DANMARKS OG GRØNLANDS GEOLOGISKE UNDERSØGELSE **RAPPORT 2024/18**

CCS2022-2024 WP1: The Rødby structure

Seismic data and interpretation to mature potential geological storage of CO_2

Tanni Abramovitz, Henrik Vosgerau, Ulrik Gregersen, Florian W.H. Smit, Morten Bjerager, Tomi A. Jusri, Anders Mathiesen, Finn Mørk, Niels H. Schovsbo, Henrik I. Petersen, Lars Henrik Nielsen, Shahjahan Laghari, Lasse M. Rasmussen & Marie Keiding

GEOLOGICAL SURVEY OF DENMARK AND GREENLAND
DANISH MINISTRY OF CLIMATE, ENERGY AND UTILITIES

G E U S

CCS2022-2024 WP1: The Rødby structure

Seismic data and interpretation to mature potential geological storage of CO_2

Tanni Abramovitz, Henrik Vosgerau, Ulrik Gregersen, Florian W.H. Smit, Morten Bjerager, Tomi A. Jusri, Anders Mathiesen, Finn Mørk, Niels H. Schovsbo, Henrik I. Petersen, Lars Henrik Nielsen, Shahjahan Laghari, Lasse M. Rasmussen & Marie Keiding

GEOLOGICAL SURVEY OF DENMARK AND GREENLAND
DANISH MINISTRY OF CLIMATE, ENERGY AND UTILITIES

G E U S

CCS2022-2024 WP1: The Rødby structure

Seismic data and interpretation to mature potential geological storage of CO_2

Tanni Abramovitz, Henrik Vosgerau, Ulrik Gregersen, Florian W.H. Smit, Morten Bjerager, Tomi A. Jusri, Anders Mathiesen, Finn Mørk, Niels H. Schovsbo, Henrik I. Petersen, Lars Henrik Nielsen, Shahjahan Laghari, Lasse M. Rasmussen & Marie Keiding

Preface

A new Danish Climate Act was decided by the Danish Government and a large majority of the Danish Parliament on June 26th, 2020. It includes the aim of reducing the Danish greenhouse gas emissions with 70 % by 2030 compared to the level of emissions in 1990. The first part of a new Danish CCS-Strategy of June 30th, 2021 includes a decision to continue the initial investigations of sites for potential geological storage of CO_2 in Denmark. GEUS has therefore from 2022 commenced seismic acquisition and investigations of potential sites for geological storage of CO_2 in Denmark.

The structures decided for maturation by the authorities, are some of the largest structures onshore Zealand, Jutland and Lolland and in the eastern North Sea (Fig. 1.1). The onshore structures include the Havnsø, Gassum, Thorning, and Rødby structures, and in addition the small Stenlille structure as a demonstration (pilot) site. The offshore structures include the Inez, Lisa and Jammerbugt structures. A GEUS Report is produced for each of the structures to mature the structure as part of the CCS2022–2024 project towards potential geological storage of CO_2.

The intention with the project reporting for each structure is to provide a knowledge-based maturation with improved database and solid basic descriptions to improve the understanding of the formation, composition, and geometry of the structure. Each report includes a description overview and mapping of the reservoir and seal formations, the largest faults, the lowermost closure (spill-point) and structural top point of the reservoir, estimations of the overall closure area and gross-rock volume. In addition, the database will be updated, where needed with rescanning of some of the old seismic data, and acquisition of new seismic data in a grid over the structures, except for the Inez and Lisa structures, which have sufficient seismic data for this initial maturation.

The reports will provide an updated overview of the database, geology, and seismic interpretation for all with interests in the structures and will become public available. Each reporting is a first step toward geological maturation and site characterization of the structures. A full technical evaluation of the structures to cover all site characterization aspects related to CO_2 storage including risk assessment is recommended for the further process.

Content

Dansk sammendrag

Regeringen og et bredt flertal i Folketinget vedtog i juni 2021 en køreplan for lagring af CO_2, der inkluderer undersøgelser af potentielle lagringslokaliteter i den danske undergrund. Der er derfor udvalgt fire store strukturer på land med dataindsamling og kortlægning til videre modning: Havnsø, Gassum, Rødby og Thorning, samt den mindre Stenlille struktur til demonstrationslagring (Fig. 1.1). Derudover indsamles nye data til kortlægning og modning for den kystnære Jammerbugt struktur, mens de to Inez og Lisa strukturer, længere mod vest i Nordsøen, kortlægges og modnes baseret på eksisterende data.

Rødby strukturen er en stor og dyb struktur, der ligger kystnært på det sydlige Lolland. Tidligere og nye seismiske data viser strukturens form og opbygning. Korrelation med de seismiske data til de nærliggende gamle dybe boringer i hhv. Rødby-1, Rødby-2, Søllested-1 og Ørslev-1 giver en vigtig viden om regionens geologiske opbygning.

Dette sammendrag opsummerer kort forundersøgelsen og den initiale vurdering af lagringsmuligheden i Rødby-strukturen. Vurderingen bygger på tolkning af eksisterende samt nye geologiske og geofysiske data og viden (Kapitel 3−4), og belyser undergrundens geologiske opbygning i og omkring Rødby-strukturen (Kapitel 5–7). Vurderingen har fokus på strukturens form, størrelse, overordnede opdeling inklusive reservoir- og seglforhold, geologiske risikofaktorer, især større forkastninger og segl, og der foretages en vurdering af statisk lagringskapacitet for det primære reservoir (Kapitel 8). Desuden opsummeres anbefalinger til yderligere modning af strukturen hen imod en mulig CO_2 lagring (Kapitel 9–10).

Datagrundlag

Rødby-strukturen er dækket af refleksionsseismiske data (Fig. 4.1.1) med 2D profiler af varierende tæthed og kvalitet indsamlet i 1960'erne, 1970'erne, 1980'erne, samt enkelte profiler fra 2012 ifm. overfladenær grundvandskortlægning. De ældre datasæt er generelt af dårlig kvalitet med meget støj. Derfor blev der i juni–juli 2023 indsamlet 10 nye 2D refleksionsseismiske profiler (i alt c. 106 km) ved hjælp af 2 vibrator-lastbiler (lydkilde), tilkoblet en landstreamer med geofoner, samt trådløse geofoner i vejsiden. Disse data har forbedret dækning og kvaliteten af data samt tolkningsmulighederne over strukturen og flankerne (se figurerne i Kap 4 og 6). En gruppe fra Uppsala Universitet gennemførte indsamlingen og processeringen på vegne af GEUS, med de seismiske lydkilder leveret fra polske Geopartner Geofizyka og med feltassistance fra universitetsstuderende fra København, Aarhus og Uppsala universiteter. COWI varetog ansøgninger om tilladelser, logistik, kommunikation og borgerkontakt. Der blev forud for indsamlingen informeret på to borgermøder hhv. i Maribo den 3. maj 2023 og i Holeby den 13. juni 2023, via webside information hhv. af GEUS og COWI, via informationsbreve og flyers, samt på en besøgsdag under selve indsamlingen den 17. juni 2023. Det nye 2D seismiske datasæt (GEUS2023-ROEDBY) har markant forbedret data grundlaget over toppen og flankerne af Rødby strukturen og muliggør derved en forbedret kortlægning.

Tolkning

Rødby-strukturen er en geologisk aflang hævningsstruktur (antiklinal med 4-vejs lukning) i form af en dome, som hovedsageligt er dannet i Mesozoisk tid over en dyb saltpude med Zechstein salt (Fig. 1.2). Saltpuden blev udviklet ved at det aflejrede Zechstein saltlag, som har mindre massefylde end de overliggende og omgivende lag i undergrunden, bevægede sig til områder med mindre tryk. Denne saltbevægelse, halokinese, pressede derved de

overliggende lag opad i en dome. Saltbevægelserne blev sandsynligvis igangsat af og udløst ved en kombination af differential sedimentbelastning pga. varierende sedimenttykkelser og tektonisk reaktivering af dybtliggende forkastninger og opløft af det krystalline grundfjeld dybt under strukturen.

I Rødby-strukturen er det primære reservoir-segl-par for potentiel CO_2-lagring tilstede i lagene fra de Triassiske Bunter Sandstone–Ørslev formationerne. Her viser tolkningen af de nye data, at strukturen af Top Bunter Sandsten Fm er veldefineret med et areal på 117 km^2 og et relief på 315 m fra toppunktet (højden af spill-point) ved ca. 1100 m til bundkonturen ved 1415 m dybde (under havniveau). Top Bunter Sandstone Fm kortet (Fig. 1.1 og 8.1.1) viser en lukning på c. 117 km2, der er lidt mindre end den tidligere kortlægning (c. 138 km^2) fra 2020 (Hjelm et al. 2022).

Det primære reservoir for potentiel CO_2-lagring i Rødby-strukturen udgøres af tre sandstensdominerede intervaller i Bunter Sandstone Fm, hvoraf den midterste reservoirenhed har højeste porøsitet (28,6 % i Rødby-strukturen (16,9–31,9 % i studieområdet)) og permeabilitet (1397 mD i Rødby-strukturen (293–2029 mD i studieområdet)). Gassum Fm, som anses for at være det primære reservoir i mange andre danske onshore strukturer (fx Gassum, Thorning, Havnsø og Stenlille), forekommer på mere grunde dybdeintervaller (< 800 meters dybde) i Rødby-strukturen, og er derfor for overfladenær til at blive betragtet som relevant for CO_2-lagring. De primære og sekundære sejl i Rødby-strukturen udgøres af hovedsageligt tykke lag af lav-permeable lersten i Ørslev–Falster formationerne, der har en samlet tykkelse på >300 meter.

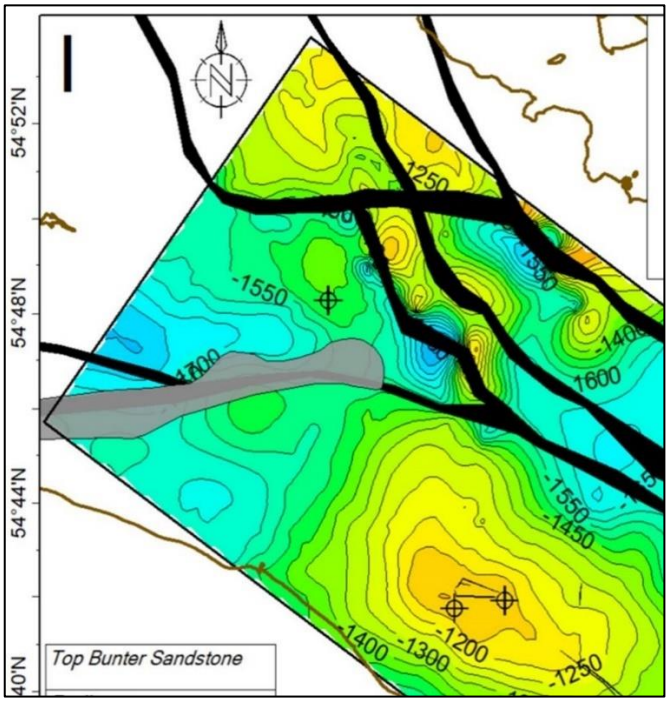

Figur 1.1 *Dybdestrukturkort i meter (m) under middelhavsniveau for Top Bunter Sandstone reservoiret. Bemærk de små forkastninger (tynde sorte linjer) på toppen af strukturen, som diskuteres i kapitel 6. De store forkastninger (sorte polygoner) i Lolland–Falster Forkastningszonen, den aflange Nybølle saltvæg (grå udfyldte polygoner) og Godsted saltdiapir NV og NØ for Rødby-strukturen, kystlinjen (brun) og boringer (cirkler + kors) er også vist.*

Rødby-strukturen er beliggende syd for et større forkastningssystem, Lolland–Falster Forkastningszonen, som afgrænser og er placeret uden for den dybeste lukkekontur på 1415 m for strukturen (Fig. 1.1). Lolland–Falster Forkastningszonen udgør derfor formodentlig ikke i sig selv en direkte risiko for potentiel CO_2-lagring inden for Rødby-strukturen. Den nye kortlægning baseret på flere seismiske linjer særligt over den østlige del af strukturen viser nogle mindre, men dog tydelige forkastninger i toppen omkring de gamle Rødby-1 og Rødby-2 boringer, som vi kalder Rødby-strukturens forkastningszone. Disse mindre forkastninger kan kun tolkes på et få seismiske linjer, hvor de ses at påvirke toppen af Bunter Sandstone Fm og gennemskære videre op gennem seglet i Ørslev-Falster Formationerne til den nedre Jurassiske Fjerritslev Fm. Da forkastningerne ikke kan kortlægges fyldestgørende med de nuværende data, anbefales det at de undersøges nærmere med indsamling af supplerende seismiske data.

Beregningerne i denne undersøgelse viser en væsentlig potentiel lagringskapacitet (*storage capacity*) af CO_2 i Bunter Sandstone Fm (Kapitel 8). Lagringskapaciteten er her estimeret for en strukturel 4-vejs lukning af strukturen på Bunter Sandstone Fm. Den gennemsnitlige statiske lagringskapacitet (*buoyant storage capacity*) for Rødby-strukturen er beregnet til ca. 107 megaton (MT) CO_2 baseret på tre forskellige scenarier, som varierer fra 69 MT CO_2 (P90)–149 MT CO_2 (P10) med en P50 på ca. 104 MT CO_2, (se Tabel 8.5.1). Den estimerede lagringskapacitet bør undersøges nærmere, f.eks. med mere konkrete data (herunder placering af injektionsboringer) og reservoir simuleringsmodeller.

Strukturen bør undersøges yderligere forud for en eventuel beslutning om injektion og lagring af CO_2. Det anbefales derfor, at supplerende seismiske data indsamles over de områder, der vurderes egnet til lagring, idet datatætheden på nuværende tidspunkt stadig er præget af for stor afstand mellem linjerne til at kunne holde til en endelig vurdering. En supplerende dataindsamling ville kunne øge den foreliggende viden om reservoir, segl og forkastninger, og derved forbedre mulighederne for modellering af CO_2 migration, risiko analyser og detail planlægning før injektion (Kapitel 10).

Viden fra forundersøgelsen af Rødby-strukturen vil indgå i myndighedernes videre arbejde med at afdække muligheder og behov, samt eventuelle krav til flere data og undersøgelser for yderligere modning af et potentielt lager.

De nye seismiske data og grids (to-vejs tid; TWT) af de vigtigste tolkede horisonter fra denne rapport er publiceret og tilgængelige via GEUS projektlinket: https://www.geus.dk/produkter-ydelser-og-faciliteter/data-og-kort/ccs-data-2022-2024

1. Summary

The subsurface in Denmark has a large number of deep structures offshore and onshore, and some of these are suited for CO_2 storage and some are also located near emission sources (Fig. 1.2). The named structures are selected for initial investigation and maturation through seismic acquisition, geological analyses, and renewed mapping from 2022 to 2024 by GEUS, and with cooperating partners on acquisition and processing (see database chapter below).

This report provides basic descriptions and interpretation of the Rødby structure (Fig. 1.1–1.3) based on a seismic database including newly acquired seismic data over the structure and with ties to nearby wells to improve the understanding of the structure in terms of its geological development, size, relief, composition, and geometry of the structure. It includes a description overview and new mapping of the reservoir and seal formations, the largest faults, the lowermost closure (spill-point) and top point at the top of the reservoir, estimations of the overall closure area and potential storage capacity.

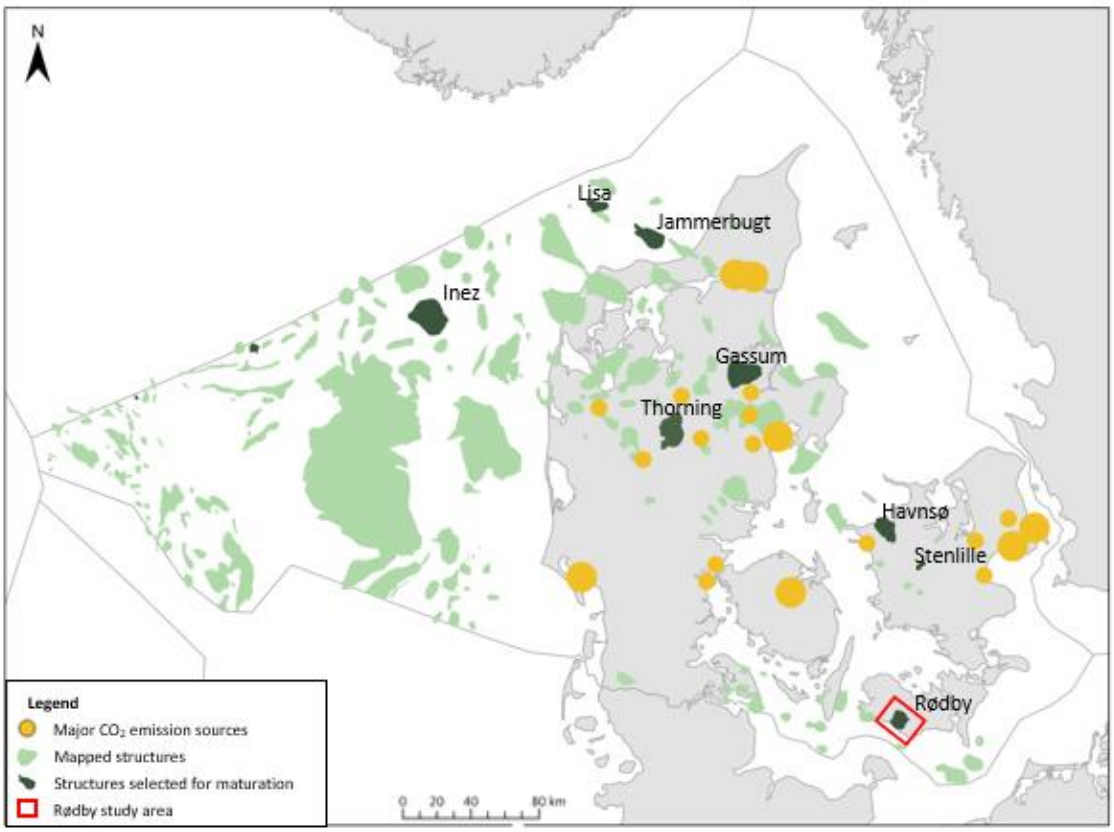

Figure 1.2. *Map of Danish structures with potential for geological storage of CO_2. The named dark green structures (Stenlille, Havnsø, Rødby, Gassum, Thorning, Jammerbugt, Lisa and Inez) are currently investigated with acquisition of new data and updated mapping in GEUS' CCS project during 2022–2024. This reporting is for the Rødby structure, and the study area is marked with a red rectangle. From Hjelm et al. (2022).*

The new 2D seismic survey (GEUS2022-ROEDBY survey) included in the present reporting was acquired in the summer 2023 to enable improved mapping of the Rødby structure and consists of c. 106 km seismic lines over the structure (Chapter 4). The Rødby structure is

located in an area with low risk for earthquakes though small earthquakes do occur (Chapter 8).

Today, the Rødby structure is a geological 4-way dip structure with the possibility of potential CO_2 storage in the reservoir-seal pair formed by the Bunter Sandstone–Ørslev Formations (Fig. 1.3). The doming of the Rødby structure evolved by separate/discrete episodes of salt pillow growth due to salt movements in the underlying Zechstein layer, forming the overlying structural doming anticlinal mainly during at least three main episodes of salt migration stating during deposition of the Falster Fm; Middle Jurassic–Early Cretaceous, and finally after deposition of the Paleocene, but before the Pleistocene.

The salt movements were probably triggered by a combination of increased sedimentary load from the overburden and re-activation of deep-seated faults causing uplift of the underlying crystalline basement block.

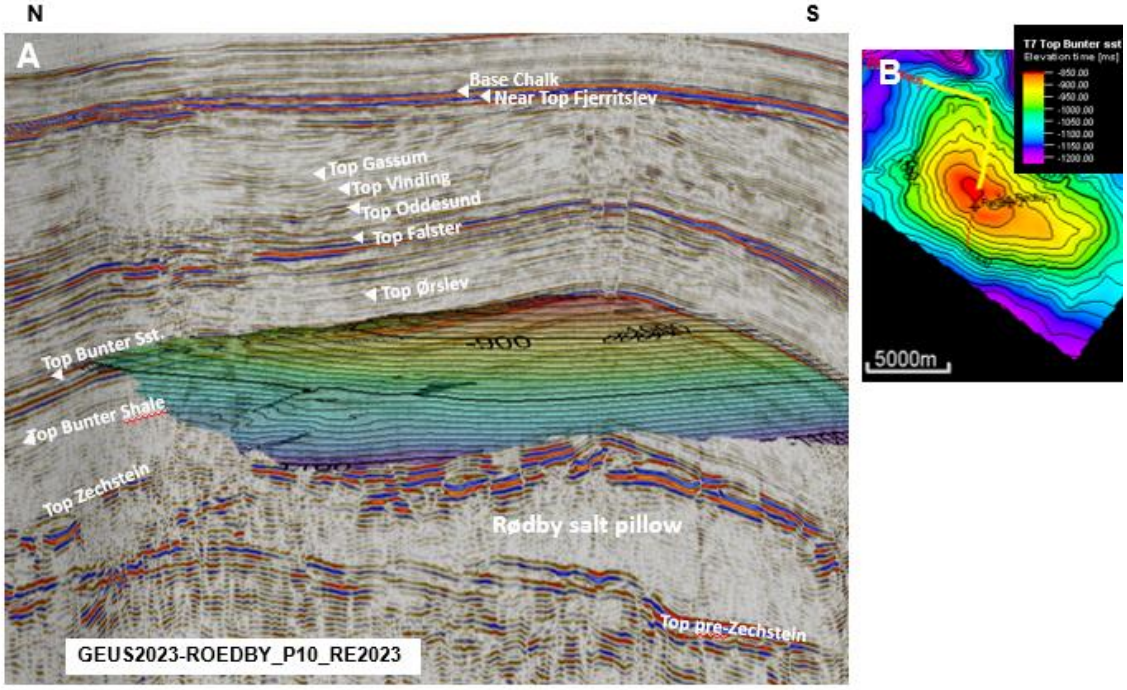

Figure 1.3. *A: 3D perspective N–S view along GEUS2023-ROEDBY_P10_RE2023 showing the shape and apex of the Top Bunter Sandstone Fm time structure map (ms TWT). B: 3D perspective view from the SW along GEUS2023-ROEDBY_P10_RE2023 showing the shape of the Top Bunter Sandstone Fm time structure map (ms TWT), with indicated positions of Top pre-Zechstein, Rødby salt pillow, Top Zechstein, Top Bunter Shale Fm, Top Ørslev Fm, Top Falster Fm, Top Oddesund Fm, Top Vinding Fm, Top Gassum Fm, Near Top Fjerritslev, and Base Chalk. B: Line position (yellow) is shown in the small database map. The Top Bunter Sandstone Fm structural closure with a NW–SE orientation is confirmed by the new data.*

The main reservoir-seal couple are the Bunter Sandstone and Ørslev Formations, which are mapped on the new seismic data showing essentially continuous thicknesses across the Rødby structure with a thickness of approximately 200–260 m for the Bunter Sandstone Fm and c. 150–200 m for the Ørslev Fm across the Rødby structure (Fig. 6.2.3). The thickness of the overlying seal in the Falster Fm is c. 150–250 m resulting in a total thickness of > 300 m seal formations, i.e. caprock in the Rødby area that complies with the recommendations from the best practices by the Global CCS Institute (Chadwick et al. 2008).

The Bunter Sandstone Formation consists of three separate reservoir units, each with distinct petrophysical properties. Each unit's properties vary due to their unique depositional environments, with the central, Detfurth reservoir demonstrating the best overall reservoir characteristics with average net thickness of 18.6 m in Rødby-1 and -2 wells (ranging from 15.2 to 30.9 m), porosities ranging between 17–32 % and permeabilities ranging between 293 – 2029 mD.

The primary seal for the Bunter Sandstone Formation is the Ørslev Formation with its low porosity (c. 2%), permeability (<1mD). The Falster Formation, although secondary, also provides effective sealing properties with generally low permeability and moderately higher porosity in specific units.

Calculations in this study show a significant storage capacity of the Bunter Sandstone Formation (Chapter 8). The area of lowermost closure on the Top Bunter Sandstone depth-structure map is c. 117 km^2 at the closing contour of c. 1415 m depth b.msl (marked in bold pink on Fig. 8.1.1). The top of the structure at the Top Bunter Sandstone map is at c. 1100 m (b.msl), and the relief of the structure at Top Bunter Sandstone is thus c. 315 m (Fig. 6.2.1I). The storage capacity of is estimated for a storage scenario in the Bunter Sandstone Formation of a 4-way closure. The mean unrisked (buoyant) static storage capacity of CO_2 in the Bunter Sandstone Formation at the Rødby structure is calculated to c. 107 MT CO_2 with a range between c. 69 MT CO_2 (P90) and c. 149 MT CO_2 (P10) and a P50 of c. 104 MT CO_2 (Figure 8.5.1).

The new seismic data have shown the existence of a minor local fault zone, here called the *Rødby Structure Fault Zone*, near the top of the Rødby structure itself with WNW–ESE striking synthetic and antithetic fault planes associated with a N-dipping main fault. The faults offsets and extends from the Top Bunter Sandstone Fm at 900 ms TWT, and up above to the Top Gassum level at 416 ms TWT. However, the throw at the Top Bunter Sandstone Fm level is very modest, <10 ms indicative of post-depositional faulting. However, due to the data scarcity, the fault zone has only been observed on three profiles, which makes it difficult to evaluate the risk it may provide to CO_2 storage without better seismic data coverage. Therefore, additional supplementary seismic data is recommended to evaluate any potential risks associated with this minor antithetic fault zone, and for a more detailed interpretation prior to potential CO_2 injection.

New 2D seismic data has been acquired across the structure, which has significantly improved the geophysical database with good quality seismic data. This improved database is used in this report for providing the updated interpretation of the size, spill-point, volume, details of reservoir- and seal successions, and faults of the Rødby structure for this initial maturation. The new seismic data and grids in two-way time of key seismic horizons are available in the GEUS project link: https://www.geus.dk/produkter-ydelser-og-faciliteter/data-og-kort/ccs-data-2022-2024

However, for further maturing the Rødby site, additional seismic acquisition over the structure and the potential injection- and storage areas is recommended, for more detailed interpretation prior to CO_2 injection, as there are still some gaps in the data coverage and distance between the 2D lines as mentioned above. This can improve site-specific knowledge with more details on reservoir, seal, and faults, and can improve modelling of CO_2 migration and risk analyses. Repeated seismic surveys in same place can serve as a baseline study and contribute to monitor the extent of the CO_2 migration, together with other monitoring (e.g., via wells, sampling, seismometers, sensor cables, satellite, etc).

New necessary data acquisition and sampling, analyses and evaluations should be carried out for further maturation, including risk analyses, to cover geological and other technical uncertainties and risks. The knowledge from the investigated structures will be included in the further work of the authorities to reveal opportunities and requirements towards further maturation, site selection and possible licensing of geological CO_2 storage.

2. Introduction

Carbon capture and storage (CCS) is an important instrument for considerably lowering atmospheric CO_2 emissions (IPCC 2022). Geological storage of CO_2 is known from more than 30 sites situated in many countries, including Norway (Sleipner), Canada (Weyburn) and Germany (Ketzin), since the first started more than 25 years ago (e.g., Chadwick et al. 2004) and more than 190 facilities are in the project pipeline (Global CCS Institute 2022).

The Danish subsurface is highly suited for CO_2 storage, and screening studies document an enormous geological storage potential that is widely distributed below the country and adjacent sea areas (Larsen et al. 2003; Anthonsen et al. 2014; Hjelm et al. 2022; Mathiesen et al. 2022). The significant Danish storage potential is based on the favorable geology that includes excellent and regionally distributed reservoirs, tight seals, large structures, and a relatively quiescent tectonic environment. The largest storage potential is contained within saline aquifers and the Danish onshore and nearshore areas contain a number of these structures with a potentially significant CO_2 storage potential (Fig. 1.2; Hjelm et al. 2022).

The Rødby structure is one of these structures and is a relatively large structure geographically located in the southern part of Lolland (Fig. 1.2), and geologically in the northern part of the North German Basin (Fig. 3.1). The structure was only covered by a limited number of old, poor 2D seismic lines, mainly acquired in the mid-1960s and early-1980s, see Table 4.1.1.

In this study, the Rødby structure is investigated further based on evaluation of the integrated database of old and new seismic data, with correlation to wells in the Lolland–Falster area, to characterize its tectonic and depositional evolution, composition with reservoir-seal couples, faults and geometry towards maturation for potentially geological storage of CO_2.

3. Geological setting

The Rødby structure is located in the northern part of the North German Basin, which towards north is separated from the Norwegian–Danish Basin by the Ringkøbing–Fyn High. The Norwegian–Danish Basin (also termed the Danish Basin) is limited towards north and northeast by the Sorgenfrei–Tornquist Zone and the Skagerrak Platform (Figs. 3.1 and 3.2). The Ringkøbing–Fyn High is part of a regional WNW–ESE trending range of high-lying basement areas in the subsurface, which in places is intersected by north–south oriented rift structures. Both the Norwegian–Danish Basin and the North German Basin are intracratonic basins formed by stretching of the lithosphere which caused Carboniferous−Permian rifting with extension and normal faulting followed by basin subsidence. The Ringkøbing–Fyn High probably formed at the same time due to less stretching than the basin areas (Vejbæk 1997, Lassen & Thybo 2012). The tectonism led to large, rotated fault blocks, intrusive volcanism, extensive erosion, and mostly coarse siliciclastic deposition (Rotliegende) affecting large parts of the basin (Vejbæk 1997; Michelsen & Nielsen 1991, 1993; Nielsen 2003). After mainly evaporites (Zechstein Group) developed in shallow basin areas during late Permian time, the region subsided and thick Triassic clay and mudstone-dominated successions formed with a few sandstones and minor carbonate and salt deposits (Bunter Shale, Bunter Sandstone, Ørslev, Falster, Tønder, Oddesund, Vinding formations; Fig. 3.3, 3.4, 3.5A,B). Sandstones are in particular known from the Bunter Sandstone Formation (Bertelsen 1978, 1980).

During Late Triassic−Early Jurassic time, sand-rich continental–fluvial, coastal near and shallow marine sand-rich systems interbedded by more clay-rich intervals formed and now constitute the widely distributed Gassum Formation (Fig. 1.4, 3.4, 3.5C). Relative sea-level rise during the Early Jurassic resulted in the deposition of thick claystone-dominated successions with some silty and sandy layers (Fjerritslev Formation), which have been correlated basin wide in several depositional sequences and members (Nielsen 2003; Michelsen et al. 2003). Mainly Middle−Late Jurassic regional uplift and salt mobilization led to formation of structures, associated faults, and major erosion in large parts of the basins, with a hiatus expanding towards the Ringkøbing–Fyn High (Fig. 3.3) (Nielsen 2003). Renewed subsidence, in the Danish part of the North German Basin most likely in the Early Cretaceous, resulted in mudstone dominated successions with local sandstones, which became gradually more calcareous during the Albian (Rødby Formation). Chalk (Chalk Group) was formed throughout the Danish Basin in the Late Cretaceous, and structures were elevated due to regional inversion. Finally, Cenozoic incl. Quaternary successions were deposited in the Danish Basin, with episodic uplift (Japsen & Bidstrup 1999; Japsen et al. 2007).

The significant amounts of sediments deposited throughout the Mesozoic period caused underlying deposits of Zechstein salt to be plastically deformed and in some places to move upwards along zones of weakness. This resulted in uplift of the overlying layers in some places (salt pillows) or breaching by the rising salt (salt diapirs). Above the salt structures, the layers may be absent or partly absent due to non-deposition or erosion, whereas increased subsidence along/in the flanks of the salt structures (in the edge depressions) may have led to corresponding layers being extra thick in these areas.

Potential sandstone reservoirs in the Danish part of the North German Basin are primarily present in the Lower Triassic Bunter Sandstone Formation and in the Upper Triassic – Lower Jurassic Gassum Formation (Mathiesen et al. 2013, Weibel et al. 2020). However, in large

parts of Lolland, including the Rødby structure, the Gassum Formation occurs above 800 meters and thus at too shallow depths to be considered relevant for CO_2 storage. Consequently, focus is on the Bunter Sandstone Formation as the prime reservoir for CO_2 storage in the Rødby structure. The primary seal for this reservoir is the Ørslev Formation and the overlying Falster Formation (Fig. 3.3).

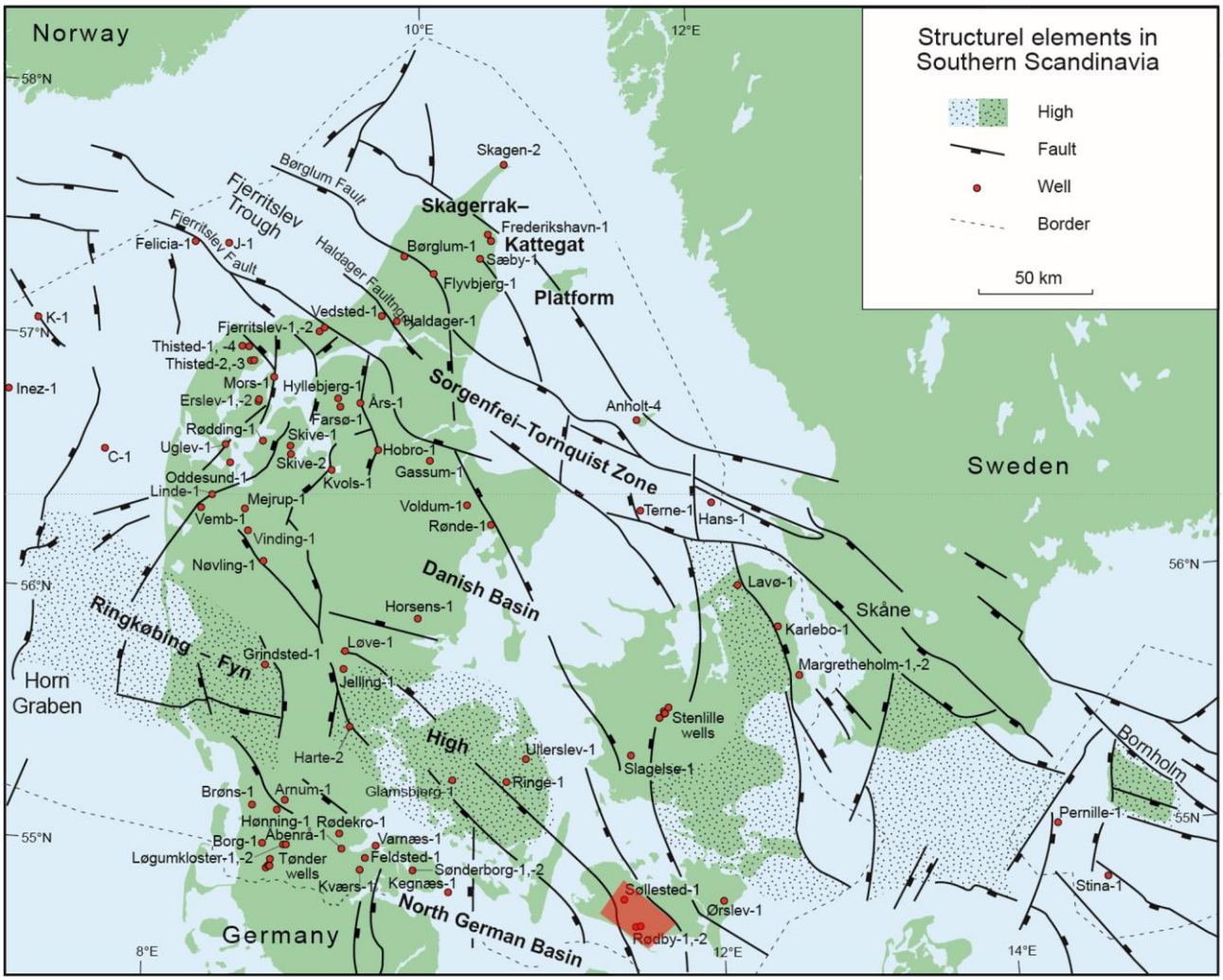

Figure 3.1. *Map of the main structural elements including highs, basins, and main faults onshore and offshore Denmark. The study area is marked with red polygon. The elements include the Danish Basin, the Sorgenfrei–Tornquist Zone, the Skagerrak–Kattegat Platform, the Ringkøbing–Fyn High and the northern part of the North German Basin. Positions of deep wells are also marked. Modified from Nielsen (2003).*

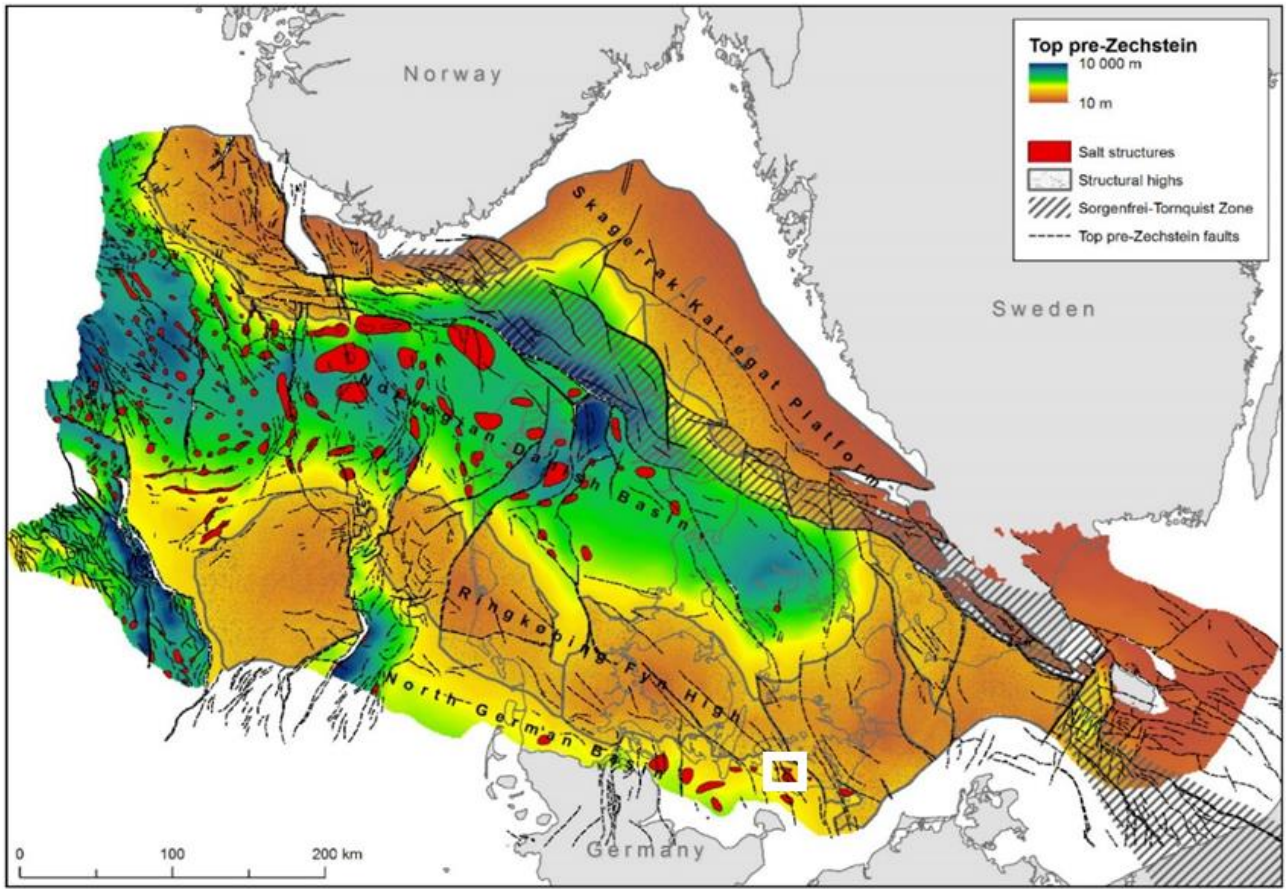

Figure 3.2. *Map of the main structural elements onshore and offshore Denmark, including highs, basins, and main faults. The location of the study area around Rødby area is marked with a white square. The elements include the Norwegian–Danish Basin (of which the eastern part in Denmark is the Danish Basin), the Sorgenfrei–Tornquist Zone, the Skagerrak–Kattegat Platform, the Ringkøbing–Fyn High and the northern part of the North German Basin. Modified from Vejbæk & Britze (1994).*

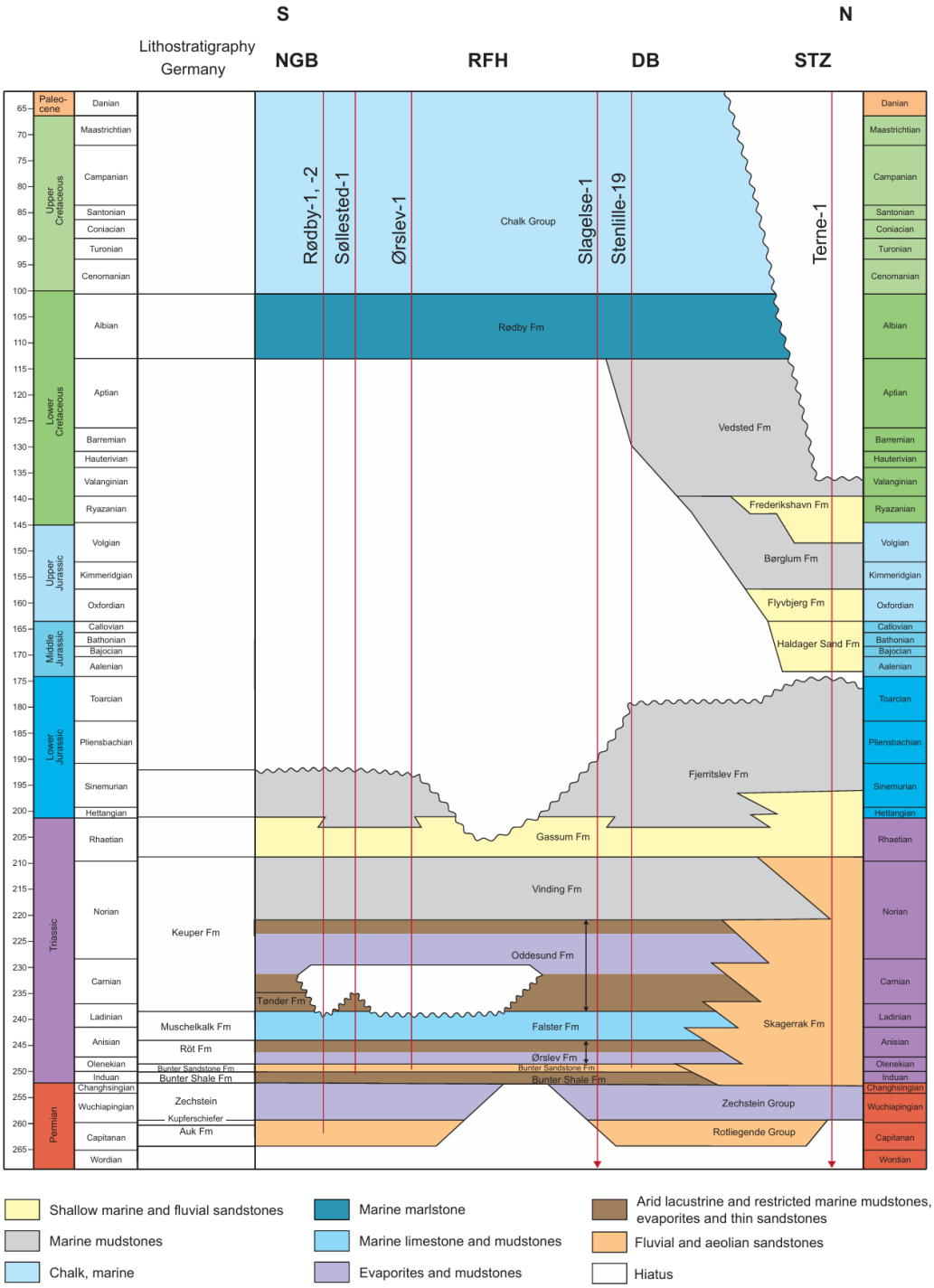

Figure 3.3. *Schematic stratigraphic S–N section from the Rødby structure in the North German Basin, over the Ringkøbing–Fyn High and into the Danish Basin. Various authors use different lithostratigraphic nomenclature, mainly for the North German Basin, as outlined in the scheme. In this study, the nomenclature to the right is followed. However, in general the lithostratigraphic subdivision of the Triassic will benefit by a major revision as only limited attention has been directed to the stratigraphic succession below the Gassum Fm in the Danish onshore area. For example, uncertainties are linked to the subsurface distribution of the Tønder Fm. Wells along the line are given at the top of the profile (the Stenlille-19 and Terne-1 wells have TD in Cambrian sandstones). Se Figure 3.1 for location of wells. Modified from Hjelm et al. (2022) who based their scheme on Bertelsen (1980), Michelsen & Clausen (2002) and Michelsen et al. (2003).*

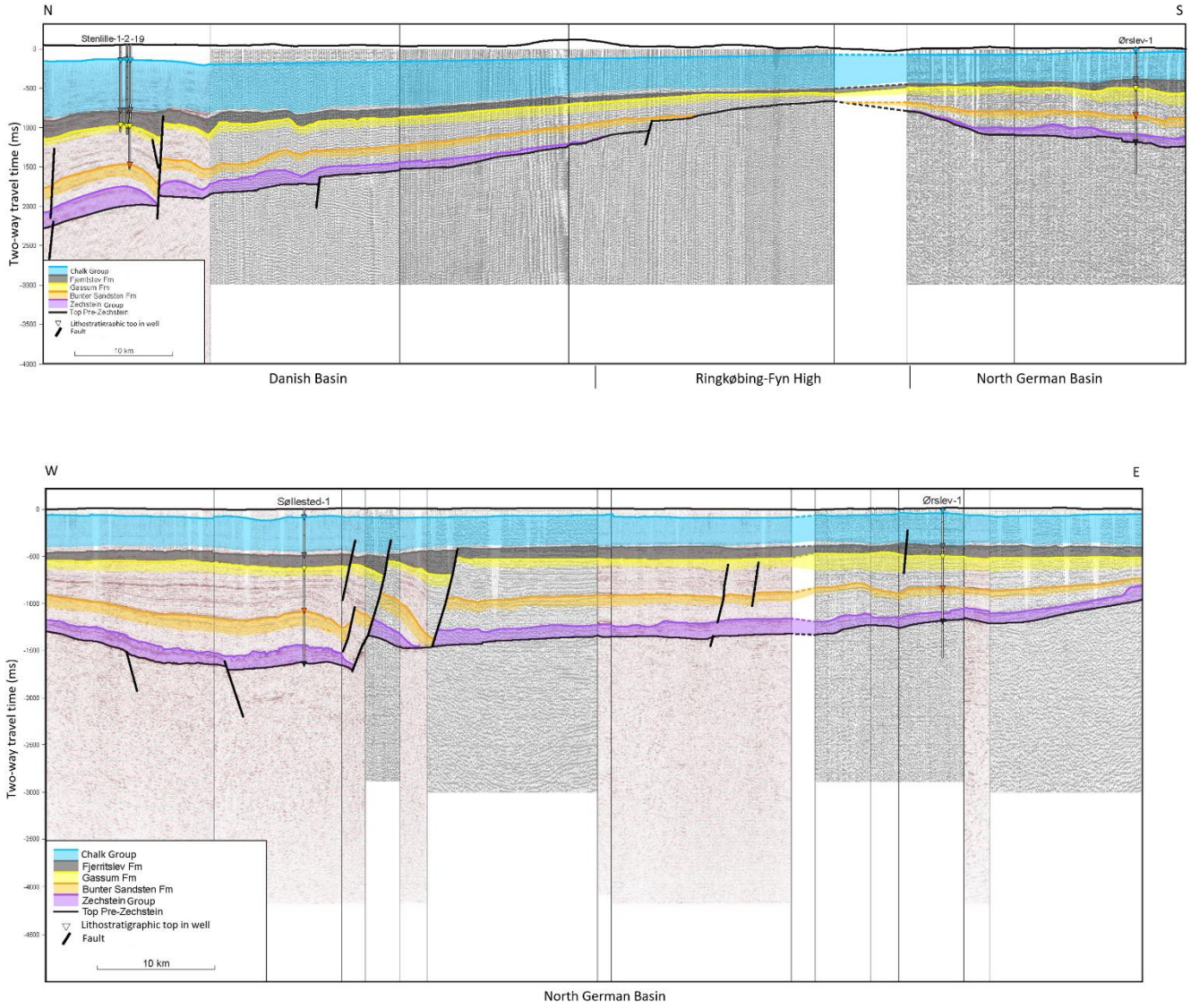

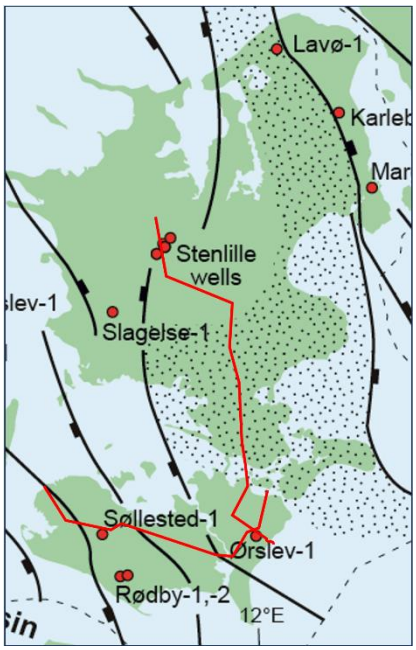

Figure 3.4. *Two regional profiles in the southeastern part of the Danish onshore area with their approximately locations shown on zoom-in on the Zealand, Falster and Lolland areas. The upper profile extends from the southern part of the Danish Basin over the Ringkøbing–Fyn High and into the North German Basin. The lower one is a W–E extending profile in the northern part of the North German Basin. Interpreted lithostratigraphy: purple indicates the deep Zechstein salt, orange the Bunter Sandstone Fm, yellow the Gassum Fm, dark grey the Fjerritslev Fm and blue the Chalk Group. Triangle positions mark lithostratigraphic well-top ties. All wells are projected onto the profiles. The composite seismic profiles are modified from https://dybgeotermi.geus.dk*

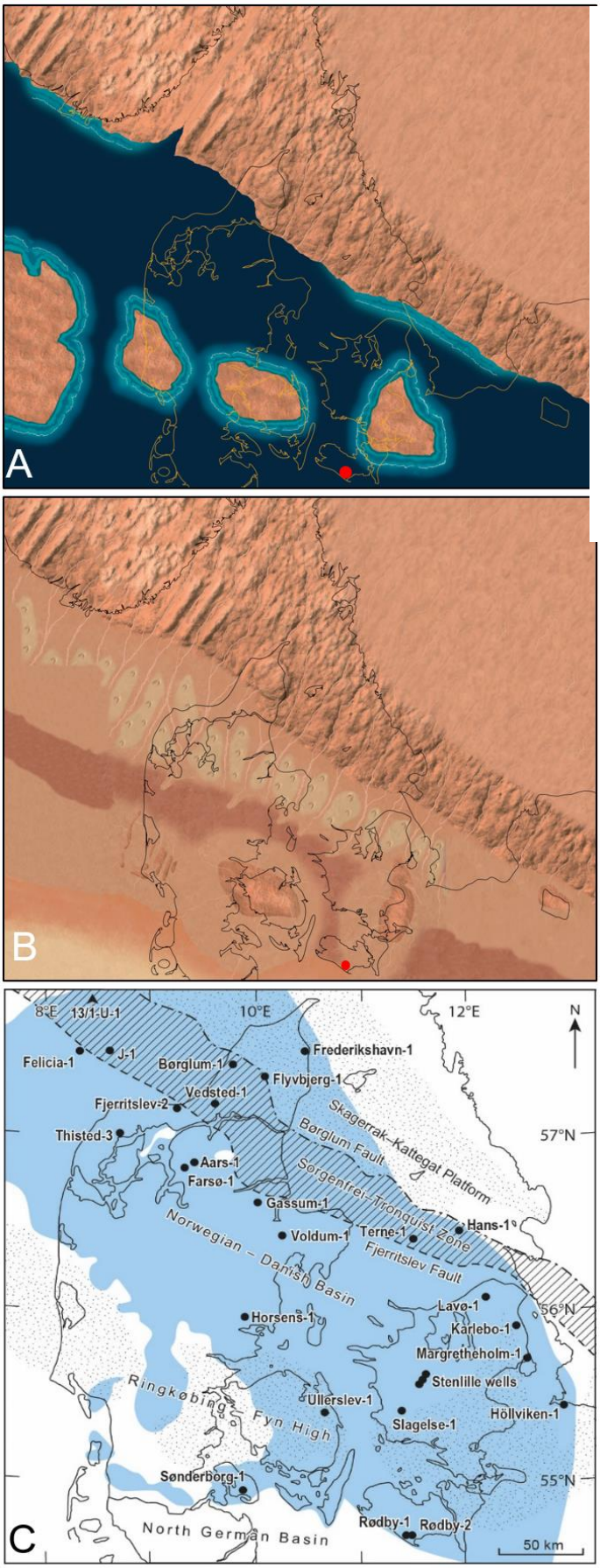

Figure 3.5. *Paleogeographic maps of Denmark and southern Scandinavia illustrating the possible distribution of general depositional environments. Red circles indicate location of the Rødby structure.*

A. Late Permian (Zechstein) sea (dark blue), coastal near areas (light blue) and onshore areas (orange red). From Rasmussen & Nielsen (2020).

B. Early–Middle Triassic (incl. the Bunter Sandstone Fm) dominated by desert with local sand dunes, lakes and sabkhas. From Rasmussen & Nielsen (2020).

C. Late Triassic (Rhaetian) to earliest Jurassic (Hettangian – early Sinemurian) Gassum Fm distribution in Denmark. From Olivarius et al. (2022).

4. Database

4.1 Seismic data

The geophysical database in the Rødby area is characterized by three decades of mostly old (1960s to 1980s), poor quality 2D seismic lines, some younger good quality 2D seismic lines from 2012, additional shallow 2D data lines recorded to 1 sec TWT for groundwater mapping purposes, and finally, the new 2D seismic data (GEUS2023-ROEDBY survey) from 2023 acquired for this project (Fig. 4.1.1). The number of wells on Lolland is sparse with only three wells in the area: Søllested-1, Rødby-1 and Rødby-2; and a fourth Ørslev-1 well located outside the study area.

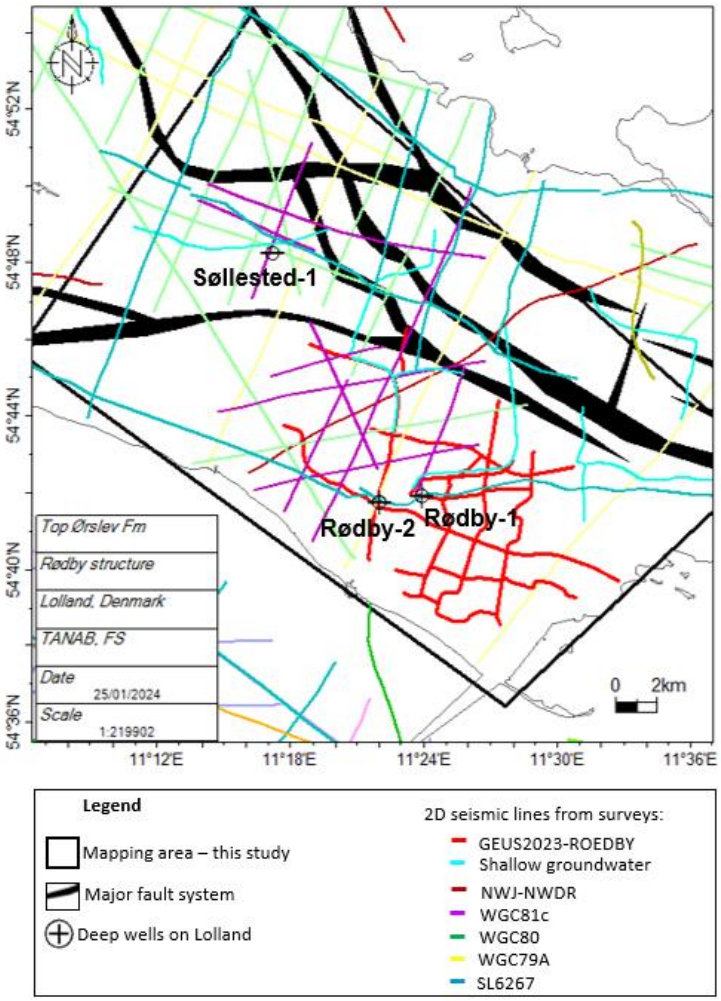

Figure 4.1.1. *Project database of the Rødby area with the new 2023 Rødby 2D seismic survey (*GEUS2023-ROEDBY*), older onshore 2D legacy data and deep wells.*

This chapter will focus on the new data of the GEUS2023-ROEDBY survey integrated with the old legacy data for mapping and interpretation of the Rødby structure as described below.

The seismic database used is shown in Figures 4.1.1 and Table 4.1.1. Seismic surveys, and acquisition and processing reports are available through GEUS (www.geus.dk), or by requests to the GEUS Subsurface Archive: info-data@geus.dk.

4.1.1 The legacy 2D data on Lolland

The quality of the seismic data in the study area is highly variable from very good to very poor (Table 4.1.1 and Fig. 4.1.2). The majority of the oldest 2D seismic surveys from the 1960s and 1970s are generally very poor to poor in quality and represented by digitalised versions of old paper sections, whereas the more recent 2D and 3D seismic data are generally of good quality and in digital format.

Table 4.1.1. *The seismic surveys and lines used for this study in and around the mapped Rødby area, with annotated age and data quality. The color coding refers to Fig, 4.1.1.*

Seismic survey	Seismic lines	Year	Color	Data quality
SSL6267 - test	SSL6267_LFC_digitized-by-geus_disp26607, SSL6267_LFC_digitized-by-geus_disp26609, SSL6267_LFH_digitized-by-geus_disp26621, SSL6267_LFP_digitized-by-geus_disp26623, SSL6267_LFP_digitized-by-geus_disp26630, SSL6267_LFP_digitized-by-geus_disp26631, SSL6267_LFP_digitized-by-geus_disp26632, SSL6267_LFP_digitized-by-geus_disp26633,	1962-67	Petrol	Poor
WGC79A	7910, 7922, 7924, 7925, 7926, 7950,	1979	Yellow	Poor
WGC80	8017, 8018, 8019, 8020, 8021, 8022, 8024, 8035, 8036, 8037,8038,	1980	Green	OK
WGC81C	8107, 8108, 8109, 8110, 8111, 8112, 8113, 8118 and 8119.	1981	Purple	OK
NWJ-NWDR	nw-dr-12-06_dmo_mig90, nw-dr-12-07_dmo_mig90, nw-dr-12-08_dmo_mig90, nw-dr-12-09_dmo_mig90	2012	Burgundy red	Ok
Shallow groundwater surveys	Lo11 final_coord , Lo15 final_coord, Lolland_LL01_fin, Lolland_LL03_mig , Lolland_LL15_mig, Lolland_LL04-05_mig, Lolland_LL10-11_mig, Lolland_LL13-14_mig		Turquoise	OK
GEUS2023-ROEDBY (processed by Uppsala University)	GEUS2023-ROEDBY_P1, GEUS2023-ROEDBY_P2, GEUS2023-ROEDBY_P3, GEUS2023-ROEDBY_P4,	2023	Not shown on map in Fig, 4.1.1	OK

	GEUS2023-ROEDBY_P5, GEUS2023-ROEDBY_P6, GEUS2023-ROEDBY_P7, GEUS2023-ROEDBY_P75, GEUS2023-ROEDBY_P8, GEUS2023-ROEDBY_P9, GEUS2023-ROEDBY_P10 GEUS2023-ROEDBY_P11			
GEUS2023-ROEDBY-RE2023 (re-processed by RTS)	GEUS2023-ROEDBY_P1-RE2023, GEUS2023-ROEDBY_P2-RE2023, GEUS2023-ROEDBY_P3-RE2023, GEUS2023-ROEDBY_P4-RE2023, GEUS2023-ROEDBY_P5-RE2023, GEUS2023-ROEDBY_P6-RE2023, GEUS2023-ROEDBY_P7-RE2023, GEUS2023-ROEDBY_P8-RE2023, GEUS2023-ROEDBY_P9-RE2023, GEUS2023-ROEDBY_P10-RE2023 GEUS2023-ROEDBY_P11-RE2023	2023	Bright red	OK

The oldest seismic dataset is the 2D seismic survey SSL6267, which was acquired in 1962–67 by Gulf Oil Co. Denmark and Shell for DUC, and eight lines were used for interpretation in area, although they mostly are of very poor quality (Table 4.1.1 and see example on Fig. 4.1.2a).

The 2D seismic survey WGC79A was carried out in 1979 by Western Geophysical Co. on behalf of Dansk Boreselskab A/S, and six lines were used for interpretation in area, although they mostly are of very poor quality (see example on Fig. 4.1.2b).

The 2D seismic survey WGC80 was carried out in 1980 by Western Geophysical Co. on behalf of Dansk Boreselskab A/S, and eleven lines were used for interpretation in area, although they mostly are of moderate quality (see example on Fig. 4.1.2c).

The 2D seismic survey WGC81C was carried out in 1981 by Western Geophysical Co. on behalf of Dansk Boreselskab A/S, and nine lines were used for interpretation in area, although they mostly are of moderate quality (see example on Fig. 4.1.2d).

The 2D seismic survey NWJ-NWDR survey was carried out in 2012 by Tesla Exploration International Ltd. On behalf of New World Resources Operations ApS, and four lines were used for interpretation in area, although they mostly are of moderate quality (see example on Fig. 4.1.2e).

Shallow 2D data lines recorded to 1 sec TWT acquired for groundwater mapping purposes can help constraining the near-surface structures of the study area and eight lines with high resolution were used for interpretation in area (see example on Fig. 4.1.2f).

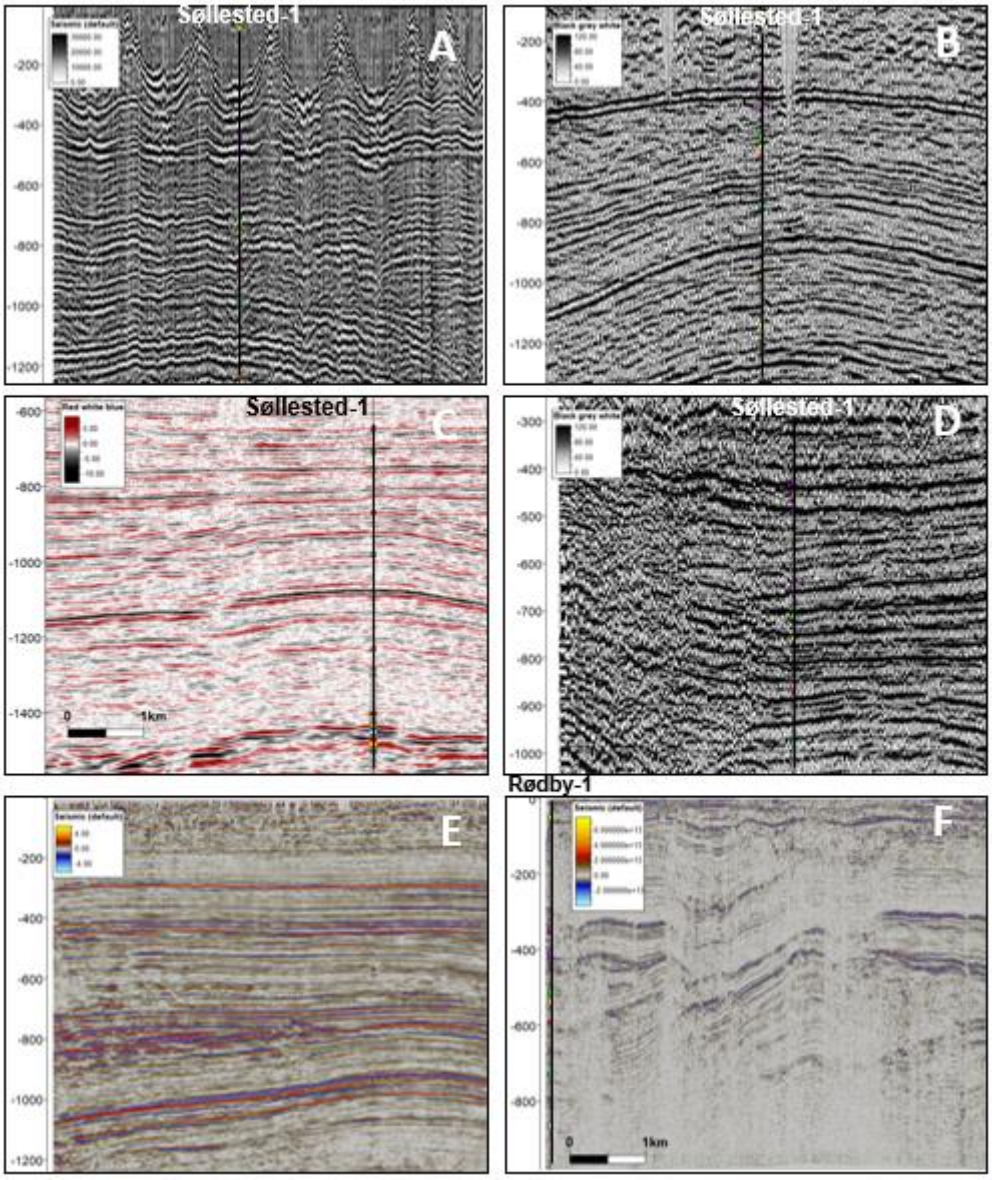

Figure 4.1.2. *Examples of seismic data quality for the 2D legacy surveys (two-way time sections). All sections have the same horizontal scale. A. Very poor data quality of 1960s data (*SSL6267_LFH_digitized-by-geus_disp26623*) across the Søllested-1 well; B. Medium poor quality of the scanned paper sections of 1979 data (*WGC79A-7925*) across the Søllested-1 well; C. Acceptable quality of the 1980 data (*WGC80-8022*), and (D) the 1981 data (*WGC81C-8112*) both sections crosses the Søllested-1 well; (E) newer high resolution data from 2012 (NWJ-NWDR-12-07_dmo_mig90), and finally (F) an example of a shallow seismic groundwater survey (Lo11_final_coord) tying to the Rødby-1 well at the SW end. All the surveys are represented in the study area (Fig. 4.1.1).*

4.1.2 GEUS new 2D seismic survey on Lolland

The new 2D seismic survey GEUS2023-ROEDBY was acquired by Uppsala University for GEUS from June to July 2023, onshore on the island of Lolland, Denmark and was organized by GEUS as part of the ongoing initial maturation efforts regarding application of CCS in Denmark as described in this report. Uppsala University carried out the acquisition and first processing of the data (Malehmir & Markovic 2024). The survey was designed to add quality data and coverage to the poorly imaged part of the eastern structure flank, where only few

and old seismic lines existed, for a better definition of the structure geometry and closure, reservoir–seal successions, and identification of potential faults.

The initial processing is carried out by Uppsala University. However, to speed up the process of having data ready for the launch of the Danish onshore CCS license application round in December 2023 and based on the experience from data acquisition on the Havnsø and Stenlille structures (Gregersen et al. 2023 & Gregersen et al. 2024), it was decided to have the data reprocessed in parallel by *Realtimeseismic* (RTS). The processing objectives were to deliver an updated Pre-Stack Time Migration (PSTM) with a good quality of imaging for facilitating a reliable geological interpretation (horizons and faults picking), prospect delineation, planning and control of future development wells and to improve vintage processing.

Data and the reports for both the initial processing by Uppsala University and the re-processing by RTS are available via GEUS: Processing summary sheet (geus.dk). Example of the data quality is displayed on Fig 4.1.3.

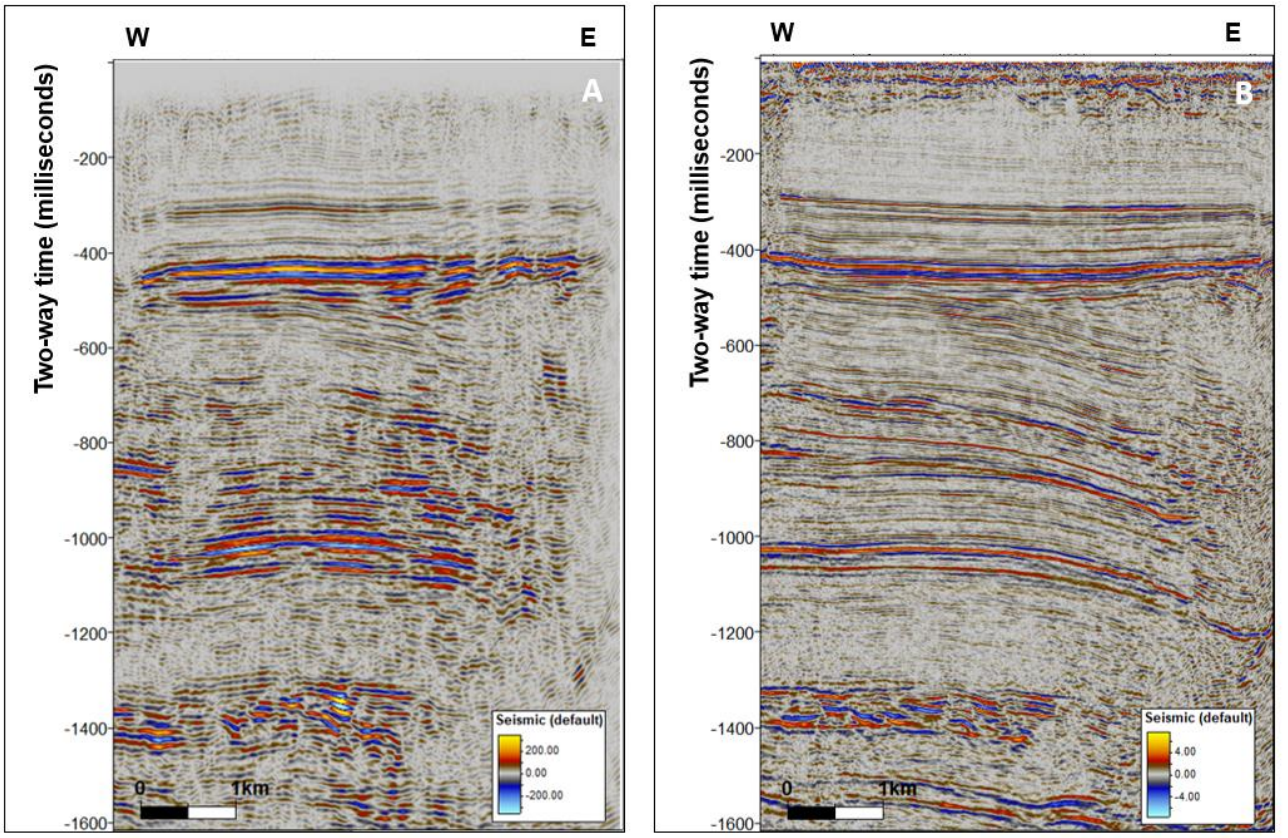

Figure 4.1.3. *Examples of seismic data quality for the* new 2D seismic survey GEUS2023-ROEDBY *(two-way time sections), both profiles show the same easternmost part of profile 1. A. The final processing carried out by Uppsala University along GEUS2023-ROEDBY-P1, B. The commercial style re-processing carried out by Realtimeseismic (RTS) along GEUS2023-ROEDBY-P1. The differences in seismic resolution will be discussed further in section 4.3.*

4.1.3 Challenges due to acquisition geometry

As observed in the new GEUS 2D seismic data acquired for both the Stenlille and Havnsø structures (Gregersen et al. 2023 & Gregersen et al. 2024), similar frequently occurring noise

can be observed in the new Rødby data especially in connection with bending of the seismic lines due to the crookedness of the acquisition geometry along minor roads. Different processing approaches on the data and line positions, such as the binning, lateral smoothing, and where lines are crocked have affected the final line positions and thus the ties, see further detailed discussion in section 4.3.2.

All released seismic surveys, and acquisition and processing reports are available through the data web portal at GEUS: Danish Deep Subsurface Data (geus.dk) or by requests to the GEUS Subsurface Archive: info-data@geus.dk.

4.1.4 Seismic data mis-ties

The 2D seismic profiles of different vintages in the study area have different datum elevations, mostly related to different static corrections, topography, etc. (Fig. 4.1.1). In this context and in relation to the data acquired, also the level of the water saturated zone (groundwater) plays a role and will be slightly different depending on the season of the year and wet or dry periods. However, the topography on Lolland and Rødby is relatively flat, rarely reaching altitudes 20 m above msl within the new 2D survey area.

To compensate for many differences in the datum elevation between seismic profiles, it was decided to use processing to mean sea level (msl) as the seismic reference datum, and for mapping purpose in this project to conduct static vertical time shifts (a constant and non-data stretched shift) of each 2D seismic profile.

The visual mis-tie screening show that there are some minor time shifts (data mis-ties) between different seismic surveys, but also between lines of the same surveys in the order of mostly approx. 5–8 ms TWT, with ranges up to -20 and 30 ms TWT in the worst cases.

To keep it simple, the 2D sections crossing the position of the wells were assumed to be at the same datum corresponding to mean sea level (msl) as the seismic reference datum. Each line was analyzed and in case of mis-tie, a manual constant time-shift for each seismic line for adjustment. The adjusted and used time-shifts are shown in Table 4.1.2 below.

Table 4.1.2. *Seismic surveys & lines used in the mapped Rødby area with time-shifts.*

Seismic survey	Line and survey: Vertical, constant time-shift (millisecond TWT) - to fit the Rødby-1 and Rødby-2 wells
SSL6267 - test	Not applicable
WGC79A	WGC79A-7926: -16 ms,
WGC80	WGC80-8033: 10 ms
WGC81C	-
NWJ-NWDR-confidential	nw-dr-12-07_dmo_mig90: -4 ms, nw-dr-12-08_dmo_mig90: -6 ms
Shallow survey	Lo12_final_coord.: -20 ms, Lo11_final_coord_flipped_SL: 30 ms

GEUS2023-RO-EDBY-RE2023	GEUS2023-ROEDBY-RE2023_P1: -8 ms; GEUS2023-ROEDBY-RE2023_P4: 12 ms; GEUS2023-ROEDBY-RE2023_P5: 8 ms; GEUS2023-ROEDBY-RE2023_P7: 5 ms

Mis-tie corrections for the surveys were only applied in this Petrel project for mapping purposes. It was not possible within the frame of this study to sort out all mis-ties, but mis-ties are described here for the present mapping and for future consideration. It is important to be aware of the mis-ties and to adjust data, to avoid errors in interpretation and mapping.

4.2 New seismic data acquired in this project

4.2.1 The new seismic survey: GEUS2023-ROEDBY

The new GEUS2023-ROEDBY 2D seismic survey acquired over the Rødby structure in June–July of 2023 is organized by GEUS for the initial maturation described in this report, and with Uppsala University in charge of acquisition and first processing of the data. Each of the survey profiles are named: GEUS2023_ROEDBY_P1, -P2, -P3, -P4, -P5, -P6, -P7, -P75, -P8, -P9, -P10 and -P11 with total lengths of c. 106 km.

The positions of the profiles are shown in Fig. 4.2.1, where they are abbreviated P1 – P11. Line extensions include a reference to the type of the geophone recording: streamer, wireless and merged (streamer & wireless together), and if the version is stacked (stk), or stacked and migrated (mig) - e.g., RODBY2023_GEUS_P1_WIRELESS_FDMIG.

Link to survey: Processing summary sheet (geus.dk).

In addition, GEUS issued a reprocessing in 2023 of the GEUS2023-ROEDBY survey: GEUS2023_ RODBY2D (RTS 2023) with a name convention indicating if the data is a post stack time-migrated section e.g., GEUS2023_ RODBY2D_P4_Final_PSTM_FullStack, also available from GEUS.

Link to survey: Processing summary sheet (geus.dk). Contact to GEUS on data by email: info-data@geus.dk.

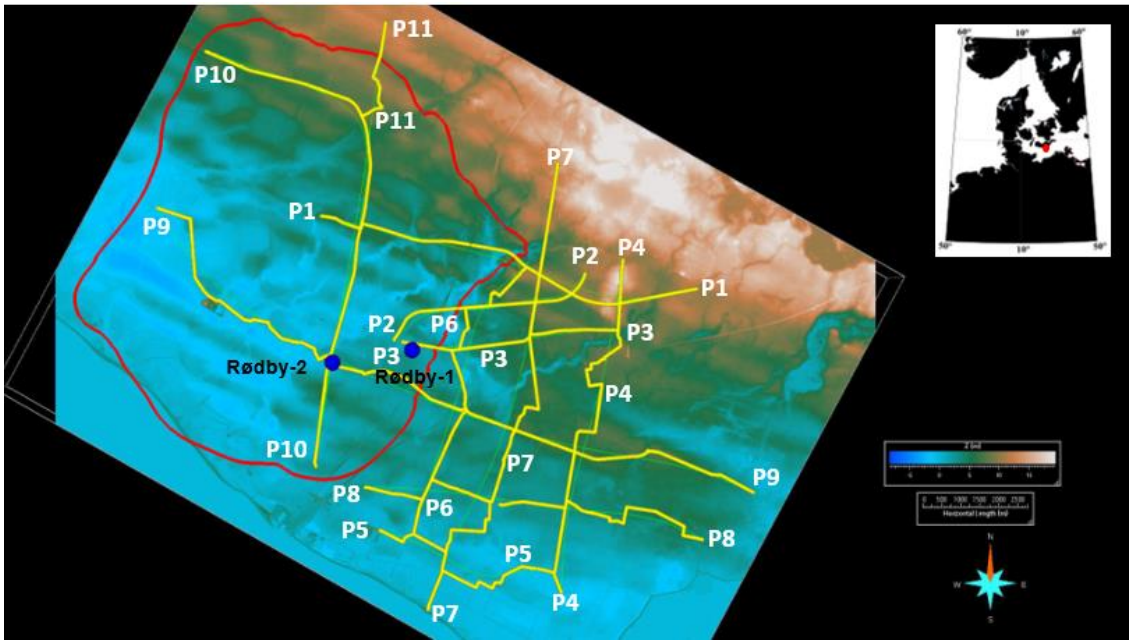

Figure 4.2.1. *Lidar elevation map with location of the seismic profiles from the acquisition and processing report (Malehmir & Markovic, 2024). Yellow lines are locations of the final migrated seismic profiles (here the profiles of wireless and merged files). The red polygon indicates GEUS earlier interpreted outline of the Rødby structure. The blue dots show the location of the* Rødby-*1 and 2 well. For information of data contact GEUS (access from website or email to info-data@geus.dk).* The most crocked lines were later geometrically adjusted into more straight lines, during the processing work to the final lines.

4.2.2 Acquisition of the survey by Uppsala University

Background and purpose

Based on the experience from the Havnsø2022 (August–October 2022) and the Gassum2023 (Feb–May 2023) projects, GEUS and Uppsala University planned and designed the seismic survey for the Rødby structure. Ten profiles were acquired to establish the tie between various legacy data and extend the current seismic coverage in the study area.

The purposes of this cooperation acquisition project are mainly:

1) to improve the database at the data-poor area and to mature the Rødby structure towards potential storage of CO_2,
2) to acquire new seismic lines to improve the data coverage with modern data,
3) to acquire modern high fold data for imaging and interpretation of the shallow and deeper subsurface, particularly the key reservoir (mainly the Bunter Sandstone Fm), seal (mainly the Ørslev Fm), faults and to obtain a better understanding of the geometry of the Rødby structure,
4) to expand knowledge of CCS operations through research and education, here in cooperation with universities.

The primary objectives of the survey are:

- Detailed and high-resolution reflection seismic imaging of geological structures including several potential reservoirs and potential faults from near surface down to 3–4 km depth,
- Test the capability of using MEMs-based 3C seismic landstreamer and the planned setup (combined landstreamer and wireless recording as well as the sources used) for similar type studies on land in Denmark,
- Generating open science data for future research purposes.

The field campaign

The survey was conducted from June 11th – July 27th, 2023 (Fig. 4.2.1 and 4.2.2). Data and discussions were delivered and reported in the acquisition and processing report of April 2024 by Malehmir & Markovic (2024) (Fig. 4.2.3).

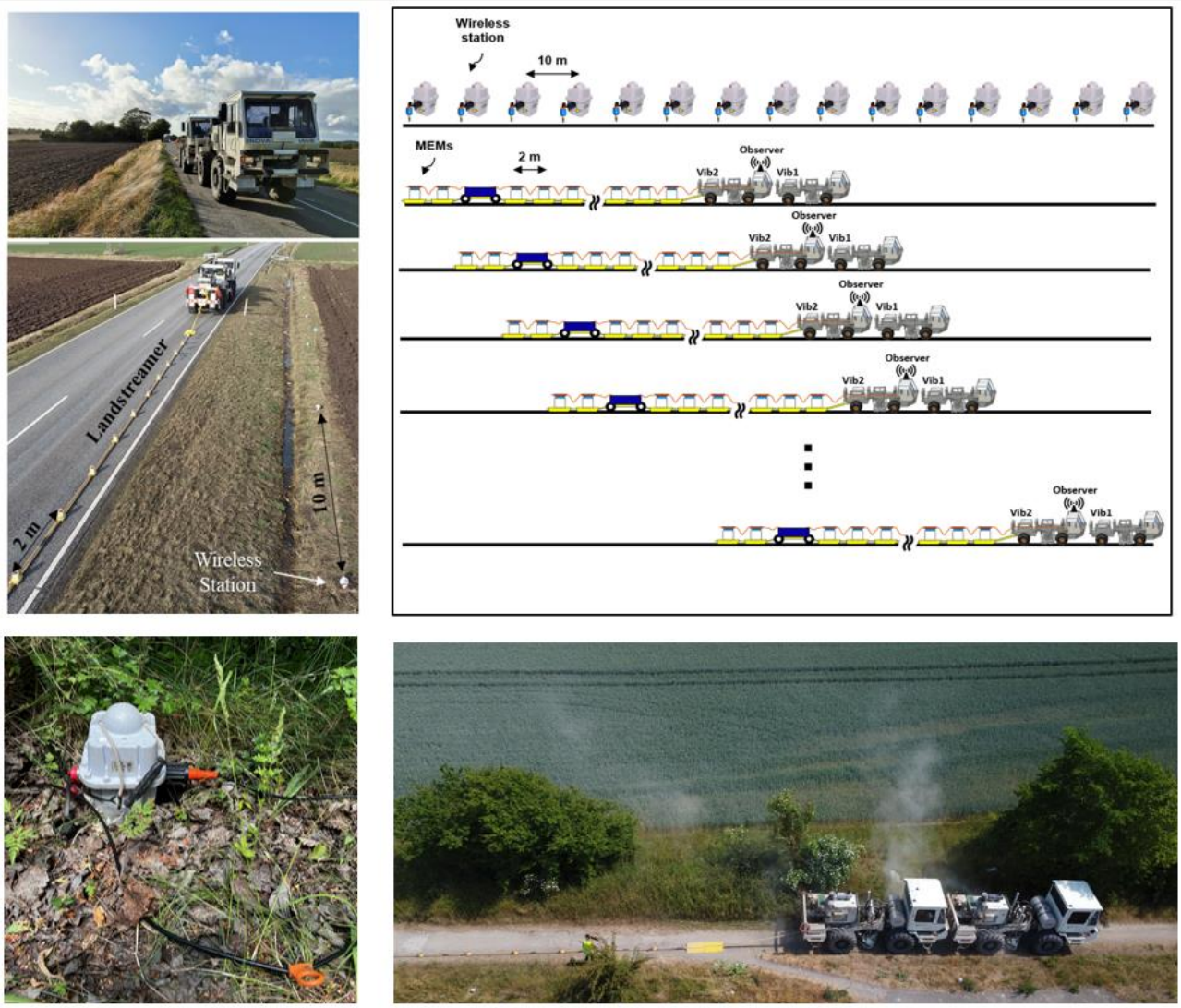

Figure 4.2.2 *Survey layout and equipment. Uppermost two left photos show how the field acquisition is carried out with the two mini-trucks equipped with vibration pistons, trailing behind a landstreamer system on the road and separate wireless geophones with a 10 m distance along the road. The illustration in the uppermost right side demonstrates the acquisition lay-out, showing the gradual proceeding of the acquisition train, with the two mini-trucks vibrating at every 10 meters, dragging the landstreamer with MEMs at 2 meters intervals, and the wireless geophones at every 10 meter along the road (Malehmir and Papadopoulou, 2023). The lower left photo is a*

close-up of a wireless geophone (GEUS). The lower right photo shows the two mini-trucks in action along a road with acquisition lay-out near Rødby (Malehmir person. Comm.).

As seismic source, two small trucks (INOVA UNIVIB-326; operating at peak-force: 95 kN) were used with synchronized vibrating hydraulic pistons lowered in firm contact with the road (Fig. 4.2.2). Each truck has a weight of 9 ton but were loaded to be 12 ton in total for a better ground contact. Before the acquisition, the field personnel followed a road-safety course, and were equipped with safety clothing during fieldwork.

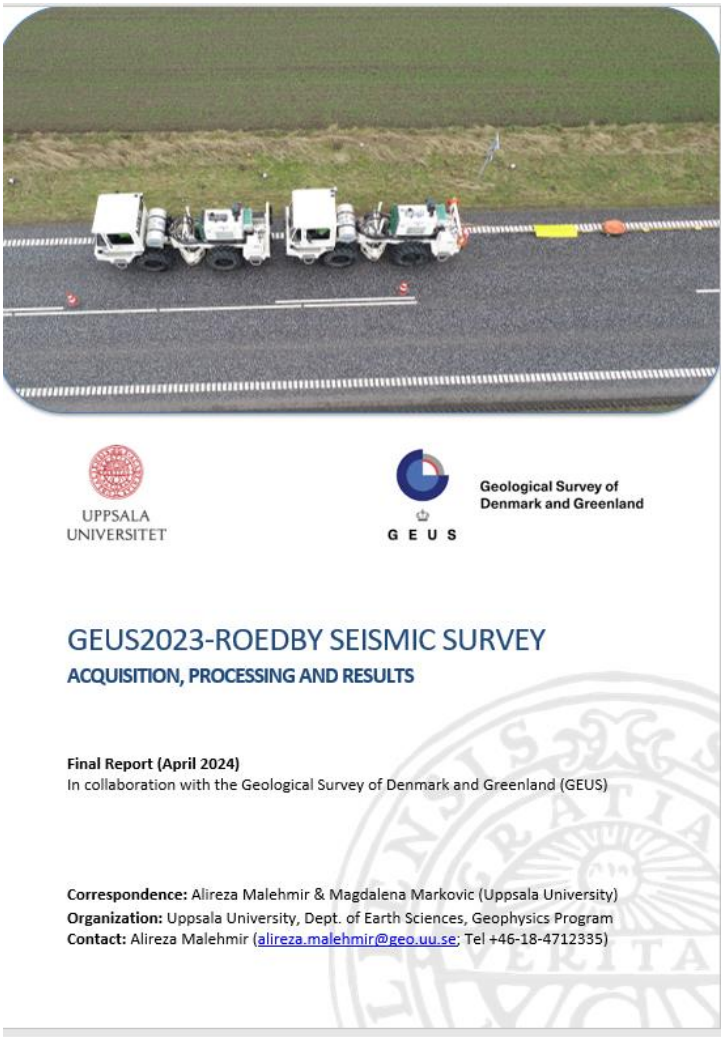

Figure 4.2.3. *The front page and contents of the GEUS2023-ROEDBY seismic survey: Acquisition, processing and results (Malehmir & Markovic, 2024), which can be purchased through GEUS (access via webpage, or email: info-data@geus.dk).*

The trucks generated simultaneous a sweep lasting 18 seconds, increasing in frequency from 10 Hz to 140 Hz (Fig. 4.2.2; Table 4.2.1). At every shot-point location this sweep was repeated three times. The three sweeps were later stacked to one shot-point during the processing to improve signal-to-noise ratio. After each shot-point with three sweeps, the trucks move 10 meters (shot-point distance) to the next shot-point. The last truck drags the attached land-streamer, adjusted along the road by field assistants (Fig. 4.2.2). The selection of the frequency range, sweep frequency, and other acquisition parameters are based on the pilot

and upscaling work conducted in Denmark prior to the Rødby survey (Malehmir et al. 2022; Zappalá et al. 2022; Papadopoulou, Myrto et al. 2023).
When passing close to private properties, control measurements with a sensitive 'Micromate' devise were carried out at the properties to secure, that vibrations stay below a threshold, as defined by the German norm DIN 4150-3. If the vibrations approached the threshold, the vibrations were stopped or continued with smaller vibration level, and in some cases with sensitive properties the shot-point was skipped.

***Table 4.2.1**: Key elements of the acquisition parameters of the Rødby seismic survey, June-July 2023 from (Malehmir & Markovic, 2024).*

Survey Parameters		
Recording system	Sercel Lite	
Source	INOVA UNIVIB-326 (2 x 12t, 95 kN per truck)	
Source sweep	10 Hz to 140 Hz linear sweep over 18 s 3 sweeps per shot point	
Shot point spacing	10 m	
Geodetic surveying	Reach RX RTK DGPS	
Recording Parameters	*Landstreamer*	*Nodal recorders*
Receiver spacing	2 m	10 m
Spread type	End-on spread	Fixed to split spread
Offset (near, far) (average)	(15 m, 215 m)	(0 m, 7500 m)
Receiver	MEMS 3C	10 Hz spike
Sampling interval	1 ms	2 ms
Record length	25 s	25 s
(before; after cross-correlation)	5 s	5 s

The landstreamer recording system was assembled within the second seismic vibrator, which was dragging the landstreamer. The inbuilt GPS antenna within landstreamer allowed accurate GPS time tagging and sampling of the streamer data, which were later used for harvesting of the data recorded on the nodal units. The operator was responsible for triggering the data acquisition, live quality control of the data, and to note in the observer's log any relevant information during the survey. Given that landstreamer was dragged along the road (including gravel roads), few of the field crew members oversaw the steering of the landstreamer to make segments straight or to follow the shape of the road. DGPS measurements were taken at every nodal unit, and vibration monitoring of infrastructure was done for safety and any damage reporting purposes.

In Rødby, depending on the length of the profiles, a fixed (e.g., if a profile was longer than 8 km) or an asymmetric split-spread roll-along geometry for the nodal arrays was used. Approximately 700-750 nodal recorders were used on average live for any shot record providing a nominal CMP fold of approximately 350, which is judged excellent for such a purpose. As for the landstreamer, depending on the complexity of the road and logistics, up to 100 units (200 m long) were used providing a nominal CMP fold of 50 for the streamer data but this was way smaller in practice. The sampling rate of the nodal recorders was set to 2 ms, while for the MEMS units sampling was 1 ms. This sampling was justified given the sweep range of 10-140 Hz used for the seismic survey. A total listening time of 25 s was used to ensure at least 5 s data can be used for data processing and for imaging purposes. Considering that landstreamer units were dragged along with the seismic vibrators, the coordinates of the

units were interpolated based on the surveyed coordinates from the fixed nodal recorders. The procedural operation of the data generation is sketched in Fig. 4.2.2.

Collaboration partners
Uppsala University contracted the Polish company Geopartner Geofizyka Sp. z. with two small trucks with vibration hydraulic pistons as source for the vibro-seismic data. Students in Geophysics and Geoscience from both University of Copenhagen and Uppsala University were hired as field assistants to conduct field support, including handling, and moving the wireless geophones with Differential GPS surveying, adjusting the landstreamer, handling the road traffic signs, distributing information folders and flyers to citizens.
COWI was contracted for acquiring permits, logistical planning, assessments in relation to landowners and supported on external contacts to authorities and citizens.

Communication & meetings
Communication with the local community was provided through two public information meetings on May 3, 2022, and November 14 2022.

A public visit day took place on June 17th, 2023, and information flyers and folders were distributed and provided to landowners in the vicinity of the acquisition prior to that date, as well as additional information on the website of project.

In addition, local medias made interviews and articles regarding the acquisition, and the local TV stations made minor recordings from the field, e.g. https://businesslf.dk/co%E2%82%82-lager-ved-roedby-skal-loese-klimaproblem/.

4.2.3 Processing of the seismic survey by Uppsala University

Immediately after seismic data acquisition seismic processing from raw SEG-D field data to final post stack migration was performed at Uppsala University. Almost identical processing sequences have been applied to the wireless data recordings and to the short offset landstreamer recordings. In the first processing step shot and receiver geometry are included in the seismic trace header and output data are in SEG-Y data format. Secondly, cross correlation of the raw recorded vibrator signal with the theoretical source sweep has been applied to get the seismic response. Subsequently the 3 sweeps for each source location are then summed together to increase the signal to noise level.

The first run of the Uppsala University processing of the GEUS2023-ROEDBY seismic survey was a relatively fast-track seismic processing of the dataset and the results have immediately been included in an updated seismic mapping of the Rødby structure (Chapter 6). For getting this fast-track processing, a conventional post stack migration has been applied to the dataset. Interpretation of both datasets have contributed to the final mapping of the Rødby structure.

Processing workflow for the wireless data from the Final Acquisition and Processing Report of the GEUS2023-ROEDBY survey (Malehmir & Markovic 2024):

1) Read SEGD
2) Theoretical sweep cross-correlation
3) Vertical stack
4) Minimum phase conversion
5) Geometry setup
6) First-break picking
7) Trace edit
8) Elevation statics
9) Frequency filter (BS 48-49-51-52)
10) Frequency filter (BP 20-30-70-90
11) Airwave attenuation (330 m/s)
12) Median horizontal filter (2200 m/s)
13) Median horizontal filter (1000 m/s)
14) DBS 16/150
15) Refraction statics
16) Constant Velocity Analysis
17) Residual statics (1 run)
18) Top mute
19) AGC (300 ms)
20) NMO corrections (60% stretch mute)
21) Stack (diversity)
22) Datum correction
23) Frequency filter (BP 15-30-90-110 Hz)
24) FX-deconvolution
25) Balance amplitude
26) FD migration

The processing workflow for the landstreamer data are almost identical to the workflow for the wireless data. Details are found in the Final Acquisition and Processing Report of the GEUS2023-ROEDBY survey (Malehmir & Markovic, *2024).*

Due to the original planning of the Rødby-deliverables before the date of the Danish application round was released, the landstreamer data and results were scheduled to be delivered by Uppsala University in Mid-February 2024 and the combined nodal and landstreamer data to be delivered by Early-April 2024, which means that neither the landstreamer data nor the combined nodal and landstreamer data were ready to be included or contributed to the final mapping of the Rødby structure in this report.

However, during processing of the Rødby data Uppsala University decided not to merge to two datasets, because the landstreamer data revealed already at the early brute stack stage, that it contained detailed information that they did not want to sacrifice at the expense of merging the two datasets *(Malehmir &* Markovic, *2024).*

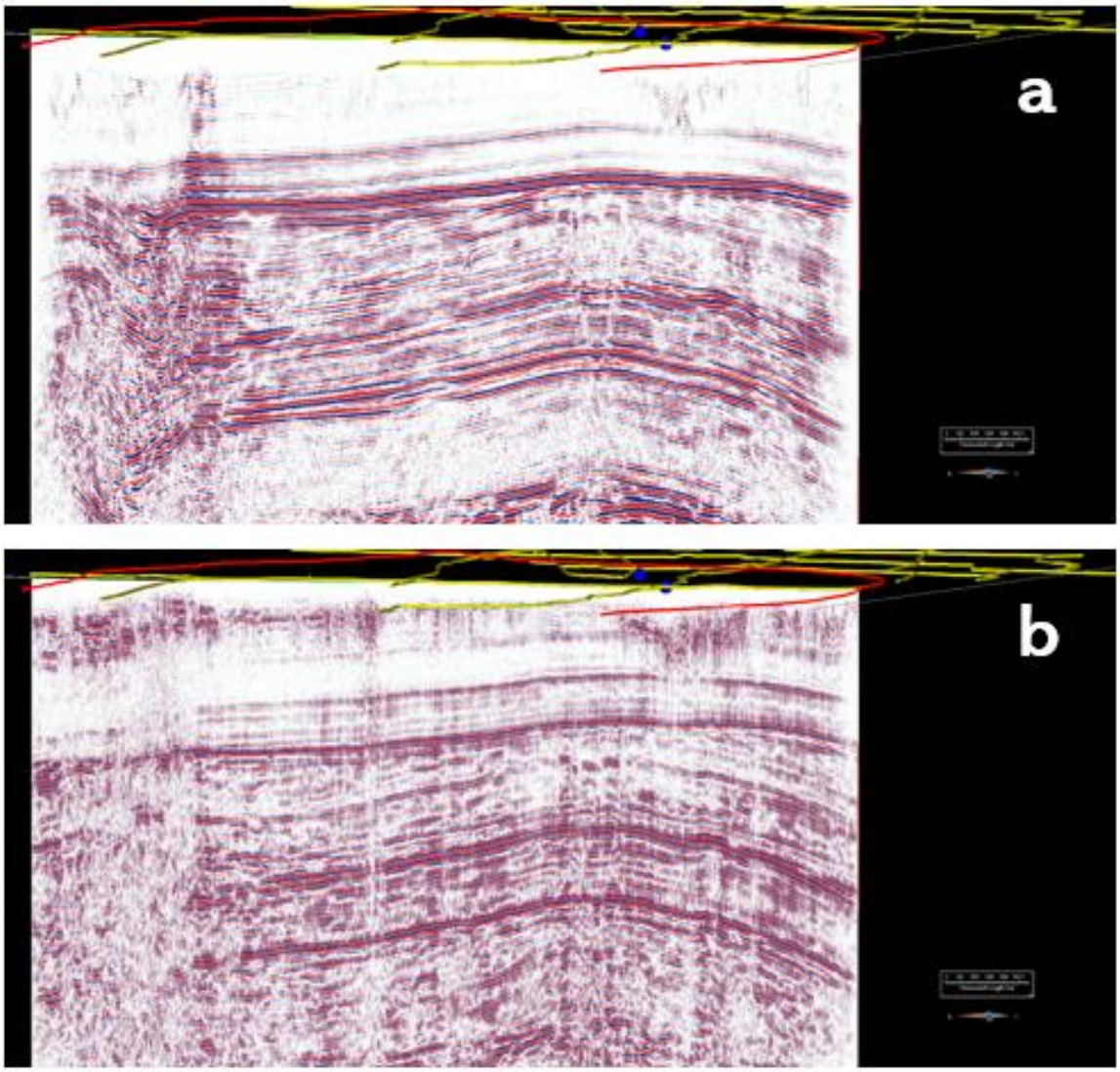

Figure 4.2.4 *Example of (a) 3D view showing key horizons successfully imaged using nodal data on P10-P11 using a post-stack migration workflow by Uppsala University. The CDP line was binned in north-south direction using limited midpoints around this line, and (b) same 3D view showing key horizons successfully imaged using landstreamer data on P10-P11 using a post-stack migration workflow by Uppsala University. The CDP line was binned in north-south direction using limited midpoints around this line. In general, the nodal recorders (i.e. the wireless data) image better the deeper parts of the subsurface and reflects the target reservoir formations (below Top Gassum Fm and Top Bunter Sst Fm), seal formations and even down to the pre-Zechstein basement.*

4.2.4 Deliverables from Uppsala University

6. Deliverables

These items have been delivered (or available) as separate files:

1. Uncorrelated raw shot gathers (SEGD format) for both landstreamer and wireless recorders
2. Correlated and reduced time shot gathers (SEGY format) ready for processing incorporating important header information
3. Refraction model: weathering velocity, weathering thickness and refractor velocity, ASCII format
4. Static corrections:
    a. Source locations, ASCII format
    b. Receiver locations, ASCII format
    c. CMP locations (floating point statics), ASCII format
5. Unmigrated stack (SEG-Y format)
6. Post-stack time migrated stack (SEGY format)
7. Pre-stack time migrated CSP gathers (SEGY format) - Pending
8. Final processed, pre-stack time migrated stack and time-to-depth converted stack (SEGY format) ready for 3D visualizations and interpretation in standard software such as gOcad and Petrel - Pending
9. Advanced processing results for PostDoc position work on depth migration and on swath 3D imaging in separate report - Pending
10. Final report summarizing the acquisition and processing works

The list of deliverables is from the GEUS2023-ROEDBY seismic survey: Acquisition and processing report (Malehmir & Markovic 2024).

4.3 Reprocessed seismic data applied in this project

Realtimeseismic (RTS) reprocessed the 2D seismic data sets from the GEUS2023-RØDBY 2D survey with the following objectives:

1. Obtaining optimal resolution for identifying key geologic formations and features in the study area.
2. Suppressing the crooked line artefacts.
3. Ensuring the optimal tie between the seismic lines.

In general, the reprocessing aimed to improve the migrated stack profiles from the original processing and help the current geological interpretation of the Rødby structure. The reprocessing project was officially named GEUS2023-RØDBY-RE2023 and took almost nine weeks, from 2 October until 30 November 2023. The reprocessed seismic data and the reprocessing report[1] can be accessed from the GEUS website portal.

The general processing sequence implemented in the reprocessing is shown in Table 4.3.1. The detailed processing sequence and parameters used in the reprocessing are given in the reprocessing report[1].

Table 4.3.1 Processing sequence implemented in the reprocessing.

No.	Processing component
1	Input analysis
2	Geometry QC
3	Firstbreak picking
4	3D diving wave tomography
5	Refraction statics
6	Residual refraction statics
7	Stacking velocity picking
8	Reflection statics
9	Surface wave attenuation
10	High amplitude noise attenuation
11	Surface-consistent amplitude correction
12	Surface-consistent deconvolution
13	Time-variant filtering

[1]Realtimeseismic, 2023. GEUS2023-RØDBY-RE2023. Reprocessing of the GEUS2023- RØDBY 2D Seismic Survey for the Geological Survey of Denmark and Greenland. Realtime Seismic Pty. Ltd., France. 57 pp. Link to info: GEUS2023-RØDBY-RE2023 report.

14	3D regularization
15	Prestack time migration
16	Migration velocity updating
17	Residual moveout correction
18	Spectral shaping
19	Time-variant filtering
20	Trim statics
21	Outside mute
22	Dip estimate
23	Structure-oriented denoising
24	PSTM common image gather stacking
25	Post-stack enhancement

4.3.1 Static effects

Processing onshore seismic data is usually challenged by static effects due to factors such as dynamic topography and near-surface velocity heterogeneities. The most common practice of static correction involves first arrival modelling using refracted ray theory (Palmer, 1980). This theory assumes that the modelled interval velocities always increase with depth and that there are no vertical velocity changes within subsurface intervals. However, those assumptions are often violated, leading to failure in removing persistent static effects. To anticipate such issues, the reprocessing utilized tomostatics - an advanced static correction technique based on a velocity model generated using turning ray tomography (Zhu et al. 1992; Zhang and Toksöz, 1998). Using a turning ray forward model, tomostatics can accommodate a vertical velocity gradient within defined velocity intervals by implementing first arrival inversion. Tomostatics can also tolerate velocity decrease with depth, given that the overall velocity gradients still enable the rays to return to the surface within the recording offset. Using tomostatics, the reprocessing anticipated potential static-related artefacts due to complex near-surface geology and missing near-surface refractors (Zhu et al. 1992; Zhang and Toksöz, 1998).

Besides the static correction, the imaging part, where the reflectors were corrected to their "correct" positions, also dictated the effectiveness of the reprocessing. The reprocessing utilized a prestack time migration (PSTM) technique to anticipate conflicting dips with different stacking velocities and complex non-hyperbolic moveouts (Yilmaz, 2001).

4.3.2 Crooked line artefacts

Due to the logistic setup of the seismic field campaign, it was only possible to acquire the seismic data along public roads. This causes significant challenges with particular seismic

signal characters in the new GEUS2023-ROEDBY 2D seismic data due to crookedness, i.e., bending of the roads and the irregular acquisition geometry as previously mentioned in section 4.1.3, as in crooked-line acquisition the CMP gathers are characterized by variable fold and uneven offset distribution.

While geometry is rarely an issue in processing seismic data from straight lines, it becomes significant in processing seismic data from crooked lines, as in the GEUS2023-RØDBY 2D survey (see Fig. 4.2.1).

Crooked lines cause irregular source-receiver offsets along the lines and shift reflection points away from the lines, producing midpoint dispersion and uneven subsurface wavefield illumination, as illustrated in Fig. 4.3.1. Crooked lines can also cause uneven fold coverage due to irregular trace distribution and missing traces in the offset classes. The low fold coverage at the crooked areas produces migration artefacts - known as migration smiles - as the migration smears the amplitudes along the wavefield isochron. This phenomenon is similar to the migration effect at the ends of a seismic profile. Strictly speaking, the crooked line artefacts found on a stack profile are made up, at least part of it, by migration smiles.

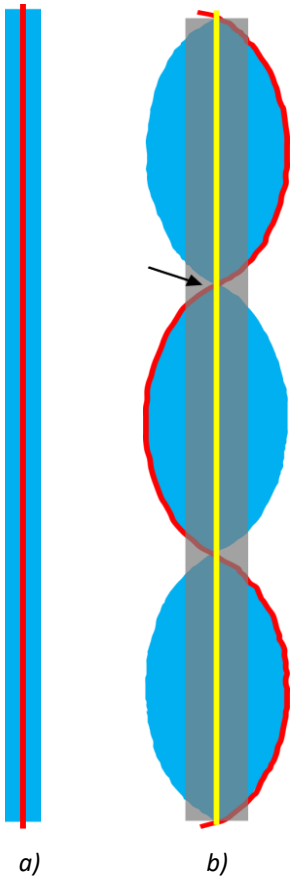

Fig. 4.3.1 *Illustration of the effects of seismic line shapes on midpoint locations. Red: seismic lines; blue: midpoint locations (midpoint dispersion in the case of the crooked line); yellow: a smoothed seismic line from the crooked line; grey: a binning area for the smoothed line; the arrow highlights an example of binned areas with missing traces. a) A straight seismic line produces midpoints exactly below the line. The blue area highlights the midpoints below the line; the crossline binning is unnecessary because all the reflections are in-plane. b) A crooked line produces midpoint dispersion away from the line.*

To deal with the crooked line artefacts, GEUS preferred the reprocessing to implement line smoothing followed by 3D regularization (Schonewille et al. 2009) to suppress the crooked line artefacts. The line smoothing aimed to have an even fold coverage. At the same time, the 3D regularization ensured obtaining the even fold coverage by filling the missing traces in the bins and offset classes.

4.3.3 Reprocessing tests to better understand crooked line artefacts.

The in-house processing team at GEUS and RTS did a test to understand the crooked line artefacts and to assess the line-smoothing approach. We used line P4 from the GEUS2023-RØDBY 2D survey (see location at Figure 4.2.1) for the test. Figure 4.3.2a shows the final PSTM stack profile from line P4 obtained without line smoothing[2] and 3D regularization, we can see prominent crooked line artefacts here. The intermediate processing output before the final PSTM stack is the raw PSTM stack, shown in Fig. 4.3.2b, and the same crooked line artefacts as in the final PSTM stack are also remarkable in the raw PSTM stack. Since the final PSTM stack is made up of the raw PSTM profile after residual moveout correction, demultiple, spectral shaping, time-variant filtering, trim statics, structure-oriented denoising, and poststack enhancement (Table 4.3.1), it is confirmed that the artefacts are not caused by any or the combination of those processes.

The effects of line smoothing and 3D regularization on the stack profile were tested. Figure 4.3.4 shows a stack profile from line P4 before the migration, with line smoothing and with and without 3D regularization. Both profiles in Fig. 4.3.2 show that the crooked line artefacts do not exist before the migration, indicating that the artefacts are caused by the migration

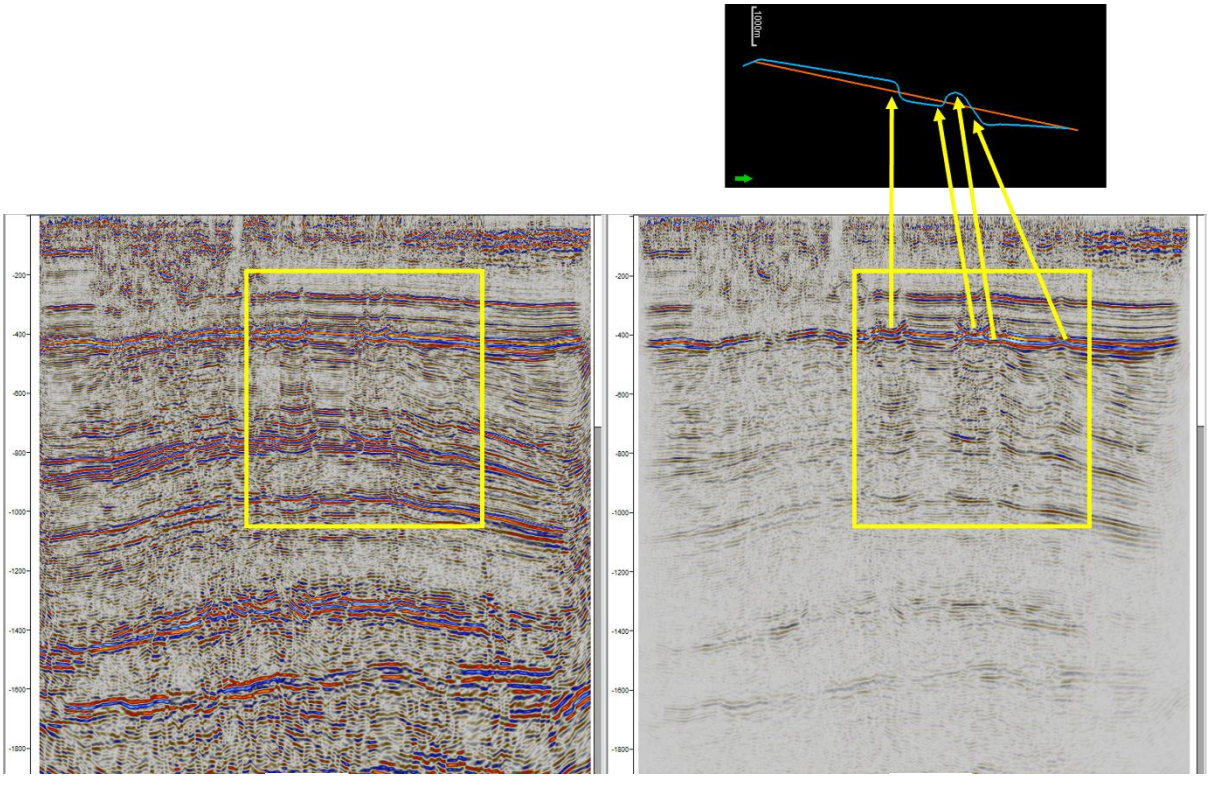

a) *b)*

only as migration smiles.

Figure 4.3.2 *Prestack time migration (PSTM) stack profiles from line P4 without smoothing. a) Final. b) Raw. The yellow boxes highlight the crooked line artefacts (migration smiles). The map*

[2] In any case, the reprocessing required subtle line smoothing for all lines without changing the main crookedness trends. "Without line smoothing" in this context is equivalent to subtle line smoothing.

shows the seismic line before (blue)2 and after (orange) smoothing. The yellow arrows show that the artefacts on the profile coincide with the crooked areas on the map.

4.3.4 Testing the effects of 3D regularization

In order to improve the reprocessing results further, we also arranged a test to see the effects of 3D regularization on the stack profile independently from line smoothing. Figure 4.3.5 shows the raw PSTM stack profiles from line P4 with line smoothing and with and without the 3D regularization. The figure shows that the migration smiles are not completely suppressed on the profile without the 3D regularization but entirely removed on the profile with the 3D regularization.

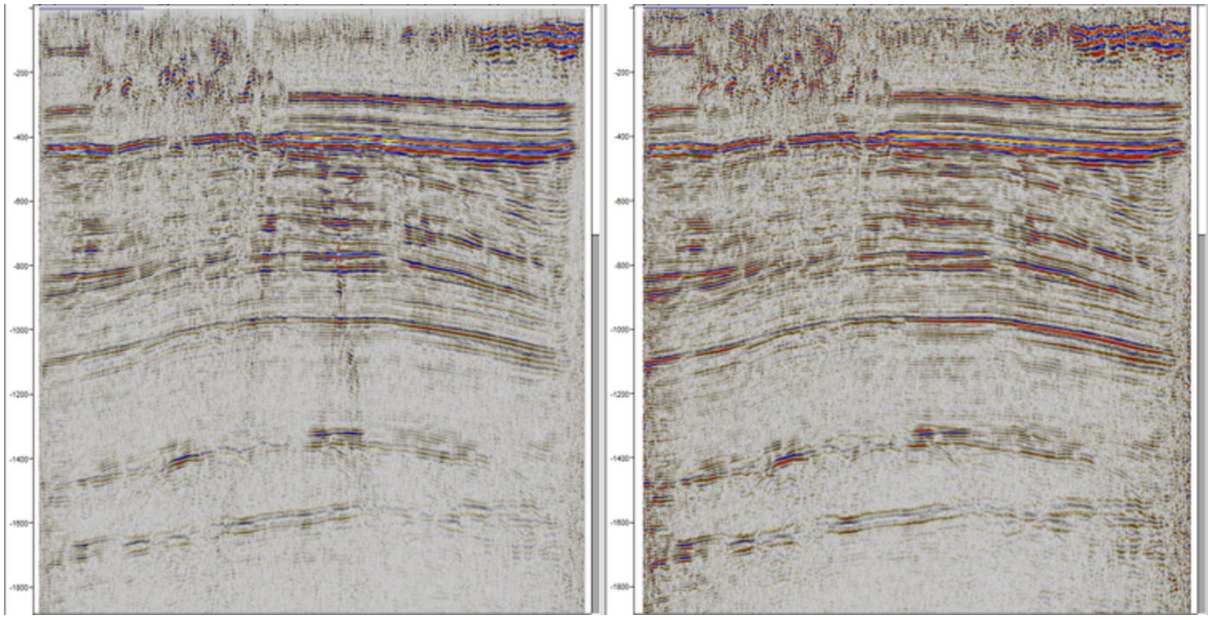

a) *b)*

Figure 1.3.4 *Stack profiles from line P4 before the migration and with line smoothing. a) Without 3D regularization. b) With 3D regularization*

Overall, the test results confirm that the migration smiles make up the crooked line artefacts and that they can be suppressed by line smoothing followed by 3D regularization.

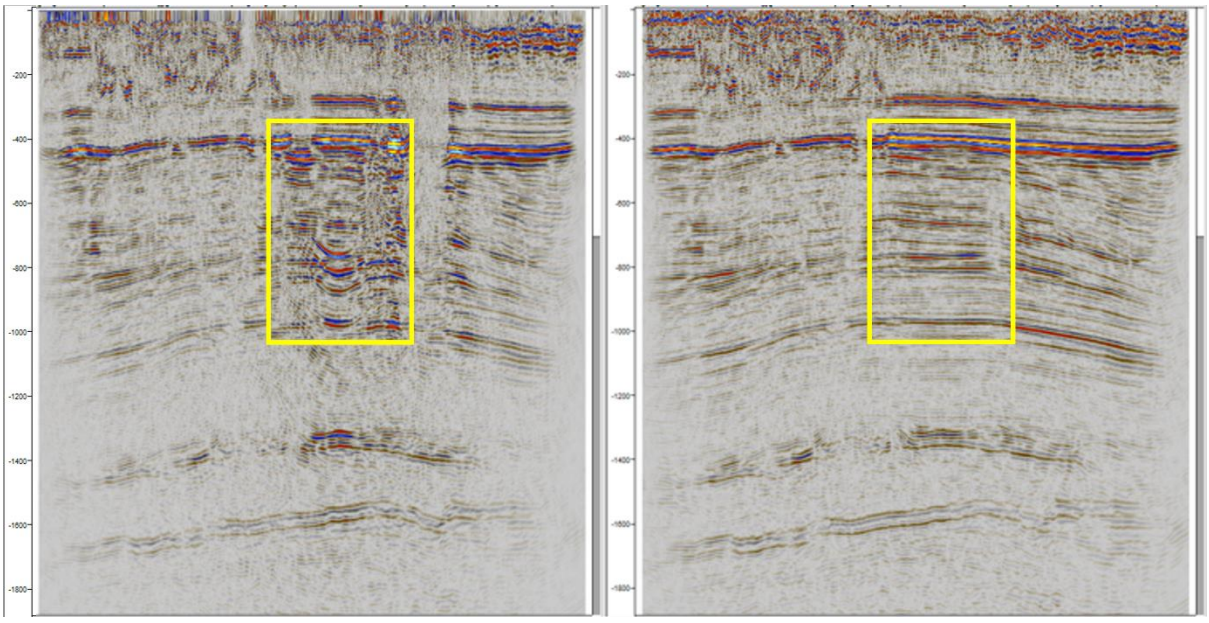

a) *b)*

Figure 4.3.5 *Raw PSTM stack profiles from line P4 with line smoothing. a) Without 3D regularization. b) With 3D regularization. The yellow boxes highlight the migration smiles that are not completely suppressed on the profile without the 3D regularization but are entirely removed on the profile with the 3D regularization.*

4.3.5 Results of reprocessing

The reprocessing results regarding PSTM stack profiles show remarkable improvement from the poststack time migration (POSTM) stack profiles produced by the original processing.

As an example, Fig. 4.3.6 shows the comparison of the original and reprocessed migrated stack profiles for line P8 (see map in Fig. 4.2.1). The comparison indicates that the reprocessed profile provides much more coherent reflections than the original profile, and such improvement has allowed us to interpret geologic features and key reflections associated with more confidence.

4.3.6 Discussion

The reprocessing certainly left room for improvement. The line smoothing approach followed by the 3D regularization is probably the simplest solution to deal with the crooked line artefacts. Yet, there are better approaches to seismic interpretation. Smoothing a crooked line means projecting the complex midpoint dispersion due to the line's crookedness into a smooth line traverse. This approach shifts the seismic interpretation onto another line traverse and includes unintended out-of-plane reflections from the dispersed midpoints. Nevertheless, although the approach of line smoothing followed by 3D regularization might not be the best to deal with the crooked line artefacts, it was the most reasonable approach that could still improve our seismic interpretation, and that could be performed within a relatively short timeframe.

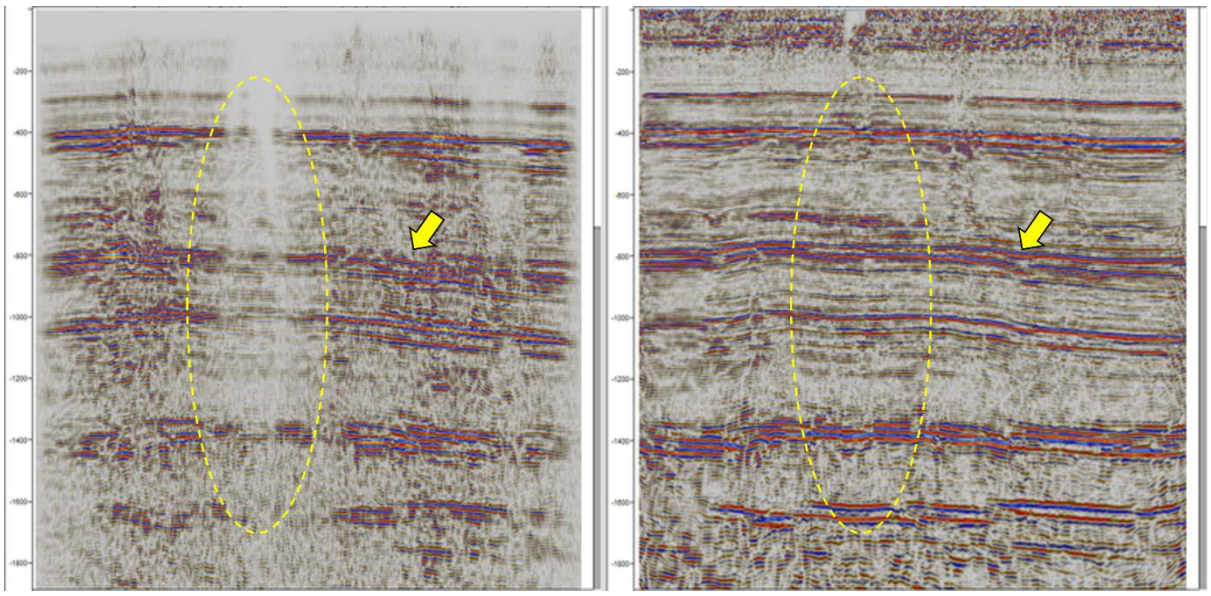

a) b)

Figure 4.3.6 *The comparison of a) the original and b) the reprocessed migrated stack profiles for line P8 (see map in Fig. 1). The yellow dash circle highlights an example of significant improvement obtained in the reprocessed profile. The yellow arrows spot an example where reflections are much more coherent and distinguished in the reprocessed profile than in the original profile.*

In principle, crooked lines violate a fundamental assumption in 2D seismic imaging - a straight-line geometry with a regular offset pattern and an even fold coverage. Therefore, problems related to the midpoint dispersion and the uneven fold coverage caused by crooked lines can hardly be resolved by conventional 2D seismic imaging (Wu, 1996). Conventional 2D seismic processing includes normal moveout (NMO) and dip moveout (DMO) corrections, which affect only the inline reflections. In addition to the NMO and DMO corrections, 2D crooked line seismic processing requires a correction also for the out-of-plane reflections in the presence of dip through so-called cross-dip moveout (CDMO) correction (Nedimović and West, 2003a). Instead of simply projecting the midpoint dispersion onto a smooth line traverse, studies show that more appropriate ways to deal with a crooked line can generally grouped into two categories, that is, 1) correcting for the cross-dip reflections and 2) processing the crooked line as 3D.

Some cross-dip analysis techniques have been developed with time, including constant shift (Larner et al. 1979), cross-dip moveout (CDMO) correction (Nedimović and West, 2003a), iterative cross-dip moveout correction (Beckel and Juhlin, 2019), generalized cross-dip moveout (GCDMO) correction (Mancuso and Naghizadeh, 2021), and 2.5D multifocusing imaging (Fam et al. 2023). Nevertheless, all these techniques have considerable limitations, including laborious computation and limited accuracy for far-offset data acquired from a severely crooked line.

On the other hand, processing a crooked line in 3D is relatively more straightforward than a cross-dip correction-based approach. Processing a crooked line as 3D takes the advantage of having the midpoint dispersion by using it as pseudo-3D or 2.5D reflection points (Schmelzbach et al. 2007; Wu, 1996). The pseudo-3D nature of midpoint dispersion from

crooked lines allows us to image complex 3D structures around the crooked areas by simply binning and processing the data from the crooked lines in 3D. The main limitation of this approach is that it can produce low-resolution images due to low fold coverage in areas not well illuminated by the recorded wavefield.

For future reprocessing, we recommend further studies implementing seismic processing techniques for overcoming crooked line artefacts, especially 2.5D multifocusing imaging (Fam et al. 2023) and crooked lines processing as 3D. The effort will be worth it as it will bring more accurate subsurface seismic images of the subsurface, leading to more reliable subsurface geologic interpretation.

4.4 Well data

The Rødby structure is drilled by two wells in 1952–53 for DAPCO: Rødby -1 and Rødby-2. For this study two additional wells, the Søllested-1 and Ørslev-1 are included and tabulated in Table 4.4.1.

Well logs are used for interpretation of lithology, and selected logs are used for well log-based sequence stratigraphy, seismic to well ties and for seismic reservoir characterization and interpretation. See Chapters 5–7 for the specific used well logs.

Original logs: Caliper (CAL), Gamma-Ray (GR), Spontaneous Potential (SP), Compressional Sonic (DT), Deep Resistivity (R_deep - mostly used), and Density (RHOB) logs.

Derived (interpreted) logs: Shale volume (V_{shale}), Effective porosity (PHIE), and Permeability (PERM_GEUS) estimates. The latter were derived from porosity-permeability relationships, established based on an analysis of core analysis data.

Table 4.4.1. *List of the wells utilized in this study, with information on the year of drilling completed, operator, Kelly Bushing (KB, meter above mean seal level), Total Depth (TD, meter below Kelly Bushing, measured drilled depth), deviation and Chronostratigraphy of the TD units.*

Well	Year	Operator	KB a. msl (m)	TD b. KB (m)	Deviated	TD
Rødby-1	1952	Dapco	5.5	1535	no	Bunter Shale Fm
Rødby-2	1953	Dapco	7.9	2725	no	Rotliegende Group
Søllested-1	1982	Mærsk Oil and Gas	11	2693	no	Rotliegende Group
Ørselv-1	1967	Gulf	22.9	2573	no	Carboniferous undiff.

5. Methods

5.1 Seismic interpretation and well-ties (see more in Chapter 6)

The Rødby structure, its formation and stratigraphy with reservoir-seal pairs, is investigated and evaluated from a structural and stratigraphic perspective, based on the available 2D-seismic data and well-ties. Seismic horizons and successions and are identified and interpreted using reflector terminations such as onlap, downlap and truncation. The seismic stratigraphic horizons are essential sequence stratigraphic and chronostratigraphic surfaces. Selected seismic horizons are in this limited area regarded as near base or near top formation boundaries. Horizon names are for simplicity identical to the formation names tied from the wells, in particular the deep Søllested-1 well. The seismic stratigraphic boundaries and sequence stratigraphic surfaces and units should on a regional scale have more neutral naming (as e.g., in Nielsen 2003; Boldreel et al. in review). At the same time, faults, salt structures, and folds were identified and mapped together with internal configuration and thickness patterns. A structural and tectonostratigraphic interpretation was carried out using the chronostratigraphic framework from the well ties.

The Petrel (2022) software was used for establishing the database, seismic interpretation with manual and auto-tracking of the horizons and seismic well-ties including generation of synthetic seismograms. In total, eleven regional seismic stratigraphic horizons were interpreted in the Rødby area to determine the stratigraphy, geological evolution, and most important to define reservoir-seal pairs and structural closures (see Chapter 6).

In addition, the deepest mappable horizons (below Top pre-Zechstein) were interpreted on most lines and correlated from the Søllested-1 to the Rødby-1 and Rødby-2 wells, to explain the earliest part of the tectonostratigraphic evolution of the region.

However, the most comprehensive and detailed mapping of horizons and faults has been performed of the successions from the Top Zechstein Gr to the Top Fjerritslev Fm, comprising the primary reservoir (Bunter Sandstone Fm), primary seal (Ørslev Fm) and part of the secondary seal (Falster Formation) to the Bunter Sandstone Fm. Lithostratigraphic and sequence stratigraphic well-log boundaries (well-tops) are adjusted by time-depth relations to the seismic data and synthetic seismograms of the wells are used to constrain the seismic interpretation (see below; Fig. 5.1).

5.2 Well-to-seismic tie and synthetic seismogram (see more in Chapter 6)

Synthetic seismograms have been produced to study and connect wells to seismic reflections for interpretation of the horizons (Fig. 5.1). Most of the legacy 2D seismic lines in the study area are of European SEG reverse polarity, where a peak is a soft kick with downward decreasing acoustic impedance (AI). We use here mostly colored seismic profiles displayed in red-white-blue (red peaks and blue troughs) or black-grey-white (black peaks and white troughs) (Fig. 6.1.1–6.1.9).

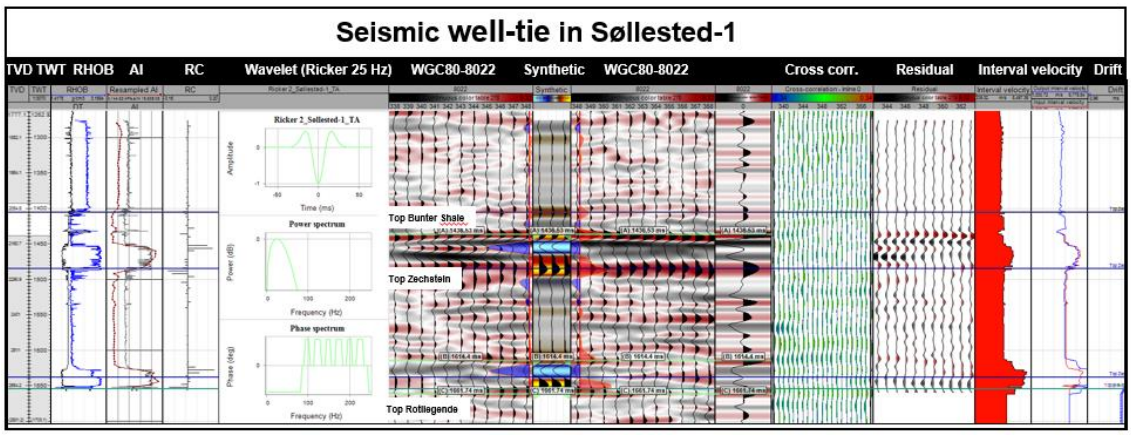

Figure 5.1. *Well to seismic tie of the Søllested-1 well using both density and sonic log, which only cover the Bunter Shale Fm and Zechstein Group. Synthetic seismic trace is shown down along the well in red-black-blue display and on the 2D seismic WGC80-8022 close to the well. Well-tops and formations are also marked.*

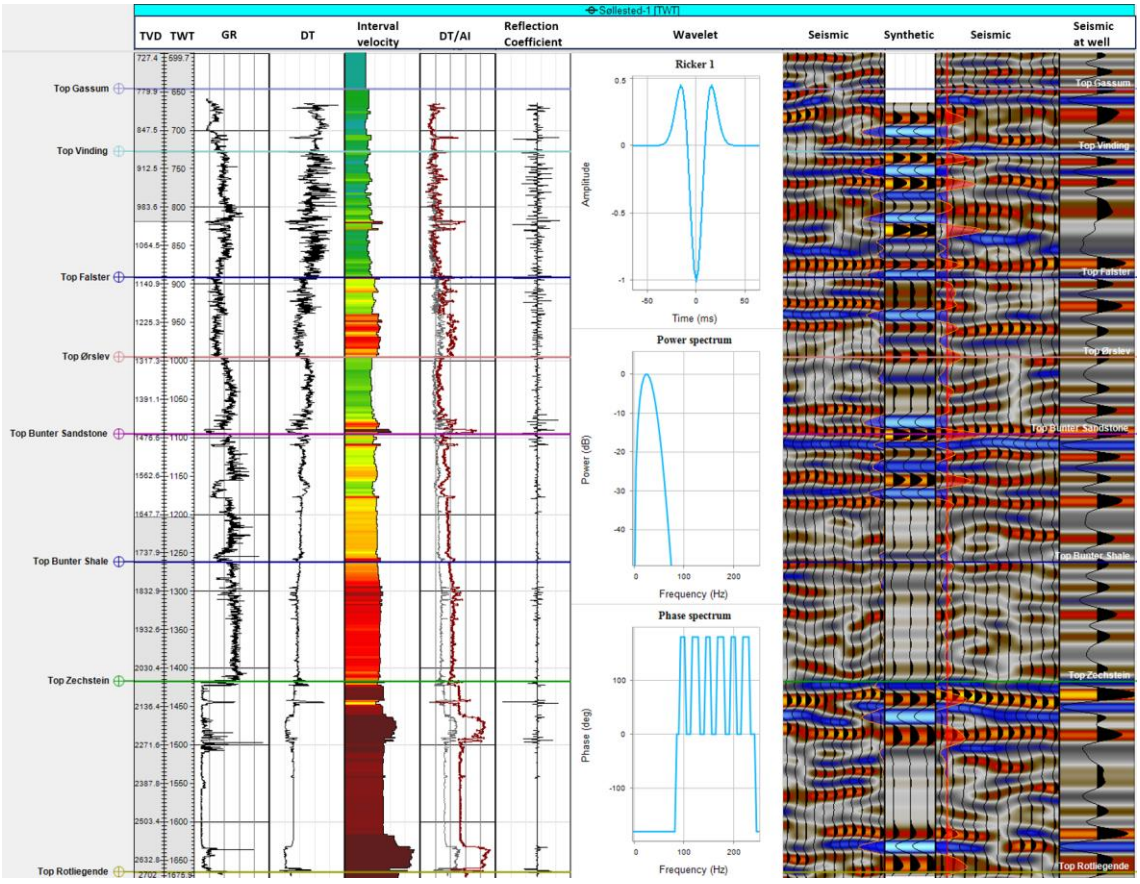

Figure 5.2 *Well to seismic tie of the Søllested-1 well using sonic log and Gartner's equation* ($\rho = 0.30925 * V_p^{0.25}$) *to compute density from sonic, since this log covers a much larger part of the stratigraphy than the density log (Figure 5.1) and helped to improve the Time-Depth Relationship.*

In order to utilize well log data and well tops (depth domain) with seismic data (time domain), a seismic-well tie procedure was performed on the Søllested- 1 well which, unfortunately, is

the only well on Lolland that contain both the sonic and density logs as well as check shots (Fig. 5.1).

However, the logs only cover the deepest part of the well from within the Bunter Shale Fm to the base of the well that terminated in undifferentiated rocks of Rotliegende age. For the seismic well-tie, a synthetic seismogram was produced for the Søllested-1 well using the available density (only available in the deeper section) and sonic logs and compared to seismic data. An analytical Ricker wavelet within the interval between the Bunter Shale Fm and Top Rotliegende (where both the sonic and density logs were recorded) gave a good match, resembling a zero-phased wavelet with reverse polarity, and having several sidelobes due to the noisy seismic data (Fig. 5.1). The well-tie was made by a combination of bulk shifts (initial shift of the Bunter Shale Fm Group reflection), and slight stretching to match the interval below Top Zechstein. The tie was quality controlled by observing reasonable interval velocities for the given lithologies. This resulted in a good correlation between the synthetic seismogram and the seismic data, thereby ensuring correct depths of well log information and well tops. Further improvements of the time-depth relationship were made by using Gartner's equation to compute a density log from the sonic log ($\rho = 0.30925 * V_p^{0.25}$), since the sonic log covered a larger part of the stratigraphy (Fig. 5.2) allowing to tie the shallower successions (Gassum Fm – Bunter Sandstone Fm).

Check shots were available for both Rødby-1 and Rødby-2 wells, which were used as an initial time-depth relationship. The time-depth relationship was adjusted manually by matching defined seismic reflections and corresponding TWT depths, and well tops in the wells.

Based on the well tie, and similarity to the Stenlille and Havnsø areas, the Base Chalk follows a peak due to a significant drop in velocity from the Chalk Group into lower velocity marl and chalk of the underlying Rødby Fm (Gregersen et al. 2022; Gregersen et al. 2023). In the Rødby study area, we similarly define each interpreted horizon in either a peak or a trough seismic reflection (Table 5.1), where e.g., the Base Chalk follows a peak, the Near Top Fjerritslev follows a trough, and the Top Gassum follows a peak reflection etc.

Table 5.1 *The most widespread use of seismic polarity of the seismic data in the study area is SEG reverse (the European–Australian convention), including the new GEUS2023-data from Rødby. On SEG reverse polarity data each horizon has been interpreted in either a peak or a trough seismic reflection, as indicated above.*

#	Seismic horizon	Correlation on SEG reverse polarity	Amplitudes
11	Top Chalk Group	Peak	Positive
10	Base Chalk Group	Peak	Positive
9	Top Fjerritslev Fm	Trough	Negative
8	Top Gassum Fm	Peak	Positive
7	Top Vinding Fm	Peak	Positive
6	Top Oddesund Fm	Peak	Positive
5	Top Falster Fm	Peak	Positive
4	Top Ørslev Fm	Trough	Negative
3	Top Bunter Sandstone Fm	Peak	Positive
2	Top Bunter Shale Fm	Trough	Negative
1	Top Zechstein	Peak	Positive

5.3 Seismic time to depth conversion

A regional velocity model was constructed to convert the interpreted horizons from the time domain to the depth domain. The model area was defined so that the velocity model includes the Søllested-1 well, since here a reasonable time-depth relationship could be established and extends around the Rødby structure with a total model area measuring 28 by 18 km (504 km^2).

Figure 5.3 *Area (28 by 18 km) of the regional velocity model, showing the used three wells, and the RMS migration velocities from the new GEUS2023-ROEDBY-RE2023 2D seismic lines (black lines).*

The data available include: 1) Top Chalk Group depth map from a public Rambøll integrated hydrological model based on Jupiter boreholes[3], since this level is at a too shallow depth to be picked confidently in the seismic data (Fig. 5.4); 2) TWT seismic horizons of the main stratigraphic units, utilizing the legacy 2D lines (listed in Table 4.1.1) and including the new GEUS2023-ROEDBY and GEUS2023-ROEDBY-RE2023 lines), gridded to 250x250m and well-adjusted to the wells; 3) Well top markers; 4) Seismic migration (RMS) velocities from the 2D lines (GEUS2023-ROEDBY-RE2023).

To account for vertical and lateral variations in average velocities found within the stratigraphic units as seen in the well TDRs and the seismic migration velocities, the velocity model was constructed in two steps, followed by depth-conversion of the TWT seismic horizons (Fig. 5.5):

[3] https://gerda.geus.dk/Modeldb/treeviewer?modelid=332

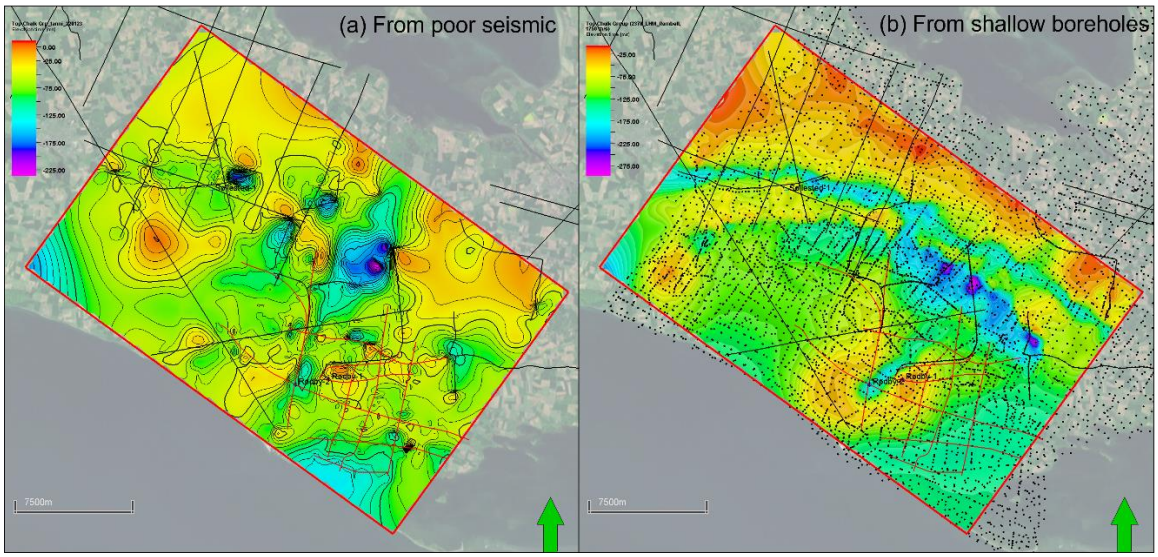

Figure 5.4 *Top Chalk Group (TWT ms); (a) from seismic data where it often difficult or impossible to pick; (b) from a hydrogeological model based on shallow boreholes (dots), time-converted with 1750 m/s. Note the improved definition of the surface and occurrence of buried glacial valleys.*

1. First, a 3D average velocity cube was constructed using kriging with 3D trend (same methodology as used in the Stenlille study (Gregersen et al. 2022)):
    a. The average velocities from the well time-depth relationships in the wells formed the primary data.
    b. Seismic migration velocities from the 2D lines were upscaled into a structural 3D grid (using arithmetic mean), and subsequently extrapolated within each zone using full tension option in Petrel (Spline in Tension algorithm). This formed the 3D trend for the kriging operation.
    c. Data analysis of the upscaled 2D seismic migration data provided azimuth and major/minor ranges information, which were employed in the kriging operation.
2. Second, a multi-layer velocity model was created using the modelled 3D average velocities as velocity input, and 3D horizons and well tops to correct the velocity values to achieve a match between depth-converted horizon and well top.
3. Finally, TWT seismic horizons were depth-converted using the created velocity model.

The workflow was performed within Petrel (2023) by the following steps:

- QC of the input data:
    - Seismic-well-ties; removing outliers in average velocities observed in the TDRs originating from overstretching and squeezing in the seismic-to-well tie procedure. Extracting the TDRs for the three boreholes as a point dataset (MD, TWT, Average velocity).
    - Adjusting the TWT seismic horizons to well markers since seismic peaks or troughs not necessarily coincide with the well tops, in order to get a good TWT to MD fit of main stratigraphic units (Fig. 5.2); checking TWT thicknesses for bullseyes originating from horizon mis-picks or extrapolation, smoothening anomalies.

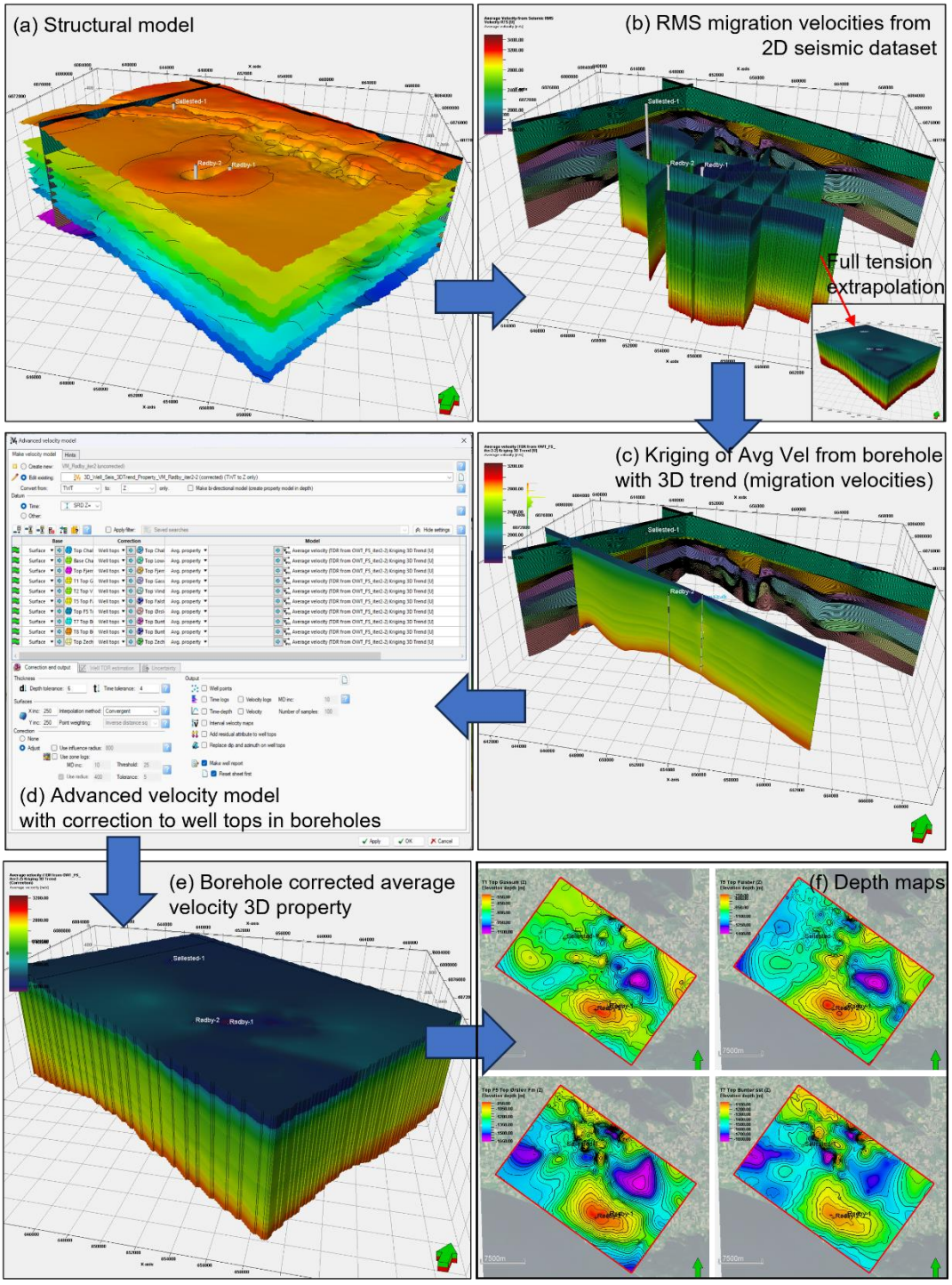

Figure 5.5 *(A) 3D perspective of the 10 horizons considered in the velocity model, which define the structural grid (250x250xc.10ms). The Rødby structure is located on the southeastern side where also the Rødby wells are indicated that were used to constrain the velocities. (B) The structural grid is indicated by the sections (0–1931 ms TWT), and the upscaled 2D average seismic migration velocities are shown (purple: 1500 m/s to red: 3250 m/s). (C) The data are interpolated within the grid using a full tension algorithm (Spline in Tension) and smoothened 10x to remove outliers where the 2D intersect. (D) An advanced velocity model is set up using the 10 horizons and associated well tops for correction. (E) Velocities are adjusted to find a match between depth-converted horizon and well tops. (F) This cube is then used to depth-convert the TWT horizons. (depth=average velocity*(surface TWT)/2).*

    - Time-convert the Top Chalk Group depth map from the hydrological model using an average velocity of 1750 m/s for the overlying succession. Adjusted the map at Rødby-2 where clearly a buried valley is observed in seismic and in the well (Fig. 5.4).
- Defining a 3D modelling grid (250x250m) based on the QC-ed TWT horizons using the Petrel structural modelling tool:
    - Model zonation according to the following horizons: MSL (0 ms), Top Chalk Gr, Base Chalk Gr, Top Fjerritslev Fm, Top Gassum Fm, Top Vinding Fm, Top Falster Fm, Top Ørslev Fm, Top Bunter Sandstone Fm, Top Bunter Shale Fm, Top Zechstein Gr (Fig. 5.5A).
    - Vertical layering was defined such that layer thickness is between 10 – 20 ms, with higher resolutions where large velocity changes occur (e.g. between Base Chalk Gp and the Lower Cretaceous strata).
- Defining a 3D average velocity property using kriging with the Petrel Petrophysical Modelling tool:
    - Average velocities from the Time-Depth Relationships in the three wells were upscaled into the 3D grid, which were used as primary data for kriging.
    - With a Petrel workflow the 2D seismic migration velocities from all profiles in the GEUS2023-ROEDBY-RE2023 dataset were sampled as a point cloud, which then were upscaled into the 3D grid. Data analysis on these upscaled cells helped to find azimuth and variogram ranges within the data, to steer the kriging operation.
    - These seismic derived upscaled cells were then extrapolated into the entire 3D grid using the full tension option in the property operations (Spline in Tension) (Fig. 5.5B, inset). We also tried the minimum curvature method, but since it maintains a gradient over long distances, it can lead to geologically unrealistic low or high velocity values. This is especially the case with sparse data points as we have in our dataset. In contrast, full tension extrapolation tends to flatten values and appears more realistic. This extrapolated volume forms the 3D trend for the kriging operation.
    - Kriging with 3D trend, using average velocity in the boreholes as primary data and seismic-derived 3D average velocity property as 3D trend (Fig. 5.5C). Azimuth and variogram ranges for each zone came from Data Analysis.
- Create an “advanced velocity model” using the same 3D seismic horizons (tied in TWT to boreholes from seismic-well-tie Time-Depth Relationship), well tops for calibration, and 3D average velocity grid from previous step as velocity model (Fig. 5.5D).
    - Without applied correction, the average depth residual was in the order of 1 – 10 m, since velocities at the boreholes are steered by the TDRs which are included in the 3D property. Away from the structures, the velocities are much more uncertain, and thus a 10% depth error is a conservative estimate.
    - The final velocity model used the well tops (“global correction”) to improve to depth-converted horizons by adjusting the velocities (Fig. 5.5E).
- Depth-convert the TWT horizons using the constructed velocity model (Fig. 5.5F).
- The velocity model is called: 3D_Well_Seis_3DTrend_Property_VM_Rødby_iter2-2 (corrected).

5.4 Investigation of reservoir and seal (see more in Chapter 7)

The geology of the reservoir and seal successions are described using well completion reports, publications, and in-house studies of well-logs and geological well samples mainly from cores. In addition, a limited number of studies focusing on lithology and biostratigraphy are available. The data used are from the wells closest to the Rødby structure. The aim of these studies is to provide a more detailed understanding of reservoir and seal characteristics (see Chapter 7).

The reservoir characteristics presented and discussed in Chapter 7 are derived mainly from the acquired wireline logs from wells on Lolland and Falster, that are calibrated against conventional core analysis, descriptions of cuttings and sidewall cores. Potential reservoir units were identified from wireline logs by low formation resistivity, characteristic neutron-density log responses, pattern of the spontaneous potential log, and low natural radioactivity as recorded by the GR log and documented by cuttings containing sand-sized quartz grains.

In petrophysical terms, a sandstone reservoir is herein defined as a rock having < 50% volume of shale, and an effective porosity (PHIE) of > 10%. The permeability is estimated using published relationships between porosity and permeability, which is based on conventional core measurements.

Seal lithology, thickness and grain-sizes were similarly evaluated based on petrophysical logs, ditch cuttings samples and cores. Sections that may act as seals were identified from wireline logs by several methods based on the availability of logs in the Rødby-1 and-2 wells.

5.5 Methods – Storage Capacity Assessment (see more in Chapter 8)

To be able to compare the potential CO_2 storage structures GEUS uses a simple widely accepted equation for saline aquifers (e.g. Goodman et.al., 2011). The static theoretical storage capacity of reservoir units with buoyant trapping is estimated from:

$$SC = GRV * N/G * \varphi * \rho_{CO2R} * S_{Eff}$$

where:

SC Storage Capacity or Mass of CO_2 (MT).

GRV Gross Rock Volume is confined within the upper and lower boundary of the gross reservoir interval (t) and above of the deepest closing contour from where spillage from the trap will occur. To get a representative GRV the lower boundary may be moved to a position closer to the upper boundary so expected the gross reservoir interval in the structure represents the surrounding wells. This will give a more correct estimation of the GRV.

N/G Average net to gross reservoir ratio of aquifer across the entire trap (GRV).

ϕ Average effective reservoir porosity of aquifer within trap (GRV).

ρ_{CO2R} Average CO_2 density at reservoir conditions across all of trap.

S_{Eff} Storage efficiency factor relates to the fraction of the available pore volume that will

store CO_2 within the trap (GRV). This fraction depends on the size of storage domain, heterogeneity of formation, compartmentalization, permeability, porosity, and compressibility, but is also strongly influenced by different well designs and injection schemes (e.g. *Wang et al. 2013*).

Evaluation and estimation of the CO_2 storage capacity (SC) in deep saline aquifers is complex and accurate estimations of storage capacity are only practical at local site-specific scales. CO_2 storage capacity estimations is furthermore difficult due to lack of knowledge on the efficiency factor that reduce the storage capacity from a theoretical to a more realistic estimation (i.e. the introduction of a storage efficiency factor, S_{Eff}).

More precise CO_2 storage capacity estimations are related to communication of fluids within the reservoir and the degree of pressurization during injection. Pressurization must not induce fracturing and depends on relation between pore pressure and volume increase, and compressibility of the rock and the fluids in the reservoir.

Injection and storage of CO2 in deep saline formations requires estimates of fluid pressures that will not induce fracturing or create fault permeability that can lead the CO2 to escape from the reservoir. To ensure this, identification of faults and analyses of fault stability are necessary and requires precise evaluation of e.g. fault orientations, pore fluid pressure distribution and in-situ stresses at the storage site. Changes in injection rates induce stress can changes formation pressures and CO2 storage volumes, why determination of in situ stresses and modelling of fault stability are essential for the safe CO2 injection and detailed modelling of storage capacity.

In open aquifers, as assumed here, the reservoir pressure is expected to stay constant during CO_2 injection, as the water will be pushed beyond the boundaries. The calculated stored CO_2 is the amount injected until it reaches the boundaries (e.g. 'lowermost closed contour'). The estimations assume a static approach where the pores in the trap is expected to be 100% connected. However, it does not include dynamic pressure build-up and movement of CO_2 and in-place brine(water) in the saline aquifer, neither in-side nor out-side the trap. Furthermore, it does not regard the solubility of CO_2 in water, where more than 10% can normally be dissolved in the water, and the presence of salt causing scales inside the storage reservoir reducing the efficiency of CO_2 injection.

A dynamic reservoir simulation will take these factors into account and will obviously produce different storage capacity results, depending on the selected parameters. A more realistic dynamic simulation of the potential storage capacity is normally carried out by the awarded license holders and operators. Dynamic reservoir simulations should be used for local-scale CO_2 storage reserves estimates and should also consider operational and regulatory factors.

The CO_2 storage efficiency factor (S_{Eff}) was first introduced in 2007 in regional-scale assessments of storage capacity in the United States and Europe. The efficiency of CO_2 storage is regarded as a combination of factors, and many published papers show values from <1% to more than 20%, emphasizing that no single value or set of values can universally be used. Regional storage efficiency values are estimated to be 1–4 % (e.g. CO_2 Storage Atlas of the US and Canada 2008), while trap specific storage efficiency have values around ~4–18% for clastic sediments (*Gorecki et.al., 2009*); ~3–10% (*US-DOE; Goodman et.al., 2011*) and ~5–20% for traps in German North Sea area (*BGR, 2023 on-going project*).

The storage efficiency factor represents the fraction of the total available pore volume of the saline aquifer that will be occupied by the injected CO_2 in the trap volume (e.g. the GRV) and is regarded as the fraction of stored CO_2 relative to the pore volume, - and has both a space

and time dependency. It depends primarily on the relationship between the vertical and horizontal permeability, where a low vertical to horizontal permeability ratio will lateral distribute the CO_2 better over the reservoir than a high ratio, why a internally layered reservoir with alternating sandstones and impermeable or poorly permeable claystones acting as seals may have an advance. Other use of the storage efficiency factor may also include the size of the storage domain, heterogeneity of the formation, compartmentalization, porosity, permeability, pressure, temperature, salinity, and compressibility, but are also influenced by number of injection wells, design and injection strategy.

The Stenlille is the best-known case in the Danish onshore area. A maximum storage efficiency factor of 40% for a 4-way dip-closure has previously been estimated and was used for the geologically excellent and well described Gassum Fm sandstone reservoir. Furthermore, the Stenlille structure has been used for natural gas storage for many years and consists of high-permeable sandstone layers with no faults offsetting the reservoir and overlying seal. Thus, for comparison reasons GEUS uses storage efficiencies of 40% in the Stenlille structure and 10% in all other potential structures. This also includes structures where the primary reservoir is not the Gassum Fm but e.g. the deeper situated Bunter Sandstone Fm. All other potential storage structures are expected to have lower storage efficiency values reaching more realistic values from 5 to 10% in structures with no well data and only minor faults offsetting the reservoirs/seals.

Storage capacity calculations are biased by imperfect seismic and reservoir data, depth conversion, reservoir thickness estimates, CO_2 density. To address the uncertainties ranges input parameters have been chosen to reflect each parameter uncertainty, and the distribution has been modelled utilizing a simple Monte Carlo simulation in-house tool. To achieve stable and adequate statistical representation of both input distribution and result output, 10.000 trials are calculated for each simulation. This methodology is simplistic and does not incorporate e.g., correlations of input parameters. However, for the purpose of initial estimation of volumes and CO_2 storage capacities, the methodology is considered relevant and adequate. The method is used for the

6. Results of seismic and well-tie interpretation

6.1 Stratigraphy of the structure

The interpreted seismic stratigraphic horizons with well-ties document the local stratigraphy of the Rødby structure and the key ties between seismic stratigraphy and the regional lithostratigraphy is shown in Figure 6.1.1. Eleven regional seismic stratigraphic horizons ('horizons') have been interpreted for the study area and are from the deepest to the shallowest: (1) Top Zechstein, (2) Top Bunter Shale (Sh.) Fm, (3) Top Bunter Sandstone (Sst.) Fm, (4) Top Ørslev Fm, (5) Top Falster Fm, (6) Top Oddesund Fm, (7) Top Vinding Fm, (8) Top Gassum Fm, (9) Near Top Fjerritslev Fm, (10) Base Chalk Group, and (11) Top Chalk Group (Figs 6.1.1−6.1.8).

The horizons are essentially interpreted as sequence stratigraphic (approximately chronostratigraphic) boundaries, which are traced in a certain reflection (here a trough or a peak, Table 5.1). In most cases, on a local scale, the seismic horizons occur close to formation boundaries as defined in the wells. Thus, the seismic horizons are here named after the approximate formation boundaries. More regionally, it may be considered to use lithostratigraphic independent naming such as letters or ages, as on a regional scale, some of the lithostratigraphic units are diachronous. However, here in this local area, the naming serves to directly relate mapped horizons and formations defined by well data and thus to describe key reservoir-seal pairs.

In addition, deeper and older horizons are interpreted in the Rødby area, e.g. the near Top basement and Top pre-Zechstein horizons that can be tied to Top Rotliegende in Søllested-1 well. The transition from the deepest sedimentary rocks and the crystalline basement is characterized by several large fault blocks, (Fig. 6.1.2.). The Slagelse-1well is the closest located deep well, which provides some insight to the oldest tectonostratigraphic evolution with a TD in Cambrian rocks. However, the Slagelse-1 is located on Zealand c. 130 km NE of the study area and is structurally separated from the Rødby area by the uplifted basement in Møn High, which forms the eastern part of the Ringkøbing–Fyn High. The Slagelse-1 well section provides ties to the deeper horizons, such as basal Palaeozoic (Cambrian) near above Top Basement, and Top Lower Palaeozoic (Schovsbo, 2011; Gregersen et al. 2023).

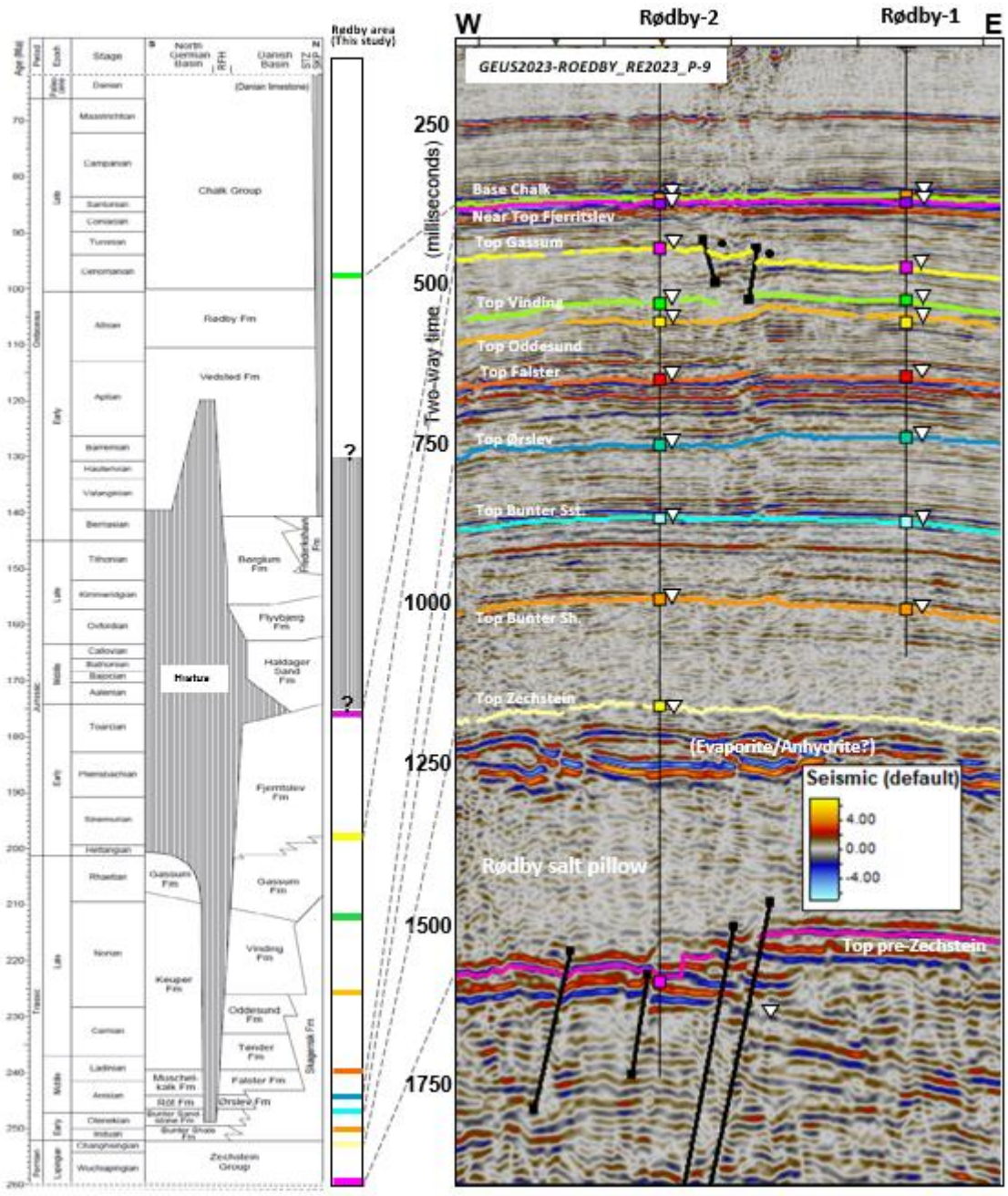

Figure 6.1.1. *Lithostratigraphy and seismic horizons with well-ties at the Rødby-2 and Rødby-1 wells in the northern part of the North German Basin, south of the elevated basement high in the Ringkøbing–Fyn High (RFH). The lithostratigraphic scheme, based on Bertelsen (1980) and Nielsen (2003), summarizes the general stratigraphy from the North German Basin in the south to the Norwegian–Danish Basin in the north. Most of the formations in the area south of the RFH are comparable to the Rødby region apart from the lacking M.+U. Jurassic formations. Colored seismic stratigraphic horizons are shown at the stratigraphic position in the separate stratigraphic column (this study), and in a seismic profile in two-way time (GEUS2023-ROEDBY_RE2023_P-9 of the 2023 reprocessing – se Chapter 4 for location of the survey). The profile shows correlation to the Rødby-2 well with well-tops (triangles, centers). Dashed horizontal lines at the top and base of the scheme (left) indicate omitted younger Cenozoic/Quaternary successions, and pre-Zechstein successions, respectively due to space limitation.*

6.1.1 Faulting

North of the Rødby structure, a set of deep-seated NW–SE striking faults occur in the Lolland–Falster Fault Zone with main offsets affecting the Triassic succession (see maps at Fig. 6.1.4 and 6.2.1–6.2.2). In places, the fault zone appears as a large flower structure (see Fig. 6.1.2 - 6.1.3) and can be followed for more than 30 km in the study area with a width of c. 5–10 km, that widens and branches out further to the west. Inside the fault zone, the structural features are mainly characterized by internal fault and fold architecture with a doming of the Triassic layers due to underlying salt pillow growth. The large faults with most significant throws occur in the Triassic–Jurassic successions and are most likely related to salt movements. The bounding fault planes of the zone are characterized by synthetic and antithetic faults, either dipping to the south or north. In some places, the major S-dipping fault planes also penetrates the Zechstein and offsets the Top pre-Zechstein before soling out into the crystalline basement indicative of additional deep-seated faults: The initiation of salt movements may thus have been affected by reactivation of older structural weakness zones in the crystalline basement (see profile SSL6267_LFN_digitized-by-geus_disp26631, Fig. 6.1.3 and Fig. 6.1.6).

However, seen from a CO_2 storage perspective it is important to note that the Lolland–Falster Fault Zone is located to the north of and c. 5–10 km away from the top of the Rødby structure (Fig. 6.1.3), where the fault zone is in a more down-dip position to the apex of the closure. The fault zone occurs outside the lowermost closure of the Top Bunter Sandstone Fm reservoir and extends parallel to the northern flank of the Rødby structure. Hence, the Lolland–Falster Fault zone most likely have very little impact on the potential storage capacity of the Rødby structure under the pre-caution that the structure is not filled to spill point with CO_2.

A minor set of WNW–ESE striking synthetic and antithetic faults associated with a N-dipping main fault are observed locally on top of the Rødby structure itself, *the Rødby Structure Fault Zone.* These faults can be mapped and traced from the old seismic profile WGC79A-7925 to the new GEUS2023-ROEDBY_P10_RE2023 and GEUS2023-ROEDBY_P2_RE2023. Here, a set of minor synthetic and antithetic faults are observed near the apex of the structure above the salt anticline less than 1 km north of the Rødby-2 and Rødby-1 wells (Fig. 6.1.2 and 6.1.7). The lateral extension of these faults is rather limited as the minor fault zone lingers off in the direction of closest seismic line WGC81C-8108, which is located less than 2 km to the west. The synthetic and antithetic faults offsets and extends from the Top Gassum level at 416 ms TWT and down to below the Top Bunter Sandstone Fm at 900 ms TWT. However, the throw at the Top Bunter Sandstone Fm level is very modest, <10 ms. This fault zone has only been observed on three profiles, which makes it difficult to classify as a high potential risk to CO_2 storage without better seismic data coverage. Therefore, additional supplementary seismic data, preferably a 3D seismic survey, is recommended to evaluate any potential risks associated with this minor antithetic fault zone, and for a more detailed interpretation.

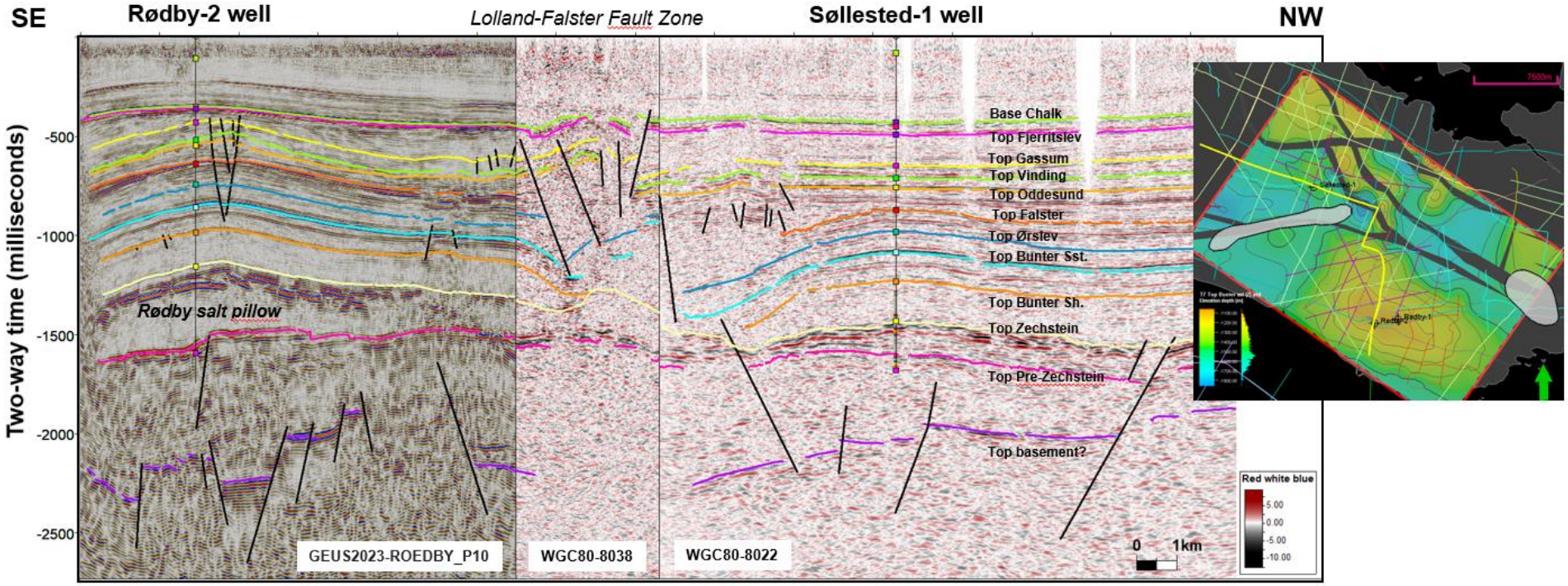

Figure 6.1.2. *Key reference profile with seismic well-ties from the Søllested-1 well to the Rødby-2 well along the composite profile along WGC80-8022, WGC80-8038 and GEUS2023-ROEDBY_P10. The Rødby structure is situated above the Rødby salt pillow and separated from a smaller salt pillow near the Søllested-1 well by a major NW–SE trending fault zone, i.e. the Lolland–Falster Fault Zone. Deep-seated basement structures are observed below the Top pre-Zechstein marker horizon. The Søllested-1 well has TD in the Top Rotliegende. Map to the right shows the location of the reference profile (yellow line) on top of the TWT map of the Top Bunter Sandstone Fm marker horizon including major salt structures (i.e. salt wall).*

6.1.2 Key horizons

The following key horizons for the Rødby structure were released and published as two-way travel time (TWT) grids: Top Bunter Shale Fm, Top Bunter Sandstone Fm, and Top Ørslev Fm. This data release was part of the GEUS presentation of the seismic acquisition and status of data processing programme on November 23, 2023, for the group of interested peers following GEUS' seismic reference as part of the preparation for the license application round announced by the Danish Energy Agency on December 11, 2023. These TWT grids are part of the present report and can be accessed via the GEUS website.

The Top Chalk horizon (Fig. 6.1.4) is mainly used for definition/construction of the Chalk Group isochore map used for time to depth conversion. However, it is challenging to map the Top Chalk towards the base of Quaternary on the legacy 2D seismic data alone. Therefore, the Top Chalk marker horizon is mainly based on input from from shallow seismic data, TEM surveys and hydrogeological wells (cf. Jørgensen et al., 2003; 2012). Several glacial valley structures, today preserved as buried valleys, were carved into the surface of the Top Chalk Group on Lolland by the Pleistocene ice. The valleys are most likely glacial related (e.g. tunnel valleys), but seems to follow the orientation of the older, deep-seated NW-SE striking Lolland-Falster Fault Zone, possibly forming weakening zones (Fig. 6.1.4).

The remaining nine horizons constitute the key stratigraphic framework in the present description of the Rødby structure throughout the study area from the 2D seismic data with well-ties as mentioned above. Horizons from Top Bunter Shale Fm and shallower can be correlated to the Søllested-1, Rødby-1 and Rødby-2 wells (Fig. 6.1.1, 6.1.3).

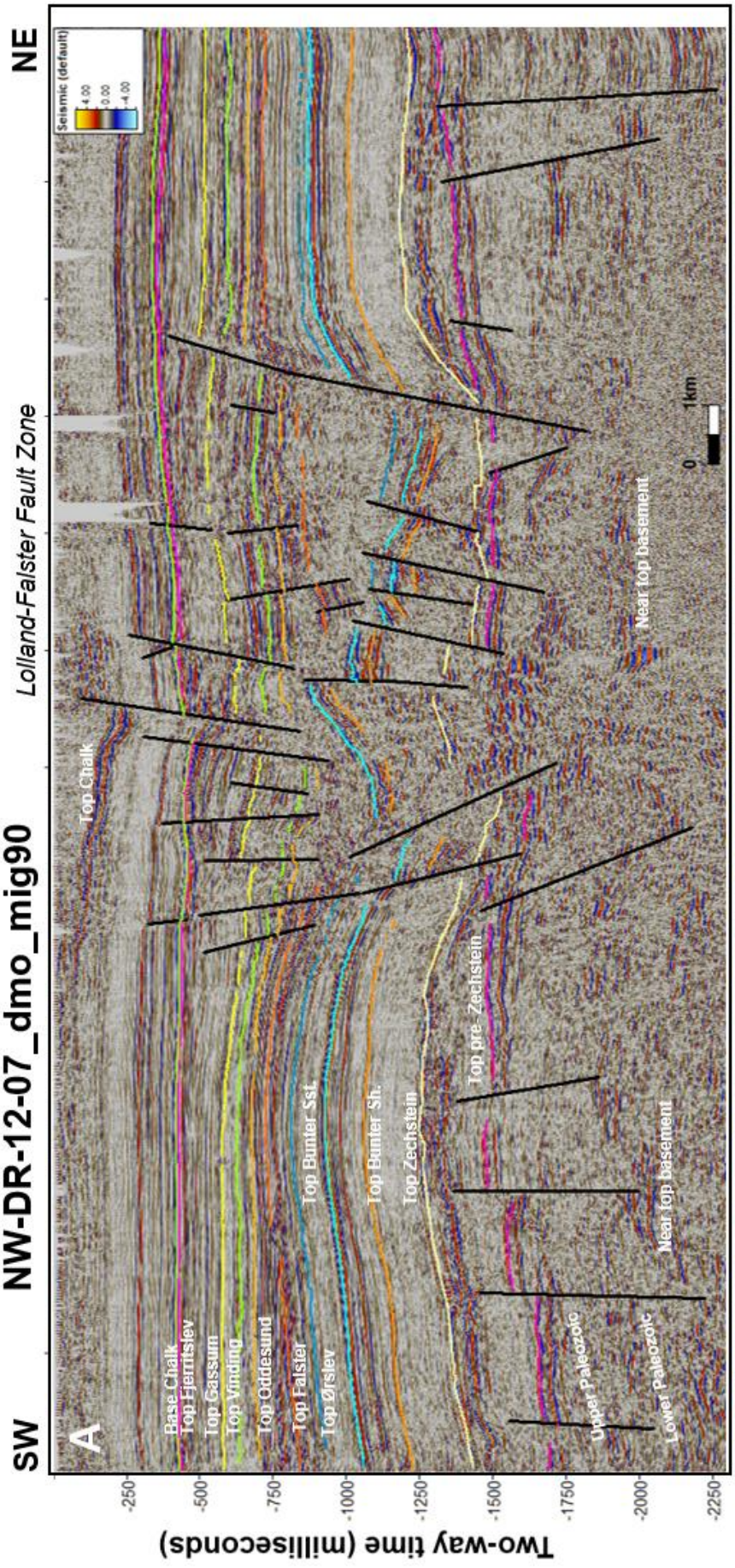
SW
NW-DR-12-07_dmo_mig90
Lolland-Falster Fault Zone
NE
A
Seismic (default)
4.00
0.00
-4.00
Top Chalk
Base Chalk
Top Fjerritslev
Top Gassum
Top Vinding
Top Oddesund
Top Falster
Top Ørslev
Top Bunter Sst.
Top Bunter Sh.
Top Zechstein
Top pre-Zechstein
Upper Paleozoic
Lower Paleozoic
Near top basement
Near top basement
0
1km
Two-way time (milliseconds)
-250
-500
-750
-1000
-1250
-1500
-1750
-2000
-2250

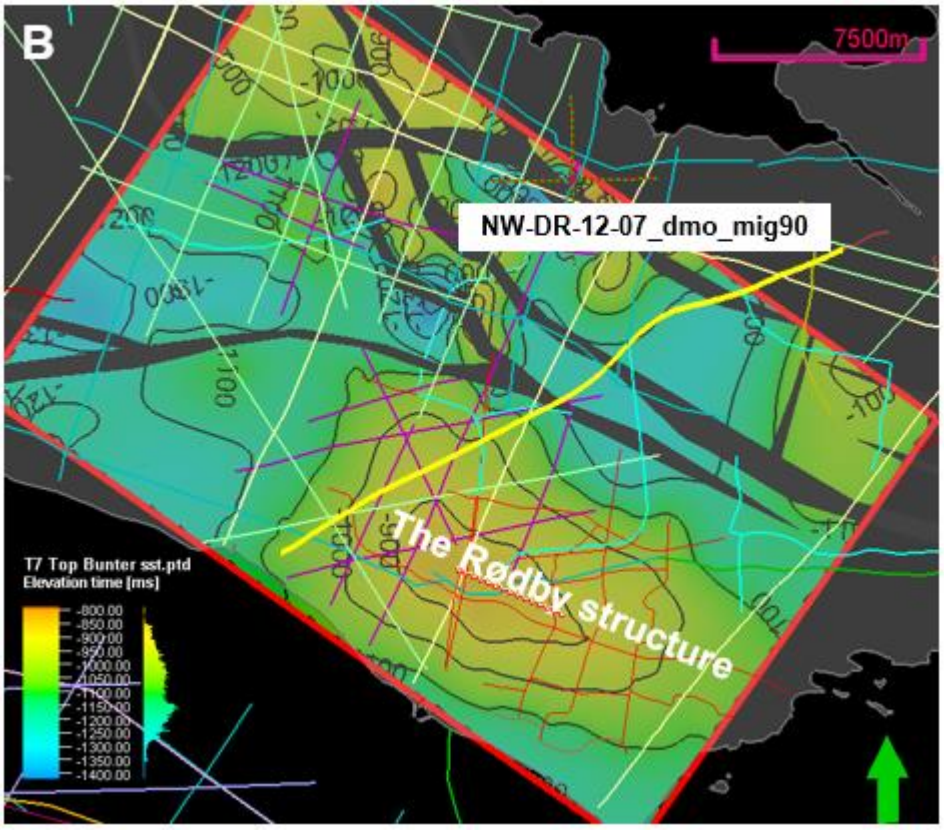

Figure 6.1.3. A: *The NE–SW striking profile, NW-DR-12-07_dmo_mig90 from 2012, depicting the mapped regional seismic stratigraphic marker horizons. The profile is located on the NW flank of the Rødby structure crossing the major deep-seated NW–SE striking Lolland-Falster Fault Zone, that mainly affects the Triassic and deeper successions. The synthetic and antithetic faults also cut the Zechstein and offsets the Top pre-Zechstein before soling out into the deeper Paleozoic succession overlying the seismic basement. B: Location of profile NW-DR-12-07_dmo_mig90 from 2012 is shown by the thick yellow line overlying the mapped structural TWT-map of the Bunter Sandstone Fm horizon and on Fig. 6.1.4.*

A majority of the older 2D seismic lines are of European SEG reverse polarity, where a peak is a soft kick with downward decreasing acoustic impedance (AI), such as the Base Chalk seismic reflection. A synthetic seismogram has been produced to tie the Søllested-1 well to seismic reflections to support the interpretation of the deeper horizons (Fig. 5.1), where the strong peak at c. 1430 ms TWT corresponds to a significant increase in velocity from the shales of the Bunter Shale Fm to the evaporites (halite and anhydrite) in the Zechstein interval defining the Top Zechstein horizon. For the study, we used mostly coloured profiles displayed in red-white-blue (red peaks and blue troughs) or black-grey-white (black peaks and white troughs) (Fig. 6.1.1–6.1.7).

We define here each interpreted horizon in either a peak or a trough seismic reflection (note the reverse polarity), where e.g., the Base Chalk follows a peak, the Near Top Fjerritslev follows a trough, and the Top Gassum follows a peak reflection etc. (Table 5.1 and Fig. 6.1.1–6.1.7).

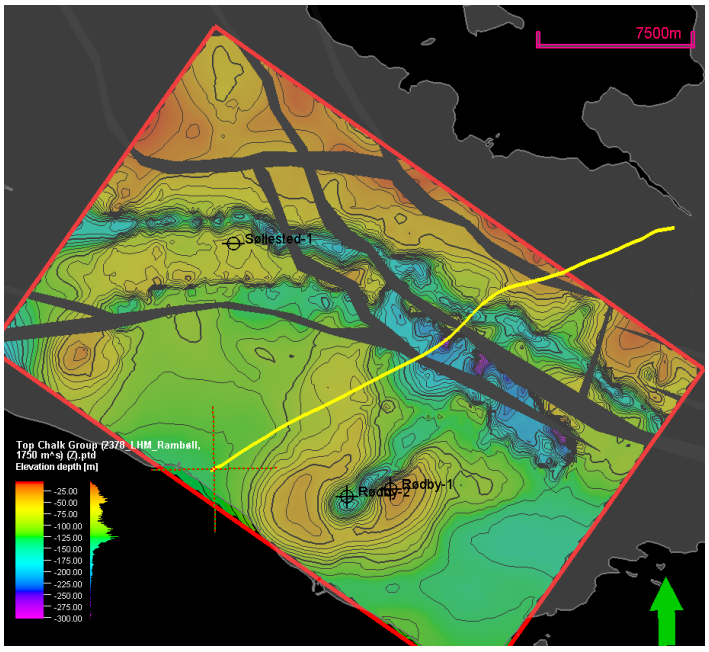

Figure 6.1.4. *The location of the NW-DR-12-07_dmo_mig90 profile displayed on the depth map (m) from Rambøll's hydrological model (cf. Jørgensen et al., 2003; 2012) for Lolland showing the main outline of the buried tunnel valley systems carved into the Top Chalk surface by the Pleistocene ice (indicated by bluish colors). The buried tunnel valley system has an orientation similar to the deep-seated NW-SE striking Lolland-Falster Fault Zone shown by the black fault polygons, which could indicate a possible link between re-activation and/or weakening zones of deeper older structural elements and areas susceptible for glacial erosion. The yellow line shows the position of the NE–SW striking profile, NW-DR-12-07_dmo_mig90, shown in Fig. 6.1.3.*

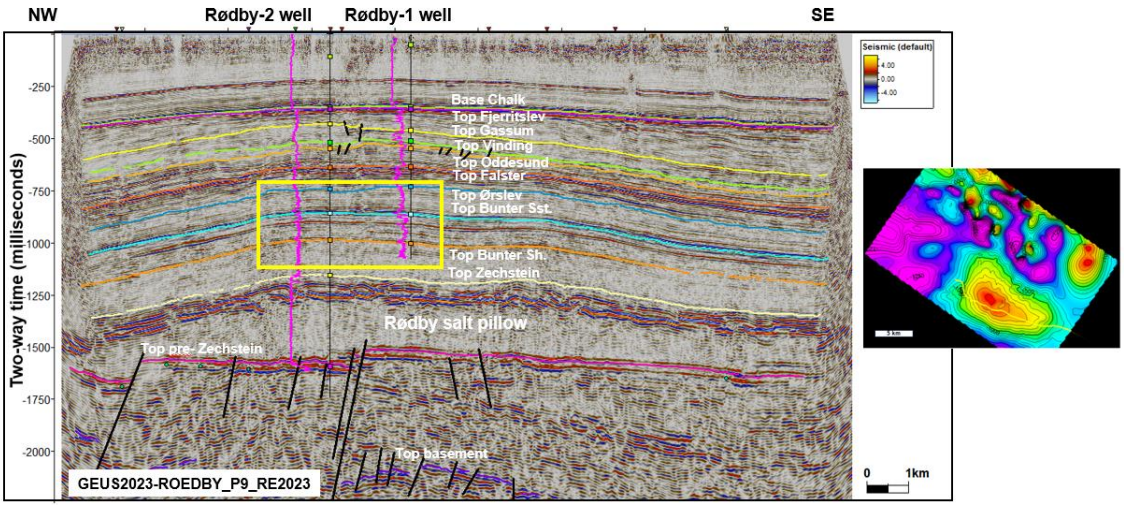

Figure 6.1.5. *Seismic key reference profile along the NW–SE striking GEUS2023-ROEDBY_P9_RE2023 across the Rødby structure intersecting both the Rødby-1 and-2 wells (overlain by the GR-log in pink). Yellow box indicates area of close-up shown in Fig. 6.1.8.*

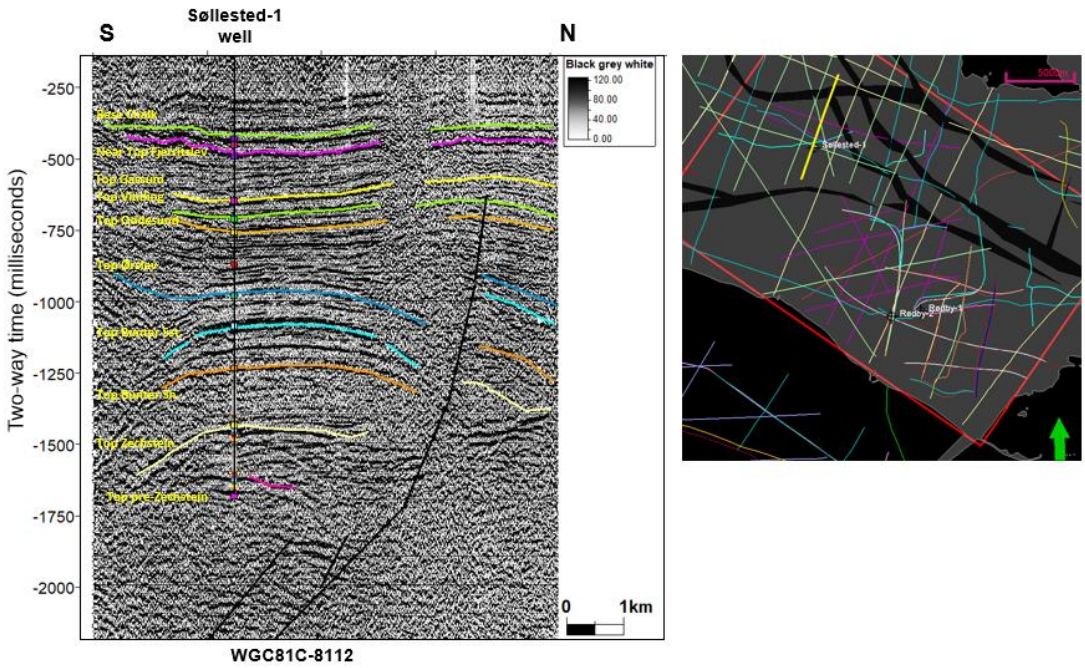

Fig 6.1.6 *To the left, the N–S striking WGC81C-8112 profile near the Søllested-1 well illustrates well the deep-seated nature of the bounding faults of the NW–SE striking Lolland-Falster Fault Zone. Deep-seated structures are observed below the Top pre-Zechstein (Top Rotliegende) marker horizon. The Søllested-1 well penetrates the Top pre-Zechstein horizon. The map shows the location of the profile (yellow line) and the dark black polygons of the fault zone.*

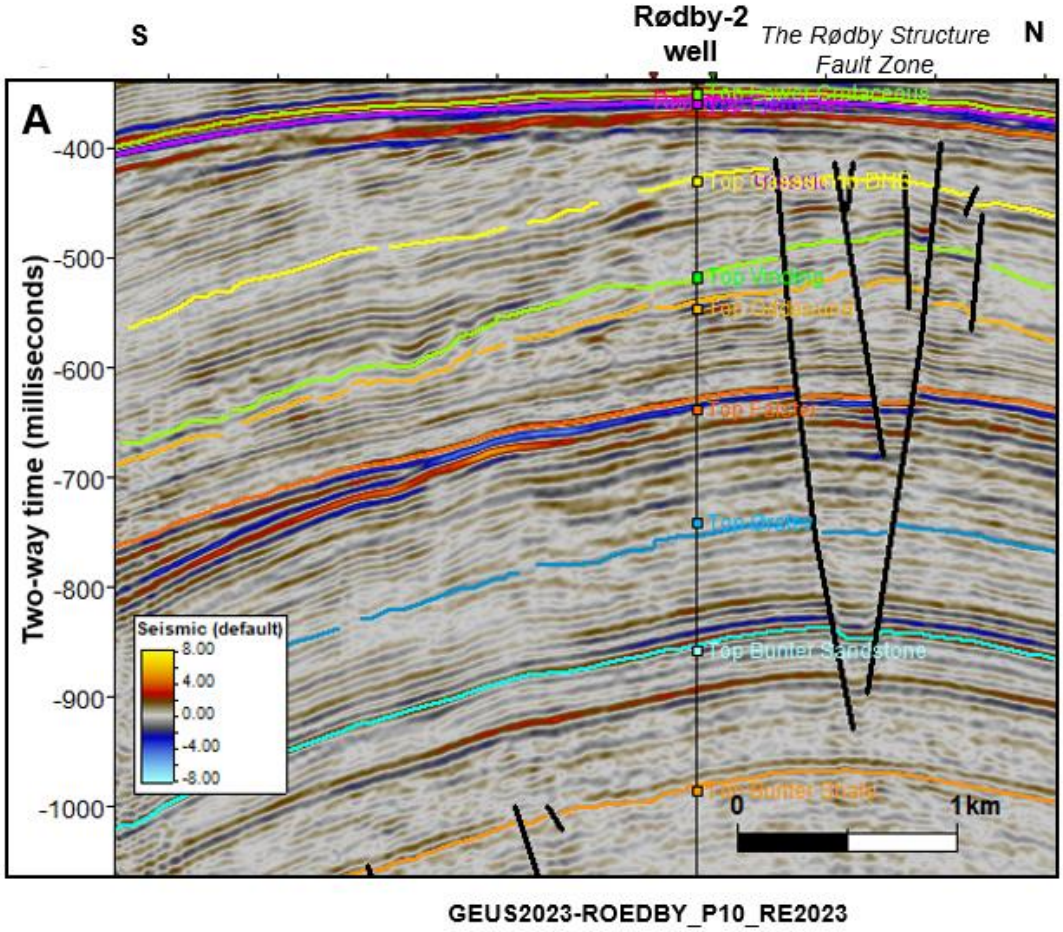

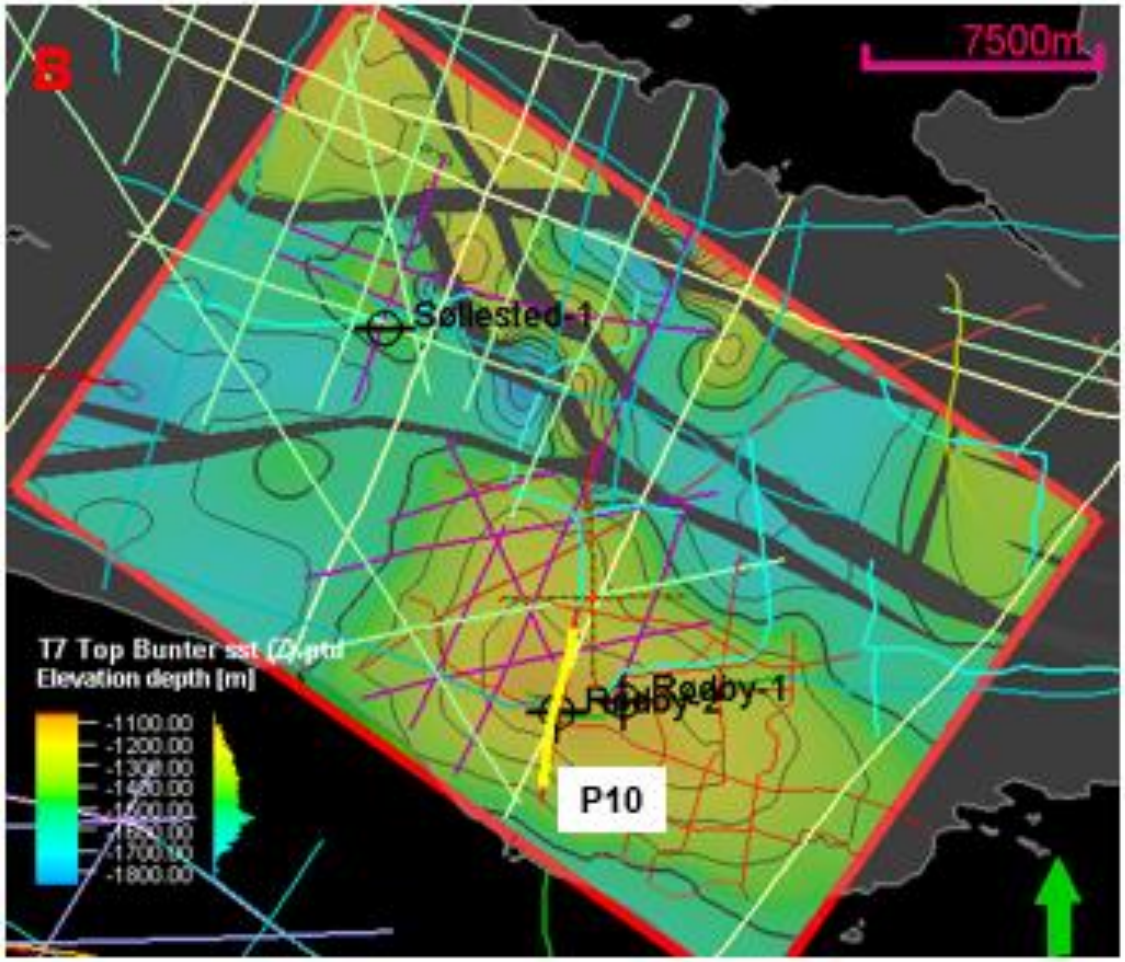

Fig 6.1.7 A: *The central part of the N–S striking GEUS2023-ROEDBY_P10_RE2023 profile images the Rødby Structure Fault Zone near the top of the Rødby structure with intra-Triassic offsets affecting successions from the Top Gassum horizon (yellow) to well below the Top Bunter Sandstone Fm horizon (turquoise) with minor throws (<10 ms at the Top Bunter Sandstone Fm level). This minor fault zone has been observed on three seismic profile which makes it difficult to evaluate the potential risk it may pose to future CO_2 storage. Therefore, new additional seismic data is recommended to supplement the present data to fully evaluate potential risks associated with this minor fault zone. Also, please note the wedge of onlapping reflectors at c. 800 ms TWT observed at the southern flank of the structure at near top Falster Fm level, that most likely indicate the presence of an intra-Triassic hiatus that developed due to salt growth. B: Location of the illustrated GEUS2023-ROEDBY_P10_RE2023 profile on top of the Top Bunter Sandstone Fm depth structure map.*

6.1.3 Internal reflectivity of the Bunter Sandstone Fm interval

The main reservoir in the Rødby area is the Bunter Sandstone Fm interval and its top is characterized by a continuous seismic horizon, that can be correlated over the entire area (peak in Figs. 6.1.5, 6.1.7, 6.1.8 and 6.1.9). The Bunter Sandstone Fm interval has a homogeneous TWT thickness of 120–160 ms corresponding to c. 228–256 m drilled in Rødby-2 and Rødby-1 wells, and up to 291 m in the Søllested-1 well, which is located above a different salt structure separated from the Rødby structure by the Lolland-Falster Fault Zone.

The internal reflectivity of the Bunter Sandstone Fm reservoir interval is characterized by three internal parallel peaks, which can be correlated over a larger area, that divides the interval into at least three parallel units A, B and C (Fig. 6.1.8), that can be related to members (see section 7.1).

The base of the reservoir interval, outlined by the Top Bunter Shale Fm, is characterized by a slightly weaker seismic horizon and represent an increase in acoustic impedance due to the transition from sandstones to shales with higher seismic velocities of the Bunter Shale Fm (trough in Figs. 6.1.5, 6.1.7 and 6.1.8). The stratigraphic subdivision of the Bunter Sandstone Formation, depositional environment and the reservoir characteristics are discussed in greater detail in section 7.1.

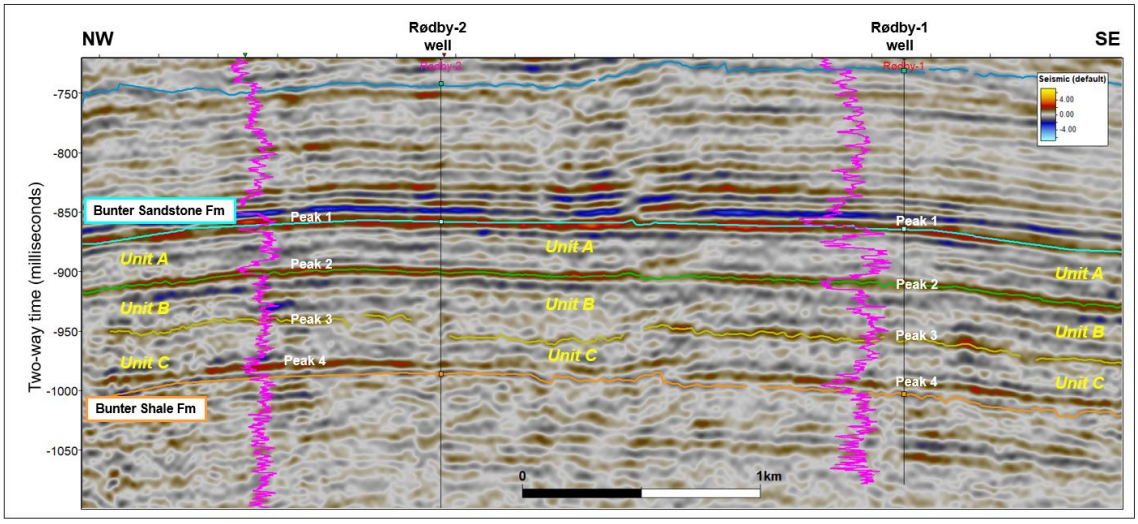

Fig 6.1.8 *The NW–SE striking GEUS2023-ROEDBY_P9_RE2023 key reference profile through both Rødby-2 and Rødby-1 wells illustrates the internal reflectivity of the Bunter Sandstone Fm interval consisting of three parallel units (A, B & C) separated by sub-parallel internal reflectors.*

6.2 Structure description and tectonostratigraphic evolution

The seismic stratigraphic interpretation is tied to well-tops in the Rødby-1, -2, and Søllested-1 wells and extended further into the 2D seismic lines as described in Section 6.1.

6.2.1 Structural maps of the Rødby structure

Structural maps in two-way time have been generated from horizons by gridding and smoothing (parameters - see each map figure). Figure 6.2.1 shows e.g., the depth-structure maps in milliseconds (ms) two-way time (twt) below mean sea level for all horizons, including the top and base of the Bunter Sandstone Fm reservoir and the top of the Ørslev Fm that constitutes the primary seal.

Figure 6.2.2 shows the depth converted maps in meters below mean sea level of all horizons from shallow to deep; A: Top Chalk; B: Base Chalk; C: Top Fjerritslev; D: Top Gassum; E: Top Vinding; F: Top Oddesund; G: Top Falster; H: Top Ørslev; I: Top Bunter Sandstone; J: Top Bunter Shale; K: Top Zechstein.

Figure 6.2.3 shows three key thickness maps of the primary reservoir (Bunter Sandstone Fm) and its primary seals (Ørslev Fm–Falster Fm). The maps in Figs. 6.2.2–6.2.3 are used in the following descriptions of the geological evolution, stratigraphy and for calculation of storage capacity.

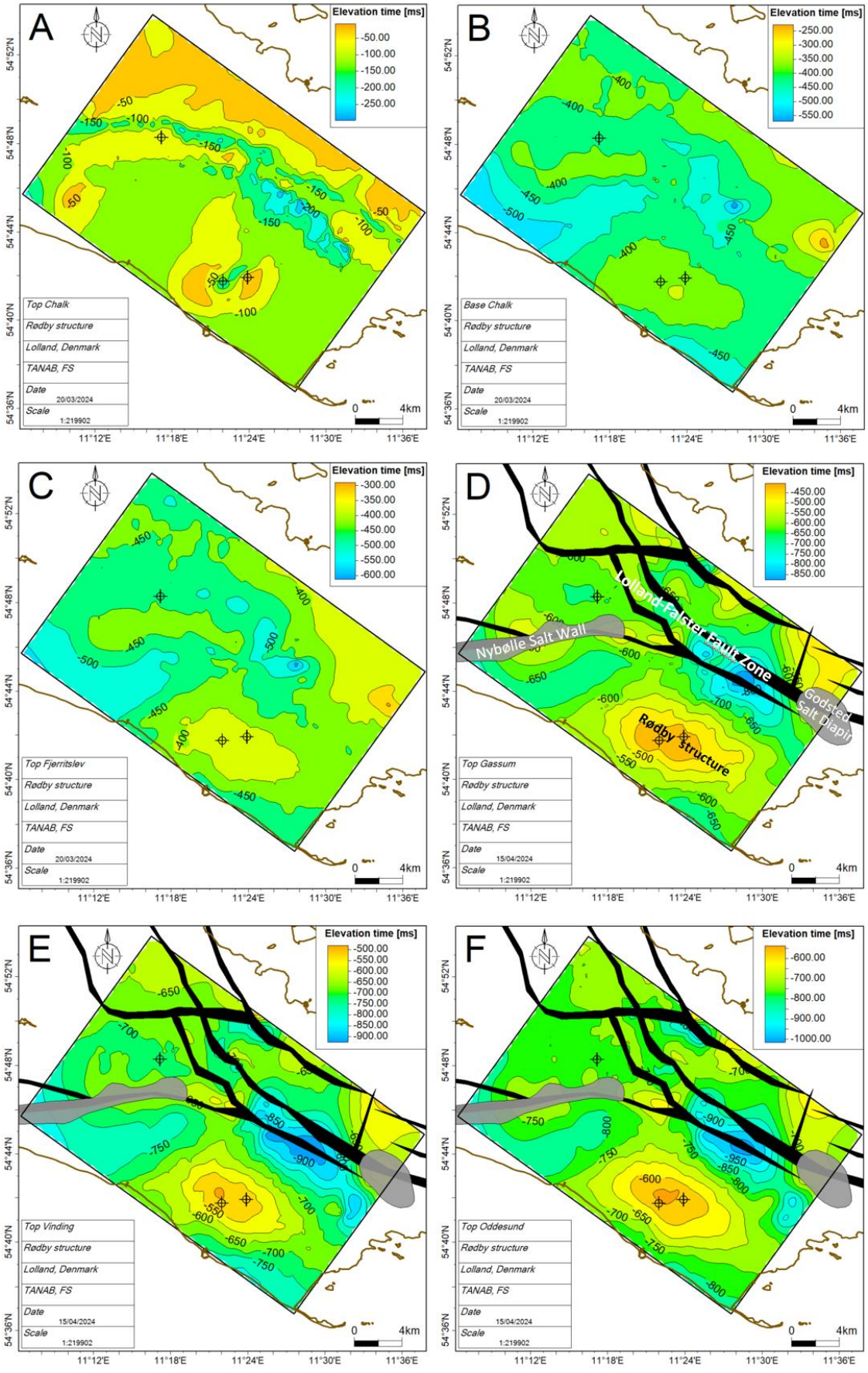
A
Elevation time [ms]
-50.00
-100.00
-150.00
-200.00
-250.00
Top Chalk
Rødby structure
Lolland, Denmark
TANAB, FS
Date 20/03/2024
Scale 1:219902
B
Elevation time [ms]
-250.00
-300.00
-350.00
-400.00
-450.00
-500.00
-550.00
Base Chalk
Rødby structure
Lolland, Denmark
TANAB, FS
Date 20/03/2024
Scale 1:219902
C
Elevation time [ms]
-300.00
-350.00
-400.00
-450.00
-500.00
-550.00
-600.00
Top Fjerritslev
Rødby structure
Lolland, Denmark
TANAB, FS
Date 20/03/2024
Scale 1:219902
D
Elevation time [ms]
-450.00
-500.00
-550.00
-600.00
-650.00
-700.00
-750.00
-800.00
-850.00
Nybølle Salt Wall
Tolland-Falster Fault Zone
Gedsted Salt Diapir
Rødby Structure
Top Gassum
Rødby structure
Lolland, Denmark
TANAB, FS
Date 15/04/2024
Scale 1:219902
E
Elevation time [ms]
-500.00
-550.00
-600.00
-650.00
-700.00
-750.00
-800.00
-850.00
-900.00
Top Vinding
Rødby structure
Lolland, Denmark
TANAB, FS
Date 15/04/2024
Scale 1:219902
F
Elevation time [ms]
-600.00
-700.00
-800.00
-900.00
-1000.00
Top Oddesund
Rødby structure
Lolland, Denmark
TANAB, FS
Date 15/04/2024
Scale 1:219902
0
4km
11°12'E
11°18'E
11°24'E
11°30'E
11°36'E
54°52'N
54°48'N
54°44'N
54°40'N
54°36'N

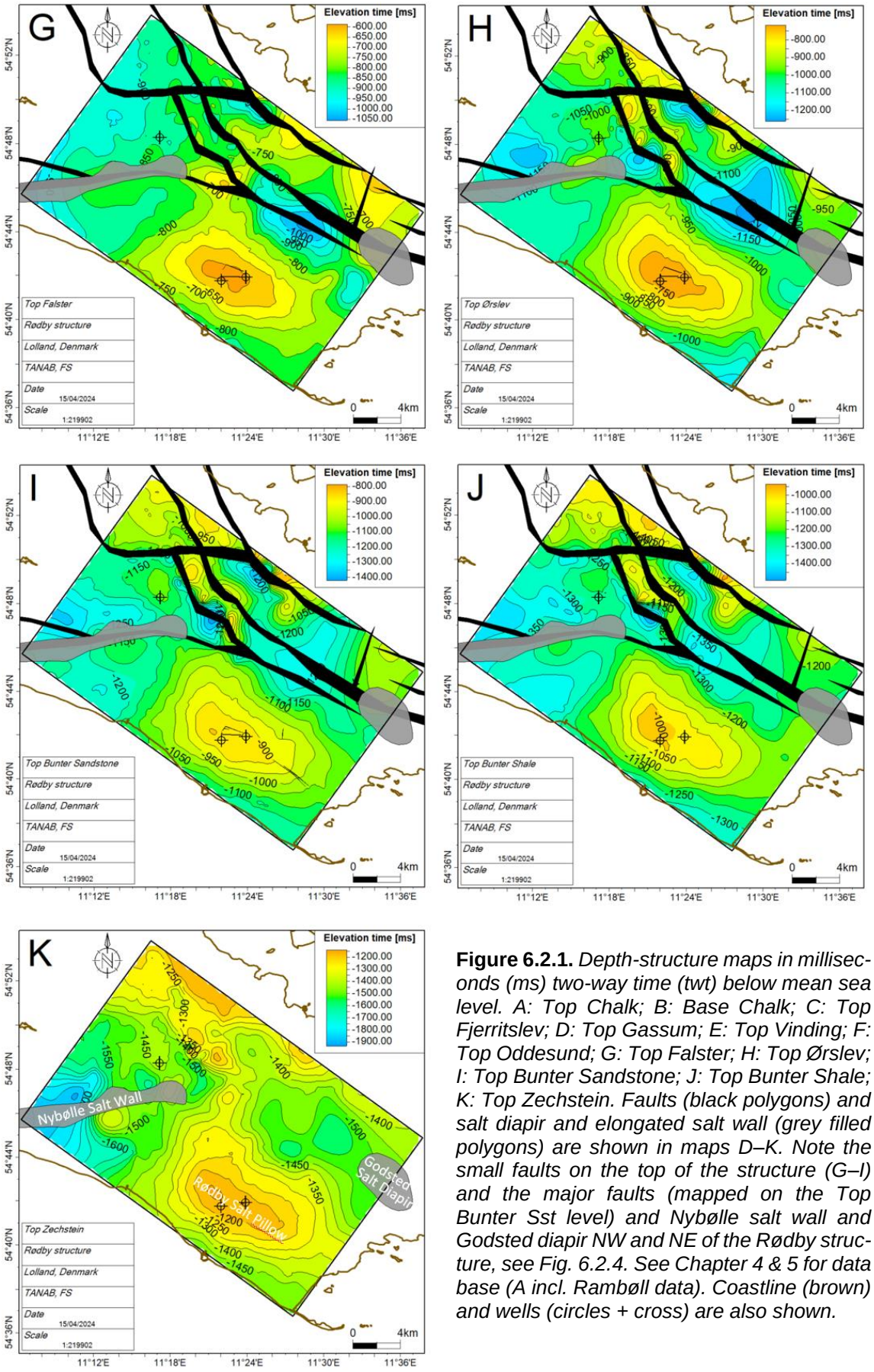

Figure 6.2.1. *Depth-structure maps in milliseconds (ms) two-way time (twt) below mean sea level. A: Top Chalk; B: Base Chalk; C: Top Fjerritslev; D: Top Gassum; E: Top Vinding; F: Top Oddesund; G: Top Falster; H: Top Ørslev; I: Top Bunter Sandstone; J: Top Bunter Shale; K: Top Zechstein. Faults (black polygons) and salt diapir and elongated salt wall (grey filled polygons) are shown in maps D–K. Note the small faults on the top of the structure (G–I) and the major faults (mapped on the Top Bunter Sst level) and Nybølle salt wall and Godsted diapir NW and NE of the Rødby structure, see Fig. 6.2.4. See Chapter 4 & 5 for data base (A incl. Rambøll data). Coastline (brown) and wells (circles + cross) are also shown.*

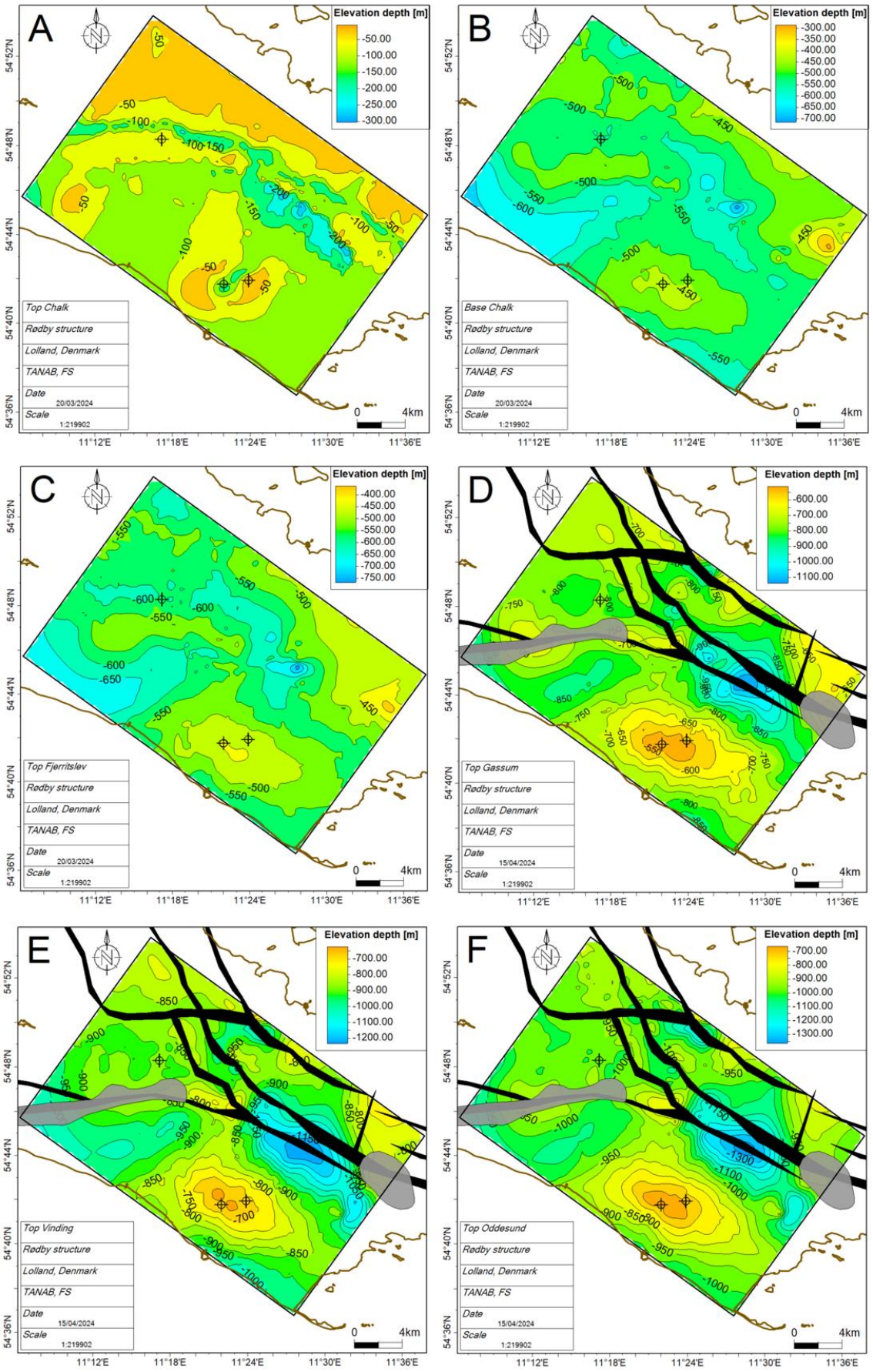
A
Elevation depth [m]
-50.00
-100.00
-150.00
-200.00
-250.00
-300.00
Top Chalk
Rødby structure
Lolland, Denmark
TANAB, FS
Date
20/03/2024
Scale
1:219902
B
Elevation depth [m]
-300.00
-350.00
-400.00
-450.00
-500.00
-550.00
-600.00
-650.00
-700.00
Base Chalk
Rødby structure
Lolland, Denmark
TANAB, FS
Date
20/03/2024
Scale
1:219902
C
Elevation depth [m]
-400.00
-450.00
-500.00
-550.00
-600.00
-650.00
-700.00
-750.00
Top Fjerritslev
Rødby structure
Lolland, Denmark
TANAB, FS
Date
20/03/2024
Scale
1:219902
D
Elevation depth [m]
-600.00
-700.00
-800.00
-900.00
-1000.00
-1100.00
Top Gassum
Rødby structure
Lolland, Denmark
TANAB, FS
Date
15/04/2024
Scale
1:219902
E
Elevation depth [m]
-700.00
-800.00
-900.00
-1000.00
-1100.00
-1200.00
Top Vinding
Rødby structure
Lolland, Denmark
TANAB, FS
Date
15/04/2024
Scale
1:219902
F
Elevation depth [m]
-700.00
-800.00
-900.00
-1000.00
-1100.00
-1200.00
-1300.00
Top Oddesund
Rødby structure
Lolland, Denmark
TANAB, FS
Date
15/04/2024
Scale
1:219902
54°52'N
54°48'N
54°44'N
54°40'N
54°36'N
11°12'E
11°18'E
11°24'E
11°30'E
11°36'E
0
4km

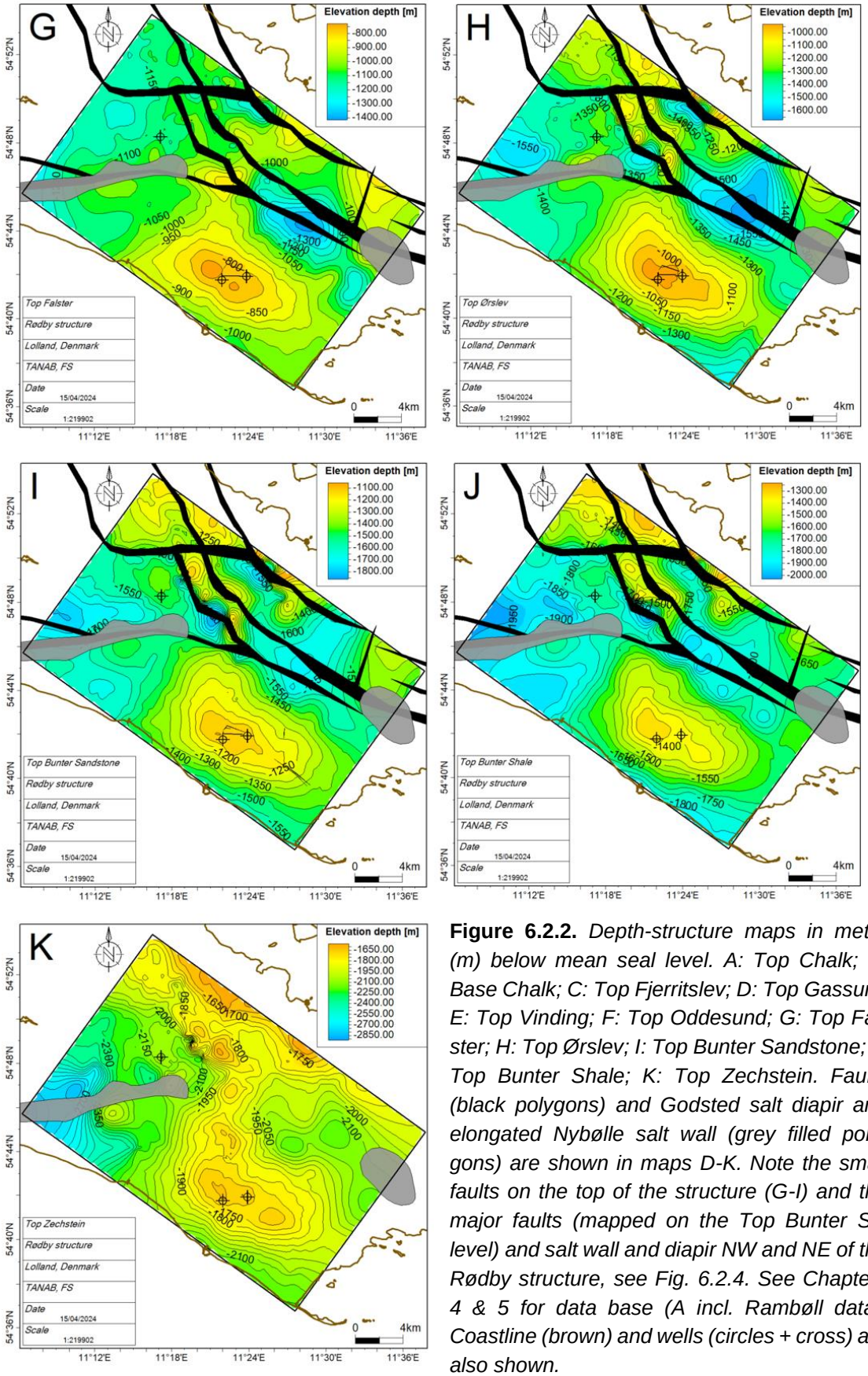

Figure 6.2.2. *Depth-structure maps in meter (m) below mean seal level. A: Top Chalk; B: Base Chalk; C: Top Fjerritslev; D: Top Gassum; E: Top Vinding; F: Top Oddesund; G: Top Falster; H: Top Ørslev; I: Top Bunter Sandstone; J: Top Bunter Shale; K: Top Zechstein. Faults (black polygons) and Godsted salt diapir and elongated Nybølle salt wall (grey filled polygons) are shown in maps D-K. Note the small faults on the top of the structure (G-I) and the major faults (mapped on the Top Bunter Sst level) and salt wall and diapir NW and NE of the Rødby structure, see Fig. 6.2.4. See Chapters 4 & 5 for data base (A incl. Rambøll data). Coastline (brown) and wells (circles + cross) are also shown.*

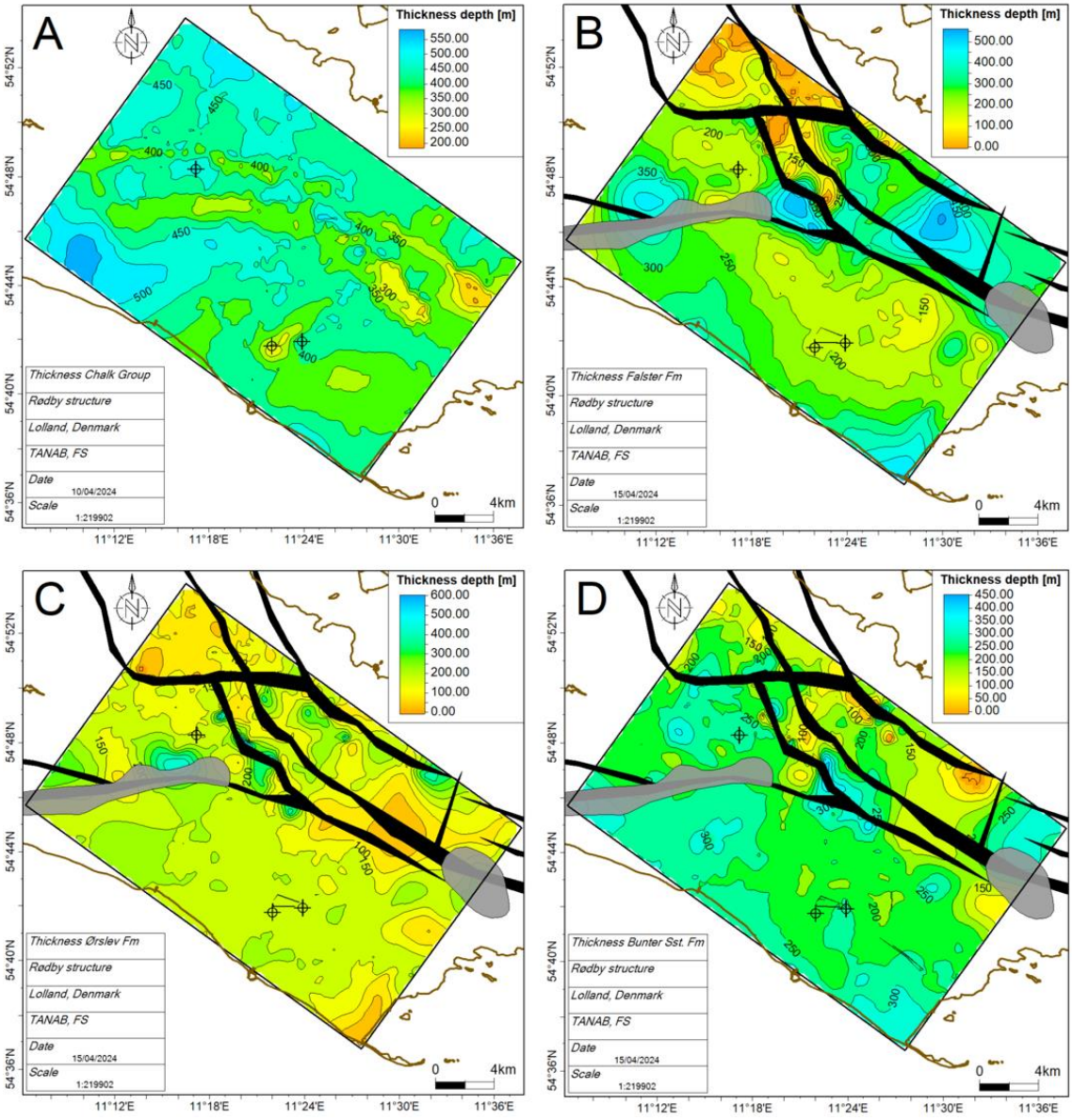

Figure 6.2.3. *Thickness maps in meter (m). A: Chalk Group; B: Falster Fm; C: Ørslev Fm; D: Bunter Sandstone (Sst) Fm. Faults (black polygons) and salt diapir and elongated salt wall (grey filled polygons) are shown. Coastline (thick brown) and wells (circles + cross) are also shown. Note that the primary reservoir Bunter Sandstone Fm is c. 200–260 m thick in the Rødby structure. Over the Rødby structure, the thickness of the primary seal Ørslev Fm is c. 150–200 m and the secondary seal Falster Fm is c. 150–250 m resulting in a total thickness of > 300 m seal formations.*

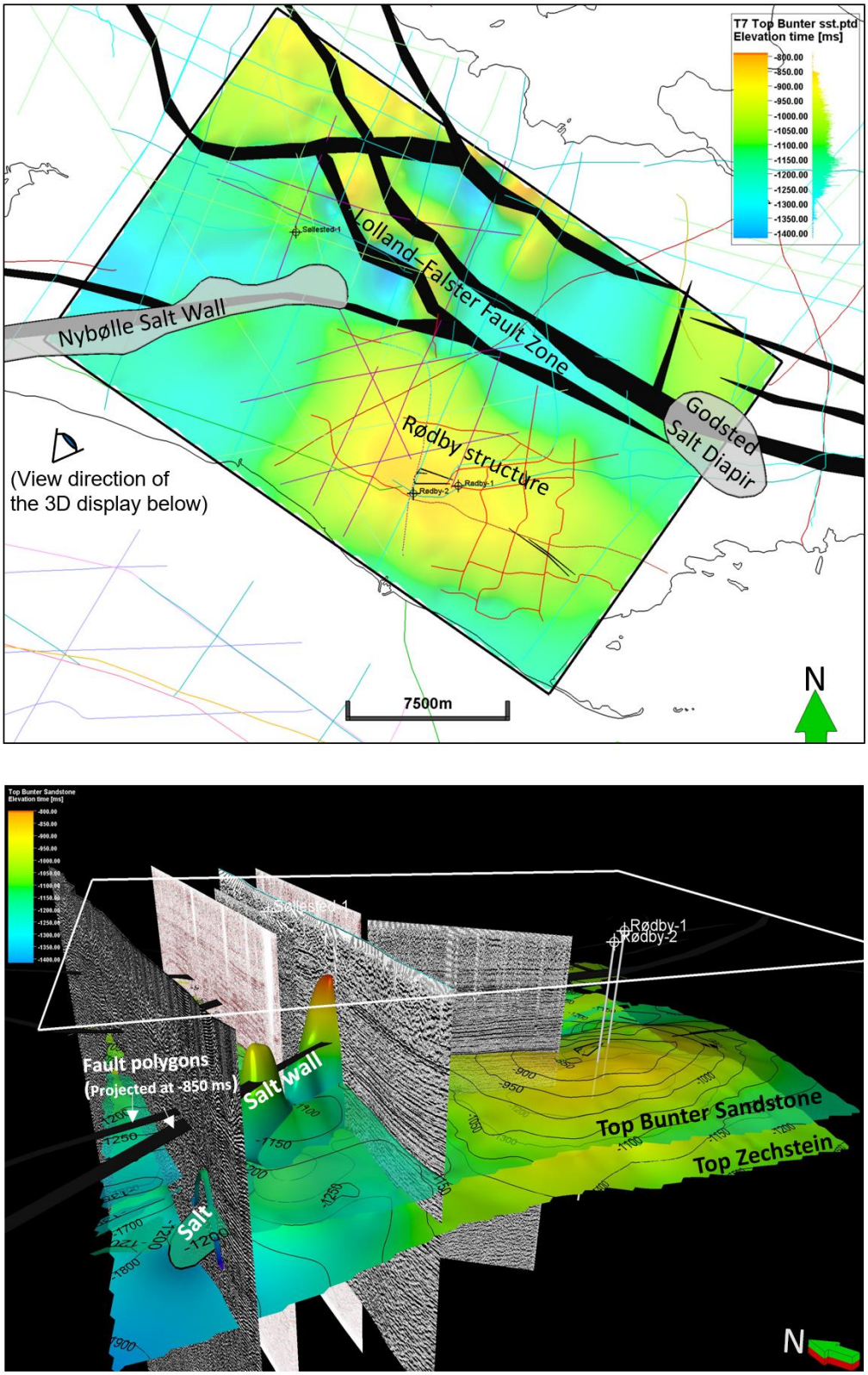

Figure 6.2.4 The 2D and 3D *maps of Top Bunter Sandstone and Top Zechstein in two-way time) with fault polygons (black), and salt wall and diapir structures (grey filled polygons in the upper map). The salt wall surface map is shown in the lower map, and also the projected black fault polygons at c. 850 ms TWT below sea level and the salt wall pierces through the Top Bunter Sandstone surface.*

6.2.2 Tectonostratigraphic evolution of the Rødby structure

Unravelling the tectonostratigraphic evolution of the Rødby structure is based on the seismic interpretation including stratigraphic control from the sparse wells, which serves as the key for understanding the Rødby structure. The interpreted tectonostratigraphic development is constrained by seismic stratigraphic horizons correlated to key wells, where lithostratigraphy and ages are defined. The stratigraphy described here includes information from completion reports and in-house GEUS work of the Rødby-1, Rødby-2, and Søllested-1 wells.

The tectonostratigraphic reconstruction and evolution of the area is summarized, based on the key profile and seismic well-ties, interpretation and mapping of seismic horizons delineating interpreted stratigraphic units and faults, using horizon flattening and back-stripping for a palinspastic restoration (Fig. 6.2.5 - 6.2.7). The tectonostratigraphic evolution of the area is described below, mainly from sections with flattened horizons, from the Top pre-Zechstein to the base of the Chalk Group (Base Chalk), suggesting that the initial formation of the Rødby structure started in the Triassic.

A 12 km long, centrally located key-tie composite seismic profile covering parts of GEUS2023-ROEDBY_P10_RE2023, GEUS2023-ROEDBY_P9_RE2023 and GEUS2023-ROEDBY_P4_RE2023 is chosen as it crosses the NW–SE axis of the Rødby structure from its northern flank along to the SE and includes important insights to both deep and shallow structures (Fig. 6.2.5).

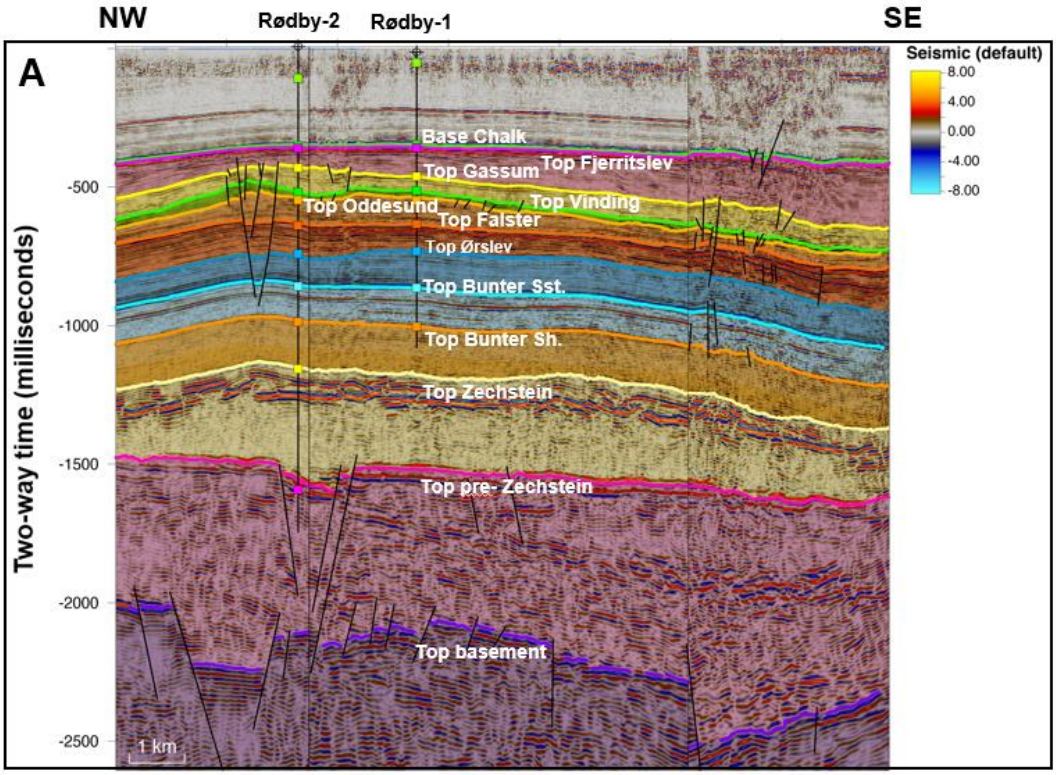

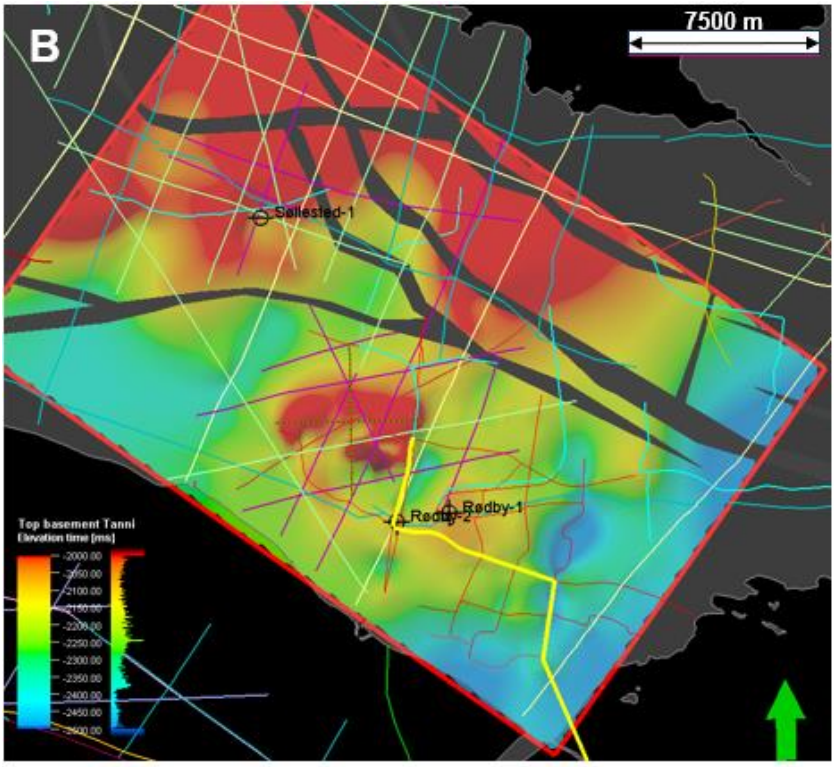

Fig. 6.2.5 – A: *A composite key reference profile across the NW–SE axis of the Rødby structure used for the tectonostratigraphic reconstruction discussed below. B: The orientation of the profile is shown as a yellow line on top of a tentative structural top basement map in milliseconds (ms) two-way travel time (twt) below mean sea level*.

The tectonic framework of the Rødby area

The Lolland–Falster and Rødby area is located south of the elevated basement block in the Møn High, the eastern continuation of the Ringkøbing–Fyn High (see Chapter 3). In contrast to the likely presence of Precambrian basement (Baltica) beneath Paleozoic sedimentary successions in the Slagelse to Stenlille areas (Gregersen et al., 2023), the composition and age of the undrilled pre-Zechstein and basement below the Rødby area is unknown due to the geographical location of the area just south of the Caledonian Deformation Front (CDF), which has been interpreted offshore Møn High (Lassen et al., 2001). The CDF has traditionally been defined as the craton-ward limit of Late Silurian–earliest Devonian folding and décollement thrusting that affected early Paleozoic sedimentary rocks and Precambrian basement during the Caledonian Orogeny between the stable Precambrian craton, the Baltica plate, and a Gondwana-derived 'micro-continent', Eastern Avalonia (Ziegler, 1990).

The CDF is an important tectonic element in the Danish geological evolution and extends westwards across the southern part of Denmark into the southern North Sea, where the CDF separates 880–825 Ma Precambrian basement to the north and east from 450–415 Ma Caledonian deformed basement and sedimentary rocks to the south and west, as demonstrated by the German Q-1 well which encountered Devonian Old Red Sandstone unconformably overlying Precambrian muscovite-biotite augen gneiss that was overprinted during the Caledonian orogeny (Best et al., 1983; Pharaoh et al., 1995) and other well-cores (Larsen, 1971; Frost et al., 1981). On deep seismic data, the CDF has been interpreted as the suture between the Baltica plate and the 'micro-continent' Eastern Avalonia during the Caledonian

Orogeny, e.g. the BABEL and MONA LISA data (BABEL Working Group, 1993; MONA LISA Working Group, 1997; Abramovitz et al., 1998; Abramovitz et al., 2000).

In the SW Baltic Sea, similar results for the southward continuation of Baltica crystalline crust buried below a northward overthrusted Caledonian deformation complex of lower Paleozoic sediments beneath the NE German Basin have been documented by drill holes (e.g. the G14 well, NE of Rügen (Krawczyk et al., 2003)) and seismic data, e.g. DEKORP-BASIN Research Group, 1999; Meissner and Krawczyk, 1999).

Hence in the Lolland–Falster area, the undrilled basement rocks most likely represent a similar tectonic complex composed by northward overthrust of Caledonian deformed lower Paleozoic sediments overlying the buried crystalline Precambrian basement (Baltica crust). Similar structures have been interpreted offshore east of the Møn High (Lassen et al. (2001)).

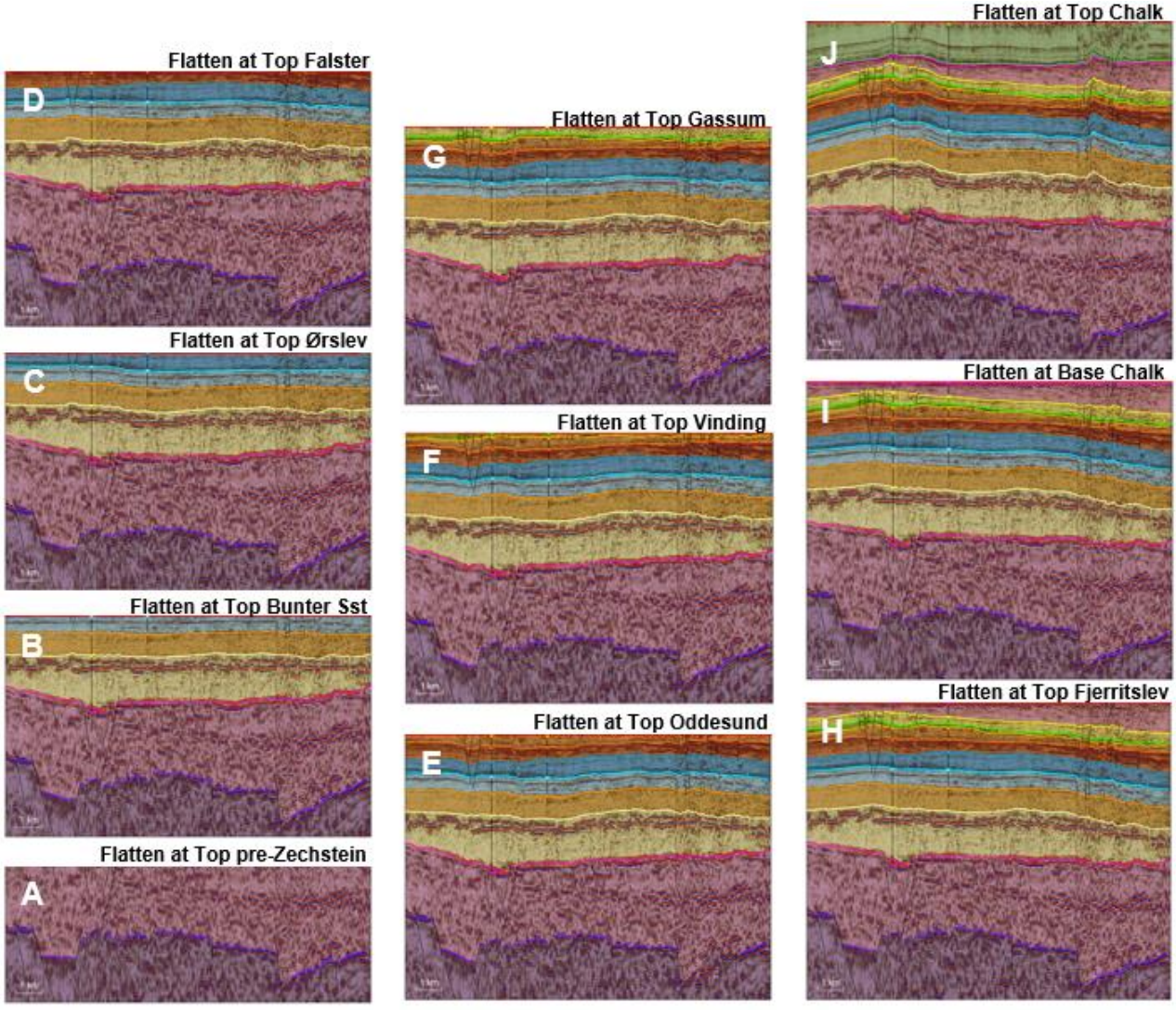

Fig. 6.2.6 *– A tectonostratigraphic reconstruction along the profile shown in Fig. 6.2.5, with horizon flattening of key-horizons illustrating the Palaeozoic to Cretaceous structural evolution of the Rødby structure described in the text. A: Top pre-Zechstein (pink), B: Top Bunter Sst (light blue), C: Top Ørslev (medium bright blue), D: Top Falster (dark orange), E: Top Oddesund (medium orange), F: Top Vinding (green), G: Top Gassum (yellow), H: Top Fjerritslev (red), I: Base Chalk, and J: Top Chalk (bright green). Notice that the deep crystalline basement is purple, the Zechstein interval is light yellow and the Bunter Shale Fm is orange.*

Precambrian to Palaeozoic

The fault-bounded near basement horizon (dark purple) is overlain by up-to 550–950 millisecond (ms) thick Palaeozoic successions (red-purple colour on Figs. 6.2.5–6.2.7), and both units are affected by faults forming a NW–SE striking structural basement high beneath the central part of the present-day Rødby structure (Fig. 6.2.5b and 6.2.6a).

The top of the pre-Zechstein (pink horizon) is penetrated by the Rødby-2 well at 2674 m below MSL (Fig. 6.2.5a), where the Rotliegende is represented by a conglomerate-dominated upper unit c. 200 m thick and a lower unit of volcanic rocks in which the well terminates after 74 m (DGU/DAPCO, 1953).

Lithosphere thinning and subsequent crustal extension during latest Carboniferous–Early Permian times was associated with widespread Rotliegende volcanism and block faulting as described by Frederiksen et al. (2001). The Top pre-Zechstein unconformity, associated with basin-wide erosional denudation, is the deepest and oldest basin-wide mappable sedimentary horizon and separates the Rotliegende syn-rift succession from the younger post-rift basin succession.

The Upper Paleozoic and younger successions started with a major syn-rift evolution of the Paleozoic that is documented by the drilled Rotliegende volcanic rocks and conglomerates in the nearby Søllested-1 well. On the composite, seismic key-profile (Fig. 6.2.5–6.2.6), the pre-Zechstein deposits consist of an upper and lower unit, separated by a SW-dipping reflective band of short, high amplitude reflections. The Rotliegende represents in places, a syn-rift wedge between the top of the Lower Paleozoic and the Top pre-Zechstein (Fig. 6.2.7).

A tentative interpretation for the pre-Zechstein evolution is presented here in a cartoon with flattening of the structures at Top pre-Zechstein level (Fig. 6.2.7), the deeply buried, faulted and rifted crystalline basement (purple) interpreted to be overlain by a central Paleozoic unit (rose red) that may be interpreted as lower unit consisting of Cambro–Silurian rocks (below the yellow stippled line) deposited on the deformed basement along the passive continental margin of the Baltica plate. This lowermost unit is overlain by with Devonian–Carboniferous rocks. However, Devonian–Carboniferous succession has not been drilled in the Rødby area, but the nearby Ørslev-1 well encountered 523 m undifferentiated Carboniferous rocks. Finally, the uppermost up-to 950 ms thick unit with little internal reflectivity (magenta color) represents an Upper Paleozoic Permian wedge-shaped unit likely consisting of conglomeratic sandstones and mudstones above a reflective band at its base, which is probably caused by volcanic eruptive rocks of Rotliegende age.

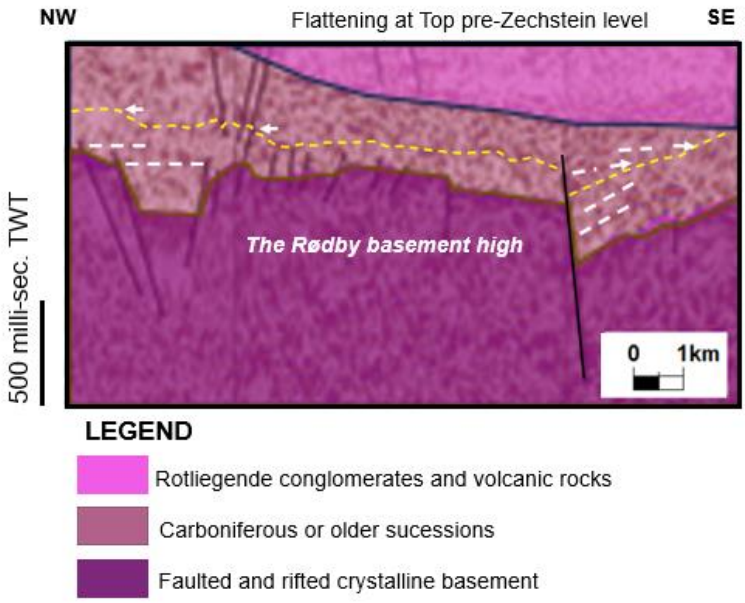

Figure 6.2.7 *A tentative interpretation of the deepest features below the Rødby structure. The faulted and rifted crystalline basement (purple) of the Rødby basement high is overlain by the presence of speculative Lower Paleozoic units (rose red) consisting of Cambro-Silurian deposits overlain by possibly ?Devonian–?Carboniferous successions, separated by the thin yellow hatched line with onlap (white arrows). A Rotliegende succession (magenta) overlies a major unconformity (black line), below the Top pre-Zechstein horizon (see text above).*

The Top pre-Zechstein unconformity was transgressed by the Zechstein Sea and restricted Zechstein seaway formed where evaporites were deposited (Vejbæk 1997). This was followed by lithospheric thermal contraction creating subsidence and accommodation space for Zechstein evaporites and the overlying thick Triassic successions.

The *Zechstein Group* (light yellow unit, Fig. 6.2.6) is interpreted between the Top pre-Zechstein unconformity and the Top Zechstein (light yellow horizon), where the succession forms a larger NW–SE trending salt pillow. The unit ties into a 1020 m thick evaporitic succession with intercalating halite, anhydrite, dolomite, and mudstone in the Rødby-2 well (Fig. 6.2.5a). The evaporites formed in an arid climate during the Late Permian time in large parts of the Danish Basin and the North German Basin, where later mobilization led to numerous diapirs and pillows.

Triassic to Early Jurassic

Near the Permian−Triassic transition, regional uplift took place which was followed by regional subsidence (Vejbæk 1997). The Triassic succession in the Lolland–Falster area, the northernmost part of the North German Basin, reflects a general transgressive evolution and subsidence resulting in Lower Triassic successions (Bunter Shale, Bunter Sandstone and Ørslev Formations), Middle Triassic carbonates and evaporites (Falster Formation), Upper Triassic red beds, sandstones and evaporites (Tønder to Oddesund Formations) and Upper

Triassic–Lower Jurassic marine shales and sandstones (Vinding to Gassum Formations) as described by Bertelsen (1980).

The lowermost Triassic unit (orange in Fig. 6.2.5a and Fig. 6.2.6) above the Zechstein layer is interpreted as the Lower Triassic *Bunter Shale Formation* by correlation to the Rødby-2 well, and it shows a nearly constant thickness around the Rødby structure. During deposition of the Bunter Shale Formation subsidence initiated along the SW part of the profile. The Bunter Shale Formation is overlain conformably by the *Bunter Sandstone Formation* with almost uniform thickness in the Rødby-2 and nearby wells. The Bunter Sandstone Fm (light blue in Fig. 6.2.6b), the potential main reservoir for CO_2 storage, is affected mostly by minor faults in the central part of the structure, that were initiated by later tectonics during deposition of the Upper Triassic to Lower Cretaceous successions (see Fig. 6.1.7).

The overlying conformable unit (medium bright blue in Fig. 6.2.5–6.2.6c) correlates to the *Ørslev Formation* (primary seal) in the Rødby-2 and nearby wells and is up-to 150–200 m thick in the Rødby area. The uniform thicknesses of the Bunter Shale, Bunter Sandstone and Ørslev Formations (Fig. 6.2.3 and 6.2.5) indicates deposition in a broadly subsiding epicontinental basin south of the barriers of the Ringkøbing–Fyn High and Møn High.

During the Middle Triassic period, the central part of the basement block beneath the Rødby structure started to uplift and subsequent salt mobilization occurred in the central and southern part of the Rødby structure possibly triggered by a combination of increased burial (temperature and pressure) and re-activation of deep-seated basement faults. The Middle Triassic unit (dark orange in Figs. 6.2.5–6.2.6) correlates with the *Falster Formation* in nearby wells, shows lateral thickness variation along the key profile with local thickening to the north and to the south of the elevated basement high below the present-day Rødby structure (Fig. 6.2.6d). The wedge of onlapping reflectors observed at the southern flank of the structure at c. 800 ms TWT near top Falster Fm level most likely indicate the presence of an intra-Triassic hiatus that developed due to salt growth (Figs. 6.1.7a).

The uplift of the basement high below the Rødby structure is most likely associated with the Late Triassic (Carnian) unconformity discussed by Clausen and Pedersen (1999). They interpreted the unconformity as formed by low-angle erosion on central parts of the eastern Ringkøbing-Fyn High (Møn High) and North German Basin due to differential subsidence along individual structural basement blocks. The intra-Triassic hiatus corresponds to the unconformity discussed in Chapter 3, that marks the top to the Falster Formation in the Rødby area may also explain why the Middle–Upper Triassic Tønder Formation was not encountered in the any of the south and eastern wells in the Lolland-Falster area, such as the Rødby-1 and -2 or Ørslev-1 wells. The Middle–Upper Triassic Tønder Formation is only drilled in the Søllested-1 well, located northwest of the Lolland-Falster Fault Zone (Fig. 6.1.2).

Deposition of Upper Triassic *Oddesund Formation* was associated with lateral thickness variations due to increased subsidence above the deep-seated faults at the northern flank and uplift above the southern flank of the Rødby basement high, combined with salt movements away from the basement block resulting in a local depocenter with increased thickness of the Oddesund Formation (orange-brown unit in Fig. 6.2.6e). An interesting observation is the onset of initial faulting along fault planes in a minor graben or fault zone, the Rødby Structure Fault Zone, that developed near the top of the Rødby structure probably associated with salt movements. These bounding fault planes extends down to the deeper successions, as the fault planes offsets the Top Bunter Sandstone Formation horizon (Fig. 6.2.8a) with a slight

throw <10 ms. Other similar minor normal faults are observed above the southern rim of the Rødby basement high (Fig. 6.2.6).

Deposition of the thin Upper Triassic *Vinding Formation* (bright green unit in Fig. 6.2.6f) was associated with minor lateral thickness variation across the Rødby Structure Fault Zone. Re-activation of the deep-seated basement faults caused the central part of the basement high to uplift combined with salt movements away from the basement block resulting in a minor local depocenter with increased thickness of the Vinding Formation above the northern flank of the Rødby basement high.

The overlying seismic stratigraphic unit ties in the nearby wells to the Upper Triassic *Gassum Formation* (bright yellow in Fig. 6.2.6g). Deposition of the Gassum Formation was dominated by subsidence that resulted in a general south-ward shift of the Gassum depocenter with increased accommodation space above the southern flanks of the Rødby basement high (horst), Fig. 6.2.6g. The change in position of the Gassum depocenter was probably caused by a combination of reactivation of the basement faults and salt migration.

Early Jurassic to Basin and the North German Basin, including the Lolland-Falster area south of the Ringkøbing−Fyn High.

Flattening at the Fjerritslev Fm horizon along the key reference profile (Fig. 6.2.6h), indicates that the Rødby area underwent a structural re-organization due to due to a Middle Jurassic–Early Cretaceous tectonic uplift and increased salt movements of the salt pillow to the north combined with subsidence over the southern shoulder of the basement high and widespread erosion along truncation patterns at the flanks of the structure.

At the Rødby structure, the truncation pattern along the mid-Cimmerian Unconformity indicates Middle Jurassic to Early Cretaceous salt-pillow growth. The Lower Jurassic Fjerritslev Fm is capped by an unconformity (and hiatus), succeeded by thinly developed Lower Cretaceous Vedsted (24 m) and Rødby Formations (14 m) in the Søllested-1 well. These formations measure merely 10 m in total in the Rødby-1 and -2 wells.

Late Cretaceous to Pleistocene

The Lower Cretaceous Rødby Formation is overlain by the regional Upper Cretaceous *Chalk Group* (green unit in Fig. 6.2.6j).

The Chalk Group is in general 400–450 m thick in the Rødby area and is overlain by Paleocene mudstones covering and draping over the Rødby structure with no indications of salt growth during the Late Cretaceous to Paleocene. The succession domes over the Rødby structure and is erosionally overlain by Pleistocene strata suggesting a renewed pulse of salt pillow growth sometime during the Cenozoic. Japsen et al., (2007) interpreted around 500 m of Cenozoic uplift and erosion in the greater Rødby area, which is in line with the observed sub-crop pattern towards the base of the Pleistocene. Here, glacial incised valleys filled with up to a few hundred meter of coarse-grained Pleistocene strata carved into the crest of the Rødby structure (Fig. 6.2.3a), as illustrated by the deep incised valley located between the Rødby-1 and -2 wells running northeast to southwest (see Fig. 6.1.4 and 6.2.1a). Located outside the deep incised valleys, only a 32–33 m thick Pleistocene unit was encountered in the Rødby-1 and -2 wells directly overlying the Upper Cretaceous Chalk Group.

6.3 Summary of the structural evolution – The Rødby structure

The structural reconstruction of the development of the Rødby structure during the Paleozoic–Mesozoic time up to the Base Chalk has been facilitated by horizon flattening at key horizons.

In summary, the Rødby structure mainly evolved by separate/discrete episodes of salt pillow growth forming the overlying structural doming anticline seen today during at least three main episodes of salt migration:

1. Initial growth of the Rødby salt pillow started during deposition of the Falster Fm as indicated by truncations along the southern flank corresponding to the missing Tønder Fm.
2. Thickness variations and truncations near the Top Fjerritslev Fm suggests growth of the salt pillow and uplift during Middle Jurassic–Early Cretaceous.
3. Final growth of the salt pillow took place after deposition of the Paleocene, but before the Pleistocene.

The structural evolution of the Rødby structure suggests that the tectonic framework and outline of the present day Rødby structure may have been controlled by the existing Paleozoic fault pattern below the Top pre-Zechstein at the base of the present day Rødby structure, and that salt movements has been triggered episodically by the re-activation of these deep-seated basement fault structures during the later tectonic phases.

7. Geology and parameters of the reservoirs and seals

The primary reservoir for potential CO_2 storage in the Rødby structure are sandstone-dominated intervals of the Bunter Sandstone Formation. The Gassum Formation, considered the primary reservoir in many other Danish onshore structures, occurs above 800 meters and thus at too shallow depths to be considered relevant for CO_2 storage (Figs. 7.1.1 and 7.1.2). The Ørslev Formation and the overlying Falster Formation are the primary seal to the Bunter Sandstone Formation (Figs. 7.1.3 and 7.1.4) whereas the overlying mudstone dominated Oddesund and Vinding formations are present at too shallow depths (above 800 m) to seal CO_2 in its supercritical phase. The Rødby-1 and Rødby-2 wells are located on the Rødby structure and have TD in the Bunter Shale Formation and Rotliegende Group, respectively. Consequently, they are the main wells for outlining information on the properties of the reservoir and seals in the structure. Interpreted well logs for the two wells and the nearest wells to the Rødby structure (Søllested-1 and Ørslev-1) are also shown in Appendix A. There are no biostratigraphic data available from the Bunter Sandstone, Ørslev and Falster formations in the included wells.

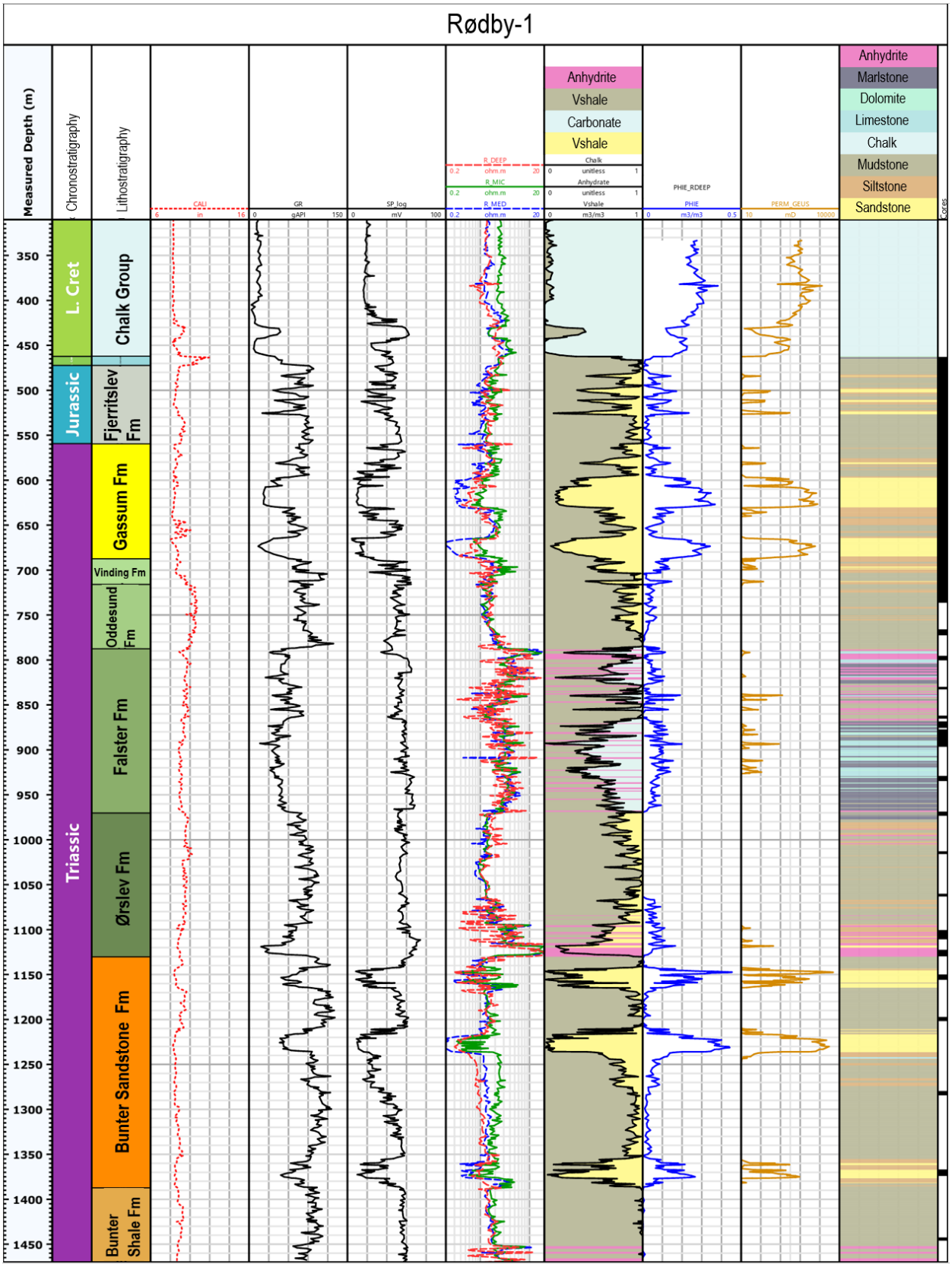

Figure 7.1.1. *Lithostratigraphic subdivision of the Rødby-1 well with interpreted lithology and formations based on petrophysical log interpretation and information from core data, cutting samples etc. Sandstones present at three distinct intervals in the Bunter Sandstone Fm form the primary reservoir.*

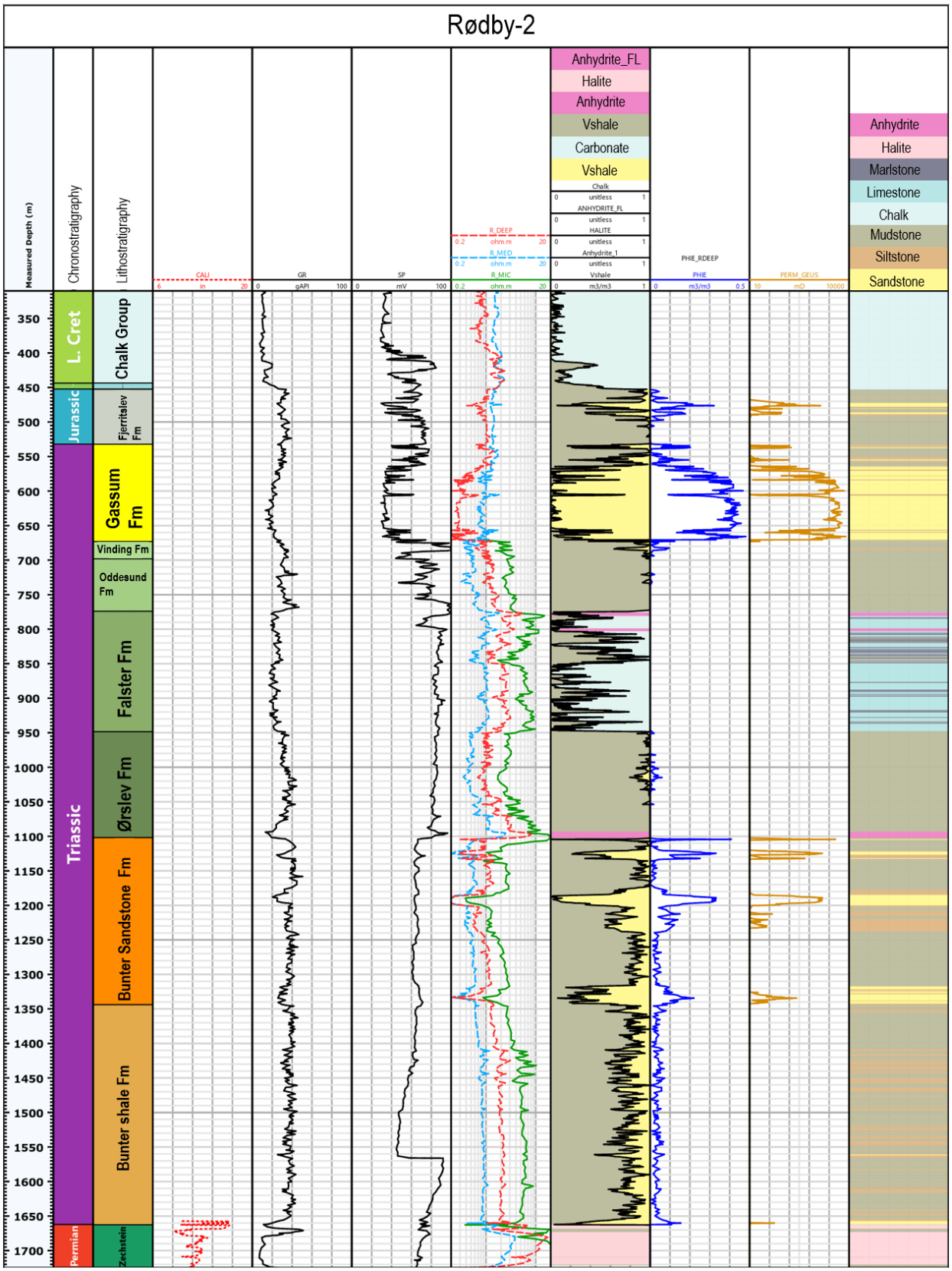

Figure 7.1.2. *Lithostratigraphic subdivision of the Rødby-2 well with interpreted lithology and formations based on petrophysical log interpretation and information from cutting samples etc. Sandstone intervals in the Bunter Sandstone Fm form the primary reservoir.*

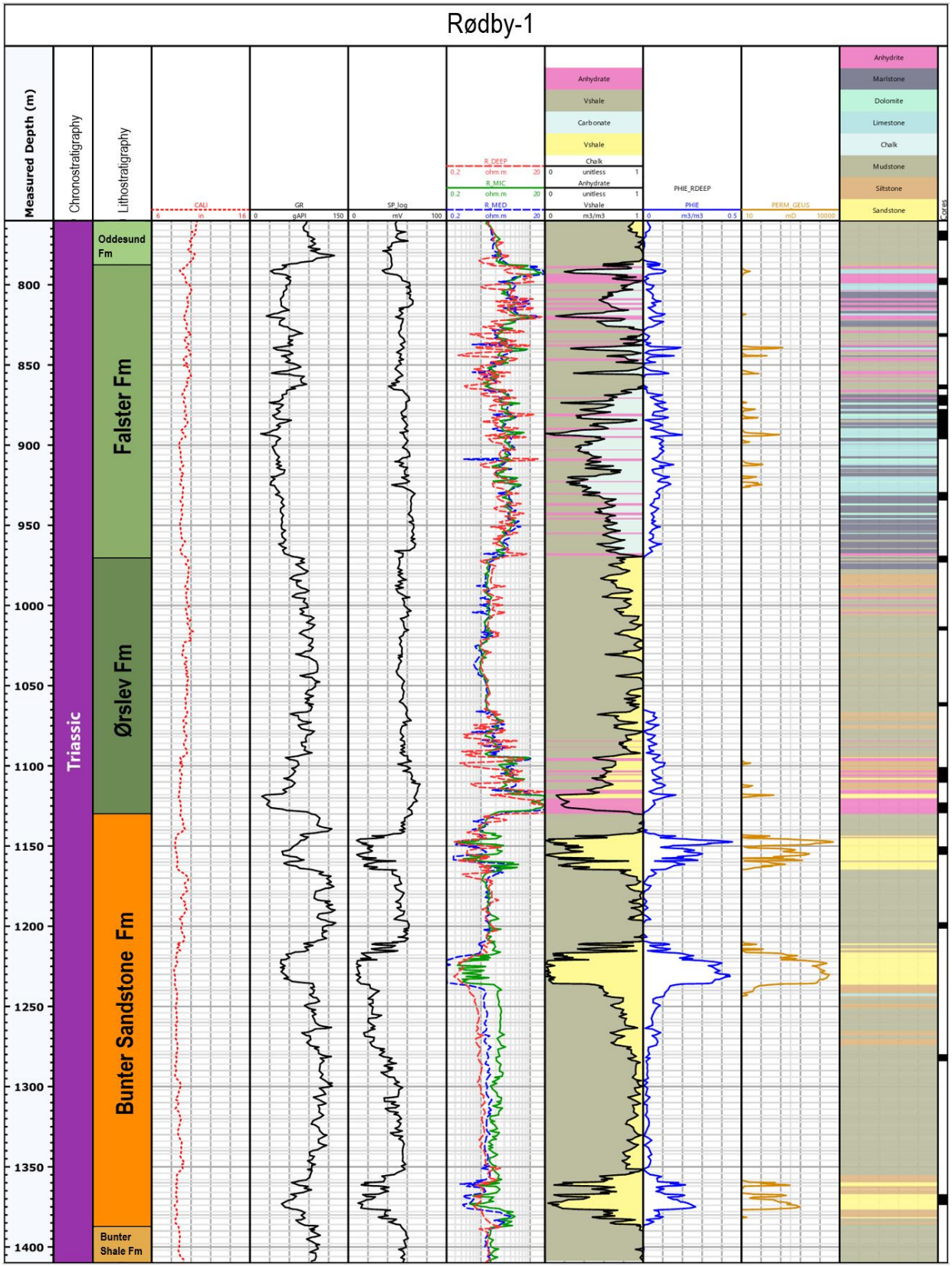

Figure 7.1.3. *The Rødby-1 well with interpreted lithology based on petrophysical log interpretation and information from core data, cutting samples etc. Zoom section of the Bunter Sandstone Fm and its primary seals (Ørslev and Falster formations) in Figure 7.1.1.*

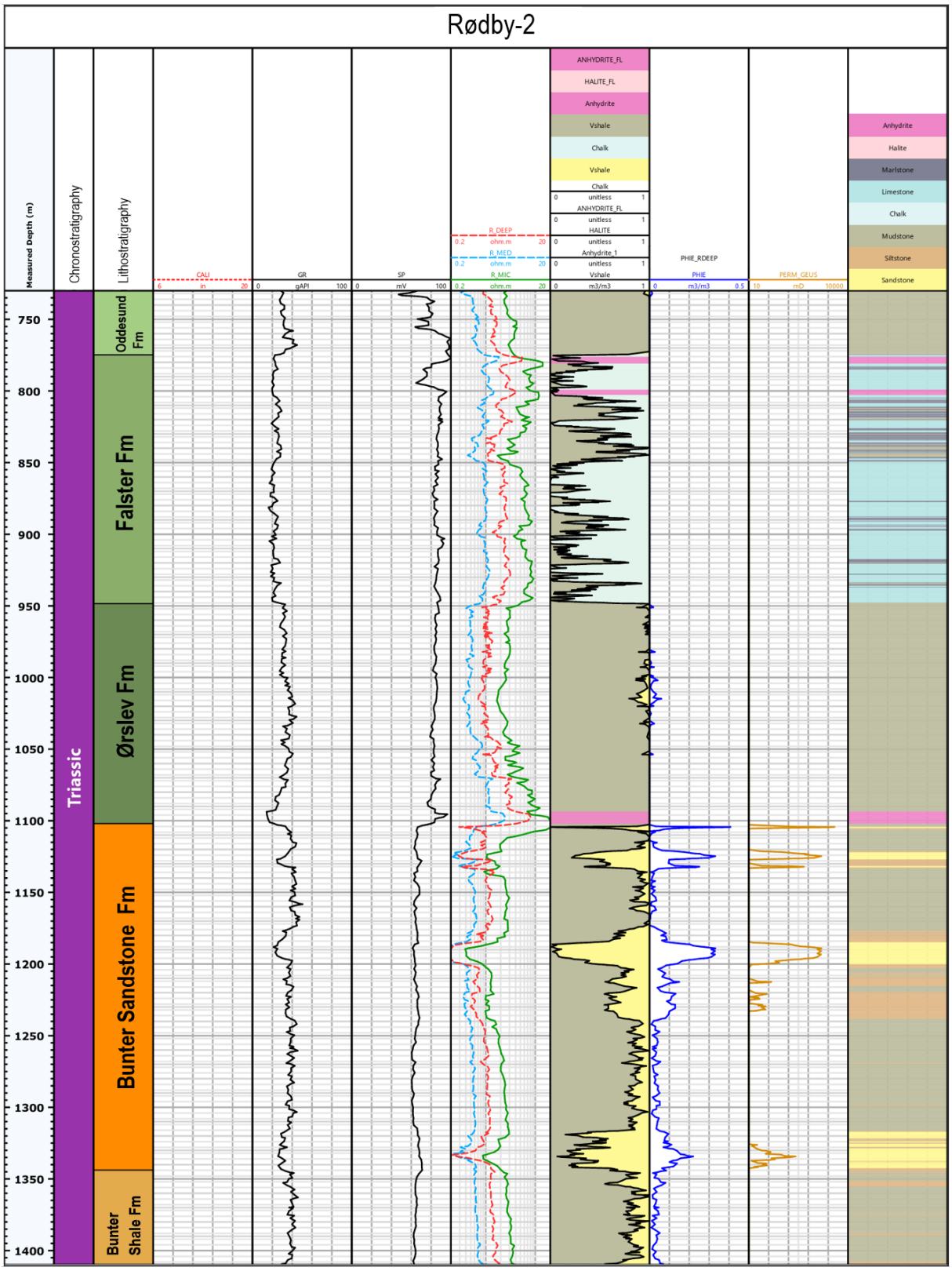

Figure 7.1.4. *The Rødby-2 well with interpreted lithology based on petrophysical log interpretation and information from cutting samples etc. Zoom section of the Bunter Sandstone Fm and its primary seals (Ørslev and Falster formations) in Figure 7.1.2.*

7.1 Reservoirs – Summary of geology and parameters

7.1.1 The primary reservoir: The Bunter Sandstone Formation

The Early Triassic Bunter Sandstone Formation was formed in a dry and hot desert climate where vegetation was extremely sparse (Fig. 3.5B). The formation is known from several deep boreholes in Denmark and Sweden and is widespread in the North German Basin and in the southern part of the Danish Basin. The geothermal plant at Margretheholm in Copenhagen was designed to use hot water from sandstone layers in the Bunter Sandstone Formation. The thickness of the formation varies greatly but is generally less than 300 meters in the southern Danish area. Over the Ringkøbing–Fyn High the formation is thin or locally absent. The high was probably partially exposed as "islands" in the Early Triassic, when smaller troughs between the islands connected the North German Basin with the Danish Basin (Michelsen et al. 1981). Northwards in the Danish Basin, the formation grades into the time-equivalent lower part of the Skagerrak Formation. However, the nature and position of this transition is poorly known. The present burial depth of the formation is 1.1–2.1 km in the Danish part of the North German Basin (Nielsen & Japsen 1991) corresponding to maximum burial depth of 1.6–2.3 km prior to exhumation events (Japsen et al. 2007). Thus, the onshore detrital mineralogy has in general only been slightly affected by diagenesis (Olivarius et al. 2015, 2017). A general but detailed description of the formation with relevant references is given in Olivarius et al. (2017) and Weibel et al. (2020). The above and following description is mainly from these publications.

The sandstones of the Bunter Sandstone Formation form the base of four depositional cycles that each grade upwards into thick intervals of lacustrine/playa mudstone (Bachmann et al. 2010; Michelsen & Clausen 2002). The depositional cycles are named the Volpriehausen, Detfurth, Hardegsen and Solling members corresponding to the German subdivision of the Middle Buntsandstein. The Hardegsen and partly the Detfurth members are of small lateral extent and thickness in the Danish area due to deep erosion prior to deposition of the Solling Member (Geluk & Röhling 1997; Michelsen & Clausen 2002). The sandstones of the members are ephemeral fluvial deposits interbedded with aeolian sand sheet deposits. The sandstones of the Solling Member were deposited during increased humidity and comprise primarily ephemeral fluvial deposits (Clemmensen 1985). The sand was supplied by northward aeolian transport from the Variscan belt and by southward fluvial and alluvial transport from the Ringkøbing–Fyn High and Fennoscandian Shield (Olivarius et al. 2017). Individual sandstone-dominated intervals are 30–50 m thick, and some of the intervals are considered to have a regional extent although not mapped in detail (Olivarius et al. 2017). The sandstones are mostly fine-grained and well-sorted, and the aeolian sand tends to be very well-sorted. In general, the sandstones are pale red to reddish brown and contain greenish grey reduction spots and light pinkish grey anhydrite nodules in some intervals. Intraclasts and detrital clays are present only in the ephemeral fluvial and playa lake deposits. Petrographical investigations of core samples show the sandstones as being arkosic to subarkosic, according to the classification of McBride (1963), with dominance of quartz and abundant feldspar. Mica, rock fragments and heavy minerals occur in small amounts. The authigenic phases comprise an average of 17–31% of the rock volume, of which calcite, dolomite and anhydrite cement are dominant. Anhydrite is found in amounts of up to 35%, but the content is highly variable, being lowest in the aeolian sandstones and highest in the fluvial sandstones. The anhydrite

cement is patchy pore-filling and partially displacive. Calcite occurs mainly as patchy cement, and dolomite rhombs are scattered in all the sedimentary rocks. Red coatings of goethite and hematite have generally formed on the sand grains (Weibel & Friis 2004). Core analyses show that several sandstones have porosity of 15–35% and a corresponding permeability of 10–3000 mD. The best reservoir qualities are generally found in the aeolian sandstones since these are largely clay-free and only weakly cemented (Olivarius et al. 2015).

7.1.2 The Bunter Sandstone Formation at Rødby:

Depth, thickness and extent: The Rødby-1 and Rødby-2 wells show a thickness of the Bunter Sandstone Formation of 257 and 243 m, respectively, corresponding to a mean thickness of 250 m. The vertical depth to the top of the formation is around 1115 m (Below Kelly Bushing, Table 7.1.1). The seismic mapping and interpretation indicate that the formation is present in the entire structure, with a thickness of approximately 200–260 m (Fig. 6.2.3D).

Table 7.1.1. *Approximately depths to the Top and Base of the Bunter Sandstone Fm and its thickness in Rødby-1 and -2 and the nearest wells (see Fig. 3.1 for location of wells). The boundary to the overlying Ørslev Fm is sat at the base of the first occurring evaporitic or carbonate deposits (implying minor deviations from the depths given in Nielsen & Japsen 1991).*

Well	Rotary Table – m above terrain	Measured/True vertical depth (meter below Rotary Table)		Thickness (m)
		Top Bunter Sandstone Fm	Base Bunter Sandstone Fm	
Rødby-1	2.3	1130	1387	257
Rødby-2	5.2	1102	1344	242
Søllested-[illegible]	6.0	1467	1760	293
Ørslev-1	6.2	1087	1210	123

Subdivision and depositional environments:

The Bunter Sandstone Formation is tentatively subdivided into the Volpriehausen, Detfurth and Solling members in the Rødby-1, Rødby-2 and Søllested-1 wells (Michelsen & Clausen 2002; Olivarius et al. 2015). The Volpriehausen and Solling members are also present in the Ørslev-1 well whereas the Detfurth Member is absent (Fig. 7.1.5). The absence of Detfurth Member in the Ørslev-1 well is probably related to the more proximal location of this well to the Ringkøbing–Fyn High compared to the other wells implying a likely more intense erosion and removal during the erosional event that took place prior to the deposition of the Solling Member. The log panel of the wells outlines that the basal sandstone intervals and the overlying mudstone intervals of the members have a large lateral continuity (Fig. 7.1.5). This is also indicated on seismic sections where the members are mappable along the seismic lines (Figs. 7.1.6 and 7.1.7). It is difficult to infer the depositional environments of the sandstones based on the seismic data as the sandstone intervals correspond only to a single reflector. However, in places a small-scale relief occurs at the base of the reflectors, probably reflecting fluvial erosion considering the general interpretation of the basal sandstones as being mainly fluvial in origin.

The sandstone intervals are thus to be considered present in the entire Rødby structure. However, comparing the petrophysical log interpretation of the lithology in the Rødby-1 and Rødby-2 wells also demonstrate that over short distances variations may occur in the thickness of the individual reservoir units as well as their silt- and mudstone content contra their sandstone content (Fig. 7.1.5). This most likely reflect variations in the depositional environment, e.g. fluvial channel sand that laterally give way to more fine-grained floodplain deposits or infills of abandoned channels.

The log panel also outlines the large thicknesses of the mudstone intervals above the basal sandstones of the members, especially for the Volpriehausen Member where the mudstone interval may be up to nearly 130 m thick (Fig. 7.1.5). Apart from considering the Bunter Sandstone Formation as one reservoir, it therefore seems reasonable also to treat the basal sandstone intervals of its members as separate reservoir units (as will be done in the following section dealing with the reservoir quality of the formation). This is outlined for the Rødby-1 well in Figure 7.1.8 where the Bunter Sandstone Formation is separated in three reservoir units informal named after the members they are associated to.

The thick mudstone-dominated interval of the Volpriehausen Member, overlying the basal sandstone interval, in places shows an uneven to chaotic reflection pattern on seismic sections (Figs. 7.1.6 and 7.1.7). Locally the reflection pattern resembles weakly developed clinoform or channel features thus indicating higher energy conditions in the depositional system than just suspension fall out of mud. One scenario could be that they represent muddy delta progradation into lakes. However, for the moment the interpretation of the seismic reflection pattern remains highly speculative. The mudstone-dominated interval of the Detfurth Member shows an overall discontinuous parallel reflection pattern – locally showing onlap onto a basal reflector (Fig. 7.1.6). This reflection pattern probably reflects a drowning of the basal fluvial sandstones of the member followed by mud deposition by suspension fall out and partly mudflows in lacustrine playa-like environments.

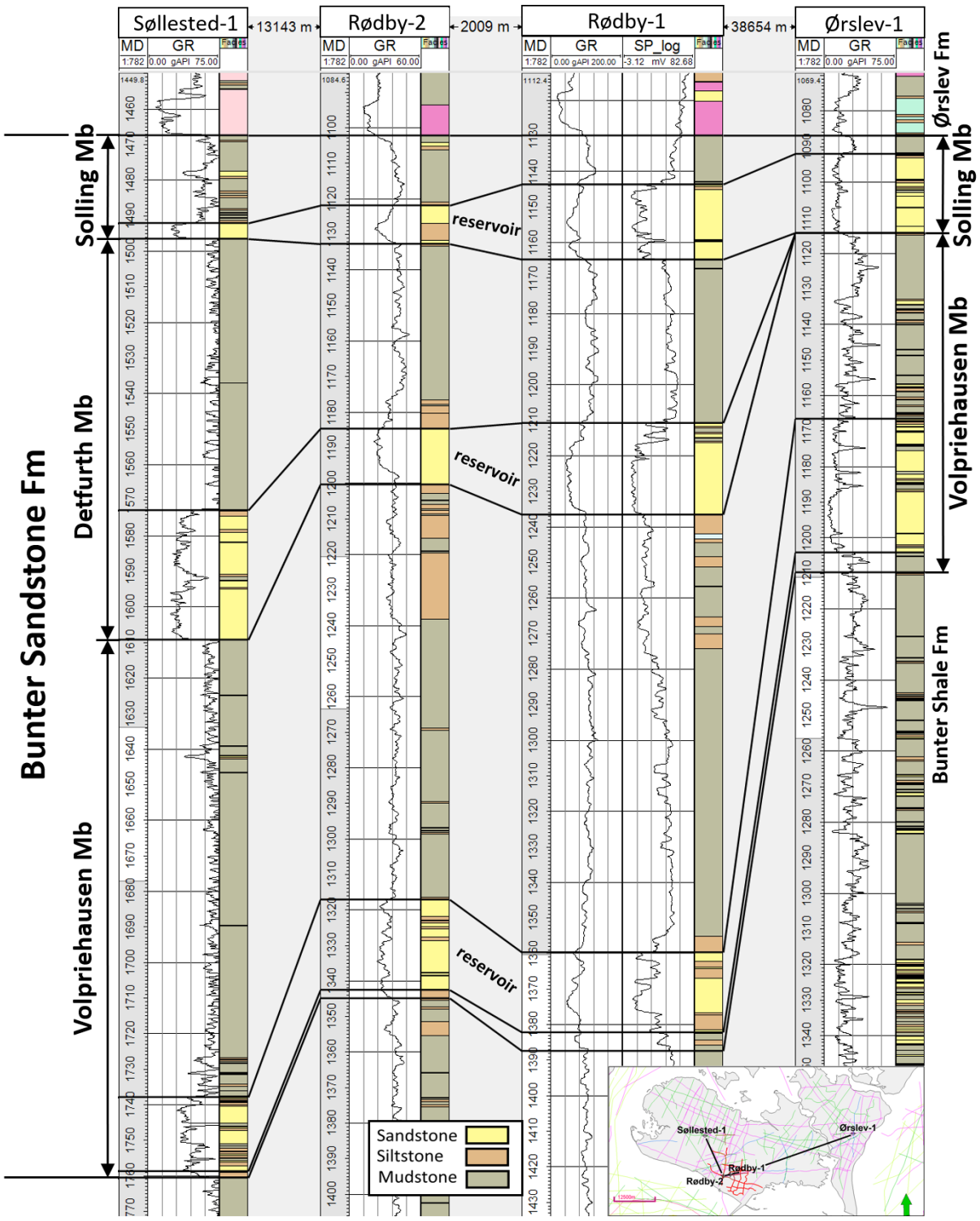

Figure 7.1.5. *Correlation panel of wells penetrating the Bunter Sandstone Fm in the Lolland–Falster area. The formation is subdivided into the Volpriehausen, Detfurth and Solling members of which the Detfurth Mb is absent in the Ørselv-1 well situated closer to the Ringkøbing–Fyn High. The basal sandstone-dominated parts of the members constitute separate reservoir intervals in the formation and are herein informal named after their associated member as outlined for the Rødby-1 well in Figure 7.1.8. The top of the Bunter Sandstone Fm is used as datum line in the panel. Lithology legend for the Bunter Sandstone Fm and location of the log panel is shown in the lower part of the figure.*

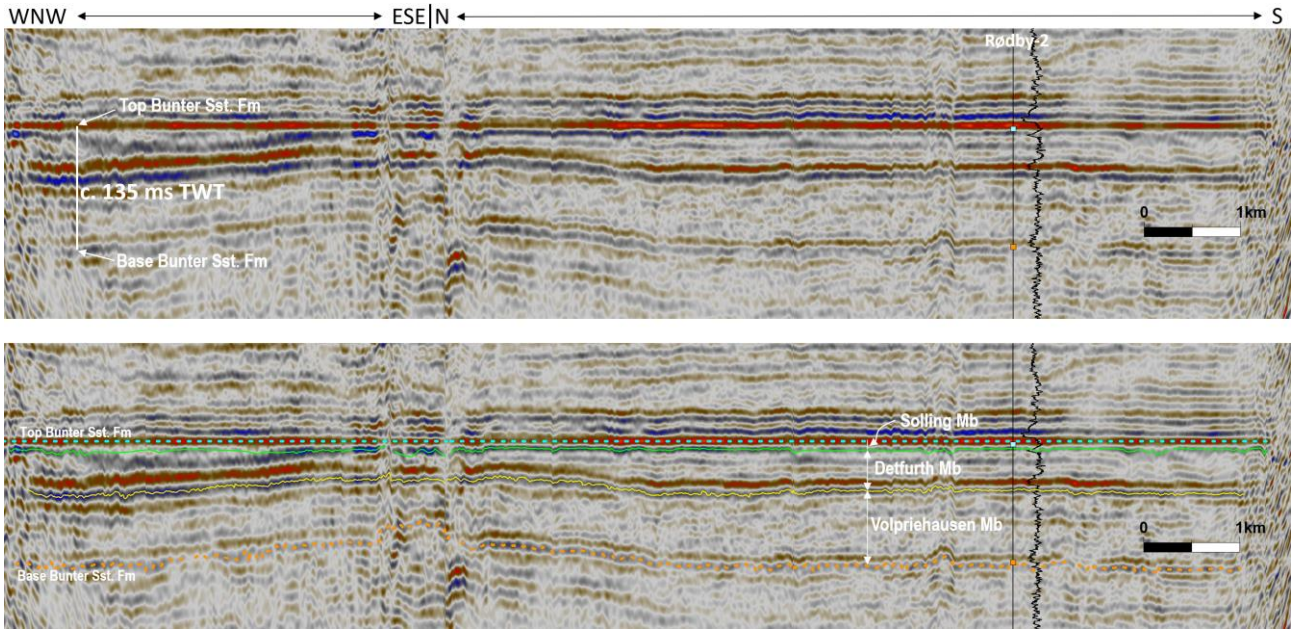

Figure 7.1.6. *Mapping of the Volpriehausen, Detfurth and Solling members of the Bunter Sandstone Fm along the reprocessed seismic line P10 (location shown in Fig. 4.2.1). The seismic section is in two-way time and is flattened at the Top Bunter Sandstone Fm surface. The basal sandstone intervals of the members correspond to a single reflector. Notice among others the uneven to chaotic reflection pattern of the fine-grained interval of the Volpriehausen Mb that in places resemble clinoforms, and an onlapping reflector within the Detfurth Mb in the central part of the section (discussed in text). The Rødby-2 well and its associated gamma-ray log well is projected onto the section from c. 115 m distance.*

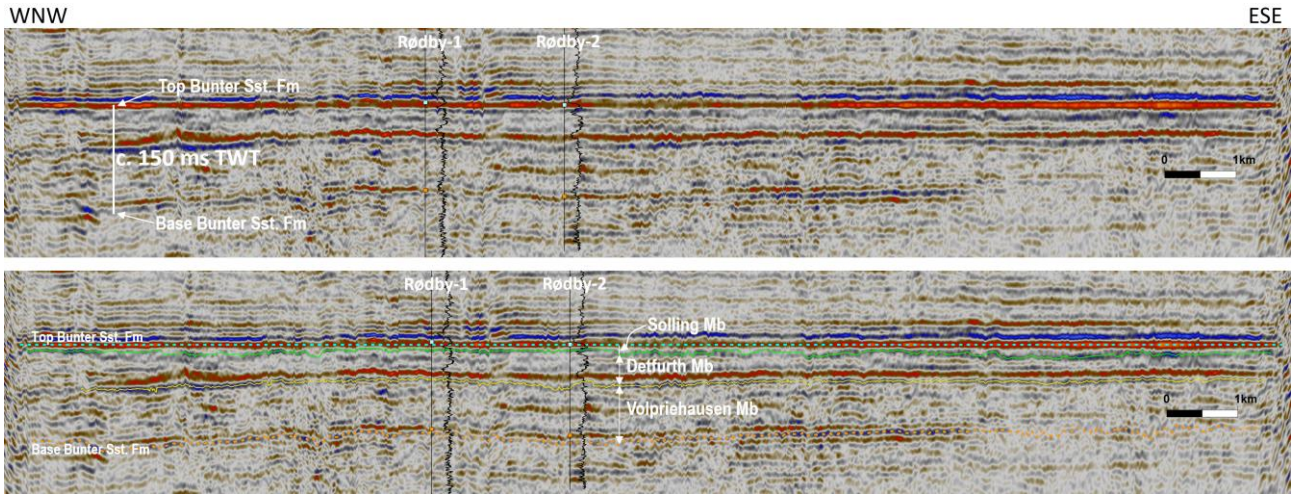

Figure 7.1.7. *Mapping of the Volpriehausen, Detfurth and Solling members of the Bunter Sandstone Fm along the reprocessed seismic line P9 (location shown in Fig. 4.2.1). The seismic section is in two-way time and is flattened at the Top Bunter Sandstone Fm surface. The basal sandstone intervals of the members correspond to a single reflector. Notice among others the uneven reflection pattern of the Volpriehausen Mb that in places resemble clinoforms, and the in comparison more discontinuous reflection pattern of the Detfurth Mb. The Rødby-1 and -2 wells and their associated gamma-ray logs are projected onto the section from c. 250 m and 970 m distance, respectively, causing some minor misfits between the gamma-ray logs and the interpreted seismic horizons.*

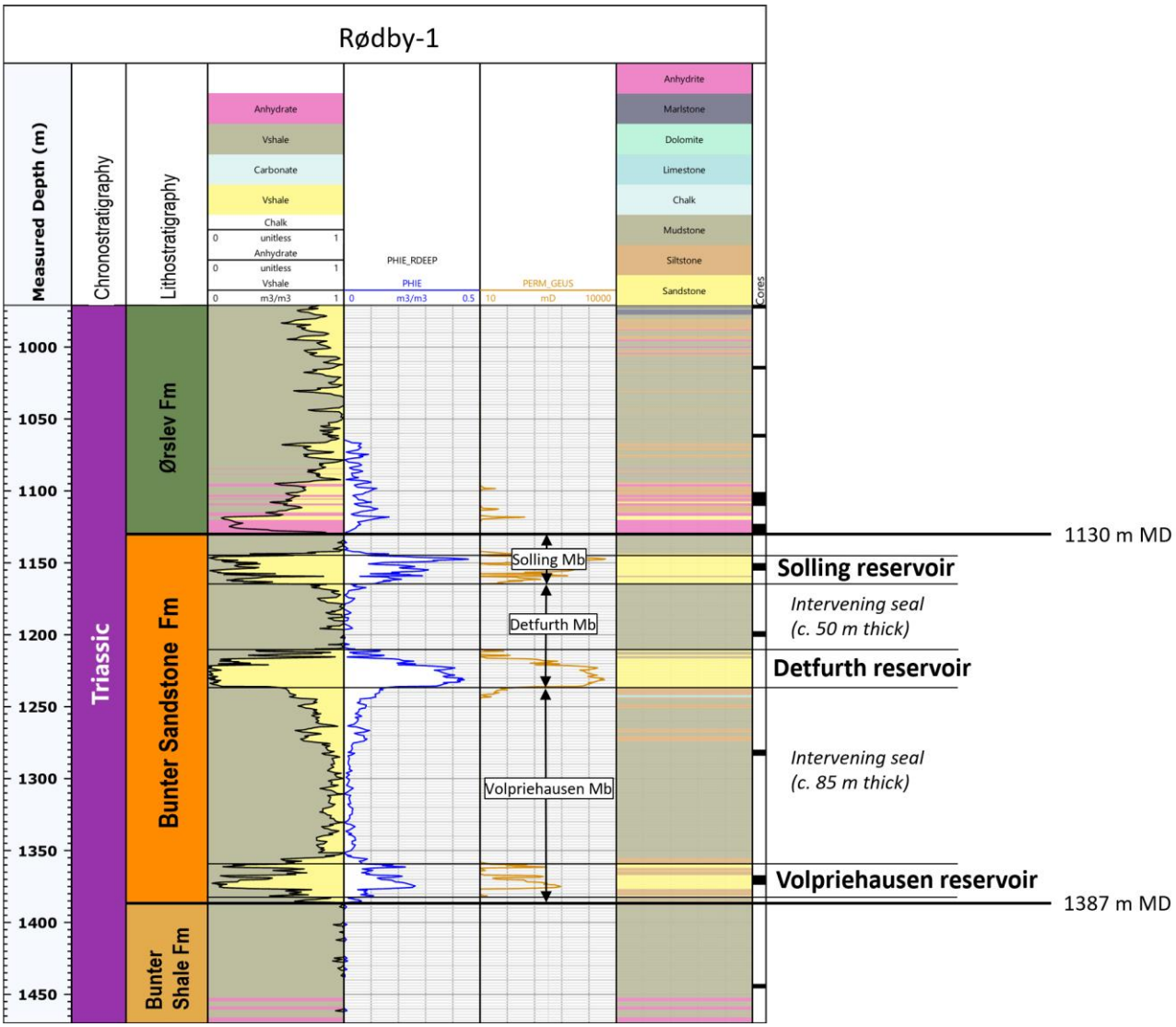

Figure 7.1.8. *The Bunter Sandstone Fm and its subdivision into members in the Rødby-1 well. Rødby-1 is the only well in the Lolland–Falster area that has cored intervals of the Bunter Sandstone Fm (the cored intervals are marked with black boxes on the log to the right). Three sandstone intervals are separated by thick mudstone intervals which may function as internal seals. The sandstone intervals are treated as separate reservoirs and are informal named after the members they are associated to.*

Lithology and provenance: According to descriptions of drill cuttings and cores given in completion reports of the Rødby-1, Rødby-1, Ørslev-1 and Søllested-1 wells, the grain size of the sandstones is mainly very fine to fine, locally medium to coarse grained (DGU/DAPCO 1952, 1953; Gulf Denmark 1968; Dansk Boreselskab 1983). The sandstones may be slightly clayey and contain lumps or thin layers of anhydrite or carbonate. Information on the degree of sorting and rounding is scarce but is in some of the completion reports described as being mainly moderately sorted and sub-rounded to rounded. Both calcareous and non-calcareous sandstones occur, and in general they are firm to hard, although the degree of cementation is not described in detail. Cores of the Bunter Sandstone Formation in the Rødby structure is limited to a few short cores in the Rødby-1 well (Figs. 7.1.3, 7.1.8 and 7.1.9).

For a general description of the mineralogical composition and diagenesis of the Bunter Sandstone Formation in the Danish onshore area see Olivarius et al. (2015, 2017). This also includes a zircon analysis of a sandstone sample from the Solling Member in the Rødby-1 well, indicating that the sand was sourced from the Ringkøbing–Fyn High.

Figure 7.1.9. *Cores of the Bunter Sandstone Fm in the Rødby-1 well showing the characteristic reddish-brown colour of the formation, however in places also with light greenish intervals or spots, probably reflecting local reducing conditions. Core diameter is c. 8.5 cm. Cored intervals are marked on the petrophysical log of the well in Figures 7.1.3 and 7.1.8.*

7.1.3 Reservoir quality (porosity and permeability):

The reservoir quality of the Bunter Sandstone Formation in the Rødby structure will in the following be estimated for the formation as a whole and for each of the three sandstone reservoirs it contains as mentioned in the previous section. Also, the chemistry of the formation water will be assessed.

The porosity variations have been determined based on interpretation of well log data from the four wells in the Lolland–Falster area that are calibrated to the core measurements and cutting descriptions, whereas the permeability estimates are based on specific porosity-permeability relationships set up for the Bunter Sandstone Formation based on core measurements that includes additional onshore Danish wells located in the North German Basin (Arnum-1, Hønning-1, Rødby-1, Tønder-3, -4 and -5).

When using log data, core analysis data and presumed porosity-permeability relationships, the various reservoir sandstone units can be characterized by generalized reservoir parameters, including net sand thickness, porosity, shale volume and permeability as tabulated below (Table 7.1.2). The table summarizes the results of existing well-log interpretations and current permeability assessments. Similarly, the net sand thickness varies in terms of shale volume, porosity and well location. Herein 'Net sand' is defined as sandstone intervals characterized by fairly high porosities (> 10%) and low shale content (< 50%). In addition to the actual estimates for the individual wells, there has been two average scenarios estimated, *i.e.* the average for all four wells and for the two Rødby wells alone. These will constitute the basis for the estimations used in the following chapters of this report.

Average porosities of the Rødby-1 and -2 wells for the reservoir zones of the respective members are 24.1 % for the Solling reservoir, 28.6 % for the Detfurth reservoir, and 16.3 % for the Volpriehausen reservoir. The Detfurth reservoir thus is characterized by the highest average porosities as well as the greatest net thickness, which might be attributed to the depositional and compositional differences between the reservoir intervals. The Detfurth reservoir sandstone is likely comprised by well-sorted aeolian sands that contains less anhydrite compared to the two other reservoir units.

Table 7.1.2. *Reservoir parameters for the Bunter Sandstone Formation Reservoir Zones relevant to the Rødby structure, including average values for all four wells and for the two Rødby wells, respectively.*

Well	Zones	Top	Gross	Net	N/G	Vshale	PHIE	PERM
		m	*m*	*m*		*v/v*	*%*	*mD*
Søllested-1	Solling	1492.0	4.4	3.1	0.72	0.12	14.3	110
	Detfurth	1572.8	36.3	30.9	0.85	0.22	16.9	293
	Volpriehausen	1737.8	21.2	9.4	0.45	0.33	13.1	70
Rødby-2	Solling	1121.8	10.7	6.1	0.57	0.34	25.3	662
	Detfurth	1184.6	15.5	15.2	0.98	0.16	25.5	765
	Volpriehausen	1317.0	25.3	14.6	0.58	0.26	14.0	49
Rødby-1	Solling	1143.8	20.8	18.7	0.90	0.21	22.8	727
	Detfurth	1210.8	25.6	22.0	0.86	0.11	31.6	2029
	Volpriehausen	1359.6	22.4	13.2	0.59	0.23	18.6	187
Ørslev-1	Solling	1091.9	22.3	15.8	0.71	0.28	18.4	198
	Detfurth	Not present						
	Volpriehausen	1166.5	37.5	20.8	0.55	0.09	21.1	327
Average All	Solling		14.5	10.9	0.72	0.24	20.2	424
	Detfurth		25.8	22.7	0.90	0.16	24.7	1029
	Volpriehausen		26.6	14.5	0.54	0.23	16.7	158
Average Rødby	**Solling**	**1132.8**	**15.7**	**12.4**	**0.73**	**0.28**	**24.1**	**694**
	Detfurth	**1197.7**	**20.6**	**18.6**	**0.92**	**0.13**	**28.6**	**1397**
	Volpriehausen	**1338.3**	**23.8**	**13.9**	**0.59**	**0.25**	**16.3**	**118**

Figure 7.1.10 displays the conventional core porosity and permeability analysis available from the onshore wells Arnum-1, Hønning-1, Rødby-1, Tønder-3, -4 and -5, as reported by Olivarius et al. (2015), where also a best-fit power function of the sandstone plots is superimposed. This correlation is used for estimating permeabilities in un-cored zones within the Rødby structure, meaning that the permeability assessments presented in Table 7.1.2 are derived from log data.

Only the core measurements performed in sandstones constitute the basis for the porosity-permeability relationship, hence the data points denoted as siltstones, heteroliths and claystones do not contribute. Furthermore, it is seen that most of the sandstone is characterized as being fine grained, and that almost all medium grained sandstone data points are located above the best-fit function curve whereas the fine-grained sandstone data points are more evenly distributed around the curve. For given porosities, higher permeabilities are thus obtained if the grain size is medium compared to fine. The grain size influencing the porosity-permeability relationship is also known from other studies, e.g. of the Upper Triassic – Lower Jurassic Gassum Formation (Weibel et al. 2017).

As there here is presented a mathematical relation of the permeability as a function of the porosity, the Detfurth reservoir is also the one with the best average permeability (Table 7.1.2). Based on the analysis, the best reservoir properties are thus present in the Detfurth

reservoir, which has an average thickness in the Rødby-1 and -2 wells of 18.6 m, while ranging from 15.2 – 30.9 m within the study area (based on the four wells). The average log derived porosity, PHIE, in this reservoir zone is estimated to 28.6 % in the Rødby structure, while ranging from 16.9 – 31.9 % when including also the Søllested-1 well. The "regional range" in permeability thus varies similarly from 293 – 2029 mD.

The Solling reservoir has an average net thickness in the Rødby structure of 12.4 m, ranging between 3.1 – 18.7 m in the study area. The reservoir properties are described by the average PHIE of 24.1 % in the Rødby structure, varying between 14.3 – 25.3 % when also including the other wells. It follows thereof, that the average permeability in the Rødby structure is 694 mD, ranging from 110 – 727 mD within the study area.

The Volpriehausen reservoir has an average net thickness in the Rødby structure of 13.9 m, ranging from 9.4 – 20.8 m when also including the other wells. Within the study area the PHIE range is 13.1 – 21.1 %, while the average for the Rødby wells is 16.3 %. Hence, the derived permeabilities range from 49 – 327 mD, averaging 118 in the Rødby structure.

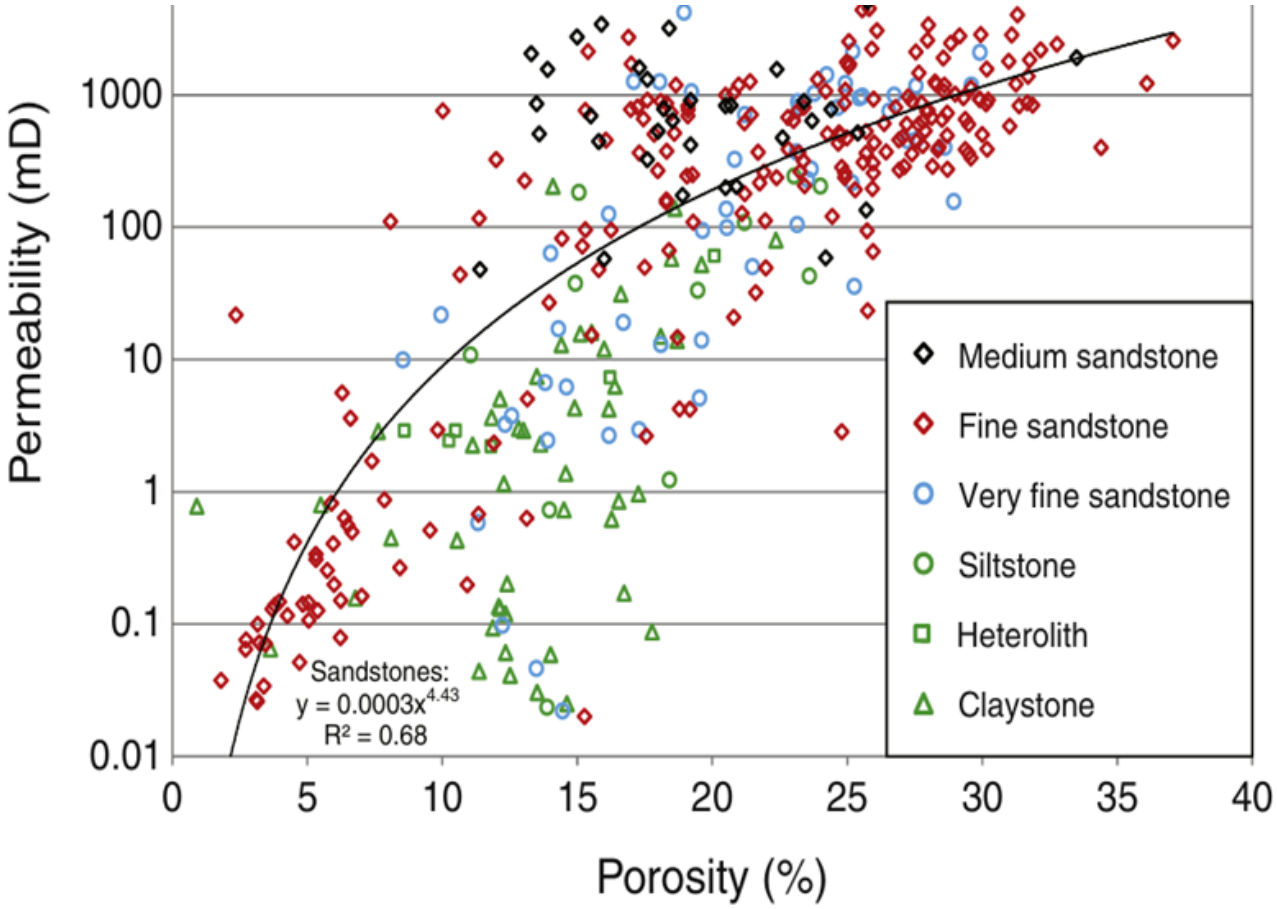

Figure 7.1.10. *Porosity-permeability plots for the Bunter Sandstone Fm based on conventional core analysis data from onshore Danish wells (Arnum-1, Hønning-1, Rødby-1, Tønder-3, -4 and -5) located in the North German Basin (Olivarius 2015). The black line is the best fit power function for the sandstone plots.*

7.1.4 Assessing the Formation Water chemistry in the Rødby structure

Risks associated with formation water composition.

Understanding the significance of salt content in the context of CO_2 storage is important for several reasons:

Corrosion and material selection: High salt concentrations can accelerate corrosion in the materials used for storage wells and associated infrastructure. This can lead to increased maintenance costs and potential safety risks. An accurate assessment of salt content is crucial for selecting the right materials and designing effective corrosion protection systems.

Scaling and operational efficiency: Salts, especially when present in high concentrations, can precipitate and form scales inside the storage reservoir and in the equipment. Scaling can reduce the efficiency of CO_2 injection and retrieval processes, potentially leading to operational challenges and increased costs.

CO_2 solubility and storage capacity: The solubility of CO_2 in formation water is affected by the salinity of the water. Higher salt content typically reduces the solubility of CO_2, which could impact the overall storage capacity of the reservoir. Understanding the salt content helps in accurately estimating how much CO_2 can be stored.

Geochemical reactions and long-term stability: Salt content can influence the geochemical reactions between CO_2, formation water, and reservoir rocks. These reactions are crucial for the long-term stability of stored CO_2. Predicting and monitoring these reactions require a thorough understanding of the formation water chemistry, including its salt content.

Background and Challenges in the Rødby Area: In the Rødby region, there are no direct measurements of formation brine chemistry, leading to uncertainties in pre-drilling evaluations. The composition of formation water in onshore Denmark is best documented in the Danish Basin. Here, it is known to vary both geographically and with burial depth, as highlighted in studies by Laier (2002, 2008) and Holmslykke et al. (2019). These compositional variations reflect the depositional environment, associations with underlying deposits, water expelled from these deposits, and mineral reactions occurring during burial, as noted by Weibel et al. (2020).

Comparative Analysis from the North German Basin: In the Danish part of the North German basin, detailed analyses of formation water chemistry are limited, with significant studies conducted only in the Tønder and Sønderborg areas. In Tønder, the Bunter Sandstone Formation exhibits very high salinity levels, often oversaturated with respect to halite (Holmslykke et al. 2019). This unique scenario is interpreted as a consequence of the presence of underlying Zechstein salt and overlying Röt salt thus embracing the Bunter Sandstone Formation.

Distinctive Conditions in Rødby: Contrasting Tønder, the Rødby area may present a different scenario. While halite is present in the underlying Zechstein deposits, as evidenced by findings from the Rødby-1 and 2 wells, no halite was observed in the cuttings from the overlying Ørslev and Falster formations during drilling of these wells. This suggests that the Rødby area may not closely parallel the formation water chemistry found in the Tønder area. This

hypothesis is further supported by new interpretations of log data from boreholes in Lolland–Falster (Rødby-1, Rødby-2 and Ørslev-1), which do not indicate thick halite layers (up to 10 meters) above the Bunter Sandstone Formation in the Ørslev Formation (Röt) as previously interpreted. In contrast to this, the presence of rock salt was mentioned in the Final Well Reports of the Søllested-1 and Ørslev-1 wells from the Triassic interval, and the occurrence of salt in Søllsted-1 is also collaborated by new well log interpretations. In the Ørslev-1 well, the Triassic was described as having seams of halite similar as in Søllested-1, however the new wire-line log interpretation is ambiguous with respect to this occurrence.

Methodology for Estimating Salinity in Rødby: For evaluating the formation water chemistry in Rødby, we have utilized the relationship between geological depth and salinity established from the Danish Basin (7.1.11). Based on this approach, we estimate that at the depth of the Bunter Sandstone Formation in Rødby (approximately 1250 m), the formation water's chloride concentration is likely to range 85,000 ppm from a (low case) of 115,000 ppm Cl^- (corresponding to 190,000 mg/l Total Dissolved Solids (TDS)) to a high case of 200,000 ppm Cl^- (330,000 mg/l TDS) representing approx. halite saturated conditions. The higher level would be more plausible if the Tønder area were a close analogue to Rødby. However, the juxtaposition of findings from various wells in the area around Rødby mentioned above highlights the complex and heterogeneous nature of formation water chemistry in this region. In Rødby, we thus currently estimate a mean case scenario (P50) of approximately 170,000 ppm Cl^- (280,000 mg/l TDS). This level is slightly lower than the saturated salinity level measured in the Tønder area and in the Zechstein at Ørslev-1 (190 000 ppm Cl^- at 1510 m – see FWR of well). The estimate thus ranges from full saturated conditions at 200,000 ppm Cl^- to a minimum of 115,000 ppm Cl^- representing the salinity expected at the depth of interest in the Danish Basin (c.f. Laier 2008).

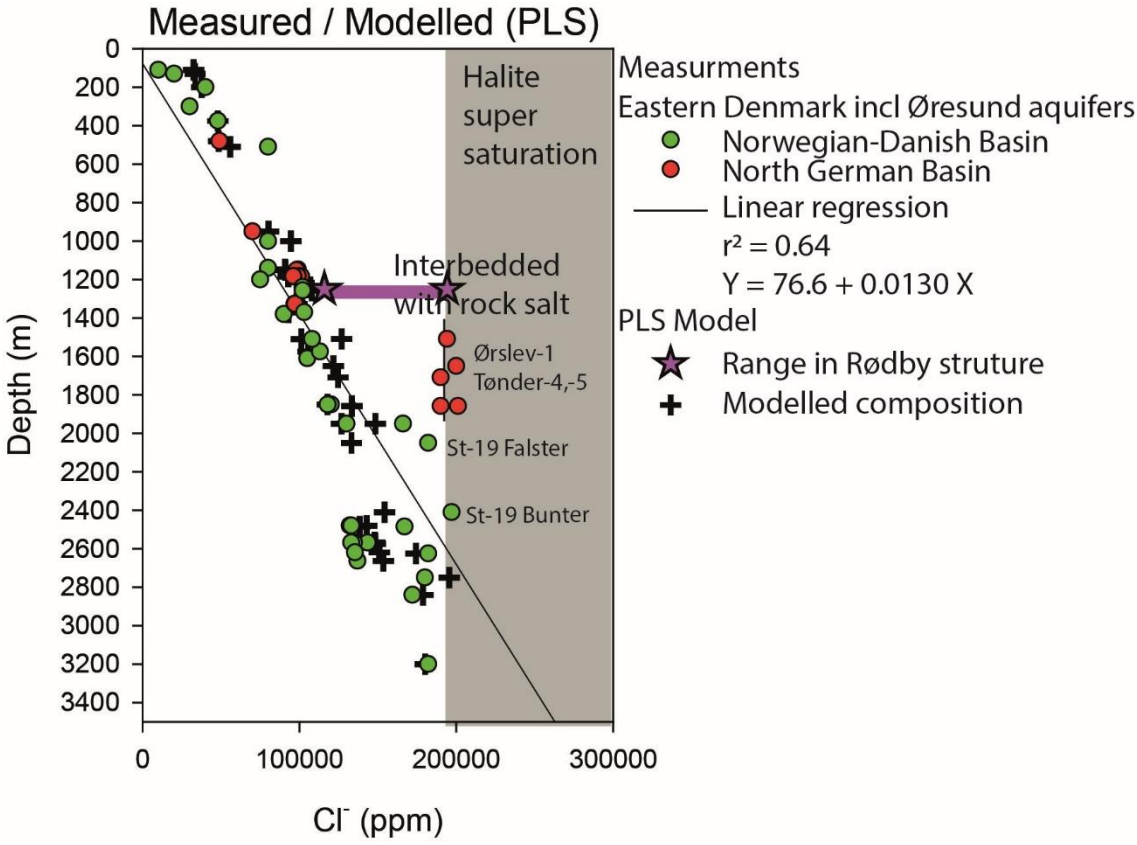

Figure 7.1.11. *Salinity with depth in Eastern Denmark and the Øresund Area illustrating the likely range in Cl concentration in the Rødby structure at a depth of 1250 m within the Bunter sand. This figure is derived from the data compilation by Laier (2008), incorporating minor updates based on recent findings in Holmslykke et al. (2019) and the Final Well Report (FWR) from the Ørslev-1 well. Modelled salinity (PLS model) is based on a numerical analysis (GEUS, unpublished; pers. com Niels Schovsbo). Field of halite (NaCl) supersaturation (grey) assumes stoichiometric concentration of Na^+ is loosely based on Holmslykke et al. (2019). No account for temperature and pressure effect has been made on the solubility.*

7.2 Seals – Summary of geology and parameters

7.2.1 The seals of the Bunter Sandstone reservoirs; Bunter Sandstone, Ørslev and Falster formations

Sealing units of Bunter Sandstone reservoirs in the Rødby area comprise intraformational mudstones of the Bunter Sandstone Formation and the overlying main seal of the Lower–Middle Triassic Ørslev and Falster formations (Fig 7.1.3, Mathiesen et al. 2022).

The three intraformational mudstone units of the Bunter Sandstone Formation comprise fluvial plain – lacustrine fine-grained deposits overlying the individual reservoir units of the Solling, Detfurth and Volpriehausen members (Fig. 7.1.5.). In the Rødby-1 and -2 the thicknesses of these sealing units are 13–20 m (Solling), 45–51 m (Detfurth) and 123–117 m (Volpriehausen), respectively.

The Lower – Middle Triassic Ørslev Formation comprises evaporitic – restricted marine evaporites and mudstones. In the Rødby-1 and -2 wells the formation is 153–160 m thick. For reference the top of the Ørslev Formation is situated 975 m b. msl. at Rødby-1. The overlying Middle Triassic Falster Formation consists of restricted marine to open marine marlstones, limestones, mudstones and evaporites (Bertelsen 1980). In the Rødby-1 and -2 wells the formation is 174–182 m thick. The top of the Falster Formation is situated at 782 m b.msl. and 786 m below terrain at Rødby-1; the uppermost part of the Falster Formation is thus not considered part of the seal with regards to the critical depth of 800 m for CO_2 storage.

The formations are defined in deep wells in the Lolland – Falster area in SE Denmark by Bertelsen (1980). A revision of the Triassic lithostratigraphy in Denmark was suggested by Michelsen & Clausen (2002), and they adapted the nomenclature from Germany and The Netherlands. In this report we retain the lithostratigraphic nomenclature of Bertelsen (1980) for the Middle–Upper Triassic as these units in general represent more basin marginal settings compared to the German – Netherlands units that mainly define the stratigraphy in deeper basinal part and southern parts of the North German Basin (Boogaert & Kouwe 1994). The lithostratigraphic correlation to the units of the North German Basin is however shown in Figure 3.3.

The Bunter Sandstone, Ørslev and Falster formations are distributed in the northern part of North German Basin and partly into the Danish Basin. The thicknesses of sedimentary units generally decrease northwards towards the structural highs of the composite Ringkøbing – Fyn High (RFH). A marked unconformity marks the top to the Falster Formation in the Rødby area (Fig. 3.3). The Tønder Formation is thus absent here and the overlying Oddesund

Formation is relative thin compared with wells towards the west (Clausen & Pedersen 1999) and north of RFH (Michelsen & Clausen 2002).

The seal performance to the Bunter Sandstone reservoirs onshore Denmark is only known from the Tønder area where a small nitrogen gas cap in a sandstone interval within the Bunter Sandstone Formation was observed to be sealed off by overlying mudstones in the uppermost part of the formation in the Tønder-1 well (DAPCO 1952). Few Gas fields in UK North Sea have also shown that the seal has proven effective on geological time scale (Ketter 1991, Brook et al. 2003, Heinemann et al. 2012). The sandstones of the Bunter Sandstone Formation are also proven petroleum plays in the southern part of the South Permian Basin (Kortekass et al. 2018). Here the effective sealing units comprise evaporites (halites) of the Röt Formation or mudstones of the Solling Member (Bunter Sandstone Formation). In anticipation that these sealing units are analogous to the succession onshore Denmark, the petroleum plays are positive indications for the sealing effectiveness onshore Denmark.

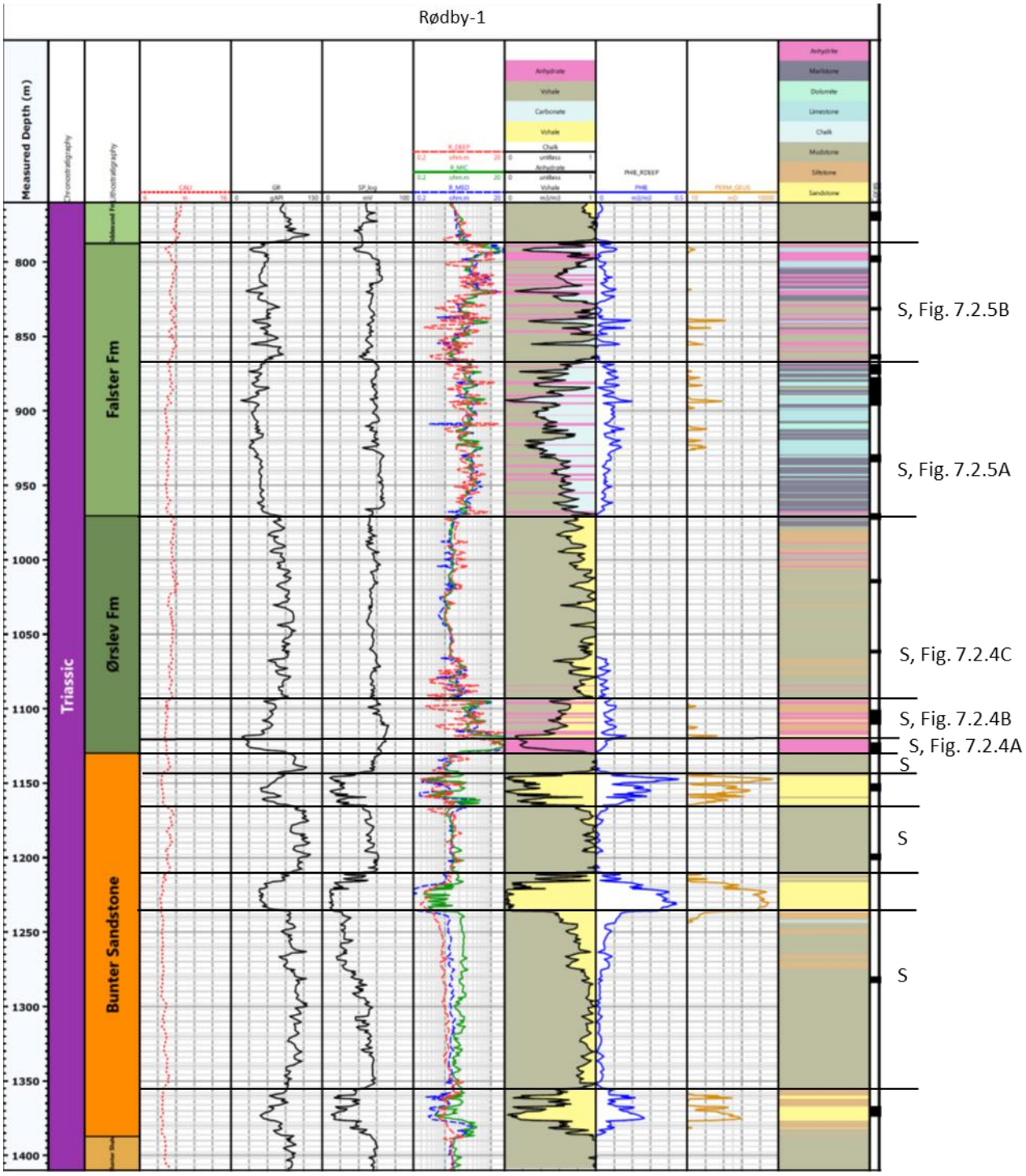

Figure 7.2.1. *Lithostratigraphic subdivision of the Rødby-1 well with interpreted lithology and formations based on petrophysical log interpretation and information from core data, cutting samples. To the right in the figure, the letter S indicates the presence of three intraformational seal units in the Bunter Sandstone Fm, three seal units in Ørslev Fm and two seal units in Falster Fm.*

The Ørslev and Falster formations are encountered in several wells onshore Denmark. The Rødby-1 and Rødby-2 wells penetrate the Rødby structure, and laterally, data from the Søllested-1 and Ørslev-1 are included in evaluation of the seal. The Rødby-1 well includes core

material from selected intervals of the Bunter Sandstone, Ørslev and Falster formations. XRF geochemistry, TOC content, thermal maturity and photos of cuttings are available from Rødby-1 and Søllested-1 in Schovsbo & Petersen (2024).

The ages of the Bunter Sandstone, Ørslev and Falster Formations are poorly constrained due to lack of age diagnostic biota in the strata. Bertelsen (1980) suggest a late Induan – early Olenekian age for the Bunter Sandstone Formation and brackets the combined Ørslev and Falster formations in late Olenekian – early Ladinian. Similar ages are suggested by Michelsen & Clausen (2002) although they refer the Ørslev and Falster formations to the German and The Netherlands lithostratigraphic nomenclatures of the Röt Formation and Muschelkalk Formation, respectively.

7.2.2 Lithological subdivision and depositional environment

The lithological description is based on representative cored intervals in Rødby-1, cutting sample descriptions and petrophysical log interpretation (Fig. 7.2.1). The seal thicknesses, given below, is based on the Rødby-1 and Rødby-2 wells.

The Solling, Detfurth and Volpriehausen reservoir units are each overlain by intraformational fluvial plain – lacustrine mudstone units. The Volpriehausen Member mudstones are 117–-123 m thick and is represented by one cored interval (4.200'–4.212'/1280–1284 m) (Fig. 7.1.3) which consist of reddish-brown mudstones (Fig 7.1.9). The core is in poor condition and the original description in the well report indicate that the mudstones were sticky and fragmented during the drilling process (DAPCO 1952). Hard parts comprise siltstone with fractures along apparent horizontal bedding planes. The petrophysical log interpretation shows that the succession has common to dominating siltstones in the upper 40 m.

The Detfurth Member mudstones are 45–53 m thick and is represented by one cored interval (3.930'–3.941'/ 1198–1201 m) (Fig. 7.1.3), which consists of mainly reddish-brown silty mudstones with few greenish bands, and few thin sand laminae (Fig 7.1.9). The core is well preserved and show common planar lamination. The petrophysical log interpretation shows that the succession solely consists of mudstones with slightly fluctuating GR readings.

The Solling Member mudstones are 13–20 m thick and have no cored intervals. The petrophysical log interpretation shows that the succession solely consists of mudstones with slightly fluctuating GR readings.

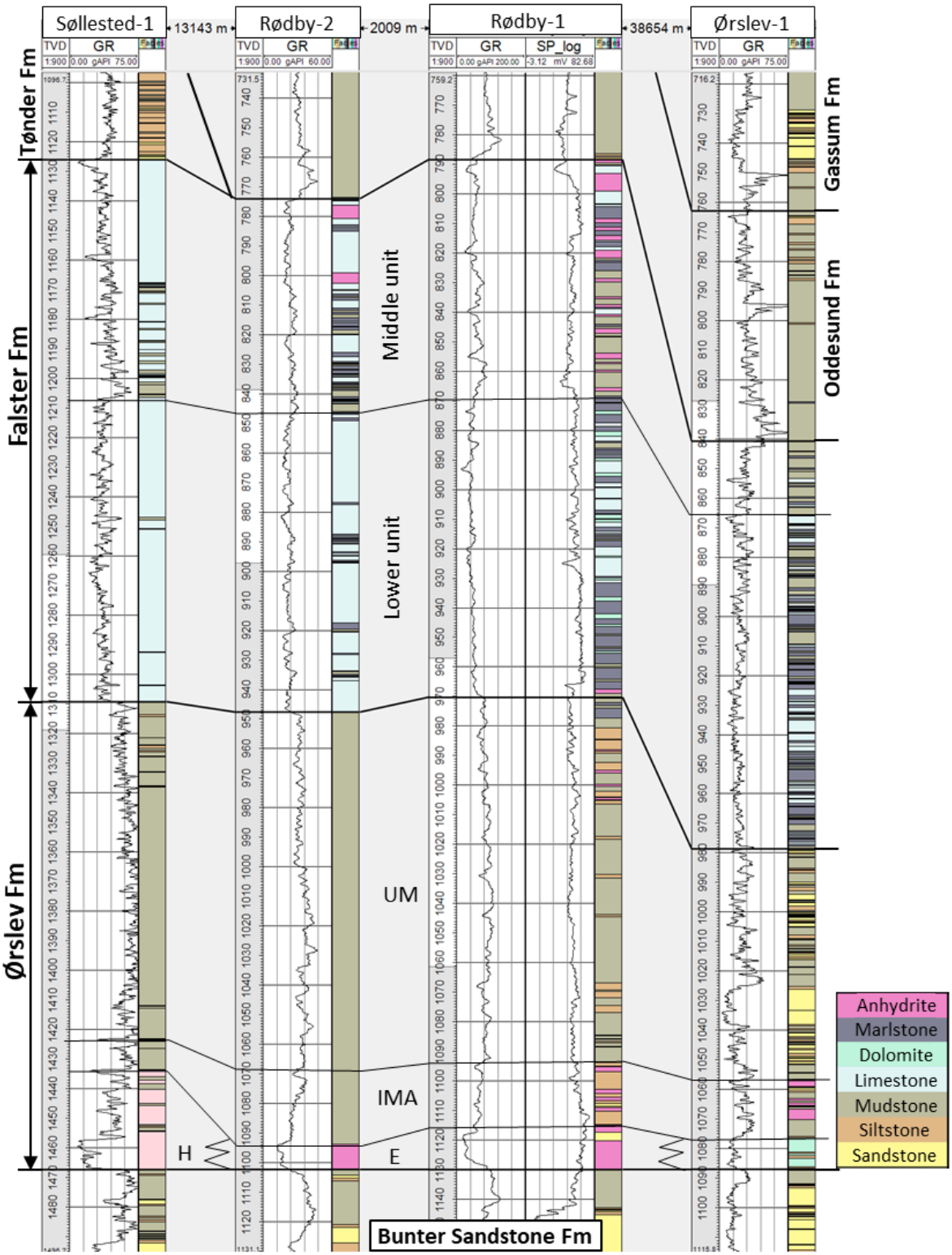

Figure 7.2.2. *Correlation panel of wells penetrating the Ørslev and Falster formations in the Lolland–Falster area. The formations are subdivided into intervals/sections representing individual sealing units. Ørslev Fm: H basal halite unit, E, basal evaporite unit, IMA Intermediate mudstone and anhydrite unit, UM Upper mudstone unit. Falster Fm: lower and middle units. The base of the overlying Oddesund Fm is a marked unconformity and the upper unit of the Falster Fm and the Tønder Fm are missing in Rødby-1, -2 and Ørslev-1. The top of the Bunter Sandstone Fm is used as datum line in the panel.*

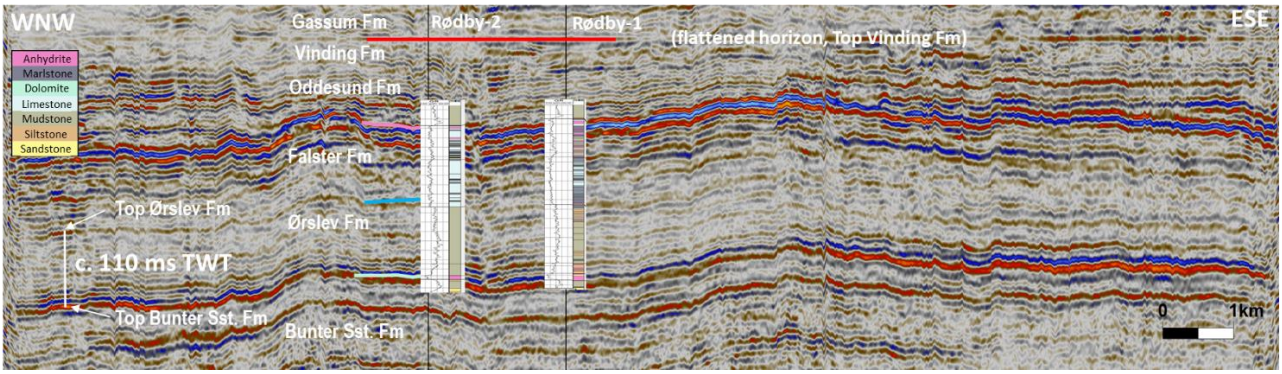

Figure 7.2.3. *Seismic line P9 showing the reflectivity in the sealing units of the Ørslev and Falster formations. The seismic section is in two-way time and is flattened at the Top Vinding Fm surface. The position of the Rødby-1 and -2 wells are shown with gamma-ray logs and interpreted main lithologies from the Ørslev and Falster formations. The wells are projected onto the section from c. 250 m and 970 m distance, respectively, causing some minor misfits between the gamma-ray logs and the interpreted seismic horizons. The basal evaporite of the Ørslev Fm corresponds to a single high amplitude reflector, the overlying mudstone dominated succession of the formation is characterised by parallel low amplitude reflectivity. The Falster Fm shows mainly high amplitude parallel reflectivity representing the heterogenous succession of limestones, dolomites, marls, mudstones, and marlstones. Location of seismic line P9 is shown in Fig. 4.2.1.*

The Ørslev Formation in the Rødby-1 and -2 wells is represented by a heterogenous succession that is 153 m and 160 m thick, respectively (Fig. 7.2.2). It consists of evaporites; mainly anhydrites and dolomites interbedded with siltstones and claystones, that are succeeded by a claystone – siltstone succession (Figs 7.2.2, 7.2.4). The formation represents deposition in evaporitic to restricted marine environments. Laterally, halite forms the lower part in the deeper basinal areas e.g. to the south in Germany and the Netherlands and to the west e.g. in the Tønder area in Sønderjylland. Local deepening of the basin with halite deposition is also seen towards NW in Søllested-1 (Figs 7.2.2, 6.1.2). Regionally in the Danish Basin, the Ørslev Formation shows a northward transition into terrestrial deposits of the Skagerrak Formation.

The formation is equivalent to the Röt Formation in North Germany and The Netherlands, where the Röt Formation can be subdivided into six units; they are from stratigraphic below and upwards the Main Röt Halite Member, Main Röt Evaporite Member, Intermediate Röt Claystone Member, Upper Röt Evaporite Member and Upper Röt Claystone Member (Michelsen & Clausen 2002). The equivalent to the Main Röt Halite Member is not present in the Rødby wells but in Søllested-1 it is 35 m thick (Fig. 7.2.2). A basal Evaporite unit, 7–14 m thick is present in the Rødby wells and it consists mainly of anhydrite beds. It is equivalent to the Main Röt Evaporite Member. The overlying unit (IMA) is 21–26 m thick and comprises alternating anhydrite beds and silt-dominated mudstones in Rødby-1. Rødby-2 does not resolve the presence of anhydrite beds but mainly shows mudstones. The unit is probably equivalent to the Intermediate Röt Claystone Member. The upper unit (UM) of the Ørslev Formation is 120–124 m thick in the Rødby wells and correlates with the Upper Röt Claystone Member. The unit is dominated by mudstones that contain interbedded siltstone beds. Levels with anhydrites are few and thin, <1m in thickness.

A few measurements on plugs on anhydrite/dolomite show an estimated average porosity of c. 2% (Michelsen et al. 1981). The petrophysical derived porosity properties of PHIE are between <0.1 and 10% and the calculated permeabilities are general <1 mD with few thin sandy units between 10 and 100 mD in the Intermediate Mudstone Anhydrite unit.

Figure 7.2.4. *Photographs of the Ørslev Fm, Rødby-1 cores. A) Section from core 69, 3685'–3705' (1123–1129 m), Evaporite unit. Layered and nodular anhydrite, with occasional thin units of mudstones and sandstones. B) Section from core 67, 3612'–3628' (1101–1106 m), intermediate mudstone anhydrite unit of laminated greenish grey mudstones with few thin anhydrite layers, note desiccation crack to right. C) Section from core 65, 3480'–3485' (1061–1062 m), upper mudstone unit of reddish-brown mudstones and muddy sandstones with reduced greenish spots. Core diameter is 8.5 cm. Cored intervals are marked on the petrophysical log of the well in Figure 7.2.1.*

The Falster Formation is subdivided into three informal and unnamed main units (Bertelsen 1980, Clausen & Pedersen 1999) and has a thickness of c. 175 m in the Rødby wells. The lower unit is 95 m and 100 m thick in Rødby-1 and -2, respectively, and it consists of intercalated marl, limestone, and dolomite beds with minor thin anhydrites (Figs 7.2.2, 7.2.5). The limestone beds become more abundant and increase in thickness upwards and bivalve shells are common. The middle unit is 76–77 m thick and consists mainly of claystone beds with minor layers of marl, limestones, and anhydrites. The upper unit is only represented by a thin anhydrite dominated unit, 5–10 m thick. Laterally to the west the thickness increases to >50 m (Clausen & Pedersen 1999) and the unit comprises intercalated limestone, marl, claystone and anhydrite beds. The formation represents deposition under restricted to more open marine conditions, and it shows a northwards lateral transition into terrestrial deposits of the Skagerrak Formation. The transgressive character of the formation is indicated by a pronounced lateral extension of the upper unit far north into the Skagerrak Formation (Michelsen & Clausen 2002). The equivalent Muschelkalk Formation in the North German Basin represents shallow-marine to open-marine deposition in a basin rimmed by carbonate platforms, where a short period of restricted conditions resulted in evaporite deposition.

Figure 7.2.5. *Photographs of the Falster Fm, lower unit in Rødby-1 cores, A) Sections from core 62, 3050'–3065' (930–934 m) Slightly greenish light-grey laminated marlstones and limestones. B) Sections from 2880–2900' (878–884 m), marlstones, light brownish grey, with undulating and planar lamination and mottled bedding. Core diameter is 8.5 cm. Cored intervals are marked on the petrophysical log of the well in Figure 7.2.1.*

The top of the Falster Formation is truncated by the Upper Triassic (intra Carnian) unconformity in the Rødby-1, -2 and Ørslev-1 wells, and is overlain by mudstones of the Oddesund Formation. The Tønder Formation mudstones are thus absent along on the Rødby structure and northwards at the Ringkøbing – Fyn High (Clausen & Pedersen 1999).

The porosity and permeability of the formation is poorly known; a few measurements on plugs of marl and claystones record estimated average porosities of 14% and 21%, respectively (Michelsen et al. 1981). The petrophysical derived porosity properties of PHIE are consistent between 5 and 10% with a few thin units <2 m thick showing PHIE of 10–20%. The calculated permeabilities are generally <0.1 mD but show values between 10 and 100 mD in the relatively high porosity units.

Table 7.2.1. *Depths to the Top and Base of the Ørslev Fm and its thickness in Rødby-1 and -2 and the nearest wells of Søllested-1 and Ørslev-1. The base of the Ørslev Fm is marked by the base of the first occurring evaporitic or carbonate deposit (implying minor deviations from the depths given in Nielsen & Japsen 1991).*

Well	True Vertical Depth (meter below Kelly Bushing)		Depth, meter below mean sea level	Thickness (m)
	Top Ørslev Fm	Base Ørslev Fm	Base Ørslev Fm	
Rødby-1	970	1130	1125	160
Rødby-2	949	1102	1108	153
Søllested-1	1310	1467	1458	157

Ørslev-1	979	1087	1065	108

Table 7.2.2. *Depths to the Top and Base of the Falster Fm and its thickness in Rødby-1 and -2 and the nearest wells of Søllested-1 and Ørslev-1.*

Well	True Vertical Depth (meter below Kelly Bushing)		Depth, meter below mean sea level	Thickness (m)
	Top Falster Fm	Base Falster Fm	Base Falster Fm	
Rødby-1	788	970	965	182
Rødby-2	775	949	941	174
Søllested-1	1125	1310	1299	185
Ørslev-1	826	979	957	153

7.2.3 Clay minerals

No data exists on clay mineralogy Lower–Middle Triassic succession i.e. from the mudstone units of the Bunter Sandstone Formation, or from the Ørslev and Falster formations in the Rødby-1, -2 wells or from wells in the vicinity.

7.2.4 Burial and exhumation

Vitrinite reflectance values are a proxy for maximum temperatures during burial. Petersen et al. (2008) measured 560 vitrinite reflectance (VR) values in samples from 26 wells in the Norwegian–Danish Basin and concluded that the Fjerritslev Formation experienced a significant post Early Cretaceous uplift in most of the basin.

Present-day depths based on chalk sonic velocities must be corrected for net-exhumation of 473 m in the Rødby-1 well and 362 m in the Ørslev-1 well further to the east (Japsen & Bidstrup 1999). Correction for net-exhumation shows that the maximum burial depth of the base Ørslev Formation in the Ørslev-1 well was only 1457 m, and aligned with the vitrinite reflectance (VR) measurements, this reveals that the Triassic in the well is thermally immature (Petersen et al. 2022). Correction for net-exhumation of the present-day depths in the Rødby-1 well indicates that the Base Ørslev-1 Formation has been buried to a maximum depth of 1604 m. Using the net-exhumation depth corrected VR curve in Petersen et al. (2022), this shows that the Triassic in this well likewise is thermally immature.

7.2.5 Characterization of the seal in Rødby-1 well by HH-XRF, organic geochemistry and photos of cuttings samples

Schovsbo and Petersen (GEUS report 2024/10 in prep) have reported new data from the Rødby-1 and Søllested-1 wells relevant for seal integrity evaluation. Here the main results are presented to compliment the description of the sealing sections in the Rødby structure.

The Rødby-1 well was spudded 1/11-1958. A few cores were cut, and a limited wireline logs suite was acquired. The hole condition was generally good and no large fall out zones were identified as the hole diameter varies between 8–10 inch. A total of 76 cuttings were selected for HH-XRF analysis (sample 934–1045) and 95 cuttings pictures (photos IMG_0877–IMG_0970) were taken in the interval 760–1380 m in the Falster, Ørslev, Bunter Sandstone and top Bunter Shale formations. The Søllested-1 well was spudded 27/10-1982. No cores were taken. The available material was insufficient for HH-XRF analysis and hence no data was acquired. However, 120 images of cuttings samples were recorded (photos IMG0764–IMG0876) between 880 and 1755 m measured depth (MD) encompassing the Gassum, Vinding, Oddesund, Tønder, Falster, Ørslev and Bunter Sandstone formations.

The colour of the cutting material for both wells are generally light grey to reddish (Fig. 7.2.6) and thus markedly different from those present in the Jurassic section, i.e., the Fjerritslev Formation. The Falster Formation and upper part of Ørslev Formation are generally very light grey (950 m and 998 m in Fig. 7.2.6) consistent with a lithology dominated by carbonate, marl and anhydrite as suggested by cutting descriptions and HH-XRF data (c.f. Fig. 7.2.9). Cuttings from the high GR responding and Al-rich Ørslev Formation (c.f. 1065 m and 1095 m in Figures 7.2.8, -9) are darker coloured in agreement with more clay-rich material in the cuttings. The cuttings from 1126 m (low GR responding) represents light grey – dark grey anhydrites, marlstones and sandstones.

Cuttings from the Bunter Sandstone Formation range in colours from light grey to reddish (e.g., 1196 m, 1232 m and 1260 m in Fig. 7.2.6). Millimetre-sized sand grains were seen in the sample from 1232 m (Fig. 7.2.7) consistent with a very quartz-rich composition as judged from the HH-XRF measurements. The reddish sediments at 1260 m represent the mudstone indicated in Figure 7.2.1. Further, the grey grains at 1377 m probably represent sandstones of the Volpriehausen Member of the Bunter Sandstone Formation.

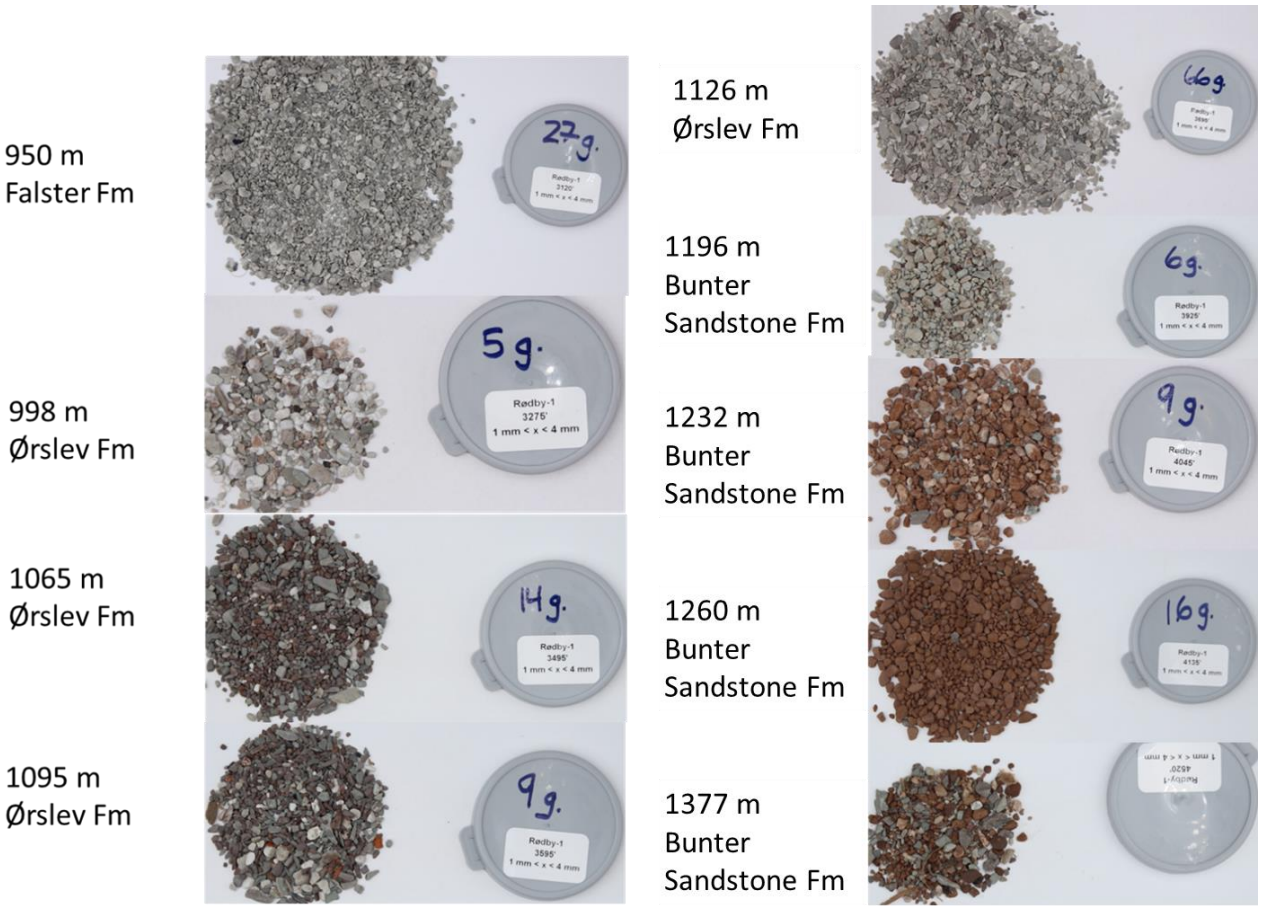

Figure 7.2.6 *Selected pictures of cuttings in the 1–4 mm fraction from the Rødby-1 well. Grey lids shown to the right have a diameter of 45 mm. Depths are given in MD below KB. From Schovsbo & Petersen (2024).*

Figure 7.2.7 *Photograph of a bulk cuttings sample from the Bunter Sandstone Fm at 1232 m (4045') below KB. The sample shows a dominance of quartz grains in the coarse sand fraction. The >5 mm grains in general consist of sandstones and claystones (DGU/DAPCO 1952). The sample also has a high Si content and a high Si/Al ratio, and an overall chemical composition*

interpreted to be dominantly composed of quartz. Grey lid shown to the right have a diameter of 45 mm. From Schovsbo & Petersen (2024).

The calculated API response on the cuttings based on the HH-XRF determination of K, U and Th are in generally good agreement with the measured GR log curve in the hole (Fig. 7.2.8). In generally it appears that API values from the cuttings are slightly offset with depths compared to the GR log respond probably representing a “lack time” reflecting a somewhat poor depth control on the cutting depth.

The low GR readings in the Falster Formation between 880–960 m correspond to the presence of carbonate whereas the overlying and underlying anhydrites appear to have medium high GR responses. In the Ørslev Formation the GR is low in the basal part of the formation.

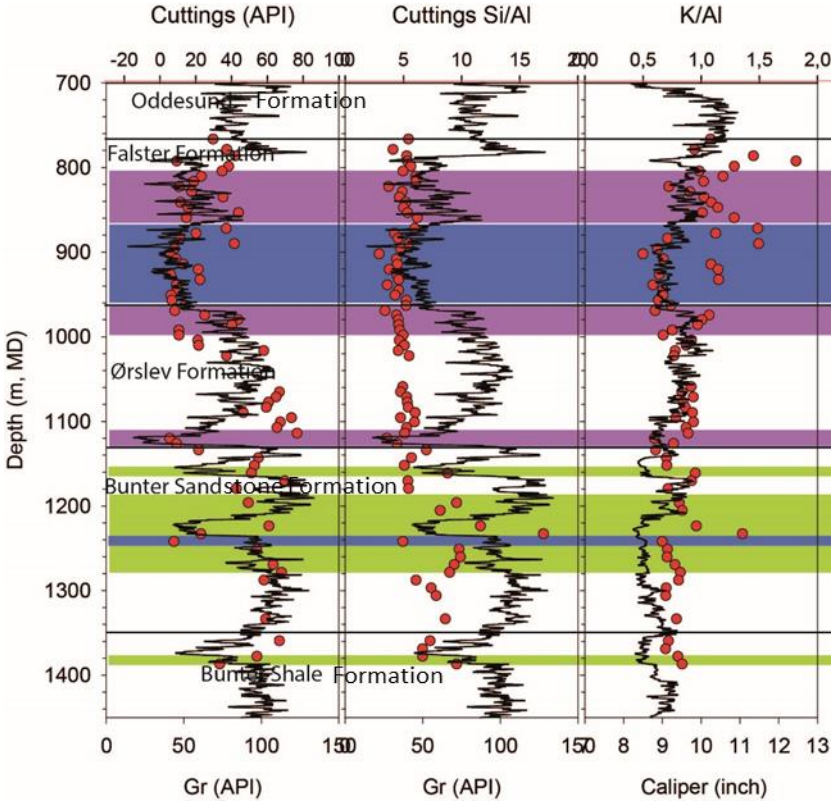

Figure 7.2.8 *GR log curves, caliper log and API values calculated from cutting samples based on HH XRF data (SGR) in the Rødby-1 well. The visual fit between SGR and GR API is in most intervals interpreted to be good. Lithologies are anhydrite (purple), carbonate (blue) and sandy (green). Red dot: measurement on cuttings sample. From Schovsbo & Petersen (2024).*

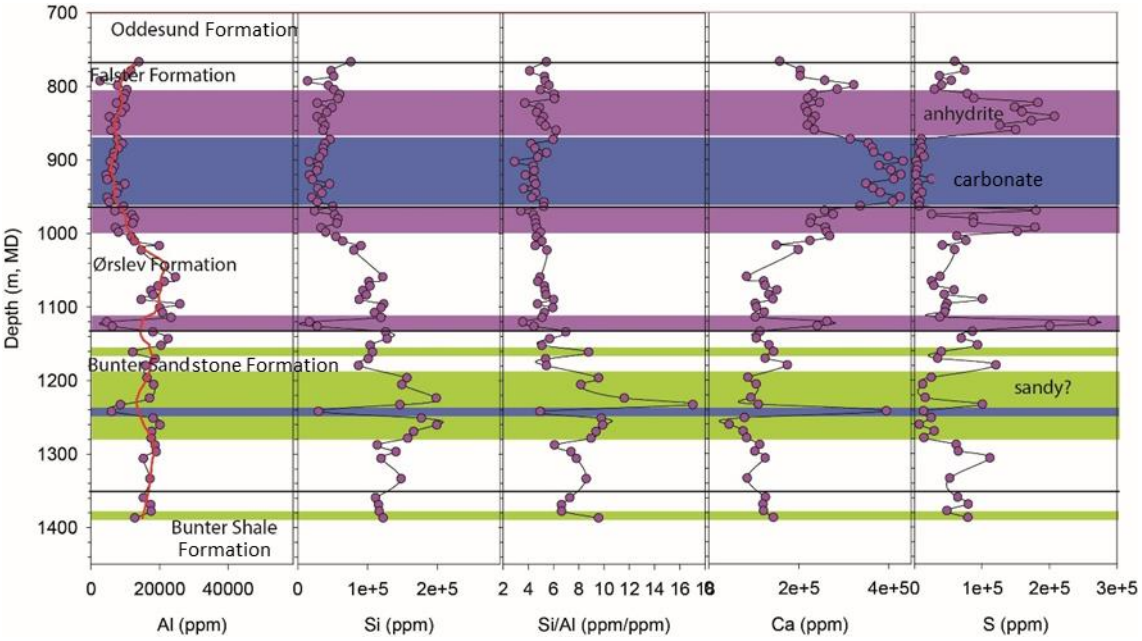

Figure 7.2.9 *Elemental logs of Al, Si, the Si/Al ratio, Ca and S in the Rødby-1 well. The dominantly lithology (anhydrite – pink, carbonate – blue, sandy – green) is interpreted from HH-XRF data represented by the red dots. Sandy beds are interpreted with a Si/Al ratio >8. Red curve in Al diagram is the LOWESS smooth trend. From Schovsbo & Petersen (2024).*

A high organic content in the caprock may reduce the seal integrity by creating an organic network for CO_2 migration. However, Guiltinan et al. (2017) investigated shales with up to almost 8 wt.% total organic carbon (TOC) and suggested they had the potential to be a suitable seal. The content of TOC in both the Ørslev and Falster formations in the Rødby-1 well is low to very low with most values <0.10 wt.% and mean values of only 0.09 wt.% and 0.06 wt.%, respectively (Fig. 7.2.10 and 7.2.11). These low TOC values are within the analytical detection limit indicating the formations are very lean in organic matter.

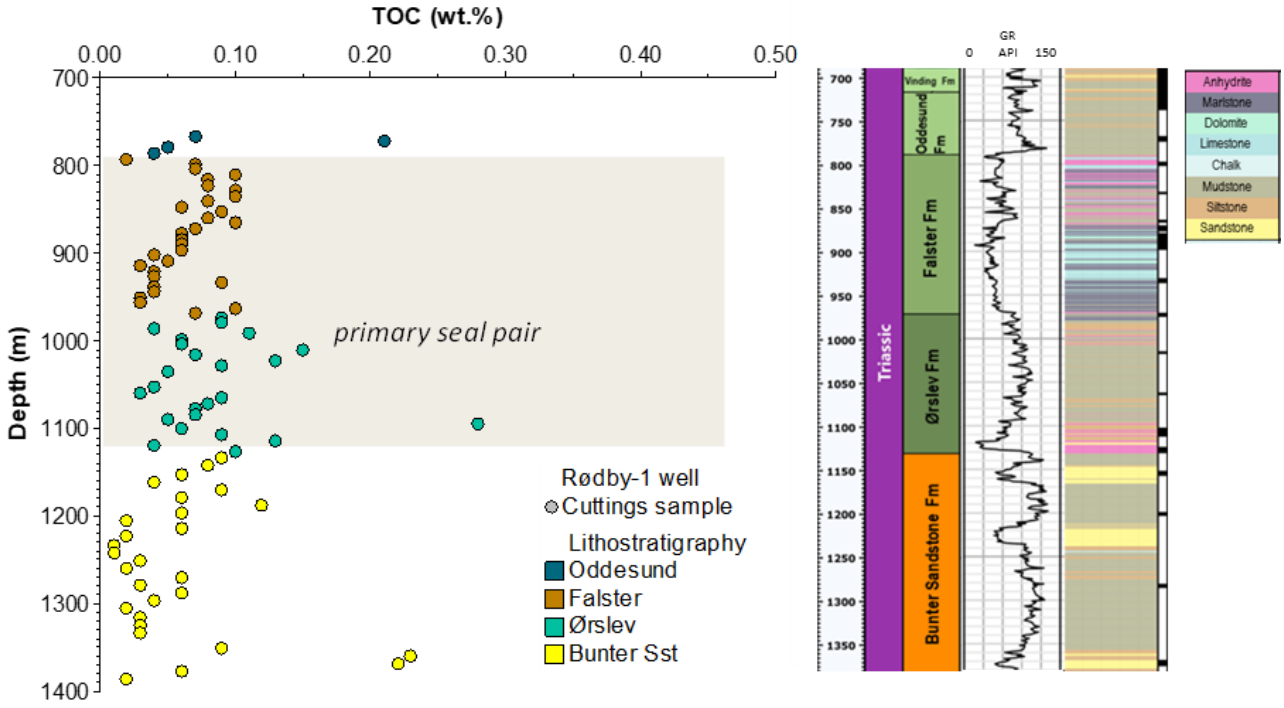

Fig. 7.2.10. *Very low TOC contents were measured in the sealing mudstones of the Ørslev and Falster formations in the Rødby-1 well. The GR log curve and petrophysical log-derived lithologies together with cored intervals marked in black are shown to the right.*

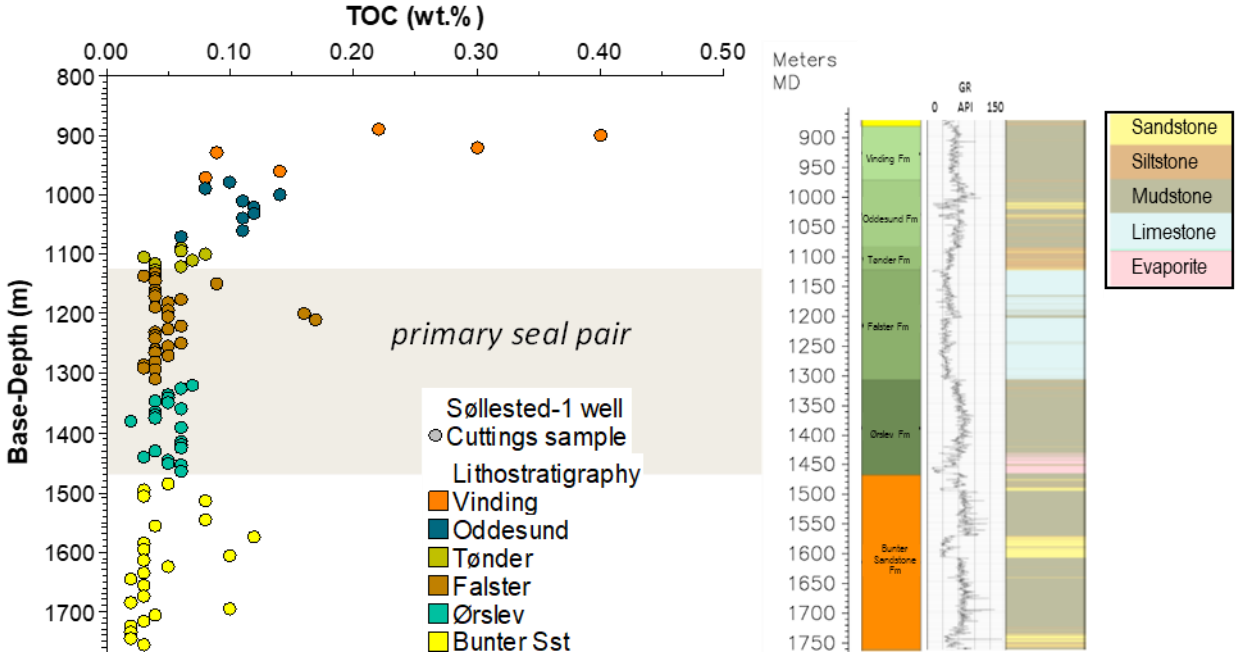

Fig. 7.2.11. *Very low TOC contents were measured in the sealing mudstones of the Ørslev and Falster formations in the Søllested-1 well. The GR log curve and petrophysical log-derived lithologies are shown to the right.*

7.2.6 Seal integrity and capacity of the Lower to Middle Triassic succession

The seal integrity and capacity of the Lower to Middle Triassic formations has not received similar attention as the Lower Jurassic Fjerritslev Formation in Denmark. In addition, whereas the Fjerritslev Formation was deposited in a humid climate under dominantly fully marine conditions, the Lower to Middle Triassic sections, including the Bunter Sandstone, Ørslev, and Falster formations, were deposited under arid to semi-arid climatic conditions with localized restricted marine to lacustrine evaporitic conditions. This makes drawing parallels between the Fjerritslev Formation and underlying Triassic seals very challenging.

Geochemically, the units are also markedly different. The Al content in the Bunter, Falster and Ørslev formation collectively only reach up to 2000 ppm (Fig. 7.2.9), which is significantly lower than in the Fjerritslev Fm (Schovsbo & Petersen 2024), suggesting that the clay volume is much less than the 40% recorded in Fjerritslev Formation (c.f. Vedsted-1 well in Mbia et al. 2014). Similarly, the Si content is lower, indicating an overall low detrital content in the Triassic formations compared to the Fjerritslev Formation. The Bunter Sandstone, Ørslev, and Falster formations all have low K/Al ratios (see Schovsbo & Petersen 2024 for full discussion), indicative of the presence of feldspars and the absence of clay types such as kaolinite and smectite. This aligns with the findings of Weibel et al. (2017), who found that K-feldspars and micas in arid to semi-arid conditions were largely unaltered, whereas under humid conditions, they were largely replaced by kaolinite. This process may be part of the explanation for the difference in K/Al ratio and lower overall clay content. This later aspect is also important if the clay volume is interpreted from the GR log as this method work best in mature geochemical sediments where the mud is natural NORM-rich, (i.e. being general rich in Natural Occurring Radioactive Material) and the sand is (NORM) poor (Pedersen et al. 2013).

In addition to the clay type and content that places the Triassic sealing formations aside of the better-known Jurassic Fjerritslev Formation, these formations also contain interbeds of anhydrite and limestone and possible also rock salt, though it has not been observed in Rødby-1. Based on these differences the good seal capacities with respect to CO_2 storage that have been determined for the Jurassic Fjerritslev Formation cannot be directly applied to the Triassic sealing formations. However, this does not exclude that these formations have a high sealing capacity. Thus, experimental sealing capacity studies of e.g. anhydrites for CO_2 storage have shown effective sealing capacity on short term and modelled limited chemical reactions of anhydrite with CO_2 on longer terms (Hangx et al. 2010). Limestones and carbonates can show a wide range of sealing capacities from high to low. The heterogeneous nature of the Ørslev and Falster formations might lower the risk for leaks with regards to fractures since fracture propagation through heterogeneous strata can be anticipated to be much more complex due to the differences in competence between the beds (Bruno et al. 2014). Additionally, if present, rock salt will also enhance the seal capacity due to its very low entry pressures and its self-healing nature towards fractures. However, rock salt has not been positively identified in Rødby-1.

7.3 Recommendations for further studies on seal characterisation in the Rødby structure

Site-specific studies on the seal capacity are needed for all structures to be matured towards CO_2 storage. For the Bunter Sandstone Formation in the Rødby structure, which is primarily sealed by the fine-grained intraformational parts of the Bunter Sandstone, the Ørslev, and the Falster formations, the need to establish fundamental knowledge of the seal properties is very high. This is because we cannot draw parallels to the better-known Fjerritslev Formation which constitutes the main seal in most of the structures for CO_2 storage that are under exploration elsewhere in Denmark.

In Figure 7.2.12, a workflow to establish the fundamental seal information is outlined. In this workflow, the studies conducted here, i.e., HH-XRF, cuttings imaging, and TOC and Rock Eval analysis, form only part of the screening data that needs to be gathered. Additional analyses should be performed on large-size samples from cores, e.g. on plugs with diameter of 2 cm, and include porosity measurements, surface area determination, mineralogy, and clay type determination combined with grain size analysis. Hereafter a sample selection for more costly but crucial analyses should be undertaken. These analyses should include measurements of pore size distribution and capillary entry pressures, as well as petrography and microfacies descriptions in order to assess the sealing capacity of the formations. The Rødby-1 well was cored in selected intervals in the main seal units of the Ørslev and Falster formations (Fig. 7.2.10), and the cores could be sampled for more detailed analyses. It should be noted that the cores are dried due to long storage, however, they may provide material that will be suitable for most types of analyses mentioned in Figure 7.2.12. Exceptions are analysis related to the pores such as their amount, size and structure as well as most geomechanical tests. For such tests analysis of dried-out material may only serve as first measure before new core material is available.

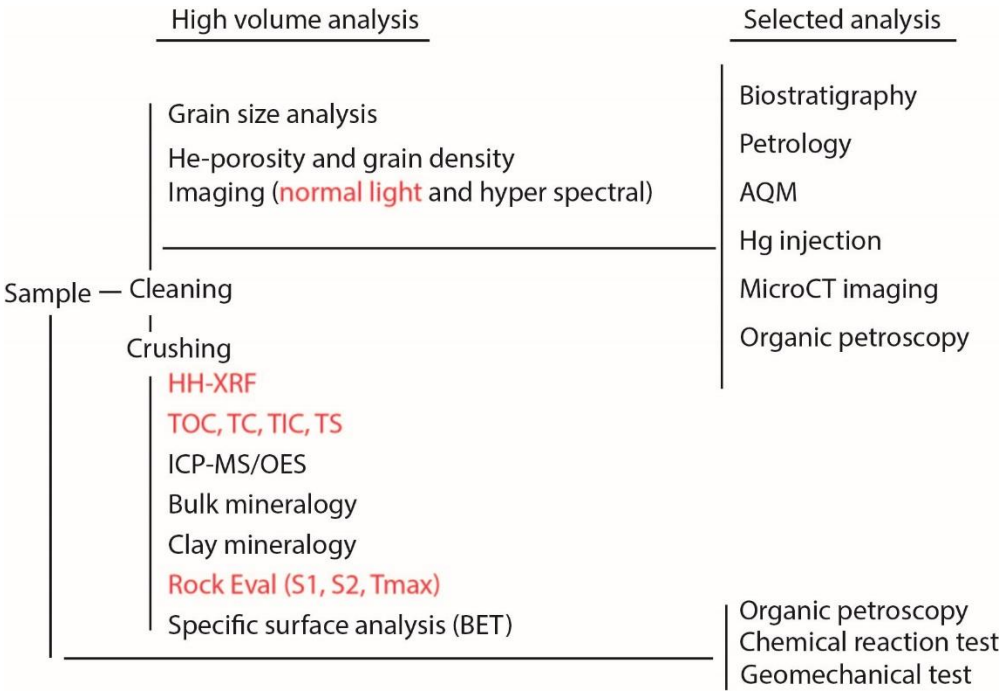

Figure 7.2.12 *Workflow for seal and reservoir characterisation. In red are methods applied here. Based on Schovsbo et al. (2023) and the present work.*

7.3.1 Summary notes on the seals

Several potential sealing units exist above the reservoirs of the Bunter Sandstone Formation, including anhydrites and mudstones of the Ørslev Formation, and limestones, marls, mudstones and anhydrites of the Falster Formation. In addition, intraformational mudstone seals are present in the Bunter Sandstone Formation.

The combined thickness of potential sealing units above the Bunter Sandstone Formation in depths >800 m is possibly more than 340 m in the Rødby structure. The principal or main sealing units depend on which reservoir unit(s) of the Bunter Sandstone Formation that will be targeted for CO_2 storage (see also Chapters 6 and 8). The heterogenous composition of the succession of potential sealing units is considered positive for the combined sealing effectiveness.

An unknown risk to the sealing units in the Rødby area is linked to the Rødby-1 and Rødby-2 wells as these are drilled near the top of the structure and the integrity and sealing capability of the plugged and abandoned wells is poorly documented.

An analytical workflow on the available cores from Rødby-1 and future fresh core material is suggested to obtain better constrains on the seal effectiveness. This includes evaluation and modelling of chemical reactions in the different seal units with CO_2 and anhydrite, dolomite, limestone marls and possibly halite that may alter the sealing effectiveness during the active storage of CO_2.

8. Discussion of storage and potential risks

8.1 Volumetrics and Storage Capacity

Primary input for the estimation of potential CO_2 storage capacity has been the seismic reinterpretation of Bunter Sandstone reservoir within the current older 2D-Survey lines combined with extended interpretation across the newly acquired 2D seismic data GEUS2023-ROEDBY survey, see also Section 4.1). The detailed well analysis and a crucial element of revising the depth conversion impacts the understanding of the reservoirs and their geometry in this moderate-relief structure (see Figure 8.1.1).

The storage capacity estimates are average values for the whole structure. The well derived data in Table 7.1.5 is the primary input for the volume calculation. The petrophysical and geological understanding of thicknesses and average net to gross reservoir ratio of aquifer across the entire trap (the N/G ratio) in the Rødby and neighboring wells is therefore transformed into structure-specific geological-based average values for the storage capacity estimation simplifying the spatial distribution/variation within the Gross Rock Volume (GRV).

Traditionally the GRV is calculated as a total volume between the top and base reservoir surfaces (see Figure 8.1.1.) The so-called Waste Rock Volume (WRV) (*James et. al., 2013*) is subtracted from the total volume to give the resulting GRV. Average reservoir thickness (i.e. net sand thickness) is not just equal to the isochore thickness (or the relief) between top and base surfaces, why the gross thickness is corrected with the N/G ratio to get a more realistic reservoir sand thickness for the GRV. Preferably, the thickness correction could also incorporate potential thin sandstone wedges between top point and the spill point on the flanks of the structure, if the seismic data support this.

For the storage capacity estimation of the Rødby structure, the Bunter Sandstone Fm have been evaluated as a structural four-way dip closure and is calculated so it can be compared to CO_2 capacities of other structures across Denmark (e.g. Gregersen et. al. 2023 and Hjelm et al. 2022).

The physical properties of the Bunter Sandstone reservoir units are described in Section 7.1. At a later stage the reservoir unit and identification of possible faulting must be assessed in more detail by 3D reservoir simulation models to ensure optimal development, injection and filling of the reservoir unit of the structure, and to ensure less uncertainty on storage capacity.

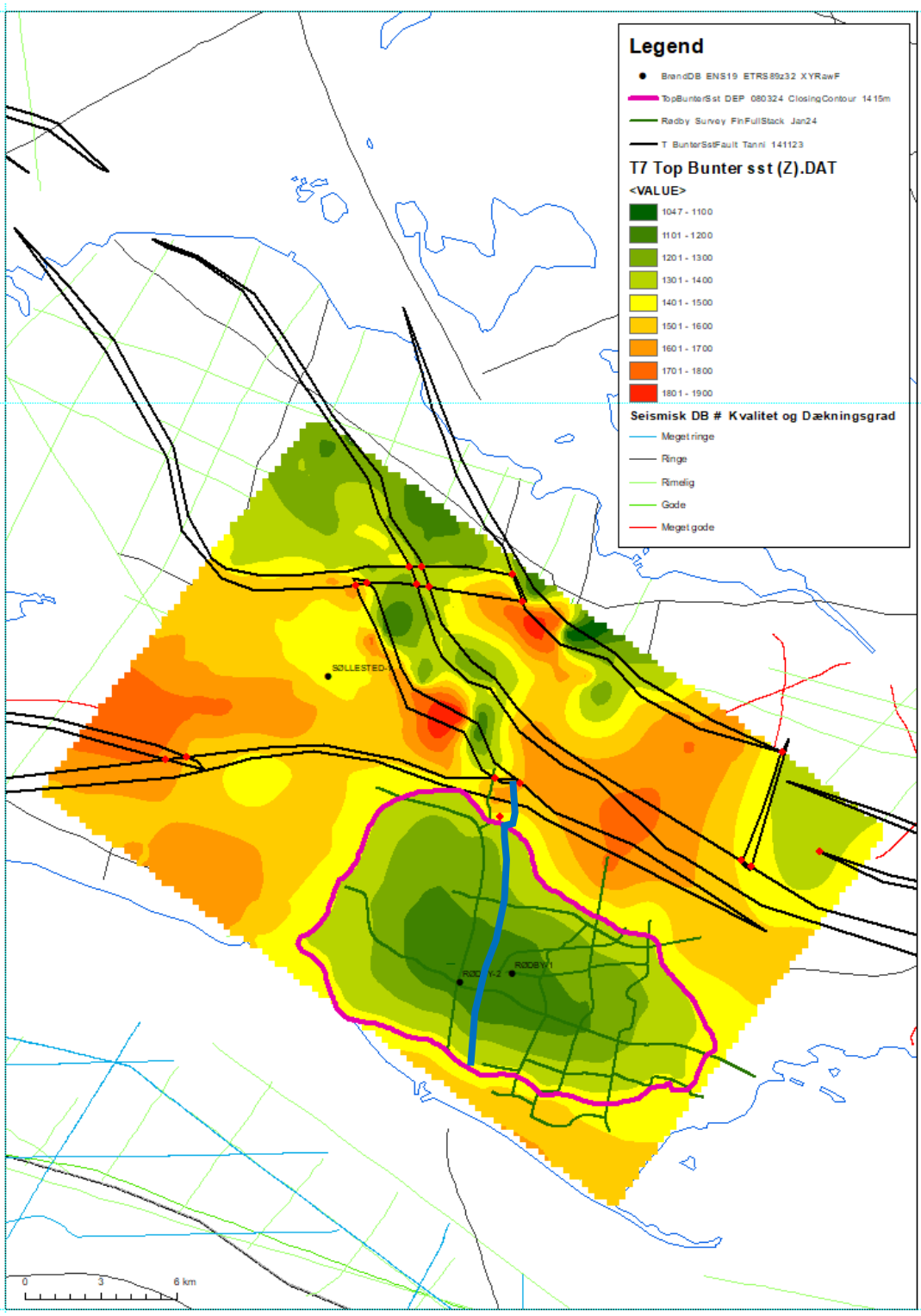

Figure 8.1.1. *The Top Bunter Sandstone depth structure map in meters (m) (generated in Petrel®, tied to nearest wells and gridded by 250x250 meter) provides the primary input to the capacity assessment. The Rødby structure are located south of a major fault system, the Lolland–Falster Fault Zone. The structural spill point is located at c. 1100 m and the deepest closing contour at 1415 m (marked in bold purple), and with an area within the spill point of c. 117 km^2. Notice that the spill point is defined as the deepest closing contour based on the dataset resulting in a minimum GRV, as saddle-points towards the south and southeast are not recognised within the dataset. See also Section 6.1.1. for fault analyses and map location. A schematic N-S profile across the structure is shown in Figure 8.1.3 (blue line).*

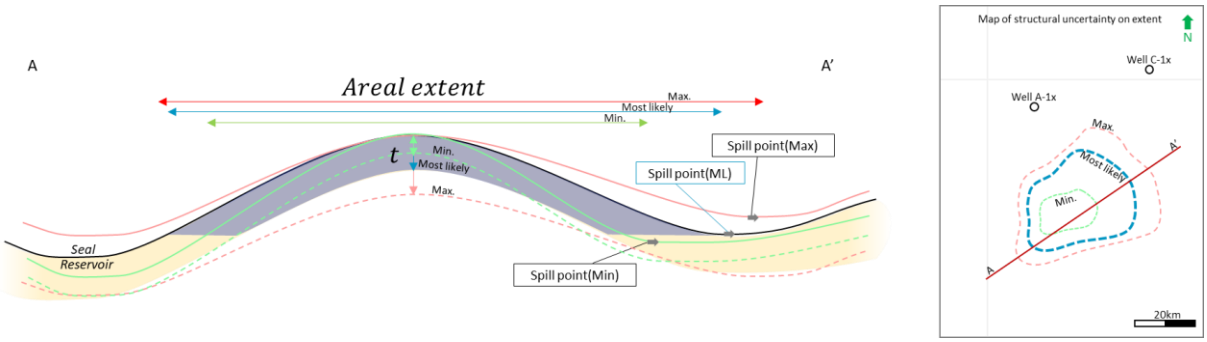

Figure 8.1.2. *Conceptual profile (A-A') across a potential structure. The uncertainty in mapping the structure results in the hypothetically min. and max. scenarios looking very different from the most likely mapped scenario. Variance in area and in thickness (t) will affect the Gross Rock Volume (GRV) of the structure. The uncertainty is addressed by applying uncertainty on the resulting GRV.*

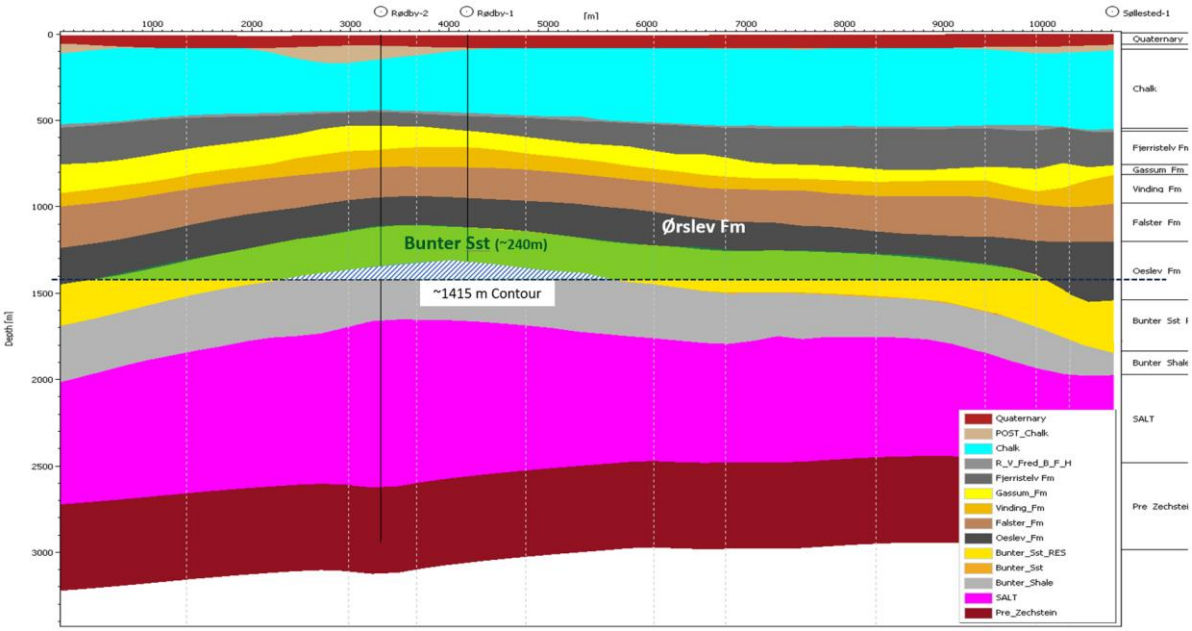

Figure 8.1.3. *N–S schematic cross section of the Rødby structure showing the location of the top and spill points for the Bunter Sandstone Fm at the 1100 m and 1415 m contours. The cross section shows the location of the base reservoir surface assuming a 240 m gross reservoir thickness based on the Rødby-1 and -2 wells. The interval between 1100 m and 1415 m is used to give a realistic GRV estimation (marked with dark green polygon above 1415 m). For the Bunter Sandstone reservoir, the GRV is calculated in Petrel as the volume between the top Bunter Sandstone and base Bunter Sandstone surfaces (i.e. the spill point). Notice the location of the two Rødby wells near the top of the Rødby structure) and that the profile towards the north enters the fault north of the Rødby structure. (see Figure 8.1.1.for location of the section).*

8.2 Volumetric input parameters

Evaluation and maturation of a CO_2 storage site includes several steps. The maturation phase, carried out by GEUS, includes static calculation of theoretical storage capacity - primary based on Gross Rock Volume (GRV), net/sand thickness, average porosity and density of the CO_2 (see also Section 7.1).

The current maturation phase does not provide dynamic capacity estimates of the potential CO_2 structures but focus on identifying and assessing extent and quality of reservoir aquifers. Furthermore, no attempts are made to address e.g. seal breach, fault leakage, fault reactivation, solubility of CO_2 in water, the effect of high concentration of salt etc.

To do detailed CO_2 storage capacity evaluation, it is important to assess aquifer quality and connectivity, i.e. to identify the existence of thick, high permeable sandstone aquifers with high connectivity with no major faults. This will require dynamic reservoir simulation, that may result in different storage capacity than static calculations and will normally be the next step for potential license holders.

8.2.1 Gross rock volume

The Gross Rock Volumes (GRV) of the Rødby structure have been based on the Area and Thickness vs. Depth methodology described by e.g. *James et al. (2013)*. The calculated Gross Reservoir Volume (GRV) is estimated from the seismic mapped and depth converted top and base reservoir surfaces, where the base surface is constrained by the spill point surface (Figure 8.1.2. and Figure 8.1.3.).

The GRV is calculated in Petrel as the volume between the top Bunter Sandstone and the base reservoir surfaces, where the base surface is adjusted by adding expected 240 m to the Top Bunter Sandstone surface to give a realistic estimate of the GRV. The expected reservoir sand thickness is multiplied with the net/gross ratio estimated from petrophysical analysis based on the nearest wells (see Section 7.1). Calculating GRV provides greater accuracy and flexibility compared to previous used correction factors for geometries with overestimated wedge volumes. This is because it allows for uncertainty ranges on GRV and reservoir sand thickness to be modeled independently. Furthermore, the method allows for a rapid GRV calculation, that can be used in a Monte Carlo simulation, to establish an unbiased estimated range of GRV.

To evaluate the uncertainty on the GRV across the Rødby structure, a minimum and maximum case was also calculated as illustrated in Figure 8.1.2. by assigned a min., mode, and max. uncertainty range, where mode is the data value that occurs most often in the data. This variation in GRV was inferred to cover uncertainty in interpretations, seismic well ties, mapping and depth conversion. To reflect this uncertainty, a distribution for the average GRV was constructed by defining the min. and max. of the distribution based on surrounding wells and supplied by c. ±20% (Table 8.2.1.). It is assumed that the GRV distribution follows a Pert distribution defined by the min., mode, and max. values. The Pert distribution is believed to give suitable representation for naturally occurring events following the subjective input estimates (*Clark, 1962*).

Table 8.2.1. *Assessment of important parameters for the Bunter Sandstone Fm reservoir in Rødby structure, where only the resulting Gross Rock Volume (GRV) min, mode and max estimates are used for the capacity estimation in Table 8.2.3. The reservoir thickness (i.e. the Gross sand thickness) is taken from Table 7.1.5.*

Unit	Apex [m, TVDSS]	Spill point [m, TVDSS]			Area [km^2]	Gross Sand TCK [m]			GRV [km^3]		
		Min.	Mode	Max.	Mode	Min.	Mode	Max.	Min.	Mode	Max.
Bunter Sst Fm	1100	1275	1415	1550	117	220	240	260	**22.6**	**28.21**	**23.9**

For the reservoir unit, the other input parameters are also given as min., mode, and max. values - Net/Gross, porosity, CO_2 reservoir density and the Storage Efficiency factor, where also assumed to follow a Pert distribution.

8.2.2 Net to Gross ratio

The Net to Gross (N/G) ratios estimated from the petrophysical analysis of the nearest wells (especially Rødby-1, Rødby-2 (and to some degree the Søllested-1 to the northwest and Ørslev-1 to the east) are evaluated and reasonable average N/G-ratios across the entire structure is defined as the mode of the distribution (see also Section 7.1). Some variance is expected due to lateral variation of the lithologies owing to differences in facies distribution, depositional environment and diagenesis. To reflect this uncertainty, a distribution for the average N/G ratio was constructed by defining the min. and max. of the distribution as c. ±20% with minor adjustments. A Pert distribution has been applied.

8.2.3 Porosity

The porosity (ϕ) was estimated from petrophysical analysis of the Rødby-1 and -2 and surrounding wells as described in Section 7.1. The well-derived estimates are considered as reasonable average porosity across the entire structure (i.e. set as mode). Some variance is expected as lateral and depth variations may occur. To reflect this, an average porosity distribution has been constructed defining the min. and max. of the distribution as c. ±20% with minor adjustments. A Pert distribution for this element has been applied.

8.2.4 CO2 density

The average in-situ density of CO_2 was estimated using the 'Calculation of thermodynamic state variables of carbon dioxide' web-tool essentially based on Span and Wagner (1996) [*http://www.peacesoftware.de/einigewerte/co2_e.html*]. The average reservoir pressure was calculated on the assumption that the reservoir is under hydrostatic pressure and a single pressure point midway between apex and max spill point was selected representing the entire reservoir.

Temperature for this midway point was calculated assuming a surface temperature of 8°C and a geothermal gradient of 30 C°/km based on the Rødby-1/-2, which is slightly higher than the typical onshore gradient of c. 28–29 C°/km estimated by Fuchs et al. (2020). Assumptions

and calculated densities for the individual reservoir units are tabulated in Table 8.2.2. For a quick estimation of the uncertainty on CO_2 density, various P-T scenarios were tested and in general terms a -5% (min.) and +10% (max.) variation from the calculated mode was applied for building a Pert distribution. All calculations showed that CO_2 would be in supercritical state.

Table 8.2.2. *CO_2 fluid parameter assumption and estimated values.*

Unit	Apex depth [TVDSS, m]	'Spill point depth' [TVDSS, m]	Structural relief [m]	Pressure HydroS.[MPa]	GeoThermal grad. [C/km]	Mid Res. Temp. [C]	CO_2 density (Kg / m^3)
Bunter Sst Fm	1100	1415	240	12.34	30	45.73	**603.6**

8.3 Storage efficiency

Storage efficiency is heavily influenced by local geological subsurface factors such as confinement, reservoir performance, compartmentalisation etc. together with injection design and operation (i.e. financial controlled factors) (e.g. *Wang et al. 2013*). A sufficient analogue storage efficiency database is not available to this study and accurate storage efficiency factor-ranges lacks at this early stage of maturation. This emphasises the need for further investigations of the subsurface and development of scenarios and dynamic reservoir simulation to better understand the potential storage efficiency ranges. In this evaluation, a range from 5% to 20% with a mode of 10% is used as a possible range. The use of a storage efficiency factor value of 10% assumes that Bunter sandstone reservoir in the Rødby structure have good reservoir characteristics based on Rødby-1/-2 and surrounding wells, and the uncertainty caused by the identification of a fault penetrating both the seal and reservoir on the new seismic data which reduces the mode value (see Section 6.1.1). A Pert distribution for this element has also been applied.

8.4 Summary of input factors

In Tables 8.4.1, input parameter distributions are listed (all selected to follow Pert distributions defined by min, mode and max). Input parameter distributions for the Bunter Sandstone reservoir is displayed in Figure 8.4.1.

Table 8.4.1. *Input parameters for the Rødby structure –* ***Bunter Sandstone Fm***

Parameter	Assumption		
	Min	Mode	Max
GRV (km³)	22.57	28.21	33.85
Net/Gross	0.20	0.25	0.30
Porosity	0.184	0.23	0.276
Storage eff.	0.05	0.1	0.2
***In situ* CO_2 density (kg/m³)**	573.4	603.6	764.0

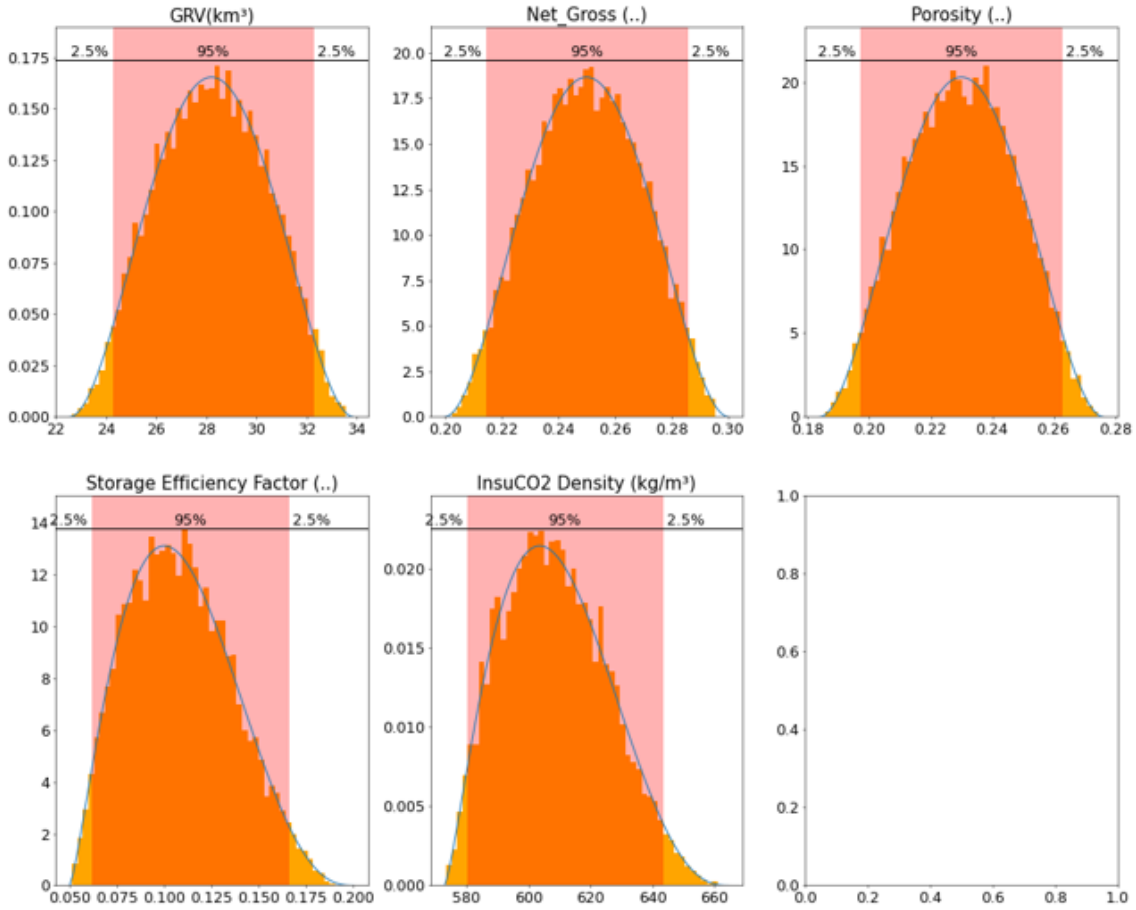

Figure 8.4.1. *Example of some of the distribution shapes (Pert distributions) for the 5 input parameters for the Gassum reservoir. The last input distribution plot is empty and not used.*

8.5 Storage capacity results

The modelled volumetrics was made on the assumption of the presence of an efficient reservoir/seal pair capable of retaining CO_2 in the reservoir. This basic assumption needs to be tested by new 3D seismic data and further geological investigation. In Tables 8.5.1, the results of the Monte Carlo simulations are tabulated. The tables indicate both the pore volume available within the trap (full potential above structural spill), the effective volume accessible for CO_2 storage (applying the Storage Efficiency factor to pore volume) and mass of CO_2 in mega-tons (MT) that can be stored. The tables present the 90%, 50% and 10% percentiles (P90, P50 and P10) corresponding to the chance for a given storage volume scenario to exceed the given storage capacity value. Mean values of the resultant outcome distribution are also tabulated and is considered the "best" single value representation for the entire distribution.

A mean unrisked static storage capacity of c. 107 MT CO_2 is calculated for the Bunter Sandstone Fm with a range between c. 69 MT CO_2 (P90) and c. 149 MT CO_2 (P10) and a P50 of c. 104 MT CO_2 (Figure 8.5.1). Due to the variability-ranges of the behind-lying factors, the modelled storage capacity has a significant range. As illustrated in Figure 8.5.2, the storage capacity uncertainty is linked with the uncertainty in gross rock volume (GRV) and storage efficiency. In comparison, CO_2 density at reservoir conditions, is believed to be of minor concern.

Table 8.5.1. *Rødby structure –* ***Bunter Sandstone Fm*** *storage capacity potential*

Results	P90	P50	P10	Mean
Buoyant trapping pore volume (km^3)	1.353	1.613	1.911	1.624
Buoyant eff. storage volume (km^3)	0.113	0.171	0.245	0.176
Buoyant storage capacity (MT CO_2)	68.83	103.90	148.78	**107.04**

Notice that the storage efficiency factor is here assumed to be 10% (compared to the previously used 40%) thus reducing the overall CO_2 storage capacity compared to previously studies. This estimation of CO_2 storage capacity must be investigated further by e.g., reservoirs simulation modelling to ensure optimal development and filling of the Rødby structure, and to ensure less uncertainty.

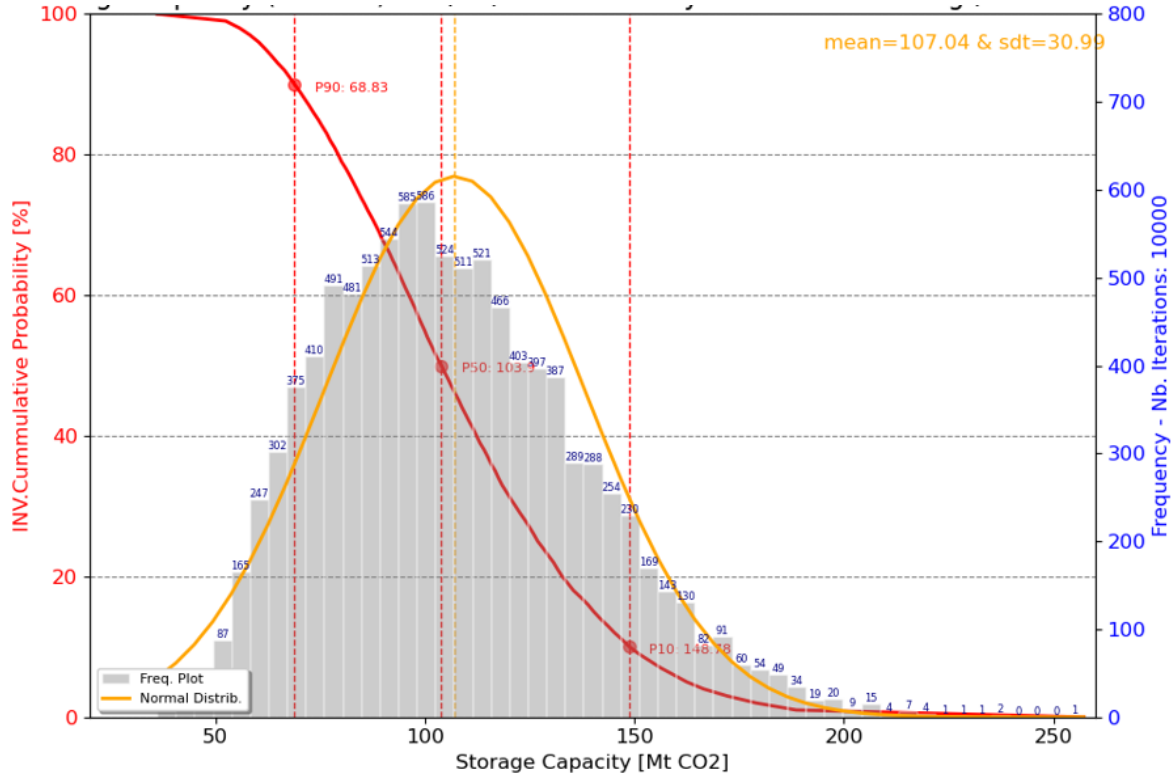

Figure 8.5.1. *Modelled statistical distribution of the combined storage capacity potential for the Bunter Sandstone reservoir in the Rødby structure.*

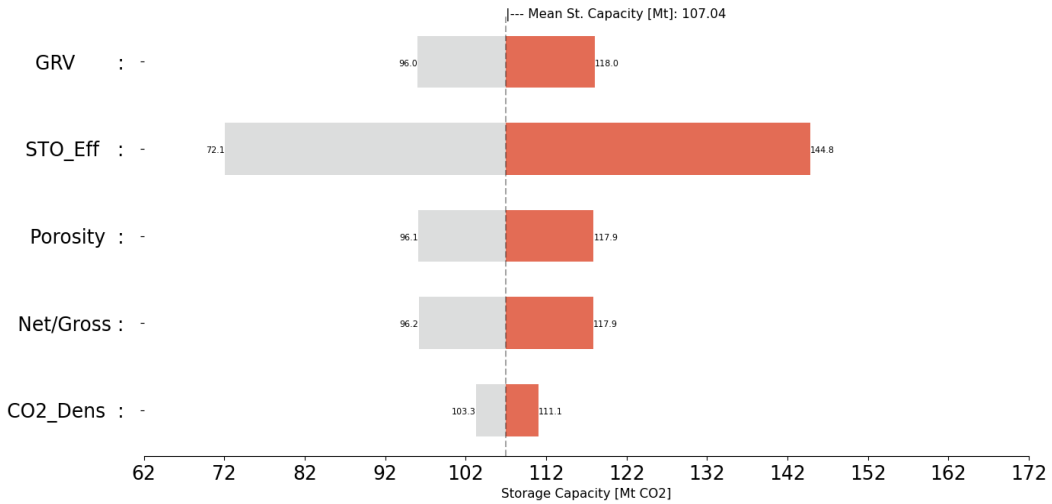

Figure 8.5.2. *Sensitivity or Tornado plot to how the various input parameters affect the estimate mean of storage capacity (c. 107 MT CO_2) of the Bunter Sandstone reservoir unit. The horizontal bars for each parameter indicate change in storage capacity given that only that parameter is changed leaving all other constant (end levels being P90 and P10, respectively, in the parameter input range). The colours show the symmetric representation of the parameters on both sides of the mean storage capacity.*

8.5.1 Seal integrity and capacity

The sealing units comprise a highly heterogeneous succession that requires detailed analysis to mitigate risks to seal integrity and capacity on the Rødby structure. The current understanding of the sealing properties of the Ørslev and Falster formations is limited to the presented hand-held XRF study and the petrophysically derived log interpretation (see Chapter 7). An analytical workflow on the available cores from Rødby-1 and future fresh core material is suggested to better constrain the seal effectiveness (see Chapter 7). This includes evaluating geomechanical properties, mineralogical composition, total porosity, permeability, and CO_2 entry pressures, along with modeling chemical reactions in the different seal units with CO_2 and minerals such as anhydrite, dolomite, limestone marls, and potentially halite, which may alter the sealing effectiveness during active CO_2 storage.

Additionally, an unknown risk to the sealing units in the Rødby area is associated with the Rødby-1 and Rødby-2 wells, as these are drilled near the top of the structure, and the integrity and sealing capability of the plugged and abandoned wells are poorly documented.

8.6 Potential risks

The present report provides an updated geological mapping describing the reservoir-seal couple, the extent, thickness, closure, reservoir quality and volume of the primary reservoir formation, as well as larger faults, but does not comprise a dedicated study of risks or risk assessment of the structure for potential storage of CO_2. Thus, the report provides a geological characterization and maturation of these identified elements and points out geological related potential risk issues, that are recommended to be included for further evaluation and maturation studies, e.g., in risk assessments.

Risks treated here are primary geological parameters incompletely understood, that may negatively affect the CO_2 storage potential. Not all risks can be identified at this early stage due to lack of dense seismic coverage and well information, while other risks identified at this stage will be mitigated by collection of new geophysical and geological data and further investigations, which together can shed new light on the critical parameters and risks. The few risks described below are not considered a full list, but rather emphasizes important points that needs further attention in future studies and data collections.

8.6.1 Fault leakage

Faulting of the Bunter Sandstone–Ørslev Fm reservoir-seal pair is considered as the primary risk at the current level of understanding. Especially, the Rødby Structure Fault Zone at the top of the Rødby structure, near the Rødby-2 well, that have been active since deposition of the Oddesund Fm and until deposition of the Lower Jurassic Fjerritslev Fm, as no signs of offset has been observed on the Near Top Fjerritslev horizon.

Besides the mentioned minor Rødby Structure Fault Zone (Figs. 6.1.7 and 6.2.4), only very few minor faults have been detected in the very thickly developed Ørslev Fm seal and overlying layers. However, when maturing the structure further, a denser seismic data coverage may reveal faults through overlying layers that could potentially introduce a possible risk of vertical leakage from storage in the Bunter Sandstone Formation.

Faults could also be a challenge to lateral migration such as reservoir compartmentalization, such as known from the Gassum Fm in the Stenlille structure, where the mapped faults are typically minor as well in lateral extension (up to few km) and with small vertical throws (typical up to 10–15 ms), and the faults are typically located kilometres apart (Gregersen et al. 2023). Such faults may reduce internal reservoir communication, and thus lower the storage efficiency and increase the number of injection wells required to fill the structure. Despite of the mapped faults in the Stenlille area, there are not registered any leakage or natural escape of gas, which has been stored in the Stenlille structure since 1989 (Laier and Øbro, 2009).

The Rødby structure has a similar trap (a four-way dip closure above a salt structure), but the reservoir-seal pair is at different Triassic interval with a different tectonic evolution, faulting history, and rheologic competence. These factors/conditions must be investigated closely to mitigate any risks and to secure the CO_2 injection and potential migration pathways are safely away from faults. Across the structure and away from the NW–SE striking Lolland–Falster Fault Zone, faults occur mostly up to near top of Bunter sandstone Fm and have only been mapped in one known area near Rødby-2 well as described in detail in Chapter 6. Other equivalent faults may occur around the rim of the structure in places not covered by GEUS's seismic field campaign in 2023.

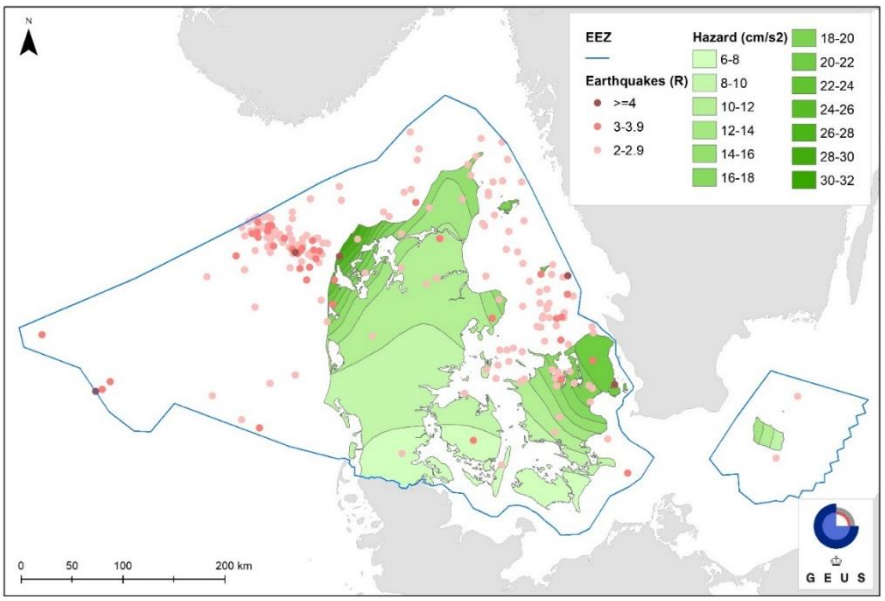

Figure 8.6.1. *The coloured contours are redrawn onshore from Voss et al. (2015) and show the estimated hazards given by the peak ground accelerations [cm/s2] for a return period of 475 years. This corresponds to a 90% non-exceedance probability in 50 years. Given values are only valid onshore Denmark. The contours are based on a validated catalogue of earthquakes over Magnitude 3 from 1960 to 2013. As the attenuation of earthquakes (ground motion prediction) has not been determined specifically for Denmark, the global reference model by Spudich et al. (1997) that describes attenuation from normal faults in hard-rock conditions was used.*

8.6.2 Earthquake hazards

Denmark is a low-risk area for earthquakes though small earthquakes do occur (Fig. 8.6.1). Estimates of earthquake hazard for Denmark can be found in Voss al. (2015), where also lists of felt and damaging earthquakes can be found. In Figure 8.6.2 all known earthquakes on Zealand and Lolland are shown. The largest is ML 4.0 (ML is the local magnitude or the local Richter scale) in 1930 ESE of Stevns (Lehmann 1931). Also, the smaller, but widely felt, earthquake in 2001 close to Holbæk is described (Larsen et al. 2008). Most earthquakes within Zealand are registered in the western part of Isefjord and the southern end of Roskilde fjord (Fig. 8.6.1–8.6.2). The depths of the earthquakes are very uncertain, but they are located within Earth's crust.

A monitoring study was carried out around Gas Storage Denmark (GSD) gas storage facility close to Stenlille (Fig. 8.6.2). Six seismic stations were in operation for almost three years, and no local events were detected. The detection limit within the storage area was calculated to be at least ML 0.0 (Dahl-Jensen et al. 2021). No earthquakes have been registered at the Rødby structure (Fig. 8.6.2).

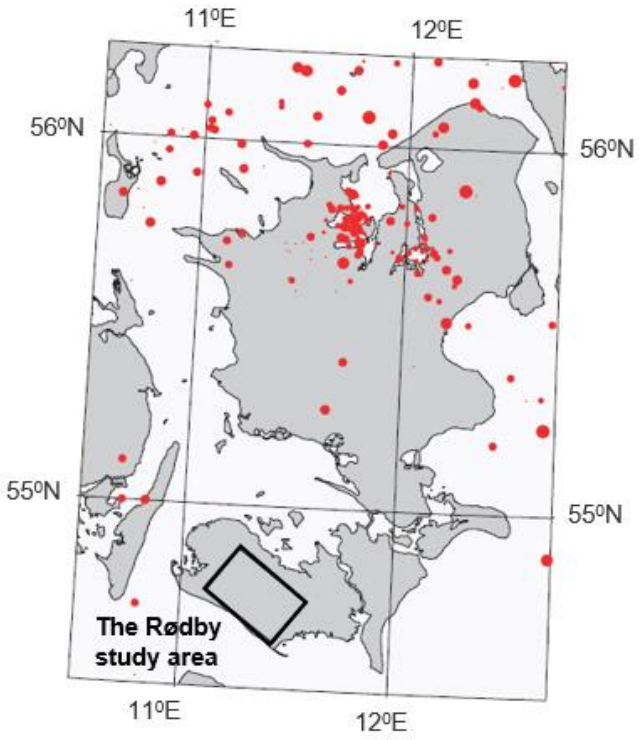

Figure 8.6.2. All known earthquakes until the end of 2022, located since 1930 within 54.5–56.25N/10.5–12.75E. The magnitude (shown by the size of the red dots) varies from ML 4.0 and down. All known and assumed man-caused explosions have been removed, but some may remain, mainly offshore. The Rødby study area of this report is marked with a black rectangle.

9. Conclusions

This study shows that the Rødby structure forms a well-defined structural anticlinal dome with a four-way dip closure, cored by a Zechstein salt pillow that is overlain by a thick Triassic−Lower Jurassic succession, and younger strata. The structure is covered by vintage seismic data, and c. 106 km new seismic 2D lines acquired during June to July 2023 to increase the coverage of the structure. The primary reservoir for CO_2 storage is sandstones interbedded with mudstones of the Lower Triassic Bunter Sandstone Formation. The thick mudstone successions of the Middle Triassic Ørslev–Falster formations form the primary and secondary seals, respectively. All formations are well-known from existing wells in the Lolland–Falster area, such as Rødby-1, Rødby-2, Søllested-1, and Ørslev-1. There is no reservoir-seal couple of the Gassum Fm–Fjerritslev Fm in the Rødby structure, as they occur at depths above 800 meters in the structure, and thus at too shallow depths to be considered relevant for CO_2 storage.

The reservoir properties of the Bunter Sandstone Fm in the Lolland–Falster area have been determined using well log data from four wells, calibrated with core measurements, and cutting descriptions. Permeability estimates are based on specific porosity-permeability relationships from core measurements, including additional onshore Danish wells in the North German Basin. The Bunter Sandstone Fm is divided into three separate reservoir units. Each reservoir unit is overlain by thick fluvial plain to lacustrine mudstone units. The Detfurth reservoir shows the best reservoir properties of the three units with the highest porosity of 28.6% in the Rødby structure (16.9 – 31.9% in the study area) and permeability of1397 mD in the Rødby structure (293 – 2029 mD in the study area)), The salinity of the formation water may range from a minimum of 115,000 ppm Cl^-, representing the salinity expected at the depth of interest in the Danish Basin, to possibly full saturated conditions at 200,000 ppm Cl^-.

The primary seal for the reservoir is the marine evaporites and mudstones of the Ørslev Fm, characterized by a 153–160 m thick heterogenous succession in the Rødby-1 and -2 wells. A few measurements on anhydrite/dolomite plugs show an average porosity of about 2%. Derived porosity values (PHIE) range from less than 0.1% to 10%, with permeabilities generally below 1 mD, except for a few thin sandy units with permeabilities between 10 and 100 mD. The secondary seal consists of marlstones, limestones, mudstones and evaporites of the Falster Fm, which is about 175 m thick in the Rødby wells. Limited measurements on marl and claystone plugs suggest average porosities of 14% and 21%, respectively. Petrophysical derived porosity values (PHIE) are between 5% and 10%, with a few thin units (<2 m thick) showing porosities between 10% and 20%. Permeabilities are generally below 0.1 mD, with some higher porosity units showing values between 10 and 100 mD. The resulting total thickness of the seal formations over the Rødby structure is > 300 m.

The Rødby structure is located south of a major fault system, the Lolland–Falster Fault Zone. The Lolland–Falster Fault Zone is located outside the deepest closing contour at 1415 m of the structure, and hence occur outside the CO_2 storage site of the Rødby structure. Faults are interpreted and described from the 2D seismic data with focus on their occurrence in the Bunter Sandstone Formation–Ørslev Formation reservoir-seal pair. A minor fault zone, the Rødby Structure Fault Zone, with synthetic and antithetic faults have been documented near the apex of the structure in the vicinity of the Rødby-2 well (see Chapter 6). The fault zone is a result of halokinesis in the underlying Zechstein salt. The distance between the old and the

new 2D lines, challenges the possibility to infer or rule out if any other faults may occur around the rim of the Rødby structure in places not covered by GEUS's field campaign in 2023. Therefore, when maturing the Rødby structure further, a denser seismic data coverage may potentially reveal additional faults through overlying layers that could potentially introduce a possible risk of vertical leakage from storage in the Bunter Sandstone Formation.

The mean unrisked (buoyant) storage capacity of CO_2 in the Bunter Sandstone Formation at the Rødby structure is calculated to c. 107 MT CO_2 with a range between c. 69 MT CO_2 (P90) and c. 149 MT CO_2 (P10) and a P50 of c. 104 MT CO_2 (Figure 8.5.1). The storage capacity estimation of the Rødby structure compared to CO_2 capacities of other structures across Denmark (e.g. Gregersen et. al. (2023) and Hjelm et al. (2022)). Here, the structural spill point of the Top Bunter Sandstone Fm is located at c. 1100 m and the deepest closing contour at 1415 m. The spill point is defined as the deepest closing contour based on the dataset resulting in a minimum Gross Rock Volume (GRV), as saddle-points towards the south and southeast are not recognised within the dataset. The areal extent of the newly mapped structure is c. 117 km^2, which is 20 km^2 smaller than indicated in the previous regional study (137,5 km^2 in Hjelm et al. 2022), which was based on a smaller amount of seismic data and velocity data. Also, the structural relief is reduced from 450 m to 315 m due to a better constrained depth conversion applying data from the new seismic survey. This reduction in the rock volume of the structure, together with an assumed storage efficiency factor of 10% compared to the previously assumed 40%, have reduced the previous estimated technical storage capacity of 341 MT CO_2 in Hjelm et al. (2022) to a mean un-risked technical storage capacity of c. 107 MT CO_2 (see also Table 8.3.1). The calculations are for static reservoir models, but the capacity may be investigated further by more site-specific assessments and reservoir simulation modelling.

The main cause of the discrepancy between the old and new estimated technical storage capacity is due to choosing a lower and more realistic value for the assumed storage efficiency factor of 10% compared to the previously assumed 40%, which only is valid in a closed confined system with good well control etc., such as in the Stenlille area. The efficiency factor is the most widely ranging parameter in the storage calculation in deep saline aquifers. In the literature, the efficiency factor varies between 0.01% and 40% but the processes underlying its derivation are not always clear (Economides and Ehlig-Economides, 2010).

It is recommended to conduct additional investigations into the faults within the Rødby structure to evaluate risk of potential fault leakage and mitigate and ensure safe CO_2 injection and containment. Faults can lead to compartmentalization of the reservoir and weaken the seal, which may pose significant risks to CO_2 injection projects. Such a supplementary exploration program can help to understand the faults' impact on reservoir connectivity and seal integrity, allowing the future operator of the Rødby site to plan CO_2 injection pathways that avoid fault zones and prevent potential leakage or migration of CO_2.

Especially site-specific studies on the seal composition, integrity, and capacity (notably CO_2 entry pressures) are needed for the seals (Ørslev–Falster formations) of the Bunter Sandstone Fm in the Rødby structure, as it is not possible to draw parallels between these fine-grained rocks to the better-known Fjerritslev Fm which constitutes the main seal in most of the structures for CO_2 storage that are under exploration elsewhere in Denmark.

10. Recommendations for further work

The new 2023 seismic data has been acquired across the central part of the Rødby structure and improved the database with ten new 2D seismic sections. The new data together with the existing data provided a comprehensive database for the present updated mapping and analyses of the size, spill-point, volume, details of reservoir- and seal successions, and faults of the Rødby structure, included in this initial maturation. However, in order to de-risk the Rødby structure, it is recommended, that a further maturation of the structure should include supplementary seismic data acquisition and an in-depth risk assessment with seal integrity study, including analyzing of leakage risk at faults and well positions.

More specific, new 2/3D seismic acquisition with denser line spacing over the potential injection- and storage areas is recommended to obtain better control of the seismic velocities over the structure for a more detailed interpretation prior to CO_2 injection. Acquisition of additional seismic data over the northern, central and eastern part of the Rødby structure can add important new data towards developing optimal scenarios for well design, mitigating the fault related risks in relation to both the minor fault zones along the apex of the structure, as well as the termination of the structure downdip toward the deep-seated Lolland–Falster Fault Zone, as well as provide data as a baseline for improved modelling of CO_2 migration. Expanding the seismic coverage over the structure to the east will allow a better definition of the deepest closing contour of the structure, which is lying very close to the edge of GEUS new 2D seismic data used in this study.

In the near future, the Rødby license will potentially be matured from an exploration and assessment phase to a development and CO_2 injection (“production”) phase, repeated seismic surveys in same area can contribute to monitor the extent of the CO_2 migration, together with other monitoring (e.g., sampling in monitoring wells, seismometers, and other instrumentation). Such data will also enable a more precise definition of trap closures and reservoir outline, which again will feed into a refined storage volume calculation. The modelled storage capacity is associated with variability-ranges and uncertainty, which e.g., are dependent on volume and closure definition.

The geometry of the structure on the mapped surface of the Top Bunter Sandstone and the relief from the deepest closure (spill-point) to the top structure is sensitive to mapping errors and depth conversion constraints despite the much-improved database. Thus, it is recommended to improve the database and conduct a careful mapping and time-to-depth models.

A further key element for the quantification of the storage potential of the structure is the understanding of the storage efficiency. The storage efficiency factor is mostly dependent on reservoir architecture and performance and thus potential heterogeneity, permeability, and compartmentalization, but also by economic aspects such as well density, well layout and injection design. Better understanding of the reservoir and dynamic simulation of reservoir flow could constrain storage efficiency better and thus narrow the estimated final capacity range.

In this study, faults have been identified and described, mainly in the primary reservoir and seal sections. The study documents the existence of the minor Rødby Structure Fault Zone near the apex of the structure in the vicinity of the Rødby-2 well. The fault zone is a result of halokinesis in the underlying Zechstein salt and has been active since deposition of the Oddesund Fm until deposition of the Lower Jurassic Fjerritslev Fm. Possible CO_2 injection in

the Bunter Sandstone Fm should be away from faults and the lowermost contour and saddle-point (spill-point) of the structure. Besides the potential storage of CO_2 within the structure as considered here, potential effects from injection and storage on reservoir and seal at the specific site(s) should also be considered, including mineral solubility, mineral trapping, pressure and stress effects, risks, etc.

New necessary data acquisition and sampling, analyses and evaluations should be carried out for further maturation, including risk analyses, to cover geological and other technical uncertainties and risks.

Site-specific studies on the seal capacity are needed for all structures to be matured towards CO_2 storage, especially to better understand the fracture propagation through heterogeneous strata. For the Bunter Sandstone Formation in the Rødby structure, which is primarily sealed by the fine-grained intraformational parts of the Bunter Sandstone Fm itself and the overlying Ørslev and Falster formations, the need to establish fundamental knowledge of the seal properties is very high. This is because we cannot draw parallels to the better-known Lower Jurassic Fjerritslev Formation which constitutes the main seal in most of the structures for CO_2 storage that are under exploration elsewhere in Denmark.

11. Acknowledgement – The new seismic data

GEUS appreciate the good cooperation and discussions with Professor Alireza Malehmir and his researcher team from Uppsala University, and Geopartner Geofizyka Sp. Z.o.o (mini-vibs) on the planning, and during acquisition and completion of the GEUS2023-ROEDBY seismic survey.

The great field assistance from all the students from the University of Copenhagen and Uppsala University are highly acknowledged and appreciated. Also, the good cooperation with COWI of applications and logistics.

The good cooperation with the geophysics company Realtime Seismic during reprocessing for GEUS in 2023 is also highly appreciated.

References

Abramovitz, T., Thybo, H., and MONA LISA Working Group 1998. Seismic structure across the Caledonian Deformation Front along MONA LISA profile 1 in the southeastern North Sea. Tectonophysics 288, 153–176.

Abramovitz T., Thybo H., MONA LISA Working Group, 2000. Seismic images of Caledonian collisional structures along MONA LISA line 2 in the southeastern North Sea. Tectonophysics, 317, 27-54.

BABEL Working Group, 1993. Deep seismic reflection/refraction interpretation of crustal structure along BABEL profiles A and B in the southern Baltic Sea. Geophys J. Int., 112 (1993), pp. 325-343

Bachmann, G.H., Geluk, M.C., Warrington, G., Becker-Roman, A., Beutler, G., Hagdorn, H., Hounslow, M.W., Nitsch, E., Röhling, H.-G., Simon, T. and Szulc, A. 2010. Triassic. In: Doornenbal, J.C. & Stevenson, A.G. (eds): Petroleum Geological Atlas of the Southern Permian Basin Area. EAGE Publications b.v. (Houten), 149–173.

Bertelsen, F. 1980. Lithostratigraphy and depositional history of the Danish Triassic. Geological Survey of Denmark. Series B, No. 4, 59 pp. https://geusjournals.org/index.php/serieb/issue/view/928

Best, G., Kockel, F. & Schöneich, H., 1983. Geological history of the southern Horn Graben. Geologie en Mijnbouw 62: 25–34.

British Geological Survey Commissioned Report, CR/03/154. 37pp.

Brook, M., Shaw, K., Vincent, C. and Holloway, S. 2003. Storage Potential of the Bunter Sandstone in the UK sector of the southern North Sea and the adjacent onshore area of Eastern England.

Bruno, M.S., Lao, K., Diessl, J., Childers, B., Xiang, J., White, N. and van der Veer, E. 2014: Development of improved caprock integrity analysis and risk assessment techniques. Energy Procedia 63, 4708–4744.

Chadwick A., Arts R., Bernstone C., May F., Thibeau S., Zweigal P. (Eds) 2008. Best practice for the storage of CO2 in saline aquifers. Observations and guidelines from the SACS and CO2STORE projects". British Geological Survey. Keyworth, Nottingham, BGS Occasional Publication No. 14. ISBN 978-0-85272-610-5.

Clausen O.R. and Pedersen P.K. 1999. Late Triassic evolution of the southern margin of the Ringkøbing-Fyn High. Marine Petroleum Geology 16, 653–665.

Clemmensen, L.B. 1985. Desert sand plain and sabkha deposits from the Bunter Sandstone Formation (L. Triassic) at the northern margin of the German Basin. Geologische Rundschau 74, 519–536.

Dansk Boreselskab 1983. Søllested-1, Completion report.

DAPCO 1952. Tønder-1, Completion report (Compiled November 1993).

DEKORP-BASIN Research Group, 1999; Deep crustal structure of the Northeast German basin: New DEKORP-BASIN '96 deep-profiling results. Geology (1999), 27 (1), 55-58.

DGU/DAPCO 1952. Rødby-1, Completion report (Compilated June 1993).

DGU/DAPCO 1953. Rødby-2, Completion report (Compilated June 1993).

Frost, R.T.C., Fitch, F.J., Miller, J.A., 1981. The age and nature of the crystalline basement of the North Sea Basin. In: Illing, L.V., Hobson, G.C. (Eds.), Petroleum Geology of the Continental Shelf of North West Europe. Heyden. London, pp. 43-57.

Geluk, M.C. and Röhling, H.G. 1997. High-resolution sequence stratigraphy of the Lower Triassic 'Buntsandstein' in the Netherlands and northwestern Germany. Geologie en Mijnbouw 76, 227–246.

Guiltinan, E.J., Cardenas, M.B., Bennett, P.C., Zhang, T. and Espinoza, D.N. 2017. The effect of organic matter and thermal maturity on the wettability of supercritical CO_2 on organic shales. International Journal Greenhouse Gas Control 65, 15–22.

Gulf Denmark 1968. Ørslev-1, Completion report.

Hangx, S.J. T., Spiers, C.J. and Peach, C.J. 2010. Mechanical behavior of anhydrite caprock and implications for CO2 sealing capacity, Journal of Geophysical Research 115, B07402, doi:10.1029/2009JB006954.

Heinemann, N., Wilkinson, M., Pickup, G.E., Haszeldine, R.S. and Cutler, N.A. 2012. CO2 storage in the offshore UK Bunter Sandstone Formation. International Journal Greenhouse Gas Control 2012, 6, 210–219.

Holmslykke, H.D., Schovsbo, N.H., Kristensen, L., Weibel, R. & Nielsen, L.H. 2019. Brine types in Danish Deep onshore sandstone reservoirs exploited for geothermal energy. Geological Survey of Denmark and Greenland Bulletin 42.

Japsen, P. and Bidstrup, T. 1999: Quantification of late Cenozoic erosion in Denmark based on sonic data and basin modelling. Bulletin of the Geological Society of Denmark 46, 79–99.

Japsen, P., Green, P.F., Nielsen, L.H., Rasmussen, E.S. and Bidstrup, T. 2007. Mesozoic–Cenozoic exhumation events in the eastern North Sea Basin: a multi-disciplinary approach based on palaeothermal, palaeoburial, stratigraphic and seismic data. Basin Research 19, 451–490.

Jørgensen, F., Lykke-Andersen, H., Sandersen, P. B. E., Auken, E. & Nørmark, E. 2003: Geophysical investigations of buried Quaternary valleys in Denmark: An integrated application of transient electromagnetic soundings, reflection seismic surveys and exploratory drillings. Journal of Applied Geophysics 53, 215–228.

Jørgensen, F., Scheer, W., Thomsen, S., Sonnenborg, T.O., Hinsby, K., Wiederhold, H., Schamper, C., Burschil, T., Roth, B., Kirsch, R., Auken, E., 2012. Transboundary geophysical mapping of geo-logical elements and salinity distribution critical for the assessment of future sea water intrusion in response to sea level rise. Hydrol. Earth Syst. Sci. Discuss. 9, 2629–2674.

Ketter, F. 1991. The Esmond, Forbes and Gordon Fields, Blocks 43/8a, 48/13a, 48/15a, 48/20a, UK North Sea. In Abbotts, I. L. (ed.): United Kingdom Oil and Gas Fields, 25 Years Commemorative Volume. Memoir of the Geological Society, London 14, 425-432.

Kortekaas, M., Böker, U., van der Kooij, C. and Jaarsma, B. 2018. Lower Triassic reservoir development in the northern Dutch offshore. In Kilhams et al. (eds): Mesozoic Resource Potential in the Southern Permian Basin. Geological Society, London, Special Publications 469, 149–168.

Krawczyk, C.M., Eilts, F., Lassen, A. & Thybo, H. 2003. Seismic evidence of Caledonian deformed crust and uppermost mantle structures in the northern part of the Trans-European Suture Zone, SW Baltic Sea. Tectonophysics, Vol. 360, Issues 1-4.

Laier, T. 2002. Vurdering af udfældningsrisici ved geotermisk produktion fra Margretheholmboringen MAH-1A. Beregning af mætningsindeks for mineraler i saltvand fra Danmarks dybere undergrund. Danmarks og Grønlands Geologiske Undersøgelser Rapport 2002/95. 48 pp.

Laier, T. 2008. Chemistry of Danish saline formation waters relevant for core fluid experiments: fluid chemistry data for lab experiments related to CO2 storage in deep aquifers. Geological Survey of Denmark and Greenland Report 2008/48. 10 pp.

Laier, T. and Øbro, H. 2009. Environmental and safety monitoring of the natural gas underground storage at Stenlille, Denmark. Geological Society London Special Publications 313(1):81-92, DOI: 10.1144/SP313.6

Larsen, 0., 1971. Kl Ar age determinations from the Precambrian of Denmark. Dan. Geol. Unders. Afh. Række 2, (97), 37 pp.

Lassen, A. and Thybo, H. 2012. Neoproterozoic and Palaeozoic evolution of SW Scandinavia based on integrated seismic interpretation. Precambrian Research, 204, 75-104.

Lassen, A., Thybo, H., Berthelsen, A., 2001. Reflection seismic evidence for Caledonian deformed sediments above Sveconorwegian basement in the southwestern Baltic Sea. Tectonics 20, 268–276.

Mathiesen, A., Dam, G., Fyhn, M.B.W., Kristensen, L., Mørk, F., Petersen, H.I. and Schovsbo, N.H. 2022. Foreløbig evaluering af CO_2 lagringspotentiale af de saline akviferer i Nordsøen. Danmarks og Grønlands Geologiske Undersøgelse Rapport 2022/15, 188 pp.

Mbia, E.N., Fabricius, I.L., Krogsbøll, A., Frykman, P. and Dalhoff, F. 2014. Permeability, compressibility and porosity of Jurassic shale from the Norwegian-Danish Basin. Petroleum Geoscience 20, 257–281.

McBride, E.F. 1963. A classification of common sandstones. Journal of Sedimentary Research 33: 664–669.

Michelsen, O. and Clausen, O.R. 2002. Detailed stratigraphic subdivision and regional correlation of the southern Danish Triassic succession. Marine and Petroleum Geology, 19, 563–587. https://doi.org/10.1016/S0264-8172(02)00028-4

Meissner, R. & Krawczyk, C.M., 1999. Caledonian and Proterozoic terrane accretion in the southwest Baltic Sea. Tectonophysics, Vol. 314, Issues 1-3.

Michelsen, O., Saxov, S. Leth, J.A., Andersen, C., Balling, N., Breiner, N., Holm, L., Jensen, K., Kristensen, J.I., Laier, T., Nygaard, E., Olsen, J.C., Poulsen, K.D., Priisholm, S., Raade, T.B., Sørensen, T.R. and Würtz, J. 1981. Kortlægning af potentielle geotermiske reservoirer I Danmark. Danmarks Geologiske Undersøgelse Serie B, Nr. 5, 96 pp.

MONA LISA Working Group, 1997. MONA LISA — Deep seismic investigations of the lithosphere in the southeastern North Sea. Tectonophysics, 269 (1997), pp. 1-19.

Nielsen, L.H. and Japsen, P. 1991. Deep wells in Denmark 1935-1990. Lithostratigraphic subdivision. Danmarks Geologiske Undersøgelse, DGU Serie A, No. 31, 177 pp.

Olivarius, M., Weibel, R., Hjuler, M. L., Kristensen, L., Mathiesen, A., Nielsen, L. H. and Kjøller, C. 2015. Diagenetic effects on porosity–permeability relationships in red beds of the Lower Triassic Bunter Sandstone Formation in the North German Basin. Sedimentary Geology, 321, 139–153.

Olivarius, M., Weibel, R., Friis, H., Boldreel, L.O., Keulen, N. and Thomsen, T.B. 2017. Provenance of the Lower Triassic Bunter Sandstone Formation: implications for distribution and architecture of aeolian vs. fluvial reservoirs in the North German Basin. Basin Research 29 (Suppl. 1): 113–130.

Pharaoh, T., England, R. & Lee, M., 1995. The concealed Caledonide basement of Eastern England and the Southern North Sea – a review. Studia geophysica et geodaetica 39: 330–346.

Pedersen, G.K., Schovsbo, N.H. and Nøhr-Hansen, H. 2013. Calibration of spectral gamma-ray logs to deltaic sedimentary facies from the Cretaceous Atane Formation, Nuussuaq Basin, West Greenland. Geological Survey of Denmark and Greenland Bulletin 28, 65–68.

Petersen, H. I., Nielsen, L. H., Bojesen-Koefoed, J. A., Mathiesen, A., Kristensen, L. and Dalhoff, F. 2008. Evaluation of the quality, thermal maturity and distribution of potential source rocks in the Danish part of the Norwegian–Danish Basin. GEUS Bulletin, 16, 1–66. https://doi.org/10.34194/geusb.v16.4989.

Petersen, H.I., Holland B. and Olivarius, M. 2022. Source rock evaluation and fluid inclusion reconnaissance study of Carboniferous and Zechstein rocks in the northern margin of Southern Permian Basin, onshore Denmark. International Journal of Coal Geology 255. https://doi.org/10.1016/j.coal.2022.103985.

Schovsbo, N.H. and Petersen, H.I. 2024. in prep. Analysis of cuttings samples from the Triassic to Jurassic interval in 8 wells in Eastern Denmark in relation to seal integrity. GEUS report 2024

Schovsbo, N.H., Weibel, R., Springer, N., Fogden, A., Sheldon, E. and Petersen, H.I. 2023. Workflow for Characterization of the Nini West Storage Site Seal, Danish North Sea. EAGE GET, p.1 – 5. https://doi.org/10.3997/2214-4609.202321010.

Weibel, R. and Friis, H. 2004. Opaque minerals as keys for distinguishing oxi dising and reducing diagenetic conditions in the Lower Triassic Bunter Sandstone, North German Basin. Sedimentary Geology 169, 129–149.

Weibel, R., Olivarius, M., Friis, H., Kristensen, L., Hjuler, M.L., Kjøller, C., Pedersen, P.K., Boyce, A., Mathiesen, A. and Nielsen, L.H. 2017. The influence of climate on early and burial diagenesis in Triassic and Jurassic sandstones from the Norwegian–Danish Basin. The Depositional Record 3(1), 60–91.

Weibel, R., Olivarius, M., Vosgerau, H., Mathiesen, A., Kristensen, L., Nielsen, C. M. and Nielsen, L.H. 2020. Overview of potential geothermal reservoirs in Denmark. Netherlands Journal of Geosciences, 99, e3, 14 pp.

Appendix A – Well-log interpretation (Lolland–Falster area)

Link to the well-log interpretation of Appendix A:

- Rødby-1
- Rødby-2
- Søllested-1
- Ørslev-1

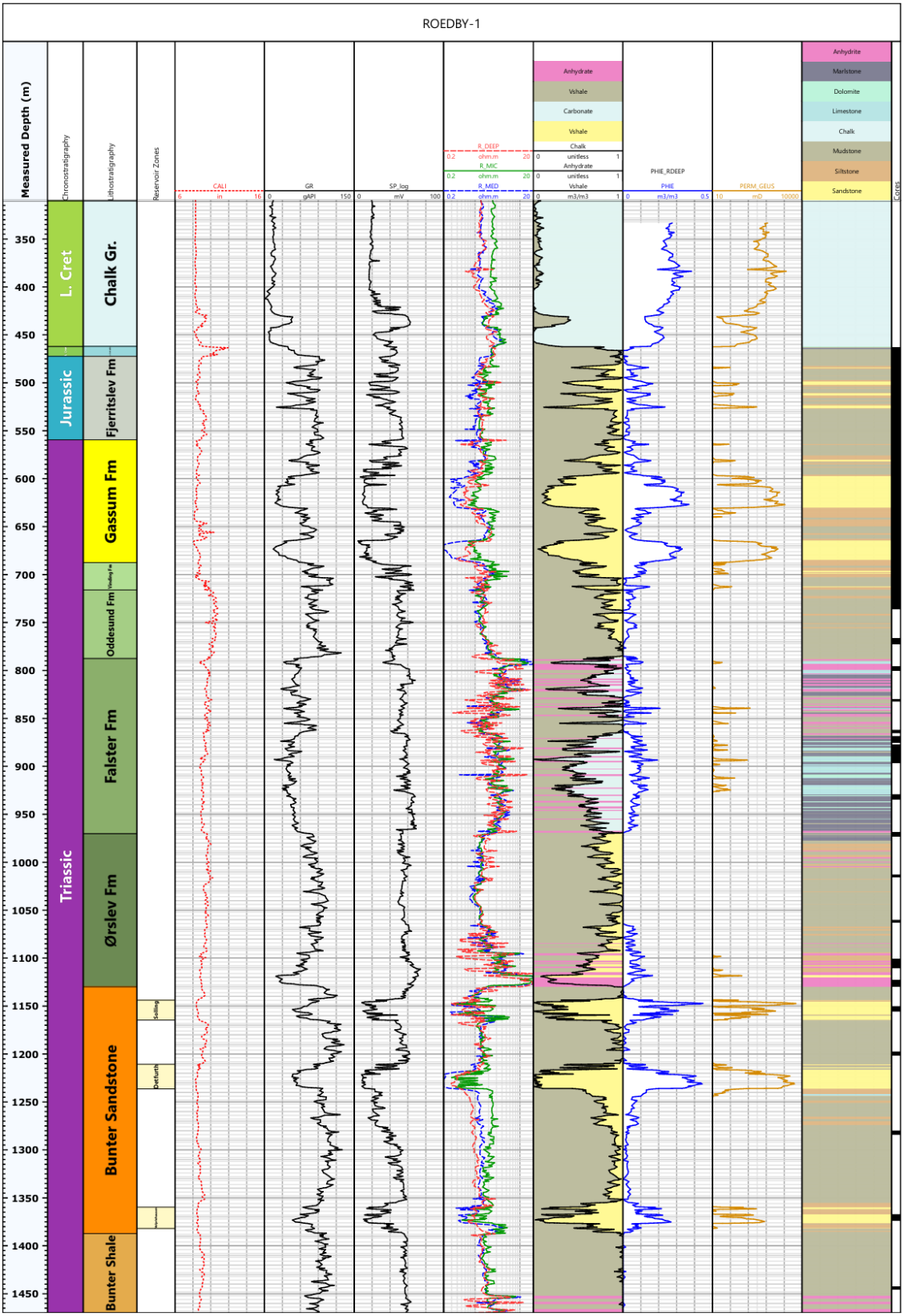
ROEDBY-1
Measured Depth (m)
Chronostratigraphy
Lithostratigraphy
Reservoir Zones
CALI
GR
SP_log
R_DEEP
R_MIC
R_MED
PHIE_RDEEP
PHIE
PERM_GEUS
Anhydrite
Vshale
Carbonate
Chalk
Marlstone
Dolomite
Limestone
Mudstone
Siltstone
Sandstone
Cores
L. Cret
Jurassic
Triassic
Chalk Gr.
Fjerritslev Fm
Gassum Fm
Oddesund Fm
Falster Fm
Ørslev Fm
Bunter Sandstone
Bunter Shale

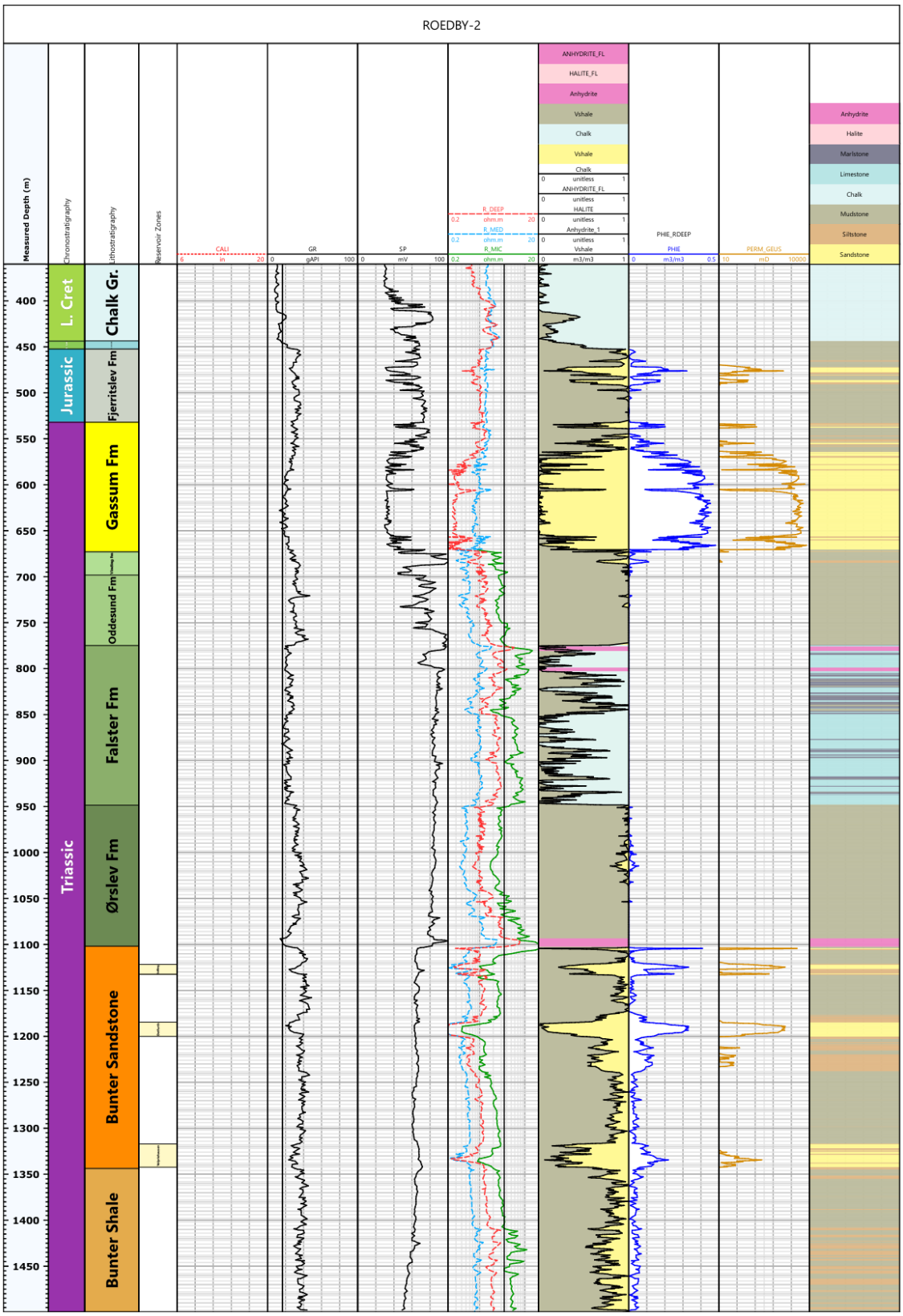
ROEDBY-2
Measured Depth (m)
Chronostratigraphy
Lithostratigraphy
Reservoir Zones
CALI
GR
SP
R_DEEP
R_MED
R_MIC
ANHYDRITE_FL
HALITE_FL
Anhydrite
Vshale
Chalk
Vshale
Chalk
ANHYDRITE_FL
HALITE
Anhydrite_1
Vshale
PHIE_RDEEP
PHIE
PERM_GEUS
Anhydrite
Halite
Marlstone
Limestone
Chalk
Mudstone
Siltstone
Sandstone
L. Cret
Jurassic
Triassic
Chalk Gr.
Fjerritslev Fm
Gassum Fm
Oddesund Fm
Falster Fm
Ørslev Fm
Bunter Sandstone
Bunter Shale

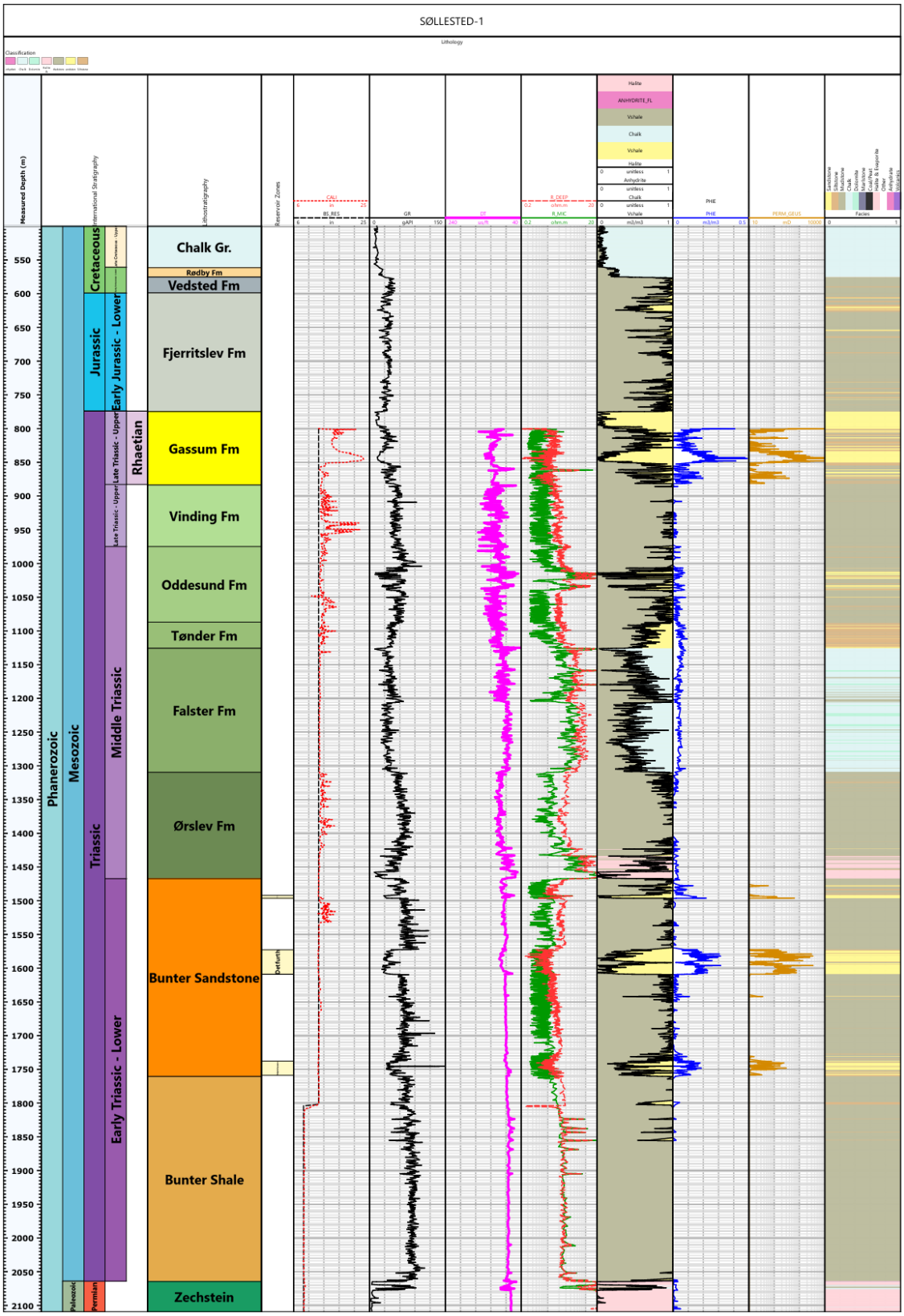
SØLLESTED-1
Lithology
Measured Depth (m)
International Stratigraphy
Lithostratigraphy
Reservoir Zones
Phanerozoic
Mesozoic
Triassic
Jurassic
Cretaceous
Permian
Paleozoic
Early Triassic - Lower
Middle Triassic
Late Triassic - Upper
Rhaetian
Early Jurassic - Lower
Late Cretaceous - Upper
Chalk Gr.
Rødby Fm
Vedsted Fm
Fjerritslev Fm
Gassum Fm
Vinding Fm
Oddesund Fm
Tønder Fm
Falster Fm
Ørslev Fm
Bunter Sandstone
Bunter Shale
Zechstein
Unconformity
Halite
ANHYDRITE_FL
Vchale
Chalk
Vchale
Halite
unitless
Anhydrite
unitless
Chalk
unitless
Vchale
CALI
BS_BES
GR
gAPI
DT
us/ft
R_DEEP
R_MIC
ohm.m
PHIE
m3/m3
PERM_GEUS
mD
Facies
Sandstone
Siltstone
Mudstone
Chalk
Dolomite
Marlstone
Coal/ Peat
Evaporite
Other
Anhydrite
Halite

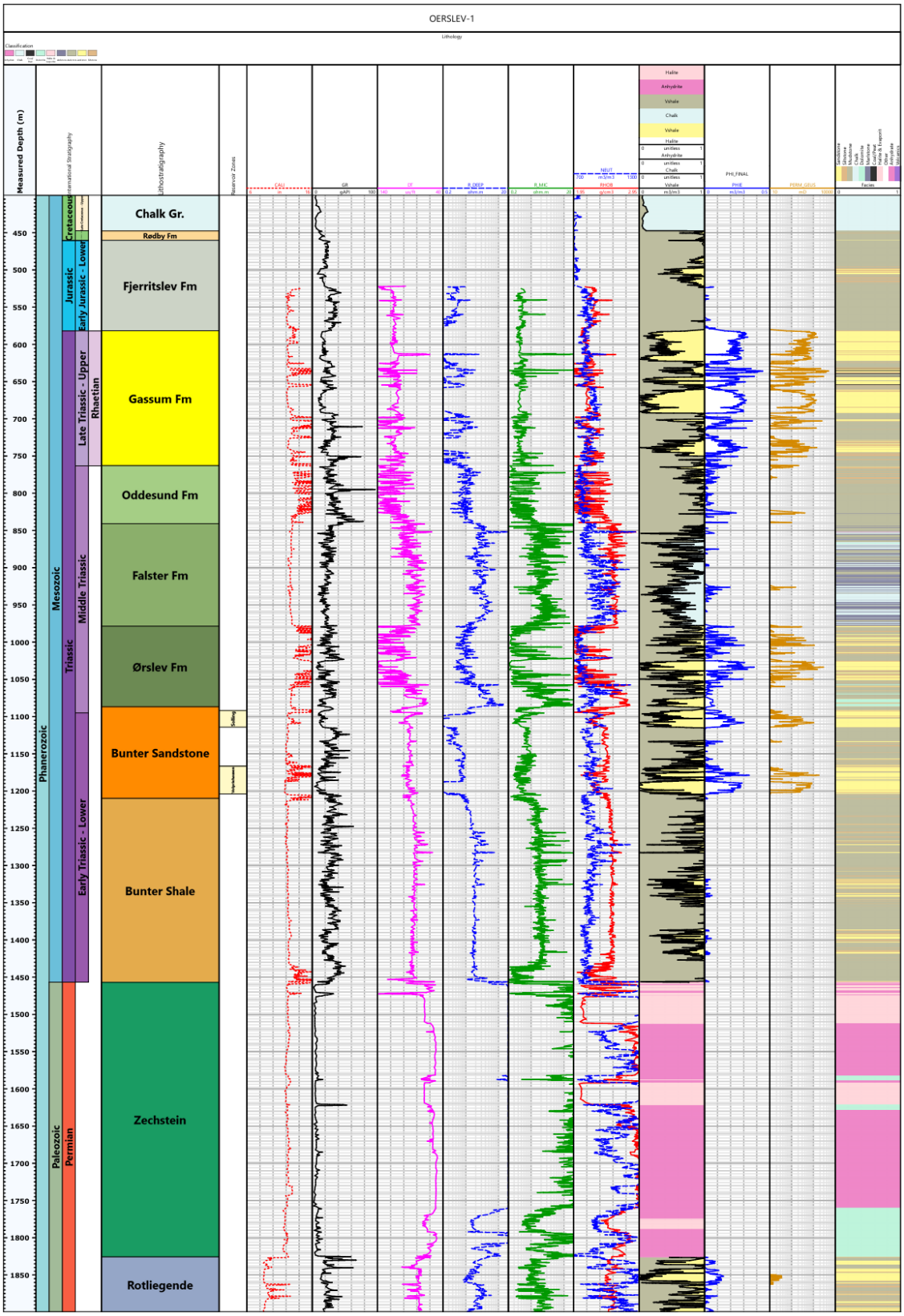
OERSLEV-1
Lithology
Measured Depth (m)
International Stratigraphy
Lithostratigraphy
Reservoir Zones
Phanerozoic
Mesozoic
Paleozoic
Cretaceous
Jurassic
Triassic
Permian
Early Jurassic - Lower
Late Triassic - Upper Rhaetian
Middle Triassic
Early Triassic - Lower
Chalk Gr.
Rødby Fm
Fjerritslev Fm
Gassum Fm
Oddesund Fm
Falster Fm
Ørslev Fm
Bunter Sandstone
Bunter Shale
Zechstein
Rotliegende
Halite
Anhydrite
Vshale
Chalk
Facies